TOWARDS THE STRUCTURE OF THE *Escherichia coli* DnaB HELICASE

by

Naďa Dammerová

A thesis submitted for the degree of Doctor of Philosophy
of the Australian National University

RESEARCH SCHOOL OF CHEMISTRY
THE AUSTRALIAN NATIONAL UNIVERSITY

August 1995

The work described herein is the author's own work, unless otherwise stated, and was carried out within the Research School of Chemistry, the Australian National University, from February 1992 until December 1994. The results presented in Section 6 were carried out by Dr José M. Carazo and Ms M. Carmen San Martin in Centro Nacional de Biotecnología (C.S.I.C.), Campus Universidad Autonóma de Madrid, Spain. The contents of this thesis have not been included in any other work submitted by the author for another degree.

Naďa Dammerová

Naďa Dammerová

ACKNOWLEDGEMENTS

I am sincerely grateful to my supervisor Dr Nicholas E. Dixon for sharing his experience with me, and continuous support throughout my postgraduate course. It has been a great privilege to work under his guidance; his passion for science together with an encouraging approach under any circumstances have made my postgraduate training a very valuable and pleasurable experience.

I would like to express my gratitude to Dr David L. Ollis and Dr Eong U. Cheah for introducing me into the world of "black art" - crystallization of proteins - as well as for their friendly support and care I have been enjoying in the past few years.

I am also very thankful to Dr José M. Carazo and M. Carmen San Martin for their collaboration. Their wonderful results of electron-microscopic studies of DnaB provided an exciting and unparalleled glimpse on the structure of the DnaB oligomer.

I would like to thank to all the members of Dr Dixon's and Dr Ollis' groups. My special thanks goes to Penny Lilley (not only for her excellent technical assistance); John Barton, Jenny Beck, Paul Carr, Jeffrey Crowther, Jenny Daniher, Chris Love, Shadi Moghaddas, Chris Penington, Anna Robinson, Peter Suffolk, Jennifer Thorn, Subhash Vasudevan, Phillippa Wyrdeman, and Jiyeon Yang are thanked for their constant friendship and assistance. I wish to acknowledge also the support of my adviser Dr Wilfred L. F. Armarego.

My postgraduate study in Australia was made possible by financial support from the Department of Employment, Education and Training through the Overseas Postgraduate Research Scholarship (OPRS) and by the Australian National University through an ANU Postgraduate Scholarship.

I would like to thank the Research School of Chemistry for providing excellent facilities for research, and all the people at RSC and ANU who offered friendship and assistance to my family and me during our stay in Canberra.

I wish to express my sincere gratitude to my parents and sister for their continuous support, love and tolerance. Assistance of my father-in-law, who spent many hours looking after our twin babies, is highly appreciated.

Finally, my special thanks belongs to my husband Dusan, and our children Jakub, Matej, and Andrej. Their love was the best kind of support I could get from them.

ABSTRACT

The DnaB helicase is the essential replicative helicase in *Escherichia coli*. The protein is involved in initiation and elongation stages of DNA replication and is primarily responsible for the unwinding of the DNA duplex at replication forks in chromosomal DNA synthesis. DnaB plays a key role also in the replication of *E. coli* phage and plasmid DNA. When acting as a helicase, DnaB unwinds the parental DNA duplex in the 5' to 3' direction with respect to the strand on which it is bound and generates single-stranded (ss) DNA in its path. The reaction is coupled with an energy-releasing DnaB-catalysed hydrolysis of nucleoside 5'-triphosphates. In its role as a replicative promoter, DnaB is believed to form a special secondary structure in ssDNA that is recognised by the DnaG primase, which in turns primes DNA synthesis on parental strands of DNA. The native DnaB protein is a hexamer of identical subunits with a monomeric molecular weight of 52,265, and is normally present in cells in a complex with the DnaC protein.

The aim of the research project was to contribute to structural studies of the DnaB helicase. The initial effort was focused on preparation of crystals of the wild-type (*wt*) DnaB protein which would be suitable for X-ray diffraction analysis. The purification procedure of *wt*DnaB was improved and quantities of ~99% pure DnaB protein and the DnaB.DnaC complex sufficient for crystallization experiments were purified. An alternative method for obtaining pure DnaB.DnaC complex by reassociation from partially purified DnaB and DnaC proteins, followed by chromatographic purification was examined. High-performance electrophoretic chromatography confirmed that the stoichiometry of DnaB and DnaC in the complex obtained in either way satisfied the strict requirements for crystallization of protein complexes. Using the knowledge that the conformation of the DnaB protein itself as well as the configuration of DnaB monomers in the hexamer are influenced by binding of nucleoside-phosphate ligands, purifications of the DnaB and the DnaB.DnaC complex were carried out in the presence of ATP and in the presence of ADP, respectively. The DnaB helicase (both ATP- and ADP-bound forms) and the DnaB.DnaC complex were crystallized. Crystals of DnaB, which had been purified in the presence of ADP, diffracted X-rays to ~8Å resolution.

Patterns of thermal diffuse scattering indicated discrete but so far undefined conformational transitions of parts of the molecules within the lattice.

An alternative strategy was employed with a view to minimize conformational changes that are induced in the DnaB molecule in connection with binding of different nucleotides. Two types of dominant-lethal mutants of the *E. coli* DnaB protein were prepared and purified on a large scale. The DnaB-R231C mutant exhibits profound defficiency in hydrolysis of ATP; DnaB-I141T is a missense mutant modified in the region that is believed to undergo conformational changes on ATP hydrolysis. The ATPase$^-$ DnaB mutant was crystallized.

The possibility of generating DnaB deletion mutants which would mimic the separate domains of the DnaB helicase, their purification and crystallization were examined. This was considered as an alternative approach to overcome the apparent conformational instability of the intact DnaB molecule. Genetic manipulations that were used in attempts to prepare systems for overproduction of DnaB domains in soluble form are described. Several systems for overproduction of the COOH-terminal domain were prepared. The NH_2-terminal domain was purified and crystallization experiments were carried out.

Suitability of the prepared dominant-lethal and deletion mutants for crystallization and high-resolution X-ray diffraction analysis is discussed.

Electron-microscopic studies of the *wt*DnaB protein and the DnaB mutants prepared and purified in our laboratory were carried out by Dr José M. Carazo and Ms M. Carmen San Martin, Centro Nacional de Biotecnología (C.S.I.C.), Campus Universidad Autonóma de Madrid. The three-dimensional reconstruction of the DnaB oligomer at 2.7 nm characterizes the aggregate as a trimer of dimers with a pronounced triangular shape and a central channel that completely traverses the oligomer.

PUBLICATIONS

Dammerova, N., San Martin, M.C., Carazo, J.M., Carr, P.D., Ollis, D.L. and Dixon, N.E. (1994)

Structural studies on the *Escherichia coli* DnaB helicase.

Proc. Aust. Biochem. Soc. 26:P-3-47.

San Martin, M.C., Stamford, N.P.J., Dammerova, N., Dixon, N.E. and Carazo, J.M. (1995)

A structural model for the *Escherichia coli* DnaB helicase based on electron microscopy data.

Journal of Structural Biology (in the press)

CONTENTS

	ACKNOWLEDGEMENTS	1
	ABSTRACT	2
	PUBLICATIONS	5
	CONTENTS	6
	ABBREVIATIONS	10
1	**GENERAL INTRODUCTION**	12
1.1	**DNA Helicases**	12
1.2	**Replication of the *E. coli* Chromosome**	15
	1.2.1 *Initiation at* oriC	15
	1.2.2 *Elongation*	17
	1.2.3 *Termination*	18
1.3	**The DnaB Helicase**	20
	1.3.1 *General Characteristics of the DnaB Protein*	20
	1.3.2 *Involvement of the DnaB Helicase in General Priming*	25
	1.3.3 *Role of the DnaB Helicase in Specific Priming*	26
	1.3.3.1 The ϕX174-Type Primosome	26
	1.3.3.2 The ABC-Primosome	28
1.4	**Analogues of the DnaB Helicase**	31
1.5	**Preliminary Structure-Function Characteristics of the DnaB Helicase**	31
1.6	**Aims of the Project**	38
2	**MATERIALS AND METHODS**	40
2.1	**Bacterial Strains and Plasmids**	40
2.2	**Growth of Bacteria**	42
2.3	**Chemicals, Reagents, Enzymes and Instruments**	42
2.4.	**Preparation of Plasmid DNA**	44
	2.4.1 *Plasmid Extraction by Alkaline Lysis*	44
	2.4.2 *Large-Scale Plasmid Preparation*	44
2.5	**Restriction-Endonuclease Digestion of DNA**	46
2.6	**DNA End-Filling with the Klenow Enzyme**	46

2.7 Electrophoresis of DNA 47
2.8 Isolation and Purification of DNA Fragments 47
2.9 5'-Dephosphorylation of Linear Plasmid DNA 48
2.10 Preparation of Oligonucleotides 48
2.11 Ligation 48
2.11.1 *Ligation of Cohesive Termini* 49
2.11.2 *Ligation of Blunt-Ended Termini* 49
2.12 Preparation of Single-Stranded Template DNA 49
2.13 Transformation of *E. coli* 50
2.13.1 *Preparation of Competent Cells* 50
2.13.2 *Transformation of Competent Cells* 50
2.14 **Determination of Protein Concentration** 50
2.15 SDS-Polyacrylamide Gel Electrophoresis 51
2.16 Oligonucleotide-Directed Mutagenesis 52

3 PURIFICATION AND CRYSTALLIZATION OF THE *wt*DnaB AND DnaC PROTEINS AND THE DnaB.DnaC COMPLEX 53

3.1 Introduction 53
3.2 Material and Methods 54
3.2.1 *Purification of* wt*DnaB, DnaC and the DnaB.DnaC Complex* 54
3.2.1.1 Purification Method A 54
3.2.1.2 Purification Method B 56
3.2.1.3 Reassociation of the DnaB.DnaC Complex and its Purification 57
3.2.2 *DNA Replication Assay* 57
3.2.3 *High-Performance Electrophoretic Chromatography* 59
3.2.4 *Concentration of Proteins* 59
3.2.5 *Crystallization of Proteins* 60
3.2.6 *Analysis of Protein Crystals* 62
3.3 Results 62
3.3.1 *Purification of the Proteins* 62
3.3.1.1 Purification of the DnaB, DnaC Proteins and the DnaB.DnaC Complex from Strain RSC680 62
3.3.1.2 Purification of DnaB and the DnaB.DnaC Complex from Strain RSC989 68
3.3.1.3 Reassociation of the DnaB.DnaC Complex 73

3.3.2 *High-Performance Electrophoretic Chromatography* 73
3.3.3 *Crystallization of the Proteins* 78
3.4 Discussion 82

4 DOMINANT-LETHAL MUTANTS OF THE *E. coli* DnaB PROTEIN 86

4.1 Introduction 86
4.2 Materials and Methods 87
4.2.1 *Construction of Phagemid pND604* 87
4.2.2 *Oligonucleotide-Directed Mutagenesis of dnaB - Construction of a Plasmid Directing Overexpression of* dnaB-R231C *and* dnaC 89
4.2.3 *Oligonucleotide-Directed Mutagenesis of dnaB - Construction of a Plasmid for Overexpression of* dnaB-I141T *and* dnaC 92
4.2.4 *Purification and Crystallization of DnaB-R231C and DnaB-I141T* 92
4.3 Results 96
4.3.1 *ATPase⁻ Mutant of the DnaB Protein* 96
4.3.2 *The Hinge-Region Mutant of DnaB* 100
4.4 Discussion 101

5 DELETION MUTANTS OF THE DnaB PROTEIN 105

5.1 Introduction 103
5.2 Materials and Methods 107
5.2.1 *Subcloning of the* dnaB *Deletion Mutants* 107
5.2.1.1 Plasmids Directing Overproduction of the DnaC Protein and the DnaBΔC Deletion Mutants 107
5.2.1.2 Plasmids for Simultaneous Overexpression of *dnaC* and the *dnaBΔN* Deletion Mutants 109
5.2.2 *Manipulations of the Region Separating the COOH- and NH_2-Terminal Domains of DnaB* 112
5.2.3 *Plasmids Directing Overproduction of DnaBΔN1-165* 115
5.2.4 *A System for Simultaneous Overproduction of the DnaC*

Protein and the COOH- and NH_2-Terminal Domains of DnaB 119
5.2.5 *Subcloning of the Regions Encoding Protease-Cleavage Sites into the* dnaB *Gene* 119
5.2.6 *Purification and Crystallization of the DnaBΔC162-470 Mutant* 124
5.2.7 *Purification of DnaB-9αα165/166, DnaB-T165/166, DnaB-F165/166* 125
5.2.8 *Proteolysis of the DnaB-T165/166, DnaB-F165/166 Mutants* 126
5.3 Results 126
5.3.1 *Subcloning of the* dnaB *Deletion Mutants* 126
5.3.2 *Mutants of DnaB Generated by the Specific Proteolyses* 133
5.3.3 *Purification and Crystallization Experiments of the NH_2-Terminal Domain of the DnaB Protein* 139
5.4 Discussion 139

6 ELECTRON-MICROSCOPIC STUDIES OF THE DnaB HELICASE 145

6.1 Introduction 145
6.2 Materials and Methods 145
6.2.1 *Electron Microscopy* 145
6.2.2 *Image Processing* 146
6.2.3 *Three-Dimensional Reconstruction* 146
6.3 Results 147
6.3.1 *Two-Dimensional Analysis of the DnaB Oligomer* 147
6.3.2 *Three-Dimensional Reconstruction of the DnaB Oligomer* 147
6.4 Discussion 151

CONCLUDING STATEMENT 158
REFERENCES 160
APPENDIX 177

ABBREVIATIONS

• A_λ	absorbance measured at wavelength λ [nm] in cuvettes of 1-cm pathway
• Ap	ampicillin
• ATP	adenosine 5'-triphosphate
• ATPase	adenosine 5'-triphosphatase
• ATPγS	adenosine 5'-(γ-thio)triphosphate
• ATPPNP	β.γ -imidoadenosine 5'-triphosphate
• bp	base pair(s)
• BSA	bovine serum albumin
• Cm	chloramphenicol
• dATP, dGTP, dCTP, dTTP	deoxyadenosine 5'-triphosphate, deoxyguanosine 5'-triphosphate, deoxycytidine 5'-triphosphate, deoxythymidine 5'-triphosphate, respectively
• DnaB	the DnaB protein
• *dnaB*	the gene encoding DnaB
• DTT	dithiothreitol
• dNTP	deoxynucleoside 5'-triphosphate
• ds	double strand(ed) (DNA)
• *E. coli*	*Escherichia coli*
• HEPES	4-(2-hydroxyethyl)-1-piperazine-ethanesulfonic acid
• kb	kilobase(s)
• LB	Luria-Bertani medium
• MPD	methylpentenediol
• MWCO	molecular weight cut-off
• $NaPP_i$	sodium pyrophosphate
• NTP	nucleoside 5'-triphosphate
• NTPase	nucleoside 5'-triphosphatase
• PAGE	polyacrylamide gel electrophoresis
• *pas*	primosome-assembly site
• PEG	polyethyleneglycol
• P_L, P_R	major leftward and rightward promoters of phage λ, respectively
• RBS	ribosome-binding site
• RF	replicative form

- rCTP, rUTP, rGTP — cytidine 5'-triphosphate, uridine 5'-triphosphate, guanosine 5'-triphosphate, respectively
- SDS — sodium dodecyl sulphate
- ss — single-strand(ed) (DNA)
- SSB — single-stranded DNA binding protein
- TCA — trichloroactetic acid
- TEMED — NNN'N'-tetraethylenediamine
- Tris — tris(hydroxymethyl)-aminomethane
- *ts* — thermosensitive
- *wt* — wild-type

1 GENERAL INTRODUCTION

1.1 DNA helicases

DNA helicases are enzymes that play an indispensable role in all aspects of nucleic acid metabolism. Processes such as DNA replication, recombination and repair, which are essential for the maintenance and faithful transmission of DNA from one generation of cells to the next, would not be possible without their involvement. Each of these processes requires at least a transient unwinding of the duplex DNA to provide a template or reaction intermediate. DNA helicases accomplish this task by disrupting the hydrogen bonds between the Watson-Crick base pairs of duplex DNA (Fig. 1.1). This is an energy-requiring reaction that is always coupled with the hydrolysis of a nucleoside 5'-triphosphate, and all helicases described to date are also DNA-dependent nucleoside 5'-triphosphatases (NTPases). Presumably the energy released in the NTP hydrolysis is utilized in the unwinding of DNA, but exactly how the two reactions are coupled is a question that remains to be answered. Like many proteins that interact with DNA, helicases exhibit a directionality with regard to the unwinding reaction. This directionality can be either 5' to 3' (Figure 1.1a) or 3' to 5' (Figure 1.1b), depending on the specific helicase (for reviews, see Matson and Kaiser-Rogers, 1990; Matson, 1991; Lehman and Kornberg, 1992; Lohman, 1992; Matson *et al.*, 1994).

DNA helicases were first discovered in 1976 (Abdel-Monem *et al.*, 1976) and are ubiquitous in nature. They have been isolated using sources ranging from bacteriophage to mammalian cells and in each cell there is always a number of different helicases that participate in many, if not all, facets of DNA metabolism (Matson and Kaiser-Rogers, 1990; Thommes and Hübscher, 1992).

Escherichia coli has at least eleven distinct DNA helicases (Matson *et al.*, 1994) (Table 1.1). At least three of them - DnaB, PriA and Rep proteins - are involved in replication of DNA. Among them, DnaB helicase is the most important. DnaB is primarily responsible for unwinding of the DNA

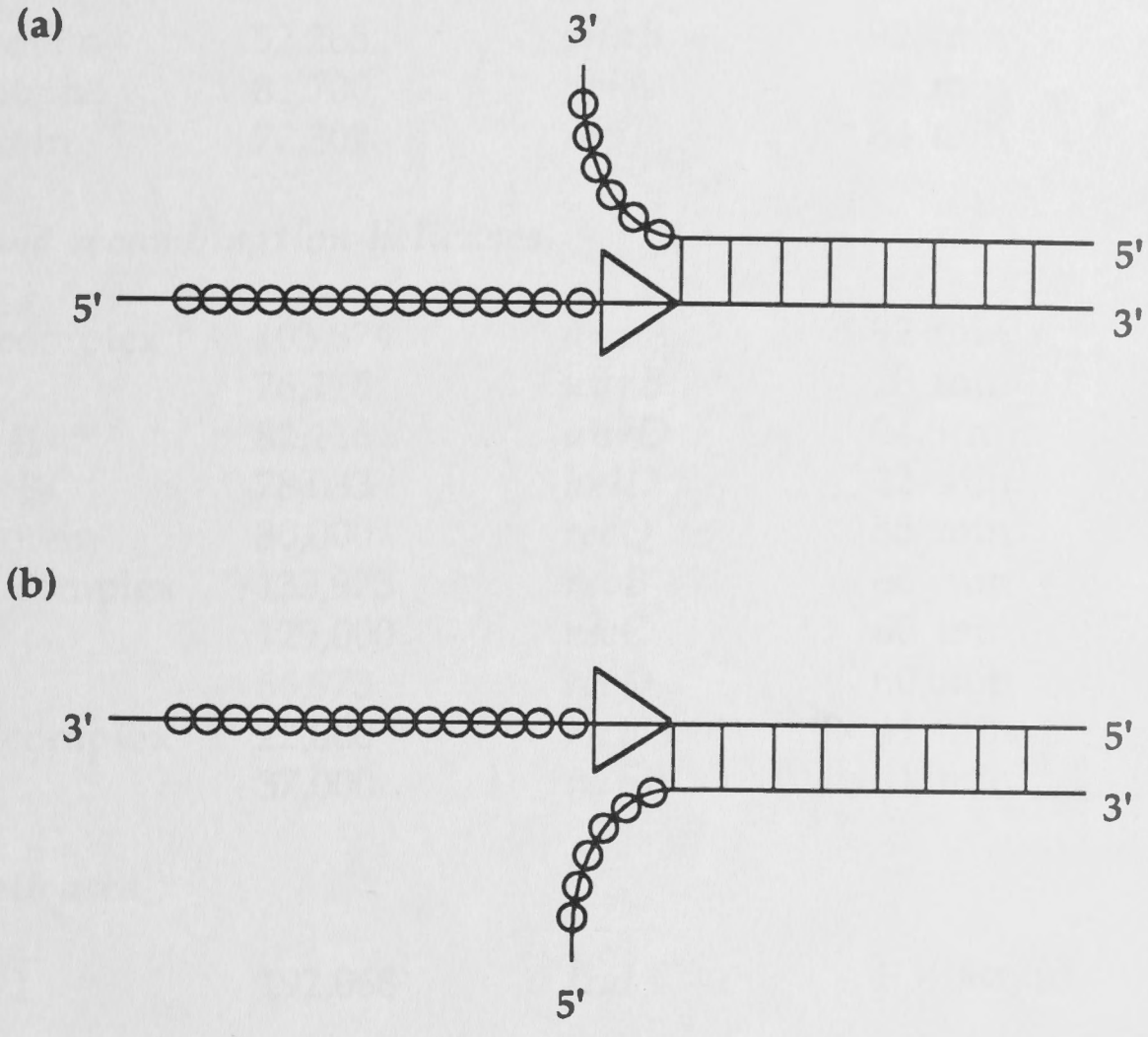

Figure 1.1

A schematic drawing representing the progressive unwinding of duplex DNA by helicases (triangles) with subsequent binding of the ssDNA by a single-stranded binding proteins (SSB, circles). The helicase with a 5' to 3' polarity is presented in Figure 1.1a; a 3' to 5' helicase is in Figure 1.1b (*e.g.* see Lohman, 1992; Matson *et al.*, 1994).

Helicase	Molecular mass	Gene	Map position	Polarity
Replicative helicases				
DnaB protein	52,265	*dnaB*	92 min	5' to 3'
PriA protein	81,700	*priA*	88 min	3' to 5'
Rep protein	72,802	*rep*	84 min	3' to 5'
Repair and recombination helicases				
UvrAB complex	103,874	*uvrA*	92 min	5' to 3'
	76,118	*uvrB*	18 min	
Helicase II	82,116	*uvrD*	84.5 min	3' to 5'
Helicase IV	78,033	*helD*	22 min	3' to 5'
RecQ protein	80,000	*recQ*	85 min	3' to 5'
RecBCD complex	133,973	*recB*	60 min	*
	129,000	*recC*	60 min	
	66,973	*recD*	60 min	
RuvAB complex	22,000	*ruvA*	41 min	5' to 3'
	37,000	*ruvB*	41 min	
Other helicases				
Helicase I	192,068	*traI*	F plasmid	5' to 3'

*The RecBCD helicase has a strong preference for unwinding blunt-ended duplex DNA substrates and does not appear to exhibit a polarity as defined for the other helicases.

Table 1.1

DNA helicases from *E. coli* (Matson *et al.*, 1994).

duplex at replication forks in chromosomal DNA synthesis (LeBowitz and McMacken, 1986) as has been confirmed both in biochemical and genetic studies (Wechsler and Gross, 1971; Zyskind and Smith, 1977; Baker and Wickner, 1992). To illuminate the key role of DnaB helicase in the replication of bacterial chromosomal, phage and plasmid DNA (Lehman and Kornberg, 1992), a short overview of *E. coli* DNA replication with respect mainly to DnaB protein follows.

1.2 Replication of the *E. coli* Chromosome

Biochemical and genetic analyses have revealed that replication of the *E. coli* chromosome - 4.7×10^6 base pairs (bp) of double-stranded (ds) circular DNA - requires action of at least 30 separate gene products (Marians, 1992). Although detailed information on exact functions of all individual replication proteins is not complete, their basic activities in DNA replication are known (for reviews, see Baker and Wickner, 1992; Lehman and Kornberg, 1992; Marians, 1992).

Replication of the *E. coli* genome is a bidirectional semiconservative process, in which each strand of the parental DNA duplex is maintained in a new duplex of DNA after serving as a template for complementary strand synthesis. Functionally, replication can be divided into three stages: initiation, elongation and termination.

1.2.1 *Initiation at* oriC

Initiation is the process by which the enzymes that synthesize DNA at the replication fork are assembled on the template at a specific sequence of DNA termed the origin of replication (Figure 1.2). *oriC* , the origin of replication of the *E. coli* chromosome, is located at 84 min on the *E. coli* genetic map (Oka *et al.*, 1980). Its minimum length was determined to be 245 bp (Oka *et al.*, 1980). The region is highly conserved among enteric bacteria (Zyskind *et al.*, 1983) and contains several specific sequence elements, the most important of which are four 9-bp repeated sequences and an adjacent region formed of three AT-rich 13-mers (Bramhill and Kornberg, 1988b). During the initiation process the *oriC* sequence is recognized by the *E. coli* initiator protein DnaA, 10 - 20 monomers of which are cooperatively bound to the 9-mers (DnaA boxes; Fuller *et al.*, 1984; Fayet and Prère, 1987). In the presence of ATP and assisted by HU protein (Dixon and Kornberg, 1984), DnaA induces a localized distortion of the duplex DNA generating thus a single-stranded bubble in the AT-rich region (Bramhill and Kornberg, 1988a; Woelker and Messer, 1993). After the DNA sequence of the origin is denatured, replication forks are formed and proceed bidirectionally to the terminus region. DnaB protein is transferred to the ssDNA with the assistance of DnaA and DnaC proteins (Funnell *et al.*, 1987; Sekimizu *et al.*, 1988; Marszalek and Kaguni, 1994). Preceeding formation of

a DnaB.DnaC complex in the presence of ATP is required (Wickner and Hurwitz, 1975; Kobori and Kornberg, 1982a; Wahle *et al.*, 1989a,b). Marszalek and Kaguni (1994) confirmed a hypothesis (Wu *et al.*, 1992a) that a direct interaction occurs between DnaA protein bound to DNA and DnaB in the

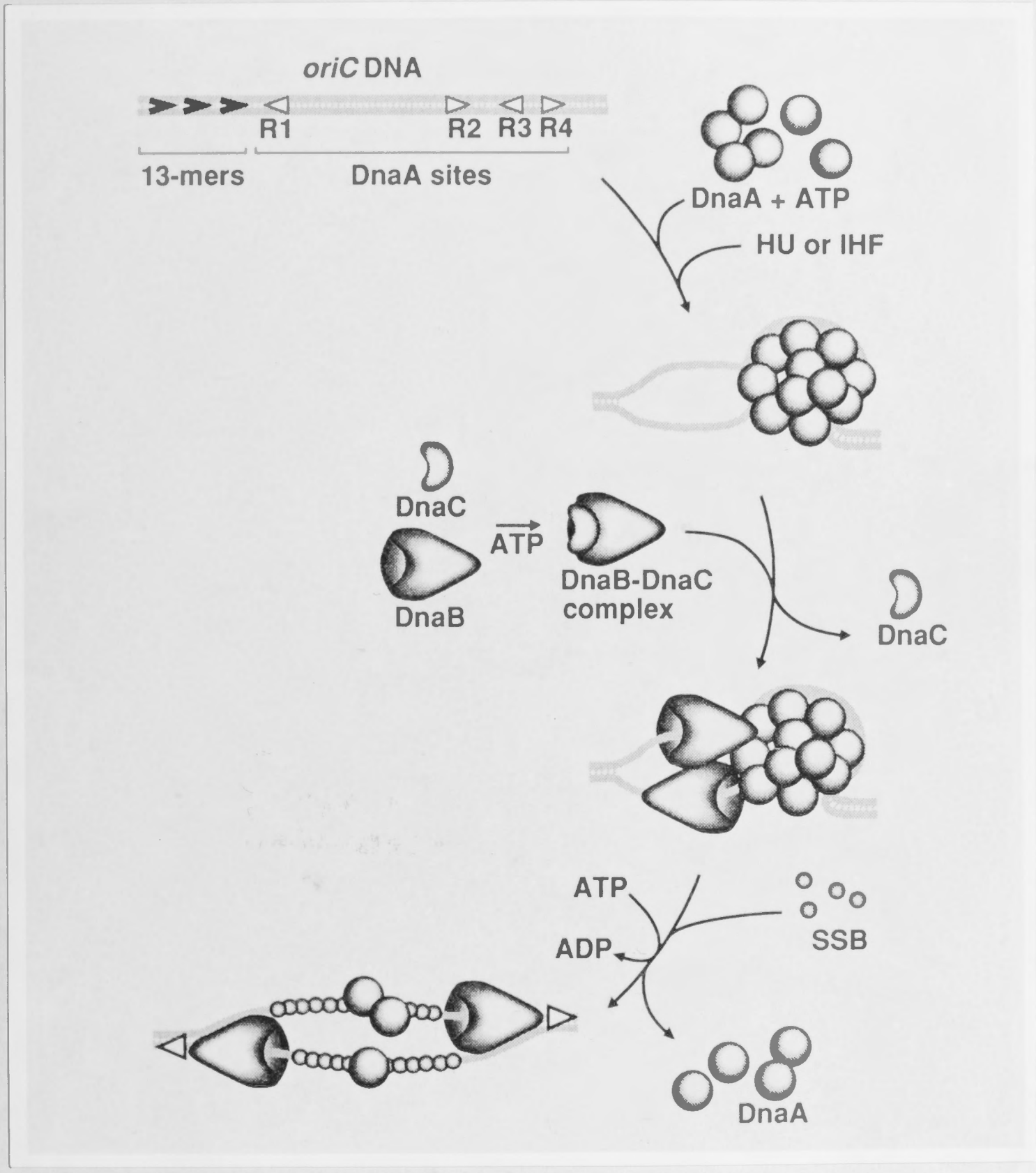

Figure 1.2

Model of the initiation of replication at *oriC*. The diagram is not meant to suggest the stoichiometry of the proteins in the postulated complexes or the molecular structure of the individual proteins (from Baker and Wickner, 1992). For details, see Section 1.2.1.

DnaB.DnaC complex to permit binding of DnaB protein and its subsequent action as a helicase. These results are in contrast with hypotheses that an interaction between DnaA and DnaC is involved in loading of DnaB protein onto a DNA template (Funnell *et al.*, 1987; Wahle *et al.*, 1989a; Masai *et al.*, 1990b; Hwang and Kornberg, 1992).

1.2.2. *Elongation*

During initiation of replication, DnaB was loaded onto the DNA template. In the following elongation stage, DnaB helicase expresses its multifunctional activity and establishes, either directly or indirectly, the rest of the replication proteins at the fork (Baker and Wickner, 1992).

The DnaB protein - the major replicative DNA helicase of *E. coli* - unwinds the parental DNA duplex in the 5' to 3' direction with respect to the single strand on which it is bound (Baker *et al.*, 1986, 1987; Figure 1.1a) and generates ssDNA in its path. Rates of the duplex melting by DnaB have been estimated to be ~730 bp/s at 30°C (Mok and Marians, 1987; Wu *et al.*, 1992a). ATP is required for the DnaB helicase activity (Arai *et al.*, 1981a) in *E. coli* cells. DnaB also activates synthesis of short RNA primers probably by generating a special secondary structure in the DNA template that can be used by DnaG primase (Arai and Kornberg, 1981a). As was demonstrated recently by functional analysis of two domains of *E. coli* primase (Tougu *et al.*, 1994), a direct interaction between DnaB and primase is also required for primer synthesis at the replication fork (Marians, 1992; Wu *et al.*, 1992b; Tougu *et al.*, 1994). RNA primers are necessary for the activity of the DNA polymerase III holoenzyme - the major replicative DNA polymerase in *E. coli* (McHenry, 1988). DNA polymerase III holoenzyme cannot start polynucleotide synthesis *de novo* but can only extend chains that have the 3'OH terminus of a nucleotide paired to a template strand extended beyond it. The dimeric assymetric multisubunit complex of the DNA polymerase III holoenzyme copies the ssDNA templates by elongating primers in the 5′ to 3′ direction. Okazaki fragments (Wu *et al.*, 1992a; Zechner *et al.*, 1992a, b) are synthesized on the lagging strand while a single stretch of DNA (leading strand) is synthesized on the other template strand. Okazaki fragments are 1000 - 2000 bp long and are joined after excision of the initiator RNA to form a continuous strand of DNA.

Other proteins involved in elongation of DNA include single-strand binding protein (SSB), PriA and PriB proteins, and DNA gyrase. DNA polymerase I and DNA ligase are required for primer removal and ligation of Okazaki fragments.

Small, heat-stable SSB proteins stabilize ssDNA by binding tightly and cooperatively to it (Chase and Williams, 1986) and melt most regions of secondary structure in ssDNA to ensure processivity of DNA polymerase III holoenzyme. DNA gyrase - an ATP-dependent type II topoisomerase - introduces negative supercoils in advance of the replication fork to facilitate unwinding by the helicases. DNA polymerase I is responsible for excising of RNA primers and their replacement with a polydeoxyribonucleotide strand. Short DNA segments of the lagging strand are converted to a continuous strand by DNA ligase (Funnell *et al.*, 1986).

Some or all of these enzymes, together with DnaB helicase, primase, DNA polymerase III holoenzyme and some other additional components, presumably form a nucleoprotein complex at a replication fork called the replisome (Kornberg and Baker, 1991; Lehman and Kornberg, 1992). Operation of the replisome at the replication fork is expected to effectively coordinate replication of both the continuously- and discontinuously-synthesized strands (Fig. 1.3).

1.2.3 *Termination*

Progress of replication forks is blocked within a large (350 kb) terminus region (De Massy *et al.*, 1987; Hill *et al.*, 1987) diametrically opposed from *oriC* on the chromosome. The region is flanked on either side by polar terminator (*ter*) sites at its left and right hand limits (Kuempel *et al.*, 1989). Blocking activity is dependent on the presence of the *ter*-binding protein (TBP - the *tus* gene product; Khatri *et al.*, 1989), which specifically binds *ter* sites with very high affinity (Hill *et al.*, 1988; Pelletier *et al.*, 1988; Kobayashi *et al.*, 1989; Hidaka *et al.*, 1991; Baker and Wickner, 1992; Hiasa and Marians, 1992).

Replication forks from either direction are not prevented from entering the terminus region, but they are prohibited from exiting when

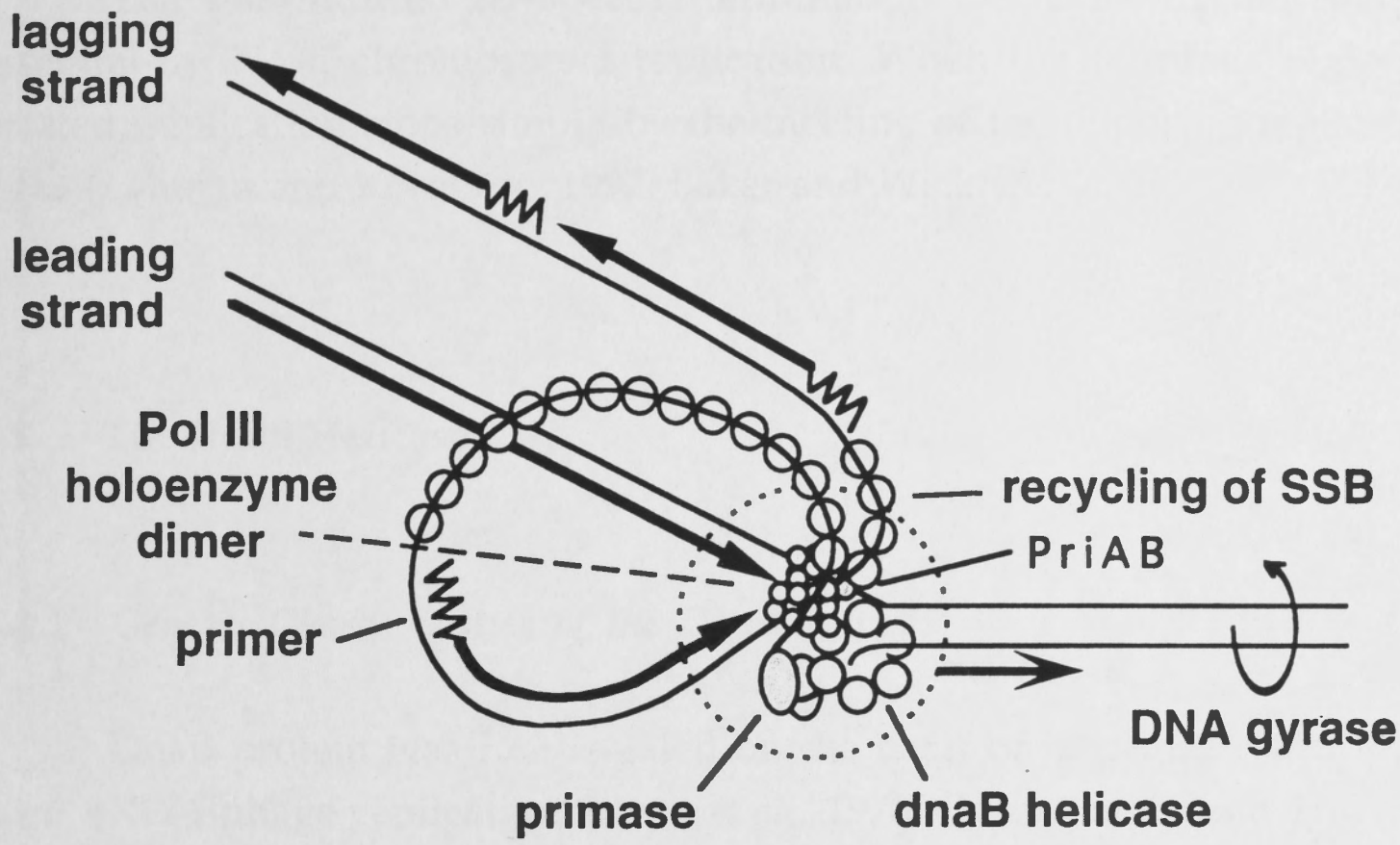

Figure 1.3

Hypothetical structure of the *E. coli* replisome - a nucleoprotein complex responsible for concerted leading- and lagging-strand DNA synthesis at a replication fork during chromosomal DNA synthesis (Kornberg and Baker, 1991). The composition of the replisome is not entirely clear. It probably contains at least DNA polymerase III holoenzyme, the primosome (containing at least DnaB and PriA helicases and the PriB protein), SSB, DNA gyrase, DNA ligase, and DNA polymerase I (see Section 1.2.2).

they progress across the terminus and reach the other site (De Massy *et al.*, 1987; Hill *et al.*, 1987). Experimental results indicate that replication fork arrest is simply a matter of inhibition of the replication fork helicase (Lee *et al.*, 1989; Khatri *et al.*, 1989).

The TBP-induced *ter*-specific termination mechanism is not strictly essential in *E. coli* chromosomal replication. When the terminus region is deleted, replication stops simply by the meeting of the opposing replication forks (Lehman and Kornberg, 1992; Baker and Wickner, 1992).

1.3 The DnaB Helicase

1.3.1 *General Characteristics of the DnaB Protein*

DnaB protein was first isolated on the basis of its requirement for *in vitro* ϕX174 phage replication (Ueda *et al.*, 1978; Reha-Krantz and Hurwitz, 1978a). The native protein is a hexamer of identical subunits (Reha-Krantz and Hurwitz, 1978a; Arai *et al.*, 1981c) with a monomeric weight of 52,265 (Nakayama *et al.*, 1984a). The sequence of the *dnaB* gene encoding the DnaB protein (Wickner and Hurwitz, 1975) was reported by Nakayama *et al.* (1984a). The gene is located near minute 92 on the linkage map (Bachmann, 1990) between the *qor* and *alr* genes (Lilley *et al.*, 1993). The *dnaB* and *alr* genes are transcribed in the same direction (Lilley *et al.*, 1993).

Isolation of *dnaB* thermo-sensitive (*ts*) mutants, that had both quick-stop (defective in chain elongation) and slow-stop (defective in initiation of replication) phenotypes, helped to identify functions of the DnaB protein in DNA replication (Baker and Wickner, 1992; Lehman and Kornberg, 1992).

As with other DNA helicases, DnaB protein catalyses two interrelated reactions: the DNA-dependent hydrolysis of nucleoside 5'-triphosphates (NTPs) (Sekimizu *et al.*, 1988; Kobori and Kornberg, 1982b; Wickner and Hurwitz, 1975; Wahle *et al.*, 1989a,b) and the unwinding of duplex DNA (LeBowitz and McMacken, 1986). Among NTPs, ATP is preferred as a substrate for ssDNA-dependent NTP-hydrolysis (Arai and Kornberg, 1981a). A K_m value for the DNA-dependent ATPase activity of DnaB protein in the

presence of ϕX174 ssDNA has been determined to be about 100 μM. However, high levels of rNTPs (>2 mM) are required for maximal helicase activity (Reha-Krantz and Hurwitz, 1978b; Arai and Kornberg, 1981a). No helicase activity has been detected in the absence of Mg^{2+} (LeBowitz and McMacken, 1986).

The unwinding reaction catalysed by the DnaB protein was demonstrated using a partial duplex DNA substrate with a 3'-terminal extension of ssDNA on the DNA fragment to be displaced (Figure 1.4), suggesting a preferred interaction with a DNA substrate resembling the replication fork (Lee and Marians, 1989; Matson *et al.*, 1994)). The minimum length of this ss tail is not known precisely, but the optimum length was determined to be ~90 nucleotides (LeBowitz and McMacken, 1986; Lohman, 1992).

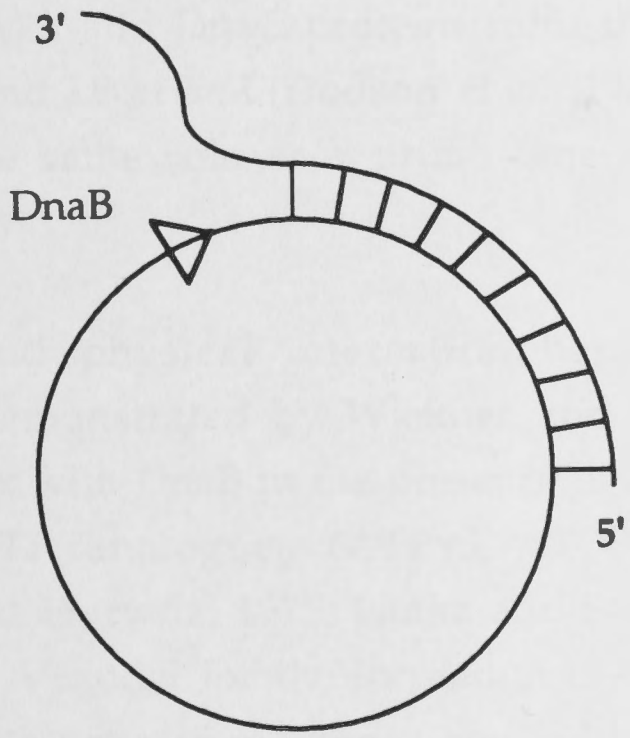

Figure 1.4

A preformed replication fork-like partial duplex DNA substrate, which was used to demonstrate the unwinding reaction promoted by DnaB protein (Matson *et al.*, 1994).

Unidirectional unwinding of the double-stranded (ds) DNA proceeds in the 5' to 3' direction with respect to the strand to which the DnaB helicase is bound (Figure 1.4; LeBowitz and McMacken, 1986). In replication of the *E. coli* chromosome, this polarity places it on the lagging strand template, ahead of the leading strand polymerase (Baker and Wickner, 1992).

Association of DnaB with DNA is inhibited by SSB due to competition for the ssDNA template (McMacken *et al.*, 1977; Arai *et al.*, 1981a; Arai and Kornberg, 1979; LeBowitz and McMacken, 1984; LeBowitz *et al.*, 1985). Nevertheless, SSB stimulates the unwinding reaction, providing DnaB is permitted to bind to the helicase substrate prior to the addition of SSB (LeBowitz and McMacken, 1986). This stimulation is probably due to SSB preserving the separation of the melted strands (LeBowitz and McMacken, 1986).

The affinity of DnaB for DNA is relatively low (LeBowitz and McMacken, 1986). The cellular abundance of the DnaB protein is very low too; there are estimated to be only 15 - 20 molecules per cell (Reha-Krantz and Hurwitz, 1978a; Ueda *et al.*, 1978). Requirement of a large excess of the protein for replication of DNA is overcome by systems of origin-initiator proteins that efficiently load DnaB onto the DNA template (Lehman and Kornberg, 1992). DnaA and DnaC proteins fulfil this role at *oriC* (Baker *et al.*, 1986, 1987), λO and λP at *oriλ* (Dodson *et al.*, 1986), and preprimosomal proteins perform the same role at a primosome assembly site (*pas*) (see Section 1.3.3.1).

Functional and physical interaction between DnaB and DnaC proteins was first demonstrated by Wickner and Hurwitz (1975). DnaC forms a tight complex with DnaB in the presence of Mg^{2+} and ATP, dATP or nonhydrolysable ATP analogues (ATPγS, ATPPNP) that can be easily isolated (Wickner and Hurwitz, 1975; Lanka and Schuster, 1983; Kobori and Kornberg, 1982a,b). A model for the formation of the DnaB.DnaC complex was presented and its properties were described by Kobori and Kornberg (1982b) and Wahle *et al.* (1989a). According to the proposed mechanism (Wahle *et al.*, 1989a, Scheme 1.1), six DnaC monomers (each of size 27.9 kDa) interact with a DnaB hexamer to form a complex of the $(DnaB)_6.(DnaC)_6$ composition, which is stabilised by the binding of 6 molecules of ATP, dATP or a nonhydrolysable ATP analog to DnaC (Wickner and Hurwitz, 1975; Kobori and Kornberg, 1982b; Biswas and Biswas, 1987). Binding of the DnaC protein to the DnaB helicase facilitates the interaction of DnaB with ssDNA, but, paradoxically, inhibits all activities of DnaB that are required for DNA replication. Only after ATP- and DNA-dependent release of the DnaC is the DnaB allowed to function (Wahle *et al.*, 1989a). The nonhydrolyzable ATP analog ATPγS supports formation of the DnaB.DnaC complex, but the complex does not direct DnaB to its targeted actions (Wahle *et al.*1989b). As

was demonstrated *in vitro* (Allen and Kornberg, 1991), the ratio of DnaB and DnaC proteins is critical for achieving optimal replication activity; an excess of DnaC inhibits DNA replication.

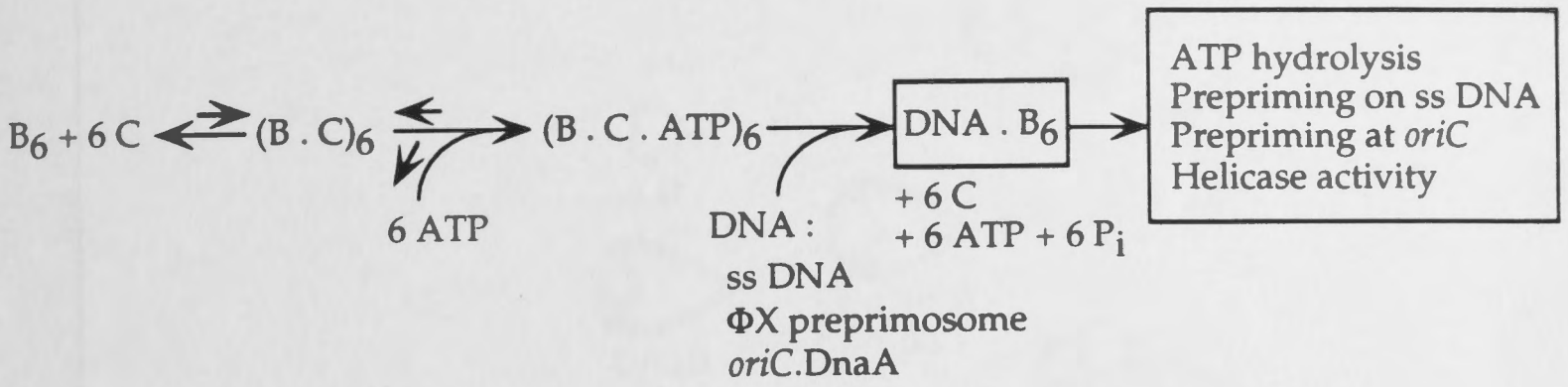

Scheme 1.1

Scheme for interaction and function of the DnaB and DnaC proteins. From Wahle *et al.*, 1989a.

An analogous reaction to the one at the *E. coli* chromosomal replication origin (*oriC*) has been observed in the replication of bacteriophage λ (Alfano and McMacken, 1989a; Dodson *et al.*, 1989; Liberek *et al.*, 1990; LeBowitz *et al.*, 1985; Figure 1.5). DNA replication initiated from *oriλ* requires the products of the phage *O* and *P* genes and many host-encoded proteins. λP protein (λ-specific analog of *E. coli* DnaC) forms a complex with DnaB protein and delivers it to the complex of λO (*E. coli* DnaA functional analog) with *oriλ* (Klein *et al.*, 1980). In the isolable DnaB.λP complex, there appears to be only three λP protomers bound to the DnaB hexamer (Klein *et al.*, 1980; Mallory *et al.*, 1990). Similarly to the DnaB.DnaC complex, λP completely inhibits the ATPase activity of the DnaB protein. Unlike DnaC, λP does not bind ATP, but enhances the binding of ATP to DnaB approximately 6-fold (Biswas and Biswas, 1987). λP is also not released spontaneously like DnaC. The DnaB protein must be separated from λP by several *E. coli* heat-shock proteins (the molecular chaperones DnaJ, DnaK and GrpE). Only then it is free to catalyze DNA unwinding (Alfano and McMacken, 1989b; Dodson *et al.*, 1986, 1989). Activation of the DnaB helicase by the preprimosomal proteins at a primosome assembly site is described in Section 1.3.3.1.

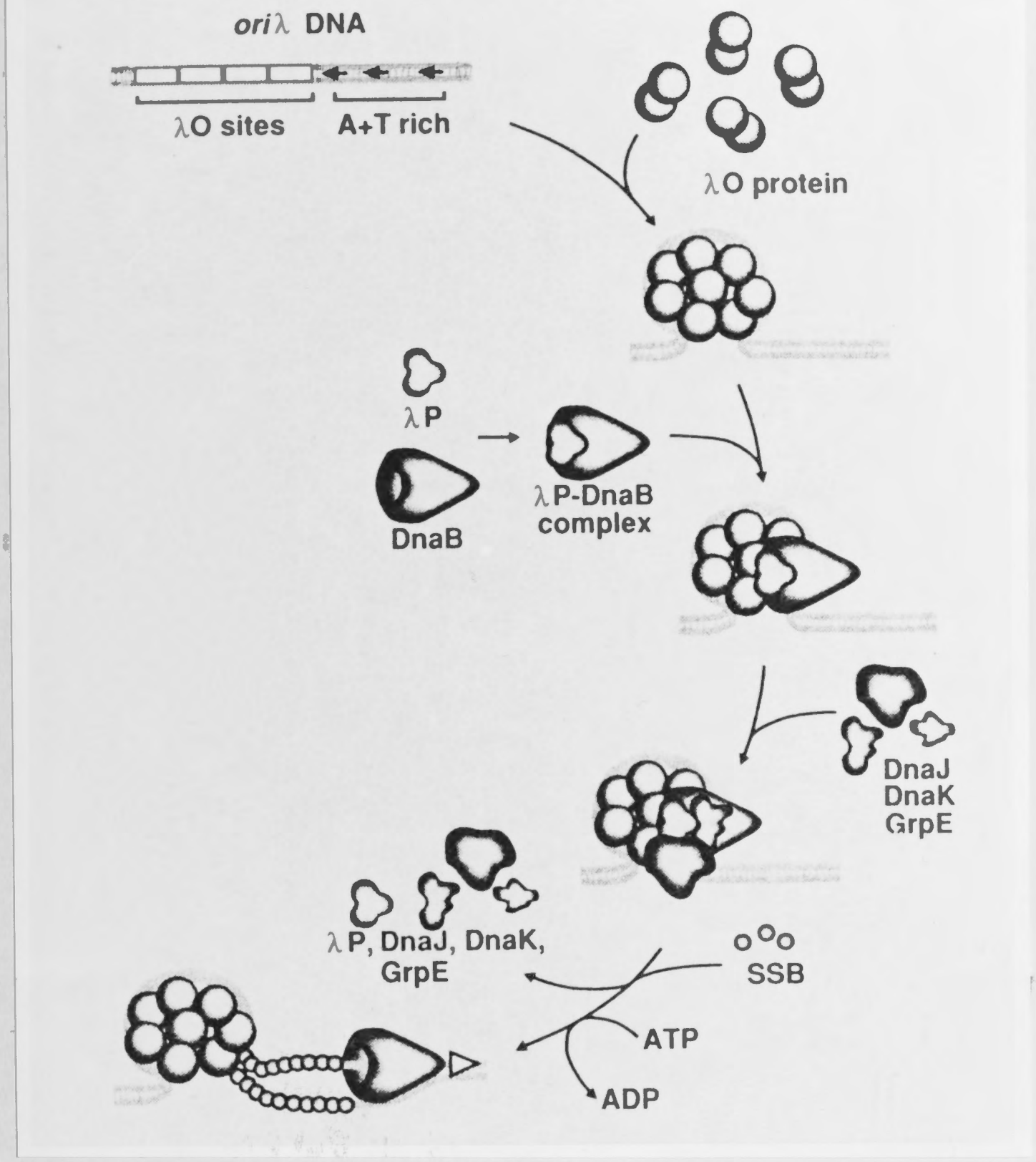

Figure 1.5

Model of the initiation of DNA replication at oriλ (from Baker and Wickner, 1992; for details see Section 1.3).

Evidence that DnaB is the principal helicase for *E. coli* chromosomal replication was obtained in genetic studies (Wechsler and Gross, 1971; Baker and Wickner, 1992) and also in biochemical assays. In purified *in vitro* systems, the DnaB protein has been shown to be the only helicase required for replication of plasmids that depend on *oriC* (Baker *et al.*, 1986, 1987) or *oriλ* (Alfano and McMacken, 1989a; Mallory *et al.*, 1990). In a concerted action of DnaB helicase and DNA polymerase III holoenzyme on a nicked duplex circle DNA with a protruding 5' tail - rolling circle replication - DnaB melted the dsDNA at the rapid rate and with the high processivity expected

of an enzyme participating in chromosomal replication (Lehman and Kornberg, 1992). The rate of the unwinding reaction was estimated at ~730 nt/s with processivity of 50,000 nts in a reconstituted replication reaction using pre-formed replication-fork-containing DNA substrates (Mok and Marians, 1987; Wu *et al.*, 1992a). In the absence of accompanying DNA synthesis, the unwinding from *oriC* proceeded in both directions at only 60 bp/s per fork at 37°C, producing "bubbles" coated with SSB (Baker *et al.*, 1986, 1987).

In addition to its ATPase and helicase activities, DnaB functions as a "mobile promoter" of primer synthesis (Baker and Wickner, 1992). Although DnaG primase alone can, under special circumstances, synthesize RNA primers, *e.g.*, on phage G4 ssDNA template (Bouché *et al.*, 1978; Masai *et al.*, 1990a), in most cases it needs to be activated by DnaB protein.

1.3.2. *Involvement of the DnaB Helicase in General Priming*

In a reaction termed general priming that occurs on ssDNA templates in the absence of SSB, DnaB and DnaG primase (in the presence of ATP) are the only enzymes required for synthesis of RNA primers (Arai and Kornberg, 1979). When binding of DnaB to the template limits the rate of priming, DnaC protein stimulates the process by forming a complex with DnaB and increasing thus the affinity of DnaB for the DNA about five fold (Wahle *et al.*, 1989b). λP protein is capable of forming a similar DnaB.λP complex, but does not stimulate general priming. The hydrolysis of ATP that fuels the helicase action of the DnaB protein is not essential for general priming.

The mechanism of activation of DnaG primase by DnaB protein is not clear. Functional interplay between both proteins is apparent - primase alone remains inert in the presence of ssDNA (Lehman and Kornberg, 1992). It is probable that DnaB generates secondary structures in ssDNA that serve as recognition sites for primase (Arai and Kornberg, 1981b). A direct physical interaction between DnaB protein and DnaG primase has been also demonstrated recently to be necessary to introduce primase to the replication fork (Tougu *et al.*, 1994). In contrast to the highly processive character of DnaB action on SSB-coated DNA (Mok and Marians, 1987; Wu

*et al.*1992a), DnaB helicase acts distributively in the process of general priming (Lehman and Kornberg, 1992).

1.3.3 *Role of the DnaB Helicase in Specific Priming*

Since general priming is inhibited if the DNA is completely coated with SSB (Arai and Kornberg, 1979; Arai and Kornberg, 1981a; LeBowitz and McMacken, 1986), specific mechanisms are needed for priming of *E. coli* chromosomal replication. Studies of the conversion of bacteriophage ϕX174 ssDNA to replicative form (RF) revealed one of the possible mechanisms (Wickner and Hurwitz, 1974; Schekman *et al.*, 1975; Weiner *et al.*, 1976; Ueda *et al.*, 1978; Low *et al.*, 1981; Shlomai *et al.*, 1981).

1.3.3.1 The ϕX174-Type Primosome

Priming on SSB-coated ϕX174 ssDNA depends on host-encoded proteins PriA, PriB, PriC, DnaB, DnaC, DnaT and the DnaG primase (Wickner and Hurwitz, 1974; Schekman *et al.*, 1975). In the absence of primase, these proteins assemble, in an ATP-dependent manner, a prepriming replication intermediate called the "ϕX174-type" primosome (Weiner *et al.*, 1976; Arai and Kornberg, 1981d; Figure 1.6).

Assembly of the preprimosome is initiated by PriA protein binding to a specific 70-nucleotide sequence in the SSB-coated single-stranded ϕX174 viral genome called the primosome assembly site (*pas;* Shlomai and Kornberg, 1980). The *pas* sequences isolated from several sources (Stuitje *et al.*, 1984; Hiasa *et al.*, 1989; Masai *et al.*, 1990b) are predicted to show considerable secondary structure, which is believed to be necessary for their recognition by the PriA protein. Binding of PriA to DNA activates its ssDNA-dependent (d)ATPase activity (Shlomai and Kornberg, 1980). PriA-catalysed hydrolysis of (d)ATP is, however, not required in primosome assembly. In solution, DnaB and DnaC proteins form the DnaB.DnaC complex composed of a DnaB hexamer and 6 DnaC monomers which is stabilized by binding 6 molecules of ATP to the DnaC protein (Kobori and Kornberg, 1982b; Wickner and Hurwitz, 1975; Wahle *et al.*, 1989a). The PriB and PriC proteins also act at early stages (Lehman and Kornberg, 1992; Allen and Kornberg, 1993), but a clear picture of their function cannot yet been

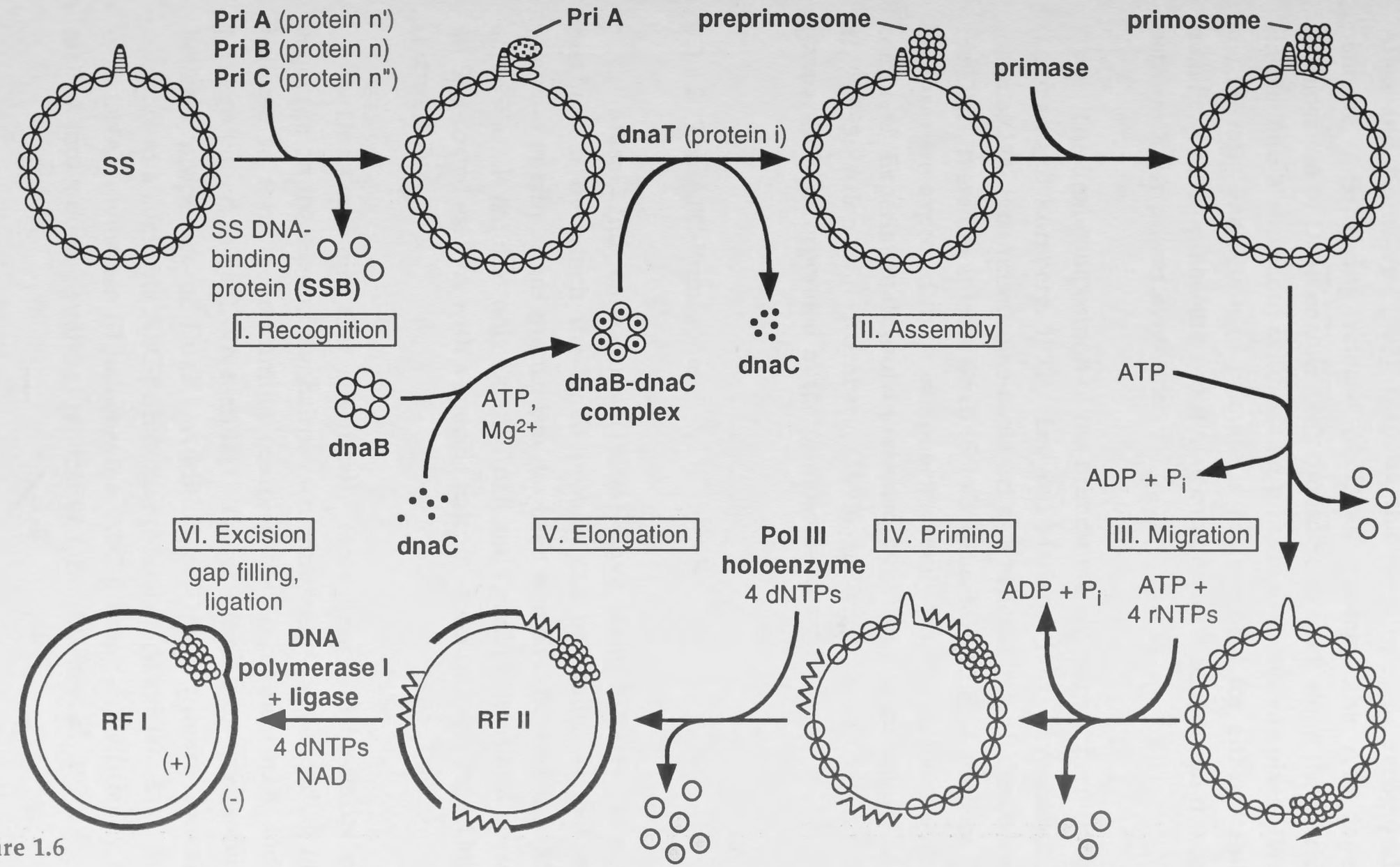

Figure 1.6

Conversion of ssDNA of phage ϕX174 to its replicative form. The mechanism of ϕX174 replication is described in Section 1.3.3.

drawn. DnaT cooperates in transfer of DnaB from the DnaB.DnaC complex in solution to the PriA.PriB.DNA structure (Lehman and Kornberg, 1992, Allen and Kornberg, 1993), forming the preprimosome recognizable by primase. Following release of DnaC protein, the ATP-dependent translocation of DnaB enables the primosome to track along the ϕX template (in the 5' to 3' direction) synthesizing primers at numerous places (Wahle *et al.*, 1989a). The action of primase is not essential for either stability or mobility of the primosome and it may continually associate and dissociate to perform RNA primer synthesis.

The final composition of the primosome has not yet been established (Lehman and Kornberg, 1992). Lee and Marians (1989) have demonstrated that a ϕX174- type primosome could act as a helicase in both directions along the DNA, therefore at least DnaB (5' to 3' helicase) and PriA proteins (3' to 5' helicase) are expected to be components stably present in the protein-DNA complex. Experimental results presented by Allen and colleagues (Allen *et al.*, 1993; Allen and Kornberg, 1993) indicated that PriB protein is permanently incorporated in the primosome as well.

1.3.3.2 The ABC-Primosome

Masai and colleagues (1990a) have demonstrated a different mechanism by which the DnaB protein can be loaded onto the DNA template *in vitro*. This mechanism has been termed ABC-priming (Masai *et al.*, 1990a). It requires only DnaA, DnaB and DnaC proteins and operates on an SSB-coated ssDNA with a specific hairpin structure carrying a DnaA box (Figure 1.7).

DnaA protein, that specifically recognizes and binds its cognate sequence on the stem of the hairpin structure, permits the loading of DnaB helicase to form a prepriming complex that contains DnaA and DnaB proteins bound to the DNA template. The prepriming complex exhibits the helicase properties of DnaB. Addition of DnaG primase converts the complex to a complete ABC-primosome (Masai *et al.*, 1990a). In conjunction with DNA polymerase III holoenzyme, ABC-priming can efficiently convert ssDNA into a double-stranded replicative form (Masai *et al.*, 1990a).

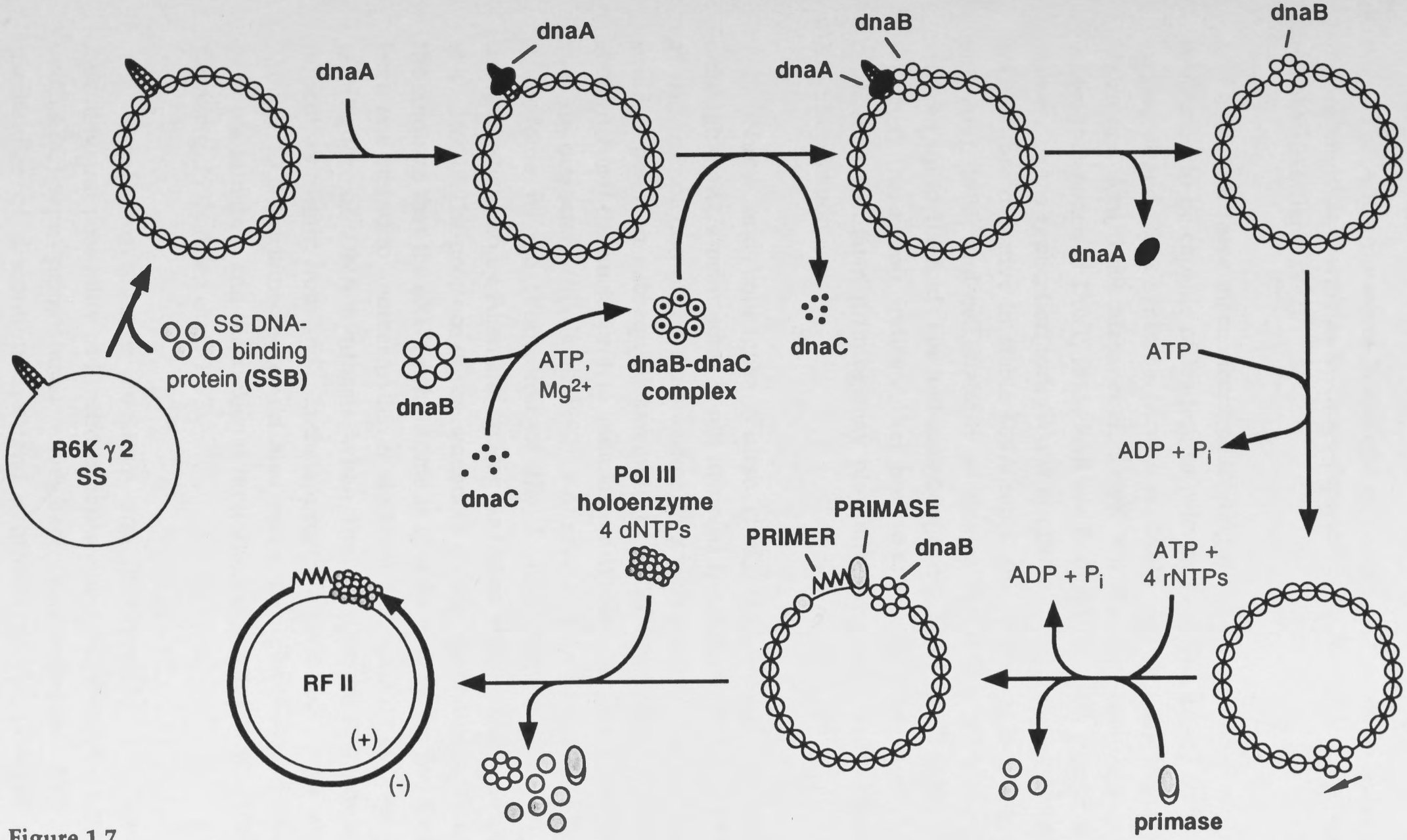

Figure 1.7

A scheme for the ABC-priming mechanism as was suggested by Masai *et al.* (1990a).

The ABC-primosome is thought to be identical or very similar to the primosome that assembles in DnaA-dependent replication at *oriC* (Masai *et al.*, 1990a; Marians, 1992).

Both of these mechanisms of loading of DnaB onto DNA have been confirmed to be capable of leading to priming of coordinated leading- and lagging-strand DNA synthesis (Arai *et al.*, 1981b; Arai and Kornberg, 1981d; Masai and Arai, 1989; Masai *et al.*, 1990b; Wu *et al.*, 1992a). ABC-priming shows that nonen of DnaT, PriA, PriB nor PriC are required to attract DnaG primase to the replication fork (Wu *et al.*, 1992a). On the other hand, *dnaT* mutants are defective in stable DNA replication (Masai *et al.*, 1986; Masai and Arai, 1988) and cell viability of strains carrying a *priA* deletion is reduced up to 100-fold (Lee and Kornberg, 1991; Nurse *et al.*, 1991). Taken together, these facts indicate that both ϕX174-primosome- and ABC-primosome-mediated priming may play important roles in *E. coli* cellular DNA replication.

Nurse and colleagues (Nurse *et al.*, 1991) have proposed that although a ϕX174-primosome is not involved in assembly of the primosome at *oriC*, completion of the chromosome in a significant fraction of the cells could depend on subsequent assembly of ϕX174-type primosomes. This could occur if the nucleoprotein complexes originally formed at *oriC* were to stall or dissociate (Marians, 1992). A special role of the ϕX174-type primosome in the replication of the *E. coli* chromosome has been demonstrated also by Allen and colleagues (Allen and Kornberg, 1993; Allen *et al.*, 1993). The presence of *pas* sequences on the chromosome, along with the findings that the ϕX174-primosome is able to transfer its DnaB helicase from one strand to another (Allen *et al.*, 1993), indicated its possible role in reinitiation of DNA synthesis when the replication fork encounters difficulties distant from *oriC*. In the appropriate conditions, a *pas* sequence and the ϕX174-primosome could also serve as a chromosomal origin to promote initiation and bidirectional replication of duplex DNA (Allen and Kornberg, 1993; Allen *et al.*, 1993).

Analogous roles of the DnaA and PriA proteins in primosomal assembly and possibility of functional replacement between ϕX174-type and *oriC*(ABC)-type primosomes have been demonstrated also in the mechanism of discontinuous-strand synthesis of the plasmid pBR322

(Zipurski and Marians, 1981; Minden and Marians, 1985). The DnaT protein is normally indispensable for ϕX174-type primosome assembly during pBR322 replication (Lehman and Kornberg, 1992). DnaA is not essential for replication of pBR322 that posesses a ColE1-type origin. However, in the presence of excess DnaA protein, DnaT becomes a nonessential component. This indicates that DnaA can bind the DnaA box near the *pas* sequence in pBR322 and function in assembly of a primosome (Seufert and Messer, 1987). DnaB protein loaded onto the template by either pathway is capable of extensive helicase activity as well as activation of DnaG primase (Lehman and Kornberg, 1992).

1.4 Analogues of the DnaB Helicase

Proteins that are considered members of the DnaB protein family substitute for DnaB in host chromosome replication, or they show significant primary amino-acid sequence similarity to DnaB and share some distinctive aspect of DnaB function (Wong *et al.*, 1988). DnaB-like proteins that have been identified so far include the *Salmonella typhimurium* DnaB protein (Maurer *et al.*, 1984a,b; Maurer and Wong, 1988; Wong *et al.*, 1988), Ban protein of coliphage P1 (D'Ari *et al.*, 1975; Lanka *et al.*, 1978b; Touati-Schwartz, 1979; Sclafani and Wechsler, 1981; Heisig *et al.*, 1987), the gene *40* product of *Bacillus subtilis* bacteriophage SPP1 (Pedré *et al.*, 1994), DnaB analogues encoded by conjugative R plasmids (Wang and Iyer, 1978), the helicase-primase of coliphage T7 (Kolodner and Richardson, 1977), the gene *12* product of *Salmonella typhimurium* phage P22 (Wickner, 1984), and the DnaB-like protein of *Chlamydia trachomatis* plasmids (Sriprakash and MacAvoy, 1988; Stamford, 1991).

The amino-acid sequences of *S. typhimurium* and *E. coli* DnaB helicases are highly conserved (with >93% identity; Wong *et al.*, 1988). Functional interchangeability of DnaB and many other replication proteins between *S. typhimurium* and *E. coli* was demonstrated by Maurer and colleagues (Maurer *et al.*, 1984b). Complementation assays revealed that every tested *E. coli* replication mutant was rescued by introducing a gene from *Salmonella*, indicating thus that near-identical biochemical pathways of replication take place in the two organisms (Maurer *et al.*, 1984b).

P1 Ban (*B-an*alog) protein has also been shown to functionally substitute for the *E. coli dnaB* product (D'Ari, 1975; Ogawa, 1975; Lanka *et al.*, 1978a,b; Touati-Schwartz, 1979; Heisig *et al.*, 1987), supressing the *ts* phenotype of DnaB mutants for chromosomal replication and restoring λ growth in *groP* (*dnaB*) mutants (Günther *et al.*, 1981). P1 Ban can interact with DnaB monomers to form functional hybrid DnaB-like multimers, the average composition of which depends on the relative quantities of Ban and DnaB in the cell (Touati-Schwartz, 1979). Activity of Ban protein is dependent on DnaC (Lehman and Kornberg, 1992).

Similarities of the other DnaB-like proteins with *E. coli* DnaB are not so extensive. *S. typhimurium* DnaB and P1 Ban protein together with the λP protein (DnaC analog; see Section 1.3.1) are the most probable candidates that could help to illuminate the principles and geometry of DnaB interactions with other proteins and DNA and indirectly solve structural problems on the DnaB helicase itself.

1.5 Preliminary Structure-Function Characteristics of the DnaB Helicase

The primary structure of the DnaB protein was determined by Nakayama and colleagues in 1984. The amino-acid sequence, deduced from the nucleotide sequence of the *dnaB* gene and consistent with the protein chemical data (Nakayama *et al.*, 1984a), has shown that the DnaB helicase is composed of 470 amino acid residues and has a calculated subunit molecular weight of 52,265 (see Appendix).

A model for secondary and tertiary structure was proposed (Nakayama *et al.*, 1984a,b) on the basis of prediction from the amino-acid sequence (Chou and Fasman, 1978) and from the results of partial tryptic hydrolysis under native conditions (Nakayama *et al.*, 1984b). According to this proposal, DnaB helicase is composed of at least two discrete structural domains joined through a hinge region, together with a hydrophilic ~14 amino-acid sequence at the NH_2-terminus that contains very little, if any, typical secondary structure (Nakayama *et al.*, 1984a,b; Figure 1.8).

The NH_2-terminal domain (residues 15-126) has a high degree of secondary structure with considerable content of α-helix. The region between residues 127 and 172 (the putative hinge region) was not detected as

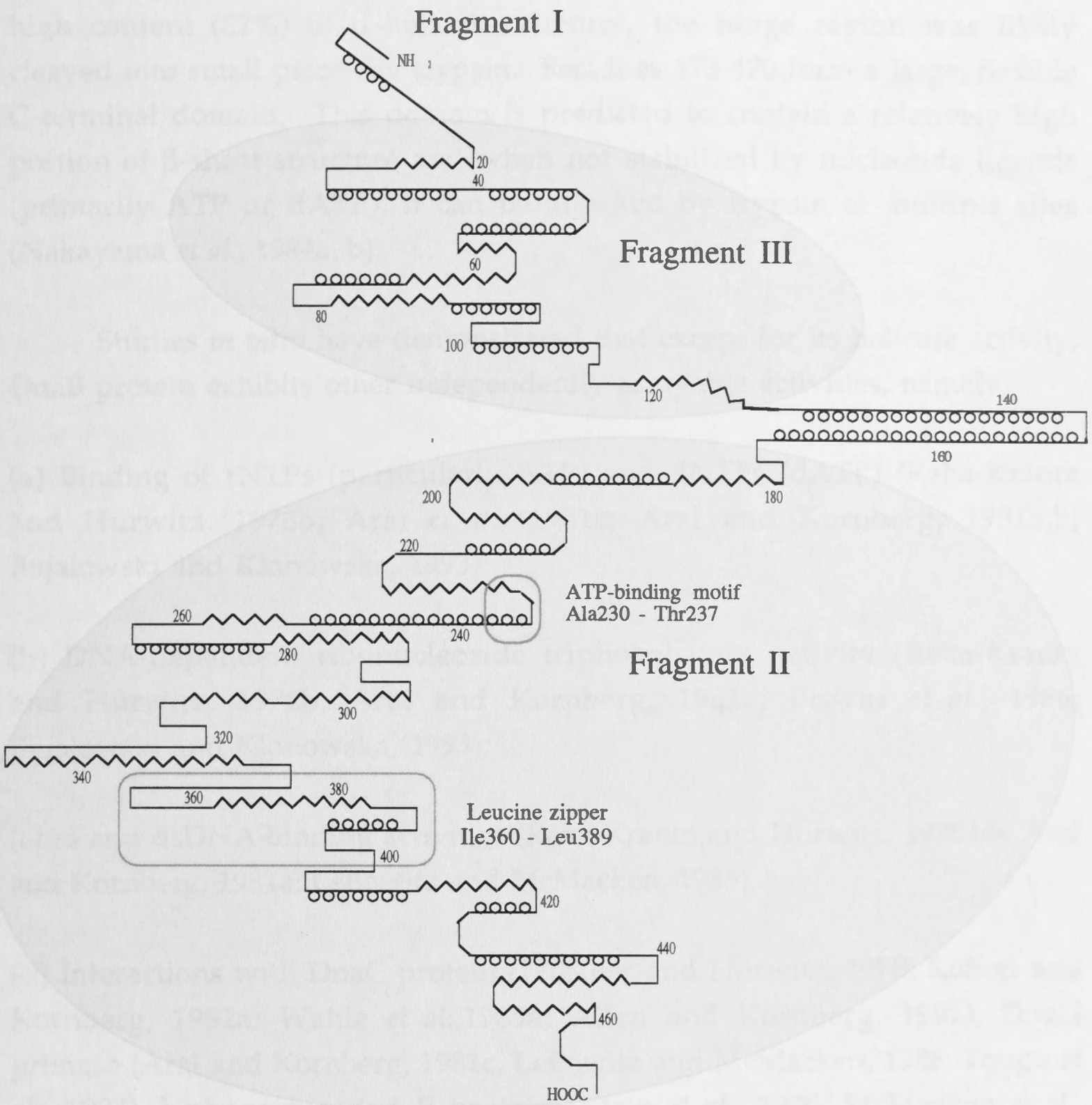

Figure 1.8

A model of secondary and tertiary structure of the DnaB protein as was proposed by Nakayama *et al.* (1984a). (ᔓ), (∧) and (←) denote α-helical, β-sheet and random coil residues, respectively. Fragment I corresponds to DnaB protein without 14 NH_2-amino-acid residues. The NH_2-terminal domain is equivalent to Fragment III (amino-acid residues 15 - 126); Fragment II (residues 173 - 470) represents the COOH-terminal domain of DnaB. Leucine zipper and the nucleotide-binding motifs are indicated (see Section 1.5).

a distinct peptide after trypsin cleavage. Despite being predicted to have a high content (82%) of α-helical structure, the hinge region was likely cleaved into small pieces by trypsin. Residues 173-470 form a large, flexible C-terminal domain. This domain is predicted to contain a relatively high portion of β-sheet structure and when not stabilized by nucleotide ligands (primarily ATP or dATP), it can be attacked by trypsin at multiple sites (Nakayama *et al.*, 1984a, b).

Studies *in vitro* have demonstrated that except for its helicase activity, DnaB protein exhibits other independently-assayable activities, namely:

(a) Binding of rNTPs (particularly ATP) and dNTPs (dATP) (Reha-Krantz and Hurwitz, 1978b; Arai *et al.*, 1981c; Arai and Kornberg, 1981a,b; Bujalowski and Klonowska, 1993);

(b) DNA-dependent ribonucleoside triphosphatase activity (Reha-Krantz and Hurwitz, 1978b; Arai and Kornberg, 1981a; Biswas *et al.*, 1986; Bujalowski and Klonowska, 1993);

(c) ss and dsDNA-binding activities (Reha-Krantz and Hurwitz, 1978a,b; Arai and Kornberg, 1981a; LeBowitz and McMacken, 1986);

(d) Interactions with DnaC protein (Wickner and Hurwitz, 1975; Kobori and Kornberg, 1982a; Wahle *et al.*,1989a; Allen and Kornberg, 1991), DnaG primase (Arai and Kornberg, 1981c, LeBowitz and McMacken, 1986; Tougu *et al.*, 1994), λ-phage-encoded P protein (Klein *et al.*, 1980; McMacken *et al.*, 1983; Biswas and Biswas, 1987; Alfano and McMacken, 1989a; Mallory *et al.*, 1990; Dodson *et al.*, 1989), P1 coliphage-encoded Ban protein (Lanka *et al.*, 1978b; Touati-Schwartz, 1979), and possibly other proteins involved in DNA replication (Marszalek and Kaguni, 1994);

(e) Interactions between DnaB monomers - oligomerization.

The products of limited digestion by trypsin were used for structure-function analysis (Nakayama *et al.*, 1984b) in efforts to localize particular catalytic sites on the DnaB monomer. The results have indicated roles of particular domains and regions of the protein.

All the DnaB catalytic activities that have been detected to date can be associated with the large *COOH-terminal domain* (residues 143 - 470). This domain forms oligomers (Nakayama *et al.*, 1984b; Biswas *et al.*, 1994) and retains nucleotide binding and DNA-dependent ATPase activities, and sites for ss and dsDNA binding. Analysis of the DnaB protein sequence for various structural motifs has indicated the presence of a motif that resembles the now-familiar "leucine zipper" [I.X6.L.X6.L.X6.L.X6.L.] between amino acid residues 360 and 389 (Turner and Tjian, 1989; O'Shea *et al.*, 1989a,b; Stamford, 1991; Biswas *et al.*, 1994; Scheme 1.2) that is generally responsible for dimerization of protein monomers (Turner and Tjian, 1989; O'Shea *et al.*, 1989b). Formation of dimers between fragments identical to the COOH-terminal domain in crosslinking studies performed by Biswas and colleagues (Biswas *et al.*, 1994) may be due to this sequence motif. A consensus basic region has been located between residues 323 and 331 (Biswas *et al.*, 1994). Basic regions frequently observed in eucaryotic sequence-specific DNA-binding proteins at the NH_2-terminus (preceeding the leucine zipper) are normally thought to be associated with binding of DNA. The functions of the "leucine zipper" and an adjacent basic region in DnaB require further investigation.

Basic Region

320 T E V *R S R A R R I A* R E H G G L I M I D Y L Q L M R V P A L S D N R

Putative Leucine Zipper

T L E *I A E I S R S L K A L A K E L N V P V V A L S Q L N R S L* E Q 390

Scheme 1.2

Amino-acid sequence of the "leucine zipper" and the proximal basic region in the COOH-terminal domain of the DnaB helicase. From Biswas *et al.* (1994)

Biswas *et al.* (1994) have proposed the existence of another site for protein-protein interactions further towards the NH_2-terminus of the COOH-terminal domain that probably effects formation of DnaB hexamers.

Based on the experimental results, they expect the COOH-terminal domains to form strong dimers and three of these dimers to interact weakly to form a hexamer.

Analysis of the primary sequence of the DnaB protein indicated also the presence of an ATP binding motif [G/S.X.X.X.X.G.K.T/S] between amino acid residues 230-237 (Biswas and Biswas, 1987; Scheme 1.3).

	230							237
DnaB	A	R	P	S	M	G	K	T
Consensus	**G/A**	**X**	**X**	**X**	**X**	**G**	**K**	**T/S**

Scheme 1.3

The ATP-binding motif in the COOH-terminal domain of the DnaB protein (Biswas and Biswas, 1987). Generally, nucleotide-binding sequences appear to be highly variable, however, the [G/A.X.X.X.X.G.K.T/S] sequence was reported to be the most conserved sequence (Walker *et al.*, 1982).

The rigid NH_2-terminal domain (~12 kDa) is thought to be monomeric and is expected to play an essential role in interactions with other proteins, namely DnaC and DnaG primase. The 14-residue NH_2-terminal part of the domain, which is highly susceptible to tryptic attack, probably stabilizes these interactions. Although no catalytic activity was detected by Nakayama *et al.* (1984b), the latest research has indicated that this domain may play an important role in the helicase activity of the DnaB protein and may have an influence on hexamer formation (Biswas *et al.*, 1994). Both of these activities have been demonstrated only indirectly (Biswas *et al.*, 1994). Although the COOH-terminal domain on its own has not displayed any measureable helicase activity nor could formation of discrete hexamers be detected, the separated NH_2-terminal domain has also been inactive as a helicase and has not formed oligomers either. It was only the entire DnaB protein or the DnaB fragment lacking only the 14 NH_2-terminal amino-acid residues that could express both activities.

Taken together, the two separate DnaB domains cannot display all of the DnaB activities. Even when examined together in a replication assay,

they do no longer support DNA replication. This indicates that mutual interactions between both domains and the conformation of the DnaB protein play important roles in completing the whole range of the DnaB activities.

The conformation of the DnaB protein itself as well as the configuration of DnaB monomers in the hexamer seem to be significantly influenced by binding of nucleoside-phosphate ligands (Arai and Kornberg, 1981a; Nakayama *et al.*, 1984a,b; Bujalowski and Klonowska, 1993, 1994). Various conformational changes have been demonstrated by:

(a) different effects of particular nucleotides on the affinity of DnaB with ssDNA. The presence of a γ-phosphate and the ribose is indispensable in inducing allosteric interaction between nucleotide and ssDNA binding sites. ATP and the nonhydrolyzable analog ATPγS increased the affinity of DnaB for ssDNA significantly; no such allosteric effect could be observed in the presence of ADP or dATP (Arai and Kornberg, 1981b);

(b) considerable alteration of the rate of trypsin digestion of the DnaB protein. Sensitivity to trypsin attack depends on the presence of the nucleotide as well as on its nature. The COOH-terminal domain was cleaved by trypsin at multiple sites in the absence of nucleotide ligands, but could be stabilized remarkably by nucleotide binding. The rate of DnaB digestion by trypsin was significantly decreased in the presence of ATPγS instead of ATP or ADP (Nakayama *et al.*, 1984b);

(c) thermodynamic studies of nucleotide-DnaB interactions. On the basis of thermodynamically rigorous fluorescence titrations, Bujalowski and Klonowska (1993, 1994) confirmed the nucleotide-DnaB hexamer stoichiometry that had been originally determined by Arai and Kornberg (1981b), and revealed that the process of binding of six nucleotides to the hexamer is biphasic and characterized by negative cooperativity between neighbouring nucleotide-binding sites. The negative cooperativity has been suggested to be a result of nucleotide-induced conformational changes in the protein.

In attempts to delineate protomer organization in the DnaB hexamer, two statistical thermodynamic models, namely, the hexagon and octahedron, have been analysed (Bujalowski and Klonowska, 1993). Both of

them can incorporate negative cooperativity among ligand-binding sites on the hexamer. However, the biphasic character of nucleotide binding to the DnaB hexamer can be described only for the hexagon model. From the thermodynamic point of view, the hexagon is the only possible model that can account for the configuration of DnaB subunits in the hexamer (Bujalowski and Klonowska, 1993).

At this stage, it is apparent that there is still much to be learned about the DnaB protein. Problems involve:

(a) exact understanding of the roles of the COOH- and NH_2-terminal domains;
(b) possible mutual interactions between the DnaB domains;
(c) function of the putative hinge region;
(d) principle and geometry of DnaB interaction with other proteins and nucleic acids;
(e) conformational changes in the DnaB monomer itself;
(f) transitions of the DnaB protomers within the hexamer during the action of the DnaB protein;
(g) conversion of the energy released in NTP hydrolysis into the directional motion of the DnaB helicase;
(h) high-resolution three-dimensional structure of the protein.

Considering the complex character of the replication system, the unique role of the DnaB helicase within its highly coordinated, efficient machinery, and the functional characteristics of the DnaB protein that are known, it seems to be obvious that we should focus now on the structural properties of the protein.

1.6 Aims of the project

Biochemical and genetic studies to date have provided preliminary structure-function characteristics of the DnaB helicase. Although most of the DnaB catalytic activities have been revealed already, there is a lack of knowledge of the DnaB structure (or indeed, the structure of any helicase).

The primary structure of the DnaB protein was deducted from the *dnaB* sequence. A model for secondary and tertiary structure has been predicted from the amino-acid sequence of the protein and from the results

of partial tryptic hydrolysis. The configuration of DnaB subunits in the hexamer has been proposed on the basis of thermodynamic studies. However, determination of the three-dimensional structure of DnaB at high resolution has not yet been successfull. The aim of the research project was therefore to study different approaches which would contribute to elucidation of this problem.

X-Ray crystallography and multidimensional NMR spectrometry are technologies that allow us to solve the three-dimensional structure of proteins at atomic levels. So far, there has not been reported any information about DnaB crystals suitable for X-ray diffraction analysis; our primary effort was naturally focused in this direction. Apart from *wt*DnaB, functional and deletion mutants of the *E. coli* DnaB helicase were considered as potentially useful candidates for this purpose. Another goal of the research project was therefore preparation of expression systems which would overproduce these mutants, as well as purification and crystallization of the mutant proteins.

Electron microscopy can provide us with information on the two-dimensional and three-dimensional structures of the DnaB oligomer at medium resolution. Electron-microscopic studies of the native DnaB protein and the DnaB mutants prepared and purified in our laboratory were carried out by Dr José Maria Carazo and Ms M. Carmen San Martin (Centro Nacional de Biotechnología, Madrid, Spain).

2 MATERIALS AND METHODS

2.1 Bacterial Strains and Plasmids

The genotypes of the *E. coli* strains used throughout this study are presented in Table 2.1. The strains prepared in order to overproduce the DnaB and DnaC proteins and the DnaB and DnaC mutants are in Table 2.2. The particular protein/proteins that can be overproduced, are indicated. The plasmid vectors presented in Figure 2.1 and their derivatives were used.

Strain	Genotype	Reference
AN1459	*K12supE44 thi-1 leuB6 thr-1 ilvC hsdR recA srlA*::Tn*10*	Elvin *et al.* (1986)
AN2666 (JM101*recA*)	*K12supE44 thi-1 Δ(lac-proAB) recA srlA*::Tn*10*	Yanisch-Perron *et al.* (1985)
TG1*recA*	*K12 Δ (lac-pro) supE thi hsdD5/F'traD36 proAB lacI*^{q} *lacZΔM15 recA srlA*::Tn*10*	Hermes *et al.*, (1989)

Table 2.1

Bacterial strains used in the experimental work.

Strain	Genotype	Antibiotic resistance	Protein/proteins overproduced by the strain	Reference
RSC535	AN1459, **pPS431**	Ap	DnaBΔN1-156	Stamford, 1991
RSC537	AN1459, **pPS433**	Ap	DnaBΔN1-177	Stamford, 1991
RSC569	AN1459, **pPS501**	Ap	DnaBΔC404-470	Stamford, 1991
RSC571	AN1459, **pPS503**	Ap	DnaBΔC162-470	Stamford, 1991
RSC680	AN1459, **pPS562**	Ap	DnaB, DnaC (*wt*)	Stamford, 1991
RSC832	AN1459, **pNA632**	Ap	DnaC, DnaBΔC404-470	Section 5
RSC859	AN1459, **pNA634**	Ap	DnaC, DnaBΔN1-156	Section 5
RSC860	AN1459, **pNA635**	Ap	DnaC, DnaBΔN1-177	Section 5
RSC861	AN1459, **pNA636**	Ap	DnaC, DnaBΔC162-470	Section 5
RSC933	AN1459, **pNA640***	Ap	DnaC, DnaBΔC166-470	Section 5
RSC934	AN1459, **pNA641**	Ap	DnaC, DnaB-9αα165/166	Section 5
RSC945	AN1459, **pNA645**	Ap	DnaC, DnaBΔC166-470, DnaBΔN1-165	Section 5
RSC951	AN1459, **pND712**	Ap	DnaB-R231C	Section 4
RSC956	AN1459, **pND713**	Ap	DnaBΔN1-165	Section 5
RSC972	TG1recA, **pPL717**	Ap	DnaB-R231C	Section 4
RSC976	AN1459, **pCN718**	Ap	DnaBΔN1-165	Section 5
RSC2032	AN1459, **pNA785**	Ap	DnaB-T165/166	Section 5
RSC2033	AN1459, **pNA786**	Ap	DnaB-F165/166	Section 5
RSC2034	AN1459, **pNA787**	Ap	DnaC, DnaBΔN1-165	Section 5
RSC2036	AN1459, **pNA788**	Ap	DnaB-I141T	Section 4
RSC2045	AN1459, **pNA785, pLysS**	Ap, Cm	DnaB-T165/166, T7 lysozyme	Section 5
RSC2046	AN1459, **pNA786**, pLysS	Ap, Cm	DnaB-F165/166, T7 lysozyme	Section 5

Strain	Genotype	Antibiotic resistance	Protein/proteins overproduced by the strain	Reference
RSC2047	AN1459, **pNA788, pLysS**	Ap, Cm	DnaB-I141T, T7 lysozyme	Section 4
RSC2060	AN1459, **pNA798**	Cm*	DnaBΔC162-470	Section 5
RSC2061	AN1459, **pNA798, pNA787**	Ap, Cm*	DnaC, DnaBΔC162-470, DnaBΔN1-165	Section 5

*Chloramphenicol at concentration 7 μg/ml was used to maintain pNA798 in the cells

Table 2.2

The strains that can overproduce *wt* and mutant DnaB and DnaC proteins.

2.2 Growth of Bacteria

Strains of *E. coli* were grown in LB medium (Luria and Burrous, 1957) supplemented with 25 μg/ml thymine (LBT) and, as required, with ampicillin (50 μg/ml) and/or chloramphenicol (30 μg/ml was used to maintain pLysS in host strains; 7 μg/ml was used in the case of pCE33 derivatives). Strains containing pCE30 and its derivatives were grown at 30°C, while others were grown at 37°C. For large-scale preparation of plasmid DNA, strains were grown in minimal 56 medium (Monod *et al.*, 1951) containing 1 mM magnesium sulfate and supplemented with caseine hydrolysate (20 μg/ml) and trace salts (Gibson *et al.*, 1977), 40 mM glucose, 1 μg/ml vitamin B1 and the appropriate antibiotic.

2.3 Chemicals, Reagents, Enzymes, and Instruments

All chemicals and reagents used in this study were of analytical grade and were obtained from commercial suppliers (Amersham, BDH Chemicals,

Figure 2.1

(a) Plasmid vector pCE30 (Elvin *et al.*, 1990) contains a segment of λ DNA inserted between the *Pst*I and *Bam*HI sites in the polylinker of pUC9 (Yanisch-Perron *et al.*, 1985). The λ segment contains the cI857^{ts} gene and the strong promoters P_R and P_L arranged in tandem to promote transcription in the same direction. Three unique sites (*Bam*HI, *Sma*I and *Eco*RI) are suitable for insertion of genes with their own RBSs.

(b) Vector pCE33 (Elvin *et al.*, 1990) contains the same λ segment as in pCE30 in the runaway-replication vector pMOB45 (Bittner and Vapnek, 1981). Derivatives of pCE33 direct overproduction of proteins at 42°C by virtue of both runaway replication and inducible transcription from the P_R-P_L promoter system.

(c) The phagemid vector pMA200U (Elvin *et al.*, 1990) has all the properties of pCE30, with the addition of the viral strand origin region of filamentous phage f1. pMA200U derivatives, transformed into an M13-sensitive strain, replicate in the presence of superinfecting M13KO7 (Mead *et al.*, 1986) to produce packaged ss plasmid DNA. If the gene is in right orientation for expression from P_R-P_L, the ssDNA contains the coding strand. The packaged ssDNA isolated from the culture supernatant can be used for DNA sequencing and for modification by oligonucleotide-directed mutagenesis. On transfection, mutant plasmids are then immediately available for high-level expression of the mutant protein.

(d) Vector pND706 (C.A. Love, P.E. Lilley and N.E. Dixon, manuscript in preparation) is a derivative of pPL452 (C.A. Love, P.E. Lilley and N.E. Dixon, manuscript in preparation). pPL452 is similar to pCE30, but is based on the pMTL-P series of vectors (Chambers *et al.*, 1988) rather than the pUC series. It thus contains the *par* region of pSC101, which contributes greater plasmid stability at high copy number in the absence of ampicillin selection, and has the cI857-P_R-P_L-polylinker region as in pCE30. In pND706, the translational initiation region of pPL452 was replaced by the ϕ10 translational initiation region of phage T7, essentially as it appears in the Studier T7 expression system (pET vectors; Studier *et al.*, 1990).

(a)

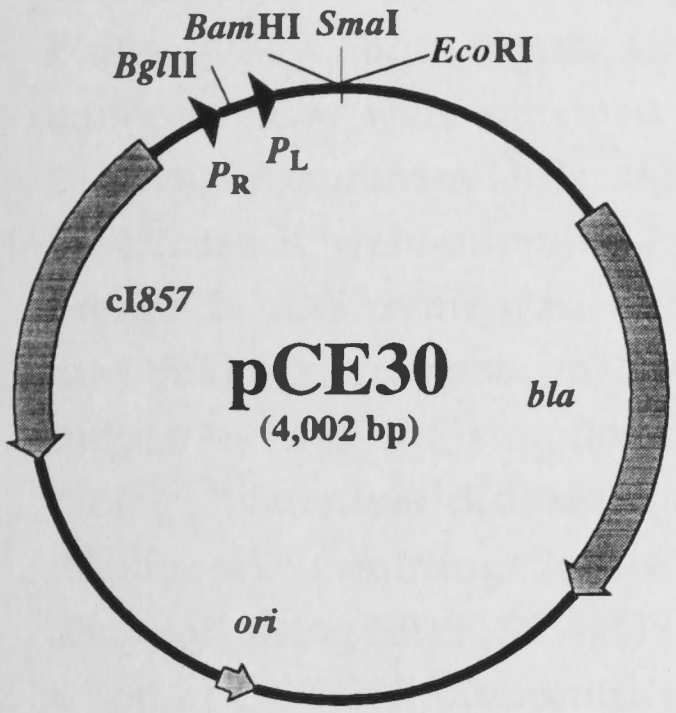

(b)

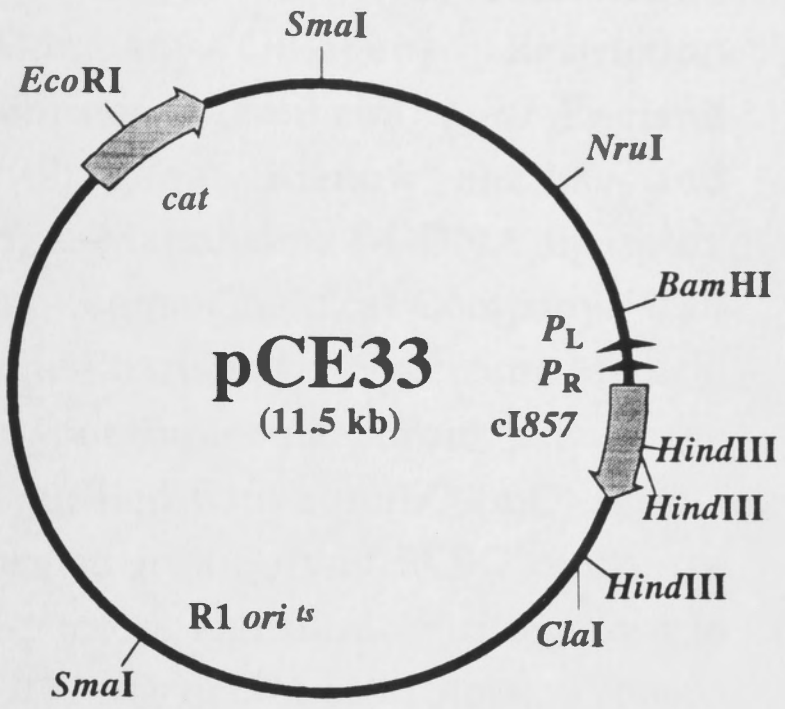

(c)

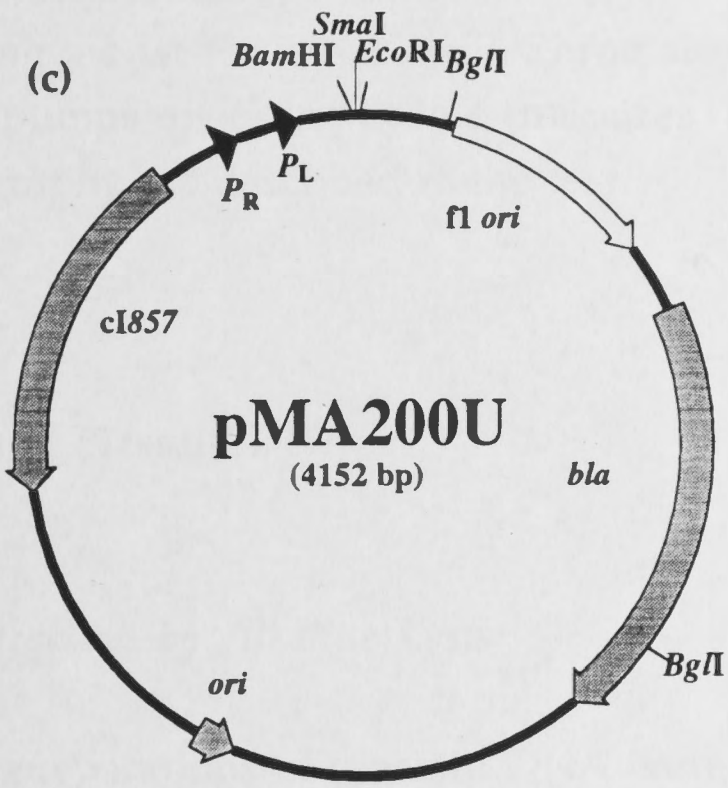

(d)

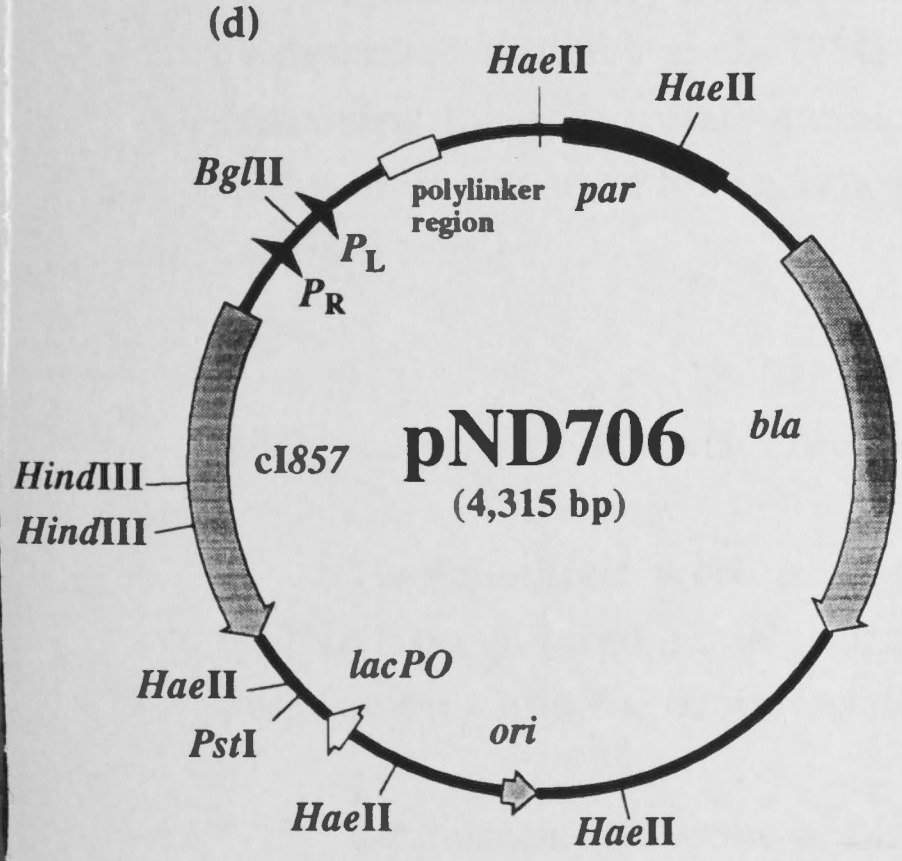

Polylinker region:

$P_R\,P_L$ ... *ClaI-SphI- NcoI- KpnI-SmaI-SstI-XbaI-*RBS*-NdeI-AatII-SalI/AccI-MluI-PstI-HindIII-XbaI-EcoRI-SstI-SmaI-KpnI-NcoI-SphI-ClaI-BglII-XhoI-StuI-NruI* ...*par*

Boehringer-Mannheim, BioRad, Difco, Upjohn Company, Pharmacia, Ajax Chemicals, Mallinckrodt Chemical Works, May and Baker, Calbiochem, Fluka AG, Cabot, Sigma Chemical Company, Quiagen). Restriction endonucleases were obtained from Boehringer-Mannheim, New England Biolabs, Amersham International or Progen. Klenow enzyme and Proteinase K were supplied by Boehringer-Mannheim, T4 DNA ligase by Bresatech. Lysozyme was purchased from Sigma Chemical Company. Calf intestinal alkaline phosphatase was from Pharmacia. Spectrum Medical Industries was the supplier of Spectra/por molecularporous membrane tubing. Water was distilled and further purified with a milliQ (mQ) system (Millipore). Centrifugations were performed in a Sorvall RC5C centrifuge (Dupont) using SE12, SS34, GSA and GS3 rotors and ultracentrifugations in a Sorval ODT 75B ultracentrifuge using TH-641 or TH-865 rotors. Proteins were purified using a Fast Protein Liquid Chromatography (FPLC) System (Pharmacia) with pumps operating at low pressures. Suppliers of resins for protein chromatography are described in the text.

2.4 Preparation of Plasmid DNA

2.4.1 *Plasmid Extraction by Alkaline Lysis*

Small-scale preparations of plasmid DNA were carried out essentially as described (Silhavy *et al.*, 1984) from cells that were grown on LBT plates containing the appropriate antibiotics (Section 2.2). Plasmid DNA obtained in this way was used for analytical purposes or transformation of competent bacterial cells.

2.4.2 *Large-scale Plasmid Preparation*

Two methods were used to prepare highly-purified plasmid DNA (pDNA) on a large scale: purification of pDNA in CsCl gradients or preparation using the commercially available Qiagen kit (Qiagen, Inc.).

Large-scale isolations of highly-purified pDNA were prepared by two successive bandings in CsCl density gradient from cells grown in minimal

media, amplified with spectinomycin and lysed with TritonX-100 using a modification of the procedure described by Davis *et al.* (1980). All procedures were carried out at 0°C unless otherwise indicated.

An overnight culture of the *E. coli* strain containing the plasmid was used to inoculate 1 l of 56-minimal medium containing the particular antibiotic and was then aerated at 30°C. When the absorbance of the culture reached A_{595}=0.5, spectinomycin was added (300 mg/l), and aeration continued at 30°C for further ~16 h. The cells were harvested by centrifugation (8,000 x g, 15 min, 4°C) and resuspended in 6.25 ml of ice-cold 50 mM Tris.HCl pH 8.0, 25% (w/v) sucrose, frozen in liquid nitrogen and stored at -70°C until use.

The cell suspension was thawed, diluted to 7.5 ml with resuspension buffer containing lysozyme at 10 mg/ml, and swirled for 5 min. Then 1.25 ml of 500 mM EDTA (pH 8.5) was added and swirled for another 5 min. Following the method of Katz *et al.* (1973), cell lysis was performed with the addition of Triton X-100 solution [10 ml; 0.1% (v/v) Triton X-100, 50 mM Tris.HCl pH 8.0, 62.5 mM EDTA]. After 10 min, the lysate was centrifuged (48,000 x g, 1 h, 4°C), the supernatant was collected and its density was adjusted by dilution to 25 ml with mQ H_2O and addition of 24.38 g CsCl. After centrifugation (13,000 x g, 1 h, 4°C), the supernatant was decanted through a tissue filter into a Sorvall T-865 polyallomer tube. The tube was filled with addition of 2.55 ml of a 10 mg/ml solution of ethidium bromide and TE (10 mM Tris.HCl pH 7.4, 1 mM EDTA) to which had been added 0.975 g/ml CsCl. The plasmid DNA was isolated in the density gradient produced by centrifugation (125,000 x g, >40h). The plasmid DNA band, visualized using a long-wave UV lamp, was collected from tubes using an 18-gauge hypodermic needle and syringe as described (Sambrook *et al.*, 1989). The plasmid DNA was transferred to a T-1270 polyallomer tube, topped up with 0.85 ml of 10 mg/ml ethidium bromide solution and buffer TE containing CsCl (0.975 g/ml) and centrifuged (125,000 x g, >40 h). The plasmid DNA was isolated as before. Ethidium bromide was removed by repeated extractions with an equal volume of propan-2-ol saturated with 5 M NaCl in TE (10 mM Tris.HCl pH 7.4, 1 mM EDTA). The solution containing plasmid DNA was then dialysed against 2 changes of 1 l of TE over 24 h. The concentration of dsDNA was determined spectrophotometrically assuming a solution with A_{260} = 1 contained 50 µg of DNA per ml. Plasmid DNAs were routinely stored in TE at -70°C.

Qiagen plasmid purification protocols for midi (up to 100 µg) and maxi (up to 500 µg) preparations were supplied by the manufacturer (Qiagen, Inc.).

2.5 Restriction-Endonuclease Digestion of DNA

Restriction-endonuclease digests were performed in buffers supplied by the manufacturers (Section 2.3). When two or more restriction enzymes with different requirements of salt concentration were used, the digest requiring lower salt concentration was performed first. Subsequently, the concentration of salt was elevated and digestion with the other enzyme was performed. In most cases, digestions were carried out at 37°C for 1 hour and were terminated by addition of 0.5 volume of restriction-endonuclease stop mix [50 mM EDTA, 17% (v/v) glycerol, 0.07% bromphenol blue pH 8.5; RE-stop mix] at 0°C.

For partial digestion, optimization of the reaction was performed on a small scale, before the plasmid DNA was digested in a preparative scale. A progressive series of two-fold dilutions of restriction enzyme were made in equivalent volumes of reaction mixtures containing identical concentrations of buffer and plasmid DNA. After a 30-minute treatment at 37°C, the reactions were stopped by addition of an equal volume of RE-stop mix at 0°C. Electrophoresis in agarose gels (Section 2.7) was used to evaluate results of the series of digests. From analysis of fragment patterns on agarose gels, the optimal conditions were determined and used in a scaled-up partial digestion.

2.6 DNA End-Filling with the Klenow Enzyme

Recessed 3'-termini created by restriction-endonuclease digestion were filled-in using the large fragment of DNA Polymerase I (Klenow enzyme) as described by Sambrook *et al.* (1989).

2.7 Electrophoresis of DNA

Agarose gels for electrophoreses of DNA were cast in a Davis system horizontal submarine apparatus (Sambrook *et al.*, 1989) using a toothed comb to form wells for loading of samples. Gels (147 x 136 x 10 mm) contained agarose at concentrations in the range 0.7% to 1.8% (w/v) in buffer TBE (89 mM Tris-borate, 89 mM boric acid, 2 mM EDTA; Sambrook *et al.*, 1989) containing 0.5 µg/ml ethidium bromide. Samples of DNA were mixed with 1/4 volume of loading buffer (0.2% bromphenol blue, 50% glycerol) and treated for 2 min at 95 - 100°C. Samples were loaded onto a gel and electrophoresed at 50 V using a Bio-Rad 2000/02 power supply until the DNA had entered the gel matrix. Electrophoresis was then continued at 100 V until the required resolution of DNA fragments was achieved.

Fragments of DNA in agarose gels separated during electrophoresis were visualized using a long-wave UV lamp or a short-wave transilluminator (UV transilluminator Model TS-15, Ultraviolet Products). Photographs of gels placed on the transilluminator were made using a model MP-4 Land Camera (Polaroid) with Polaroid 4x5 type 57/high-speed films. λ *cI857Sam7* DNA (Boehringer-Mannheim) digested with *Eco*RI-*Hin*dIII restriction enzymes was used as a DNA fragment size standard.

2.8 Isolation and Purification of DNA Fragments

Electroelution of DNA fragments from agarose onto NA45 membrane (Schleicher and Schuell) or electroelution into dialysis bags were techniques used for recovery of DNA fragments that had been separated in agarose gels. These methods were generally used for isolation of fragments generated by restriction-endonuclease digestion and for removal of enzymes after Klenow end-filling and dephosphorylation.

Both methods were carried out essentially as described (Sambrook *et al.*, 1989). The DNA recovered from gels was purified by phenol/chloroform extraction (Sambrook *et al.*, 1989). Extractions with phenol and chloroform were also used for removal of enzymes following Klenow end-filling,

dephosphorylation reactions, and the use of Proteinase K in preparations of ssDNA.

2.9 5'-Dephosphorylation of Linear Plasmid DNA

To suppress self-ligation of vector DNA, the 5'-phosphate groups of plasmid DNA linearized by restriction endonucleases were removed. Dephosphorylation of linear plasmid DNA was carried out essentially as described by Sambrook *et al.* (1989) using calf intestinal alkaline phosphatase.

2.10 Preparation of Oligonucleotides

Synthetic oligonucleotides used in site-directed mutageneses and cloning experiments were prepared at the Biomolecular Resource Facility (Centre for Molecular Structure and Function, ANU) using an Applied Biosystems 380B DNA Synthesizer. The oligonucleotides were deprotected following 12-hour treatment at 56°C in ammonia solution, and dried. Before use, they were resuspended in 500 µl of TE and spun in a microcentrifuge (MSE Micro Centaur Microfuge) at 4°C for 10 min. The concentration of oligonucleotides in the supernatants were determined by measurements of A_{260}. Molar extinction coefficients of the particular oligonucleotides were calculated from their nucleotide composition and nucleotide molar extinction coefficients at 260 nm (Sambrook *et al.*, 1989).

2.11 Ligation

Ligations were carried out with T4 DNA ligase and purified fragments of DNA (Section 2.8). Concentrations of insert and vector in a particular ligation were adjusted according to recommendations of Legerski and Robertson (1985), unless otherwise stated.

2.11.1 *Ligation of Cohesive Termini*

DNA fragments with cohesive termini were ligated using the ligation buffer described by Sambrook *et al.* (1989). Reactions were routinely carried out at 14°C for 16 h in volumes of 20 to 50 µl.

2.11.2 *Ligation of Blunt-Ended Termini*

Fragments of DNA with blunt-ended termini were ligated in blunt-end ligation buffer (Sambrook *et al.*, 1989) at 30°C for 2 h in volumes of 20 to 50 µl.

2.12 Preparation of Single-Stranded Template DNA

Single-stranded DNA used as templates in oligonucleotide-directed mutageneses and dideoxy sequencing of DNA were prepared essentially as described by Vieira and Messing (1987). All procedures were carried out at 4°C unless otherwise indicated. For preparation of phagemid particles, the strain harbouring the phagemid was grown at 30°C in 500 ml of LBT with an appropriate antibiotic to A_{595}~0.5. The culture was then infected with M13K07 helper phage (5 x 10^9 pfu/ml) and aerated for 16 h at 30°C. Phage particles were then prepared using the procedure of Hines and Ray (1980). Cultures were chilled, cells were removed by centrifugation (7,600 x g, 30 min), and phage particles were precipitated (2 h) by addition of 1/5 volume of 2.5 M NaCl, 25% (w/v) PEG 6K. After their sedimentation (7,600 x g, 30 min), they were resuspended in 0.5% (v/v) Sarkosyl in TE (5% of the volume of the original culture). The suspension was clarified by centrifugation (12,000 x g, 30 min). The phage particles were reprecipitated with PEG 6K as before. The pellet was passively resuspended in a minimal volume of TE, the suspension was clarified and the density of the supernatant was adjusted by the addition of CsCl to 2.3 M. This was centrifuged in Beckman Ultra-Clear (14 x 89 mm) centrifuge tubes (100,000 x g, 48 h). The opalescent band containing phage was extracted from the tube and the density of the phage solution was increased to 3.3 M by the addition of CsCl. This was overlaid in an Ultra-Clear centrifuge tube with 2.3 M CsCl in TE. Centrifugation and isolation of the phage were repeated as described

above. The solution containing purified phage particles was dialysed against 2 x 1-l TE over 16 h and stored at 4°C.

To recover ssDNA from the phage, the viral coat proteins had to be first denatured and digested. After treatment with 2 % (w/v) SDS at 60°C for 5 min, Proteinase K was added (200 µg/ml) and the solution was treated at 37°C for 30 min. Further Proteinase K was added to a final concentration of 300 µg/ml, and after 30 min at 37°C, NaCl was added to 100 mM. Following phenol/chloroform extraction (Section 2.8), the ssDNA was isolated by precipitaion with ethanol.

2.13 Transformation of *E. coli*

2.13.1 *Preparation of Competent Cells*

Cells of *E. coli* were made competent for transformation with plasmid DNA using $CaCl_2$ (Morrison, 1979). Cells were either used immediately or stored for up to 6 months at -70°C in 15% (v/v) glycerol.

2.13.2 *Transformation of Competent Cells*

Competent cells were transformed with plasmid DNA using the method of Morrison (1979), except that after addition of plasmid DNA and 30 min storage on ice, they were routinely treated at 30°C for 2 min before incubation in LBT broth. LBT plates containing the appropriate antibiotic were used for selection of transformants.

2.14 Determination of Protein Concentration

Concentration of proteins was determined either by the protein-dye binding method of Bradford (1976) or by measuring A_{280}. The Bradford assay was used during protein purification and for ABC-primosome assays. Bradford reagent was purchased from BioRad; bovine serum albumin (BSA;

Pharmacia) was used as a standard. Quantification of proteins prepared for high-performance electrophoretic chromatography (HPEC) was carried out by measuring A_{280} on a Varian Cary 1E UV-VIS Spectrophotometer or AN 850A UV-VIS Spectrophotometer (Hewlett-Packard) using 1-ml quartz cuvettes (Starna) of 1-cm path length. Molar extinction coefficients of DnaB and DnaC at 280 nm were estimated from their amino acid composition as described by Gill and von Hippel (1989).

2.15 SDS - Polyacrylamide Gel Electrophoresis

Electrophoresis of proteins under denaturing conditions was performed as described by Laemmli (1970).

The resolving gel contained 12.5% (w/v) acrylamide (30:2.7 acryamide:bisacrylamide), 375 mM Tris.HCl pH 8.8, 0.1% (w/v) SDS, 0.033% (w/v) ammonium persulfate and 0.033% (v/v) TEMED. Stacking gels contained 4.5% acrylamide (30:2.7 acylamide:bisacrylamide), 125 mM Tris.HCl pH 6.8, 0.1% (w/v) SDS, 0.08% ammonium persulfate, 0.08% TEMED. Slab gels (1.5 x 200 x 150 mm) were prepared in vertical glass moulds. The buffer for SDS-PAGE contained 51 mM Tris base, 384 mM glycine and 0.1% (w/v) SDS. Protein samples were mixed with an equal volume of sample buffer [300 mM Tris base, 15% (v/v) glycerol, 0.6% (w/v) bromophenol blue, 50 mM DTT, 1% SDS] and heated at 95 - 100°C for 2 minutes. Samples of low protein concentration were concentrated prior to mixing with sample buffer; 100% (w/v) trichloroacetic acid (1/10 sample volume) was added to the sample which was kept at 4°C for 30 minutes. The pellet after centrifugation (15 min in a microcentrifuge, 4°C) was resuspended in 30 µl of sample buffer, boiled for 2 min and loaded on a gel.

BioRad 2000/02 or Pharmacia EPS 500/400 instruments were used as power supplies. A potential difference of 60 V was applied until samples reached the interface between the stacking and resolving gels. Resolution of proteins was achieved by further electrophoresis at 140 V.

Gels were fixed and stained for a minimum of two hours in staining solution [40% (v/v) methanol, 10% (v/v) acetic acid, 0.3% (w/v) Coomassie Brilliant Blue R] and destained in buffer containing 10% (v/v) propan-2-ol and 10% acetic acid. Photographs for laboratory documentation were taken

using a Polaroid camera (Model MP-4 LandCamera) and Polaroid Type 55 high-speed film. Photographs presented in this thesis were taken by Mr B. Wight from the Photography Unit (Research School of Chemistry).

2.16 Oligonucleotide-Directed Mutagenesis

The oligonucleotide-directed Sculptor *in-vitro* mutagenesis system (Amersham) was used for site-directed mutagenesis of *dnaB* essentially as recommended by the manufacturer.

3 PURIFICATION AND CRYSTALLIZATION OF THE *wt*DnaB AND DnaC PROTEINS AND THE DnaB.DnaC COMPLEX

3.1 Introduction

X-ray crystallography has proved to be the most powerful tool for elucidation of the detailed structure of large biomolecules. Although very efficient, the method is extremely demanding on quality and quantity of the examined protein. A good source of the protein and an efficient purification method significantly increase the chance of obtaining suitable crystals.

The DnaB helicase, like many other replication proteins, is present in normal cells at very low levels - only about 15 to 20 molecules (Ueda *et al.*, 1978; Reha-Krantz and Hurwitz, 1978a). Recombinant DNA technology enabled construction of bacterial strains that overproduce DnaB protein to levels several thousand times higher (Arai *et al.*, 1981c; Stamford, 1991) than wild-type *E. coli* cells (Ueda *et al.*, 1978). High overproduction of the protein was, for example, achieved by cloning the *dnaB* gene in a "run-away" replication vector pKC7 (Arai *et al.*, 1981c) and in derivatives of the pCE30 expression vector (Stamford, 1991, Section 2.1). *E. coli* strain RSC680 containing recombinant plasmid pPS562 (Stamford, 1991), a derivative of pCE30, is the best currently available DnaB overproducer. Overproduction of DnaB has been reported to be 6,400 times higher than in wild-type cells (Ueda *et al.*, 1978; Stamford, 1991). Complete solubility of the overproduced DnaB protein has been achieved by simultanoeus overexpression of the *dnaB* and *dnaC* genes. Several protocols for purification of the DnaB protein from various *E. coli* strains have been published (Reha-Krantz and Hurwitz, 1978a, Ueda *et al.*, 1978; Arai *et al.*, 1981c; Stamford, 1991), but only strain RSC680 enabled simultaneous purification and separation of the DnaB and DnaC proteins and the DnaB.DnaC complex in large quatnities (Stamford, 1991).

The DnaB protein has already been purified to homogeneity (with purity >95%) in the large quantities required for extensive structural studies in several laboratories (Ueda *et al.*, 1978; Reha-Krantz and Hurwitz, 1978a; Arai *et al.*, 1981c). Nevertheless, no information about DnaB crystals or

crystals of the DnaB.DnaC complex suitable for X-ray structural analysis has been published to date. The initial goals of the project were therefore to purify DnaB, DnaC and the DnaB.DnaC complex in quantity and quality sufficient for X-ray crystallography and to set up crystallization experiments with the *wt* proteins.

In the work reported here, the method for purification of DnaB and DnaC was improved and large quantities of both proteins along with the DnaB.DnaC complex were purified. The ABC-primosome assay (Madsai et al., 1990a; Stamford, 1991) was used to determine enzymatic activities of the proteins. An accurate chromatographic method - high-performance electrophoretic chromatography (HPEC) - was used to confirm the molar ratio of DnaB and DnaC in the isolated DnaB.DnaC complex. Kobori and Kornberg (1982b) have demonstrated that purified DnaB protein when mixed with purified DnaC in the presence of ATP forms a stable complex that can be isolated. Using this knowledge, an alternative method for preparation of pure DnaB.DnaC complex from partially-purified DnaB and DnaC proteins was examined. Crystals of the DnaB protein and the DnaB.DnaC complex were prepared. X-ray diffraction analysis of DnaB crystals indicated the further direction of the research project.

3.2 Materials and Methods

3.2.1 *Purification of* wt*DnaB, DnaC and the DnaB.DnaC Complex*

3.2.1.1 Purification Method A

Buffers used in the purification procedure were 50 mM Tris.HCl pH 7.6, 10% (w/v) sucrose, 100 mM NaCl, 2 mM DTT, 10 mM spermidine.HCl (lysis buffer); 50 mM Tris.HCl pH 7.6, 20% (v/v) glycerol, 5 mM $MgCl_2$, 2 mM DTT, 100 µM ATP, NaCl as specified in the text (Buffer A); 50 mM Tris.HCl pH 7.6, 20% (v/v) glycerol, 200 mM NaCl, 5 mM $MgCl_2$, 2 mM DTT, 100 µM ATP (Buffer B); 50 mM HEPES-Na.HEPES pH 7.5, 15 % (v/v) glycerol, 1 mM EDTA, 2 mM DTT, 100 µM ATP; NaCl was added as indicated in the text (Buffer CM).

A column of a DEAE-Fractogel [TSK DEAE-650 (M); Merck] was prepared according to the manufacturer's instructions, washed with two column volumes of Buffer A containing 1 M NaCl and equilibrated with ten column volumes of Buffer A containing 25 mM NaCl. Sephacryl S-400 (Pharmacia) was washed with five volumes of Buffer B before the protein samples were applied. The CM-Fractogel [(TSK CM-650 (M)] column was prepared as directed by the manufacturer (Merck) and after washing with two column volumes of Buffer CM containing 1 M NaCl, the resin was equilibrated with ten column volumes of Buffer CM containing 25 mM NaCl.

Strain RSC680 (AN1459/pPS562; Stamford, 1991) was grown in 6 x 1 l of LBT broth containing 50 mg/l ampicillin to A_{595} = 0.5. Overproduction of DnaB and DnaC proteins was induced by temperature shift to 42°C. To make the temperature shift as quick as possible, cultivation media were heated to 42-43°C in a 60°C water bath. Following this, cultures were incubated at 42°C for another 4 hours. Cultures were chilled and cells were harvested (8,000 x g, 15 min, 4°C), resuspended in 50 mM Tris.HCl pH 7.6, 10% (w/v) sucrose (2 ml per 1 g of cell paste), poured into liquid nitrogen and stored at -70°C. The yield from 6 litres of cell culture was routinely about 15 grams of cell paste.

The cell suspension was thawed and diluted in lysis buffer (300 ml/15 g cell paste). Lysozyme was added to 0.25 mg/ml and the mixture was stirred on ice for 20 minutes and left for 2 hours at 0°C. Lysis occurred during treatment of the mixture at 37°C for 6 minutes (with gentle stirring). After chilling in ice for 15 min, cell debris was sedimented by centrifugation (12,000 x g, 20 min, 2°C) and proteins were precipitated from the supernatant (fraction FI) using finely-ground ammonium sulfate (0.2 g/ml). After being stirred for 2.5 hours, the suspension was centrifuged (40,000 x g, 45 min, 0°C) and the pellet was either stored at -70°C or resuspended immediately in 30 ml of Buffer A (containing 25 mM NaCl) and dialysed against the same buffer (1 l for 2 hours and 1.5 l overnight, respectively). The suspension was clarified by centrifugation (12,000 x g, 15 min, 4°C); the protein concentration in the supernatant (fraction FII) was adjusted to ~5 mg/ml and loaded on a column of DEAE-Fractogel (12.5 x 2.5 cm). The column was washed with 120 ml of Buffer A (with 25 mM NaCl) and bound proteins were eluted with a 600-ml linear gradient of NaCl (25 to 500 mM) in Buffer A at a flow rate of 54 ml/hour.

The DnaC protein did not bind to DEAE-Fractogel and was washed from the column before the gradient of NaCl was applied. The fraction containing DnaC was dialysed (fraction FIIIC), loaded onto a column of a cation-exchange resin (CM-Fractogel; 12.5 x 2.5 cm). The column was washed with two column volumes of Buffer CM (containing 25 mM NaCl). A 600-ml NaCl gradient (25 to 500 mM) in the same buffer was applied at a flow rate of 54 ml/hour. Fractions containing DnaC protein were frozen in liquid nitrogen and stored at -70°C.

DEAE-Fractogel fractions containing the DnaB protein and the DnaB.DnaC complex were pooled separately and precipitated with ammonium sulfate (0.4 g/ml). Pellets obtained after centrifugation (40,000 x g, 45 min, 0°C) were dissolved in 3 ml of Buffer B and dialysed for 2 x 2 hours against 1 l of Buffer B. After centrifugation (12,000 x g, 15 min, 4°C), the supernatants (fractions FIIIB and FIIIBC) were separately loaded onto columns (42 x 2.5 cm) of Sephacryl S-400 gel filtration resin (Pharmacia). The DnaB and the DnaB.DnaC complex were eluted at a flow rate of 42 ml/hour. Separate fractions FIVB (DnaB protein) and FIVBC (DnaB.DnaC complex) were frozen in liquid nitrogen and stored at -70°C.

3.2.1.2 Purification Method B

Buffers A and B were as in Section 3.2.1.1 unless otherwise stated. Buffer C contained 400 mM K_2HPO_4 - KH_2PO_4 pH 7.17, 20% (v/v) glycerol, 200 mM NaCl, 5 mM $MgCl_2$, 2 mM DTT, 0.1 mM ATP (or ADP where indicated).

The anion-exchange resin, DEAE-Fractogel, was used as described in Section 3.2.1.1. A column of hydroxyapatite (Macro-Prep Ceramic Hydroxyapatite; Bio-Rad) was prepared according to the Bio-Rad protocol. The column was then washed with two column volumes of Buffer C and equilibrated with ten column volumes of Buffer B. All buffers and samples for hydroxyapatite chromatography were filtered through a 0.2-µm filter (Sartorius) before use.

Strains overproducing the DnaB and DnaC proteins were grown, induced and harvested as described in Section 3.2.1.1. Cell paste was frozen in liquid nitrogen and stored at -70°C. Unlike the protocol for Method A,

the cell suspension in lysis buffer was treated with lysozyme (0.2 mg/ml) for 1.5 hour at 0°C. After a 4-minute treatment in a 37°C water bath, fractions FI, FII, FIIIB, FIIIC, FIIIBC and FIVC were obtained as described in Section 3.2.1.1.

Hydroxyapatite chromatography was used instead of gel filtration as a final purification step for the DnaB protein and the DnaB.DnaC complex. FIIIB and FIIIBC fractions were treated in an identical fashion. Each was filtered through a 0.2-µm filter and loaded onto a column (6.2 x 2.5 cm) of ceramic hydroxyapatite. The column was washed with 45 ml of Buffer B. Buffers B and C were mixed to produce a linear gradient (380 ml; 0 to 160 mM K_2HPO_4-KH_2PO_4 pH 7.17) for elution of protein. Fractions containing the DnaB protein and the DnaB.DnaC complex were frozen in liquid nitrogen and stored at -70°C.

3.2.1.3 Reassociation of the DnaB.DnaC Complex and its Purification

Partially-purified DnaC (~20 mg of the protein; fraction FIIIC) was precipitated with ammonium sulfate (0.4 g/ml). The precipitate was sedimented (40,000 x g, 45 min, 0°C) and dissolved in 40 ml of fraction FIVB containing approximately 5.75 mg of 90%-pure DnaB protein. The solution was dialysed against 1 l of Buffer A containing 25 mM NaCl (see Section 3.1.4.1) two times for three hours, ATP was added to 1 mM and the sample was treated at 30°C for three minutes. After cooling in ice for 10 min, 36 ml of the sample was loaded on a column of DEAE fractogel (15 x 1 cm). The column was washed with 12 ml of Buffer A (containing 25 mM NaCl) and the protein was eluted using a 120-ml linear gradient of NaCl (25 mM to 550 mM) in Buffer A at a flow rate of 0.2 ml/min. Fractions containing the DnaB.DnaC complex were frozen in liquid nitrogen and stored at -70 °C.

3.2.2 *DNA Replication Assay*

The ABC-primosome assay was used to determine activities of DnaB, DnaC and the DnaB.DnaC complex in the process of DNA replication. All of the replication proteins required in the assay were prepared in the research group of Dr N. E. Dixon: DnaA (4.08 x 10^6 units/mg), SSB (8.8 x 10^6 units/mg) and DnaG primase (1.36 x 10^6 units/mg) were purified by Mr C.A.

Love, the β subunit of DNA polymerase III holoenzyme (3×10^6 units/mg) was prepared by Dr J.L. Beck, DNA polymerase III* (5.5×10^5 units/mg) was obtained from Dr N.E. Dixon, DnaC (2×10^5 units/mg) and DnaB (1.2×10^5 units/mg) were supplied by Dr N.P.J. Stamford. Single-stranded R6K-γ2 (M13A-site) ssDNA template (Masai *et al.*, 1990a) was a gift from Dr H. Masai (DNAX Research Institute of Molecular and Cellular Biology).

The protocol (Masai *et al.*, 1990a; Stamford, 1991) was modified and the assay was carried out as follows. Reaction mixtures prepared at 0°C contained: 20 mM Tris.HCl pH 7.5; 100 μg/ml BSA; 8 mM DTT; 0.01% (w/v) Brij-58; 8 mM magnesium acetate; 125 mM potassium glutamate; 1 mM ATP; rCTP, rUTP, rGTP (250 μM each); 12 ng of DnaA; 1 μg of SSB; 36 ng of DnaG primase; 100 ng of DNA polymerase III*; 26 ng of β subunit of polymerase III holoenzyme; dATP, dCTP, dGTP, and [^{3}H]-TTP (50 μM each) and R6K-γ2 ssDNA (220 pmoles, as nucleotide). When DnaB activity was measured, the DnaC protein (340 ng) was added; when quantifying DnaC activity, DnaB (740 ng) was present in the reaction mixture. Proteins, the enzymatic activities of which were going to be measured, were diluted in buffers as follows: 50 mM Tris.Cl pH 7.4, 5 mM $MgCl_2$, 20% (v/v) glycerol, 1 mM ATP, 1 mM DTT and 200 mM potassium glutamate (DnaB protein); 50 mM Tris.Cl pH 8.3, 20% (v/v) glycerol, 20 mM potassium glutamate, 1 mM EDTA, 0.5% Triton X-100, 0.1 mg/ml BSA, 5 mM DTT (DnaC). The DnaB.DnaC complex was diluted in a buffer prepared by mixing the dilution buffers for DnaB and DnaC in a 1 : 1 ratio. Aliquots (25 μl) of reaction mixture were prepared at 0°C and after the addition of the protein the activity of which was to be determined, they were treated at 30°C for 10 min. Cooling to 0°C and addition of 1 ml of stop solution (10% TCA, 0.1 M $NaPP_i$) terminated replication of DNA. After 10 min at 0°C, the mixtures were filtered through Whatman GF/C filters and washed with ~50 ml of 1 M HCl containing 0.1 M $NaPP_i$. Filters were then washed with ethanol, dried and counted in a Beckman LS 6000 IC liquid scintillation counter. Ready-Safe liquid scintillation cocktail was purchased from Beckman. Activity of the proteins in DNA replication were calculated in units (U), where one unit of replication activity denotes incorporation of one picomole of nucleotide into product per minute at 30°C.

3.2.3 *High-Performance Electrophoretic Chromatography (HPEC)*

High-performance electrophoretic chromatography (Model 230A HPEC System Version 1.0.0; Applied Biosystems) under denaturing conditions was used for determination of the molar ratio of DnaB : DnaC in samples of the DnaB.DnaC complex.

Polyacrylamide gels were prepared in glass columns (50 x 2.5 mm) and contained 7% acrylamide (30 : 2.7 acrylamide:bisacrylamide), 75 mM Tris.PO_4 pH 7.5, 0.07% (w/v) ammonium persulfate and 0.07% (v/v) TEMED. Proteins were detected by their absorbance at 280 nm. The upper electrode buffer contained 75 mM Tris.PO_4 pH 7.5 and 0.1% SDS. 75 mM Tris.PO_4 pH 7.5 was used for the lower electrode and elution of proteins. A potential difference of 300 V was applied to gel columns for 4 h prior to loading of protein samples to elute most of the UV-absorbing contaminants from the gels. Proteins were dialysed *vs* 7.5 mM Tris.PO_4 pH 7.5 buffer, then concentrated in Millipore concentrators (5,000 MWCO). Glycerol to 15% and SDS and β-mercaptoethanol to 0.5% were added and protein samples were treated at 100°C for 2 minutes. Proteins (20-100 µg in 3-50 µl) loaded on the gel column were electrophoretically separated at 300 V (2 mA) and eluted from the gel at a flow rate of 1.2 ml/hour. Fractions (120 µl) were collected. Elution profiles were generated on the basis of A_{280} measurements. Recordings of elution profiles were enlarged to 155%, copied five times, peaks were cut out, weighed with an analytical balance and an average weight of the particular peak was calculated. The molar ratio of proteins in the DnaB.DnaC complex was determined from the equation:

$$\frac{\text{DnaB}}{\text{DnaC}} = \frac{\text{Average weight of the DnaB peak}}{\varepsilon_{280}\,(\text{DnaB})} + \frac{\text{Average weight of the DnaC peak}}{\varepsilon_{280}\,(\text{DnaC})}$$

Molar extinction coefficients at 280 nm (ε_{280}) were calculated from the amino acid compositions by the method of Gill and von Hippel (1989).

3.2.4 *Concentration of Proteins*

Four methods of protein concentration were used: precipitation with ammonium sulfate (see Section 3.2.1.1), concentration in Amicon stirred ultrafiltration cells, use of Centricon concentrators, and vacuum ultrafiltration. Amicon stirred ultrafiltration cells (Model 8050 and 8200)

were used with Diaflo ultrafiltration membranes (type YM-10, YM-30 and YM-100). The maximum pressure of nitrogen applied to cells was 375 kPa. Concentration of proteins in Centricon concentrators (C-10, C-30; Amicon) was carried out at 3,000 x g at 4 °C. A vacuum ultrafiltration apparatus (Schleicher & Schuell) was used with cellulose nitrate ultra thimbles (25,000 MWCO) according to instructions supplied by the manufacturer.

3.2.5 *Crystallization of Proteins*

Experimental techniques used for protein crystallization were as described by Ollis and White (1990). Crystals were grown using the hanging drop method of vapour diffusion. Linbro tissue culture multi-well plates (24 flat-bottom wells of size 1.7 x 1.6 cm; Flow Laboratory) with plastic cover slips (22 x 22 mm; Polysciences) were used for crystallization experiments.

Highly-purified proteins were dialysed against buffers Dial B, Dial BC and Dial C respectively and concentrated (Section 3.2.4) prior to setting up crystallization experiments. Except when indicated otherwise, Dial B contained 10 mM Tris.HCl pH 7.6, 20 mM NaCl, 5 mM $MgCl_2$, 0.1 to 0.25 mM adenosine phosphate (ATP or ADP, as indicated in the text); Dial BC was identical to Dial B except that ATP only was used at 0.1 mM and DTT was added to 1 mM. For DnaC crystallization experiments, Dial C buffer (10 mM HEPES pH 7.5, 20 mM NaCl, 0.1 mM ATP, 1 mM DTT) was used.

A "fast screen method" (Table 3.1) was routinely used for an initial examination of a wide range of conditions for crystallization of the particular protein. In each case, 3 µl of protein solutions (5-10 mg/ml) were mixed with 3 µl of crystallization buffers (Table 3.1) onethanol-washed plastic coverslips and placed over the mouths of wells of tissue culture plates into which had previously been placed 1 ml of the same crystallization buffer used in the particular drop. The gap between coverslip and well was sealed with petroleum jelly. Parallel experiments were set up at 4°C and 25°C. After the principal conditions under which protein had crystallized were found, larger amounts of protein were used for fine tuning of the crystallization conditions. Usually 7 to 9 µl of protein solution (5-10 mg/ml) in a 10 µl drop was used. The compositions of crystallization buffers, protein concentrations in the drops and compositions of buffers in

Table 3.1

A list of buffers routinely used for a "fast-screen" in initial crystallization experiments (Section 3.1.10). *pH of the cold solution was estimated using pH indicator paper. Abbreviations used in this table: AmAc - ammonium acetate, AmS - ammonium sulphate, K P_i (dibasic) - K_2HPO_4-KH_2PO_4, NaAc - sodium acetate, Na formate - sodium formate, Na tartrate - sodium tartrate.

1) 0.2 M $CaCl_2$, 0.1 M NaAc pH 4.7, 30% MPD	25) 0.1 M HEPES pH 7.5, 1 M NaAc
2) 0.4 M Na tartrate pH 6-6.5	26) 0.2 M AmAc, 0.1 M citrate pH 5.5, 30% MPD
3) 0.4 M K P_i (dibasic) pH 8.5	27) 0.2 M NaCit, 0.1 M HEPES pH 7.5, 20% isopropanol
4) 0.1 M Tris pH 8.5	28) 0.2 M NaAc, 0.1 M cacodylate pH 6.5, 30% PEG 8K
5) 0.2 M NaCit, 0.1 M HEPES pH 7.5, 40% MPD	29) 0.1 M HEPES pH 7.5, 0.8 M Na tartrate
6) 0.2 M MgCl2, 0.1 M Tris pH 8.5, 15% PEG 3.4 K	30) 0.2 M AmS, 30% PEG 8K
7) 0.1 M cacodylate pH 6.5, 1.3 M NaAc	31) 0.2 M AmS, 30% PEG 3.4K, *pH 5
8) 0.2 M NaCit, 0.1 M cacodylate pH 6.5, 30% isopropanol	32) 2 M AmS *pH 5
9) 0.2 M AmAc, 0.1 M citrate pH 5.5, 15% PEG 3.4 K	33) 4 M Na formate *pH 6-6.5
10) 0.2 M AmAc, 0.1 M NaAc pH 4.7, 30% PEG 3.4 K	34) 0.1 M NaAc pH 4.7, 2 M Na formate
11) 0.1 M citrate pH 5.5, 1 M K Pi (dibasic)	35) 0.1 M HEPES pH 7.5, 1.8 M Na tartrate
12) 0.2 M MgCl2, 0.1 M HEPES pH 7.5, 30% isopropanol	36) 0.1 M Tris pH 8.5, 8% PEG 8K
13) 0.2 M NaCit, 0.1 M Tris pH 8.5, 30% PEG 400	37) 0.1 M NaAc pH 4.7, 8% PEG 3.4K
14) 0.2 M $CaCl_2$, 0.1 M HEPES pH 7.5, 28% PEG 400	38) 0.1 M HEPES pH 7.5, 1.35 M NaCit
15) 0.2 M AmS, 0.1 M cacodylate pH 6.5, 30% PEG 8K	39) 0.1 M HEPES pH 7.5, 2% PEG 400, 2 M AmS
16) 0.1 M HEPES pH 7.5, 1.5 M Li_2SO_4	40) 0.1 M citrate pH 5.5, 20% isopropanol, 20% PEG 3.4K
17) 0.2 M Li_2SO_4 ,0.1 M Tris pH 8.5	41) 0.1 M HEPES pH 7.5, 10% isopropanol, 20% PEG 3.4K
18) 0.2 M MgAc, 0.1 M cacodylate pH 6.5, 20% PEG 8K	42) 0.05 M K Pi (dibasic), 20% PEG 8K, *pH 8.5-9
19) 0.2 M AmAc, 0.1 M Tris pH 8.5, 30% isopropanol	43) 30% PEG 2000 *pH 5.5
20) 0.2 M AmS, 0.1 M NaAc pH 4.7, 30% PEG 3.4K	44) 0.2 M Mg formate
21) 0.2 M MgAc, 0.1 M cacodylate pH 6.5, 30% MPD	45) 0.2 M ZnAc, 0.1 M cacodylate pH 6.5, 18% PEG 8K
22) 0.2 M NaAc, 0.1 M Tris pH 8.5, 30% PEG 3.4K	46) 0.2 M CaAc, 0.1 M cacodylate pH 6.5, 18% PEG 8K
23) 0.2 M $MgCl_2$, 0.1 M HEPES pH 7.5, 30% PEG 400	
24) 0.2 M $CaCl_2$, 0.1 M NaAc pH 4.7, 20% isopropanol	

the wells were optimized as indicated. By increasing the volume of the drops, we attempted to grow larger crystals.

3.2.6 *Analysis of Protein Crystals*

Size, morphology and appearance of protein crystals were evaluated using an optical microscope Olympus SZ PT at 4°C. Crystals were photographed using a Pentax camera and Ectachrome 64 ASA films. Photographs of crystals presented in this thesis were developed from colour diapositives at the Instructional Resources Unit, ANU.

X-ray analysis of crystals was carried out by Dr P. Carr from the Research School of Chemistry using an RAXIS-II image plate X-ray diffractometer. All X-ray diffraction experiments were conducted with the crystals in sealed capillary tubes with the crystals dried but in vapour pressure equilibrium with a small amount of the crystallization solution. At the time of the experiments, no stabilising buffer for DnaB crystals was available but we have subsequently determined the composition of a suitable stabilising buffer as 600 mM sodium citrate pH 6.5, 8 mM Tris.HCl pH 7.6, 16 mM NaCl, 4 mM $MgCl_2$, 1 mM ADP. Figure 3.10b (Section 3.3.3), showing a diffraction pattern recorded from a crystal of DnaB prepared as described in Section 3.3.3., was taken from the computer screen by Mr B. Wight (Research School of Chemistry, Photographic Unit).

3.3 Results

3.3.1 *Purification of the Proteins*

3.3.1.1 Purification of the DnaB, DnaC Proteins and the DnaB.DnaC Complex from Strain RSC680

The DnaB, DnaC proteins and the DnaB.DnaC complex were purified from the lysate of strain RSC680 using Method A (Section 3.2.1.1). This method is similar to the procedure described by Stamford (1991). The

following modifications were introduced into the protocol: (i) DEAE-cellulose resin was replaced with DEAE-Fractogel to achieve better resolution of the proteins and to allow increased flow rates through the column during protein purification; (ii) a shallower gradient of NaCl (25 mM to 500 mM) was used to improve protein resolution; and (iii) purification of the DnaC protein was made quicker and more efficient by using cation-exchange chromatography on CM-Fractogel for purification of Fraction FIIIC. The purification procedure described in this section will be called Purification A.

Contamination of the DnaB fractions with the DnaC protein after chromatography on a column of DEAE-cellulose was the main problem reported by Stamford (1991). This was overcome by using DEAE-Fractogel resin and lowering the highest concentration of NaCl in the salt gradient to 500 mM (Figure 3.1). From 6.5 litres of the heat-induced cell culture, 88 mg of the DnaB protein and 59 mg of the DnaB.DnaC complex were isolated. Total enrichment of the proteins (calculated from their specific activities) was 8.5 - fold for the DnaB protein and 8.8 - fold for the DnaB.DnaC complex. The purity of both was ~98% as judged by SDS-polyacrylamide gel electrophoresis (Figure 3.3). No DnaC protein contaminant was detected when 20 μg of fraction FIVB was visualized on the gel (Figure 3.3). The ABC-primosome assay (Section 3.2.2) was used for quantification of protein activities in DNA replication. The specific activity of the DnaB protein (fraction FIVB) was determined to be 53.4 x 10^3 units/mg; 130 x 10^3 units/mg was the value for the DnaB.DnaC complex (fraction FIVBC).

Purification of the DnaC protein not associated with DnaB (fraction FIIIC) was not optimal when Blue dextran-Sepharose and Sephacryl-S200 were used (Stamford, 1991). Using CM-Fractogel, 31 mg of DnaC was purified to >99% purity (Figure 3.2) from the DEAE-Fractogel flowthrough (fraction FIIIC; 47 mg of total protein). No other protein contaminants were detectable when 20 μg of purified DnaC (fraction FIVC) were run on an SDS-polyacrylamide gel (Figure 3.3). The specific activity of the DnaC protein in FIVC was 247 x 10^3 units/mg. This represented its 23.1-fold increase when compared to the DnaC specific activity in the cell lysate (fraction FI). The yield in the three-step DnaC purification was 47%. Progress of Purification A is summarized in Table 3.2.

Figure 3.1

(a) Elution profile of the DnaB protein and the DnaB.DnaC complex from chromatography on a column of DEAE-Fractogel (Purification A). Chromatography was performed as described in the text (Section 3.2.1.1). Elution of the DnaC protein not associated with DnaB is not shown. The protein had been washed from the column before the gradient of NaCl (25 mM to 500 mM) was applied. Protein concentrations were determined by Bradford assay (Section 2.14). Volumes of the fractions were 6.1 ml.

(b) SDS-PAGE of the proteins eluted from DEAE-Fractogel in the gradient of NaCl. A sample of Fraction FII (lane B, Section 3.2.1.1) and 8-µl portions of selected fractions (numbered as indicated above the photograph) were prepared for electrophoresis and run on 12.5 % SDS-polyacrylamide gel as described in Section 2.15. Protein markers (Pharmacia) in lane A were phosphorylase b (94 kDa), bovine serum albumin (67 kDa), ovalbumin (43 kDa), carbonic anhydrase (30 kDa), soybean trypsin inhibitor (20.1 kDa), and α-lactalbumin (14.4 kDa). Proteins were visualized by staining with Coomassie brilliant blue (Section 2.15).

(a)

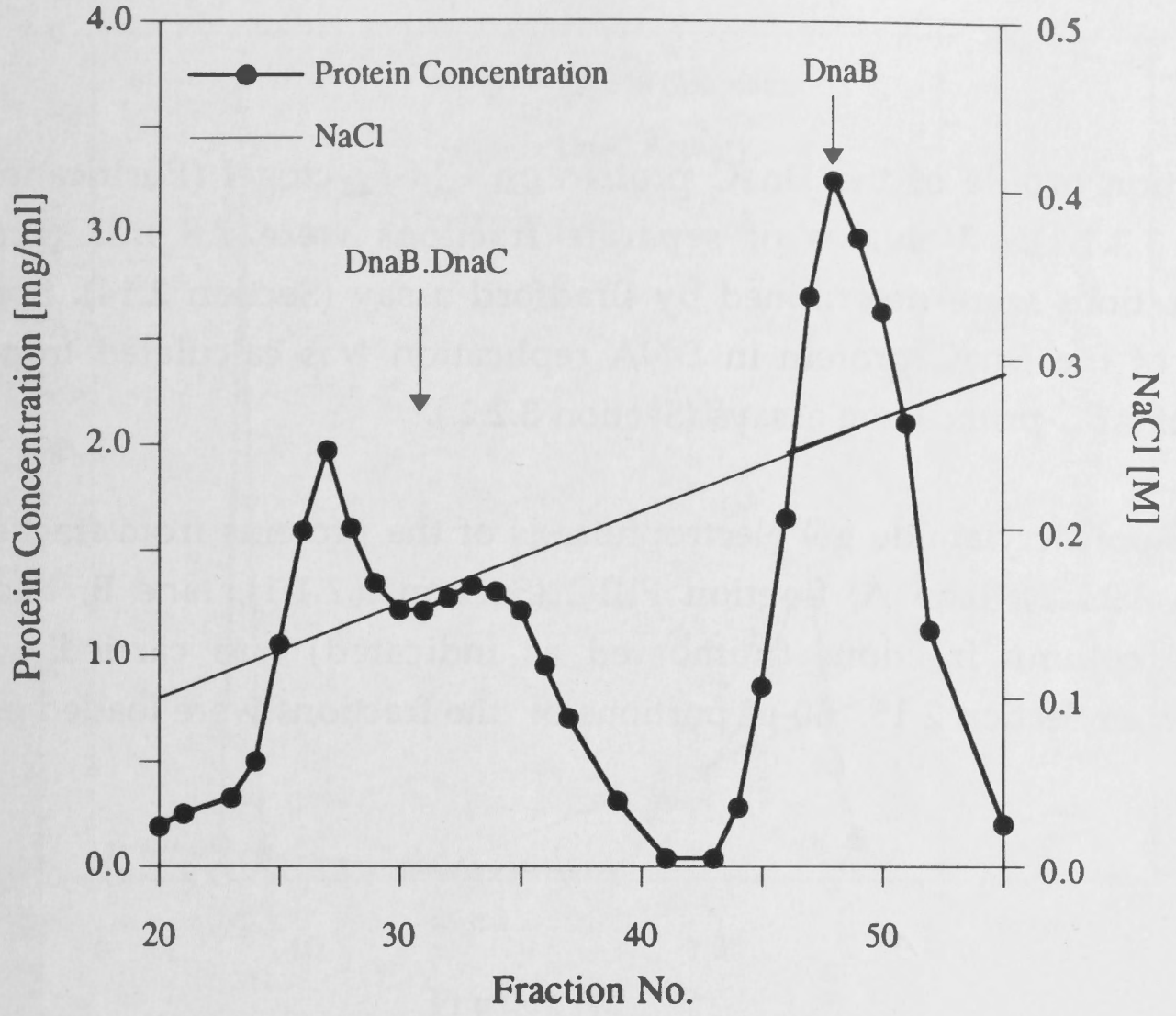
Protein Concentration
NaCl
DnaB
DnaB.DnaC
Protein Concentration [mg/ml]
NaCl [M]
4.0
3.0
2.0
1.0
0.0
0.5
0.4
0.3
0.2
0.1
0.0
20
30
40
50
Fraction No.

(b)

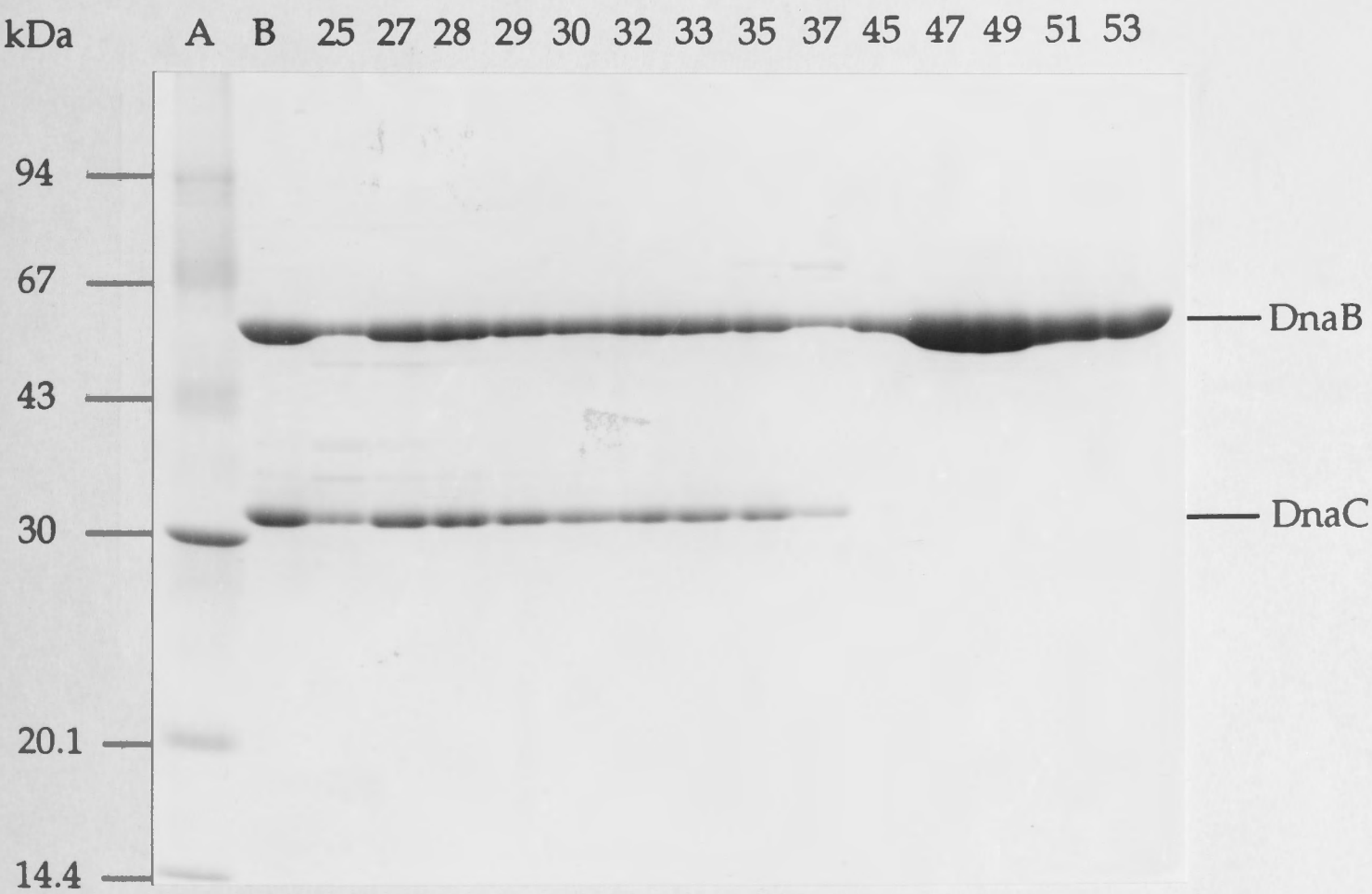
kDa
A
B
25
27
28
29
30
32
33
35
37
45
47
49
51
53
94
67
43
30
20.1
14.4
DnaB
DnaC

Figure 3.2

(a) Elution profile of the DnaC protein on CM-Fractogel (Purification A; Section 3.2.1.1). Volumes of separate fractions were 7.8 ml. Protein concentrations were determined by Bradford assay (Section 2.14). Specific activity of the DnaC protein in DNA replication was calculated from the results of ABC-primosome assays (Section 3.2.2.).

(b) SDS-polyacrylamide gel electrophoresis of the proteins from fraction FI (Section 3.2.1.1), lane A; fraction FIIIC (Section 3.2.1.1), lane B; and the separate column fractions (numbered as indicated) was carried out as described in Section 2.15. 50-µl portions of the fractions were loaded on the gel.

(a)

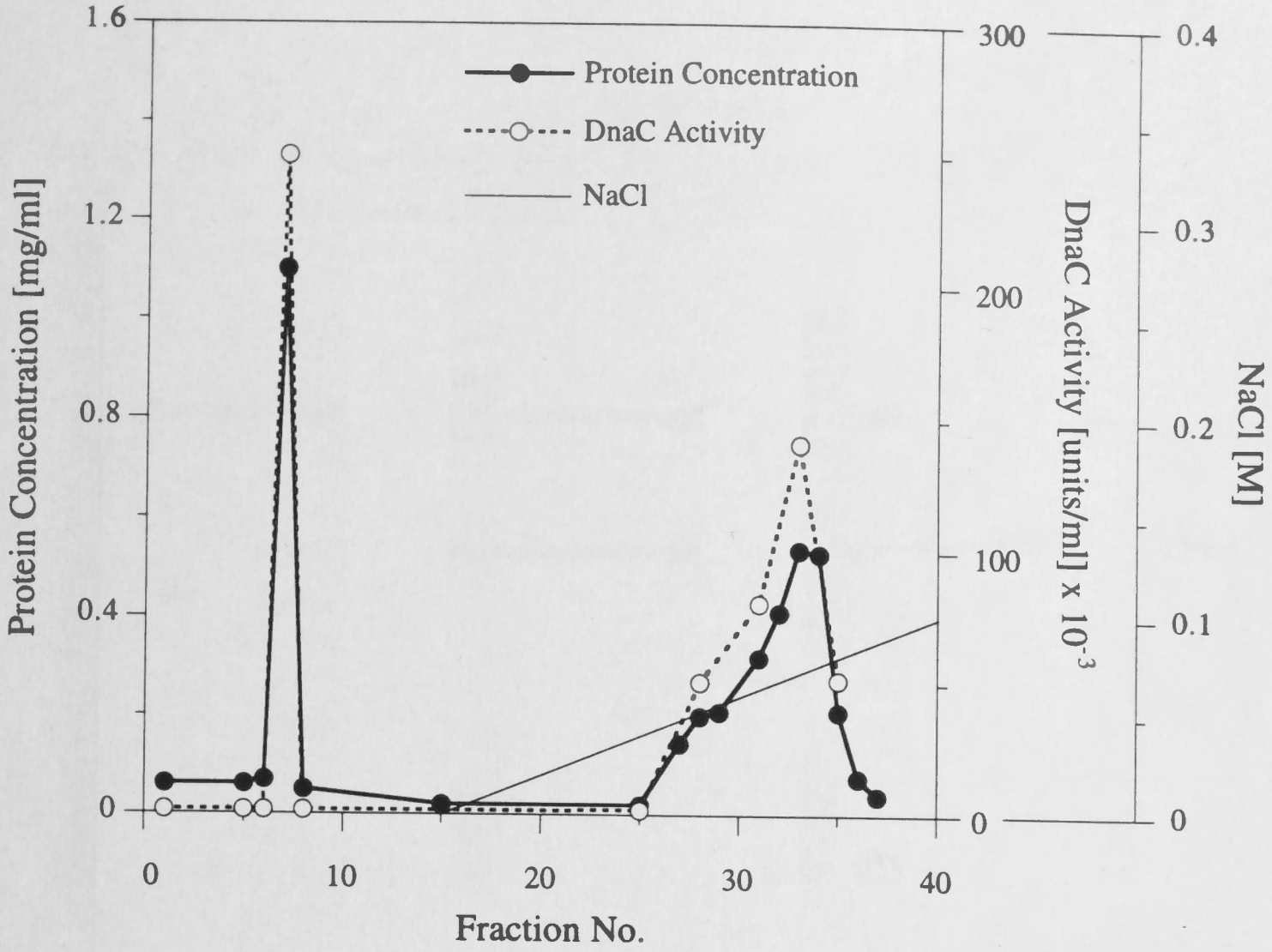
Protein Concentration
DnaC Activity
NaCl
Protein Concentration [mg/ml]
DnaC Activity [units/ml] x 10-3
NaCl [M]
Fraction No.
1.6
1.2
0.8
0.4
0
300
200
100
0
0.4
0.3
0.2
0.1
0
0
10
20
30
40

(b)

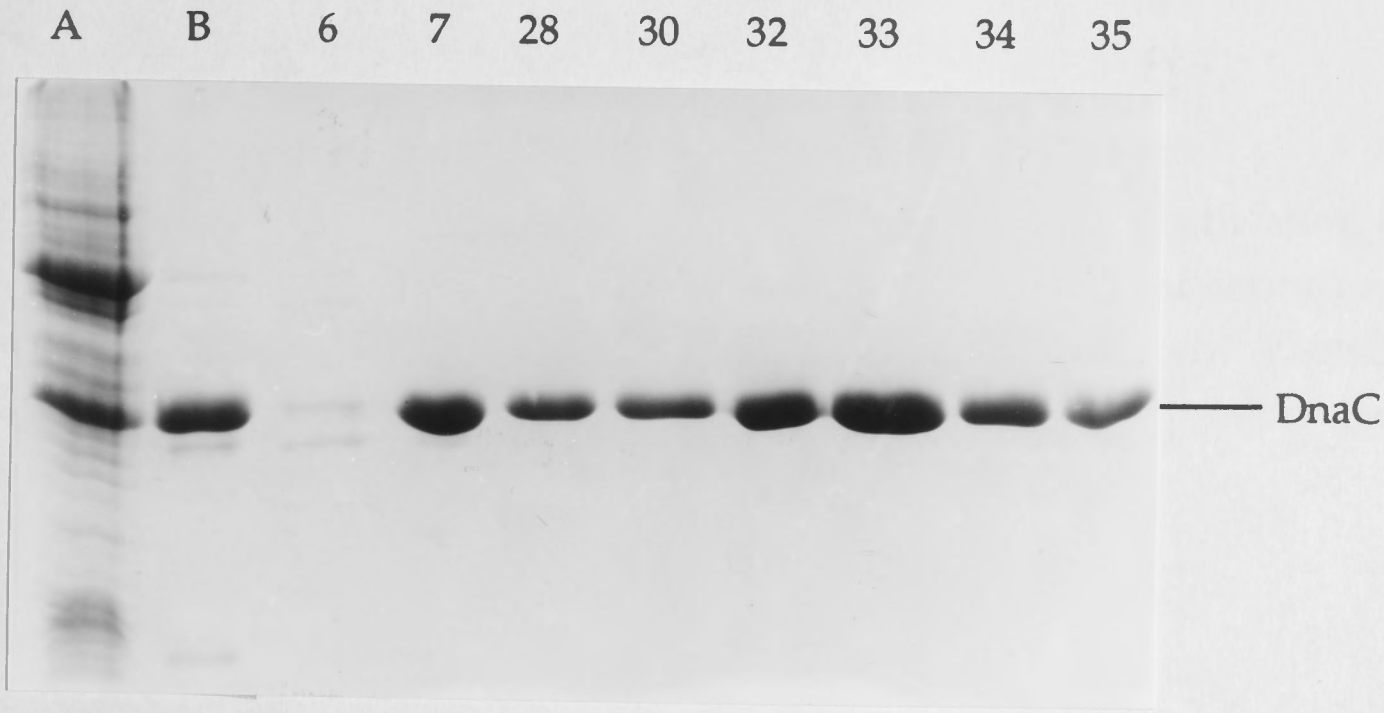
A
B
6
7
28
30
32
33
34
35
DnaC

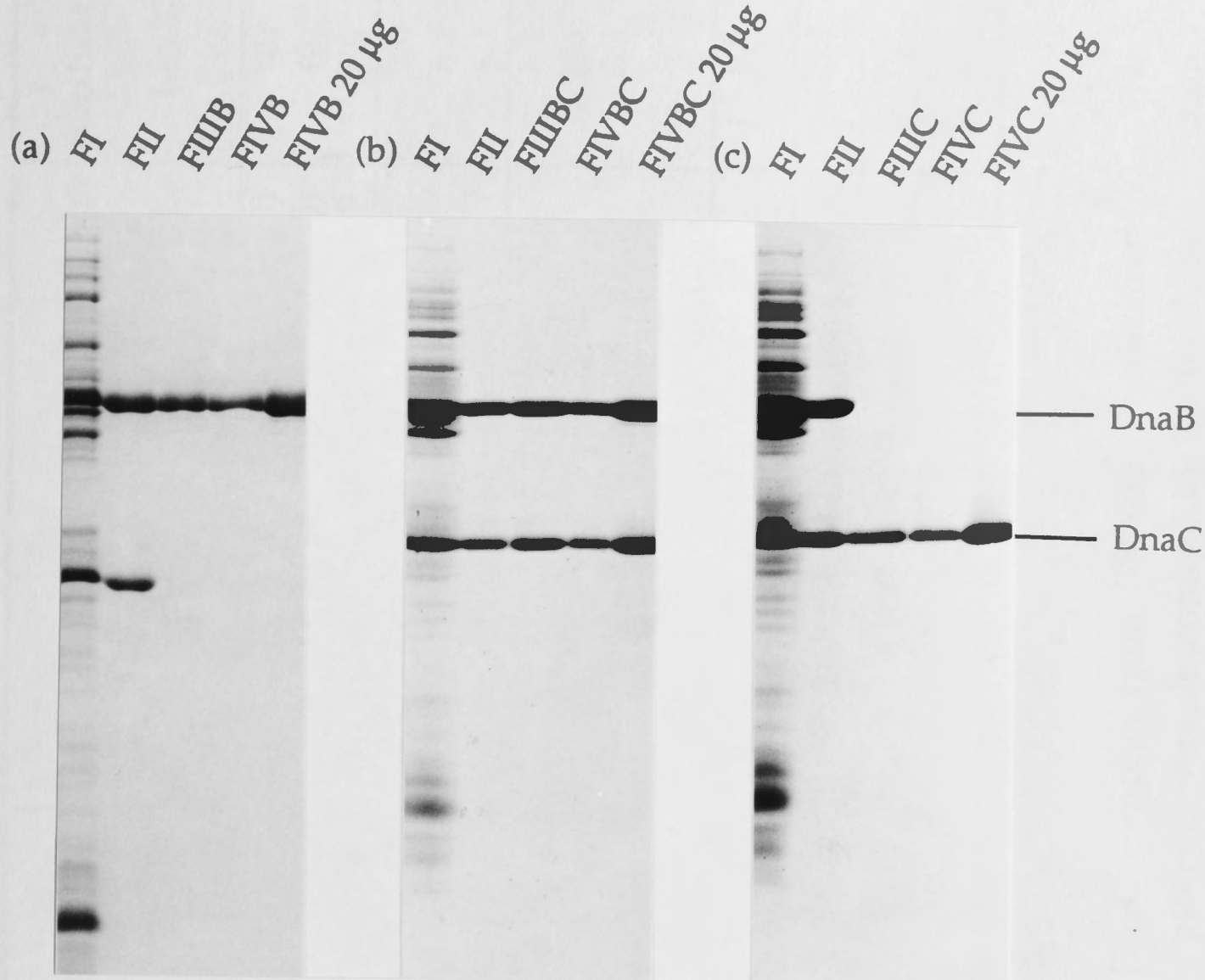

Figure 3.3

Photographs of SDS-PAGE gels documenting progress of the purification of DnaB (a), the DnaB.DnaC complex (b) and DnaC (c) (Purification A). Designation of fractions are as described in Section 3.2.1.1. Except when 20 µg of the protein was loaded on a gel, samples of the particular protein were always of equal total enzymatic activities.

Fraction	Protein	Volume [ml]	Protein concentration [mg/ml]	Total protein [mg]	Total activity [U] x 10^{-6}	Specific activity [U/mg] x 10^{-3}	Yield [%]	Purification [-fold]
FI *cell lysate*	DnaB	435.0	3.50	1523	9.6	6.3	(100)	(0)
	DnaC				16.3	10.7	(100)	(0)
	DnaB.DnaC				22.3	14.7	(100)	(0)
FII *ammonium sulfate precipitation*	DnaB	33.5	6.85	230	8.6	37.6	90	6.0
	DnaC				16.0	69.7	98	6.5
	DnaB.DnaC				21.6	94.0	97	6.4
FIIIB	DnaB	10.25	10.0	103	5.3	51.6	55	8.2
FIIIC	DnaC	170.0	0.275	47	9.0	194	55	18.0
FIIIB/C *DEAE-Fractogel chromatography*	DnaB.DnaC	5.1	12.5	64	7.7	121	35	8.3
FIVB *S400 gel filtration*	DnaB	68.0	1.3	88	4.7	53.4	49	8.5
FIVC *CM-Fractogel chromatography*	DnaC	78.0	0.395	31	7.6	247	47	23.1
FIVBC *S400 gel filtraton*	DnaB.DnaC	52.4	1.13	59	7.7	130	34	8.8

Table 3.2

Purification of the DnaB protein, DnaC protein and the DnaB.DnaC complex from RSC680 (Purification A). The purification method is described in Section 3.2.1.1. Concentrations of proteins were determined by Bradford assay (Section 2.14); the ABC-primosome assay (Section 3.2.2) was used to determine enzymatic activities of the proteins.

3.3.1.2 *Purification of DnaB and the DnaB.DnaC Complex from Strain RSC989*

Method B (Section 3.2.1.2) was used for purification of the DnaB protein and the DnaB.DnaC complex from strain RSC989 (RSC680/plysS). Cells were grown and induced in the same way as RSC680 (Purification A), except that LBT broth was supplemented not only with ampicillin (50 mg/l) but also with chloramphenicol (30 mg/l) to maintain plasmid pLysS in the cells. The introduction of pLysS that contains the gene coding T7 lysozyme into RSC680 improved lysis of the cells: 1742.45 mg of total protein was obtained from 14.5 g of RSC989 cell paste, whereas only 1523 mg was obtained from 15.5 g of the cell paste of strain RSC680. The time for lysis was significantly shorter (see Section 3.2.1.2), the heat treatment was applied for 4 minutes instead of 6 minutes, and the concentration of egg lysozyme was decreased to 0.2 mg/ml.

The DnaB protein purified from strain RSC680 in Purification A was ~98% pure, free from DnaC, and conditions for its crystallization were found (Section 3.3.3). However, the quality of the DnaB crystals was not appropriate for structural studies of the protein (Section 3.3.3).

As was demonstrated by Nakayama and colleagues (1984b), the molecule of the DnaB protein (especially its COOH-terminal domain) is very flexible and undergoes conformational changes easily. The hypothesis, that the conformations of the DnaB.ATP and DnaB.ADP complexes are different (Arai and Kornberg, 1981b) was confirmed by circular dichroism spectroscopy (Nakayama *et al.*, 1984b). When Method A (Section 3.2.1.1) was used for purification of proteins, ATP, Mg^{2+} and glycerol were present in all buffers (except lysis buffer) for stabilization of the DnaB.DnaC complex and uncomplexed DnaB protein. To eliminate the possibility of conformational changes in the DnaB molecule that are induced by hydrolysis of ATP, ATP (100 μM) was replaced with ADP (100 μM) in all buffers used through the purification of the DnaB protein.

Purification Method B, unlike Method A, used chromatography on hydroxyapatite instead of gel filtration on Sephacryl S400. Hydroxyapatite chromatography was used previously by Ueda *et al.* (1978) as a final

purification step after ammonium sulfate precipitaion, DEAE-cellulose and phosphocellulose chromatographies. A substantial increase in specific activity of DnaB was achieved.

Two purifications of DnaB and the DnaB.DnaC complex were carried out using Method B: one in the presence of 100 μM ATP (Purification B1), another in the presence of 100 μM ADP (Purification B2).

The elution profile of proteins from DEAE-Fractogel chromatography in Purification B1 was similar to that presented in Figure 3.1. Hydroxyapatite chromatography of DnaB (fraction FIIIB) is illustrated in Figure 3.4. Results of Purification B1 are summarized in Table 3.3. 90.15 mg of the DnaB protein were obtained from 14.5 g of RSC989 cell paste. Although the total enrichment of the protein was only 5.43-fold (8.5-fold in Purification A), the specific activity of the final product (fraction FIVB) was 59.5×10^3 units/mg (53.4×10^3 units/mg for FIVB in Purification A). This indicated better overproduction of the DnaB and DnaC proteins in cells used for Purification B, that can be documented also with the following results. Specific activities of DnaB in cell lysates were 10.95×10^3 units/mg (Purification B1) and 6.3×10^3 units/mg (Purification A). Precipitaion of proteins with ammonium sulfate increased the specific activities 4.65-fold in Purification B1 and 6-fold in Purification A. Results of the DEAE-Fractogel chromatographies were comparable (1.1-fold and 1.4-fold increase of the DnaB specific activities with respect to Fractions FII); 1.09-fold further enrichment was achieved by chromatography on the column of ceramic hydroxyapatite (fraction FIVB/Purification B1; Figure 3.5). The specific activity of DnaB was 1.036-fold higher after Sephacryl S400 gel filtration than it had been in Fraction FIIIB (Purification A). Results of DnaB (Purification B1) crystallization are reported in Section 3.3.3.

Purification of DnaB protein in the presence of 100 μM ADP (Purification B2) was performed in the same way as Purification B1, except that strain RSC989 was grown and induced in 4 litres of LBT broth supplemented with ampicillin (50 mg/l) and chloramphenicol (30 mg/l). 53 mg of DnaB complexed with ADP was the yield from 9.9 g of RSC989 cell paste. The purity of the protein (fraction FIVB/Purification B2) was ~99% as judged by SDS-polyacrylamide gel electrophoresis (Figure 3.5). For the results of crystallization of the DnaB.ADP complex, see Section 3.3.3.

Figure 3.4

(a) Elution of the DnaB protein in a gradient of K_2HPO_4-KH_2PO_4 pH 7.17 during chromatography on hydroxyapatite (Purification B1). Details of the method are described in Section 3.2.1.2. Volumes of collected fractions were 3.48 ml. Concentrations of proteins were determined as described in Section 2.14.

(b) SDS-PAGE of samples (5 µl) of selected fractions (numbered as indicated above the picture) and a sample (10 µl) of fraction FIIIB (Section 3.2.1.2). Protein markers are as in Figure 3.1. Electrophoresis was carried out as described in Section 2.15.

(a)

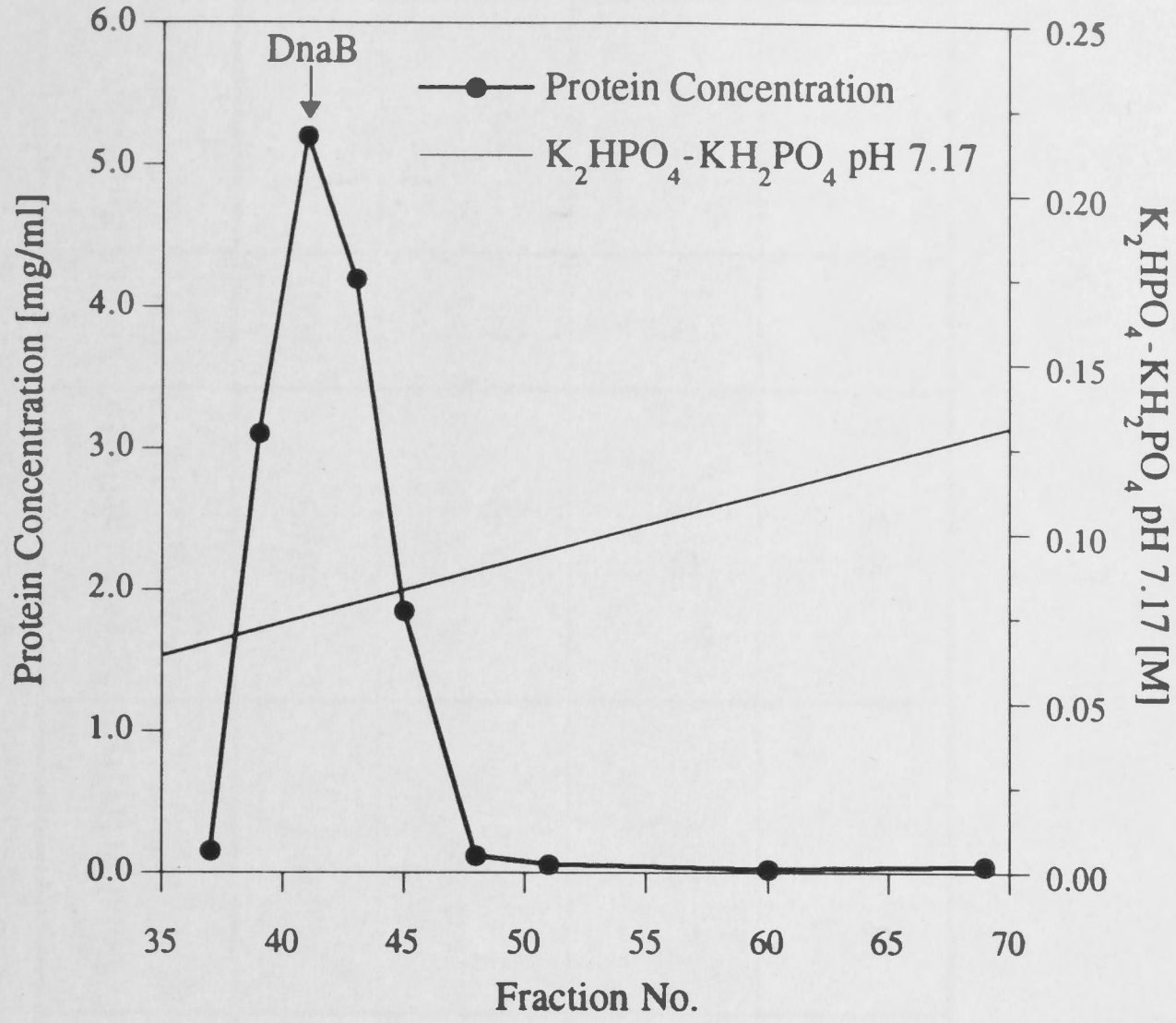
DnaB
Protein Concentration
K_2HPO_4-KH_2PO_4 pH 7.17
Protein Concentration [mg/ml]
K_2HPO_4-KH_2PO_4 pH 7.17 [M]
6.0
5.0
4.0
3.0
2.0
1.0
0.0
0.25
0.20
0.15
0.10
0.05
0.00
35
40
45
50
55
60
65
70
Fraction No.

(b)

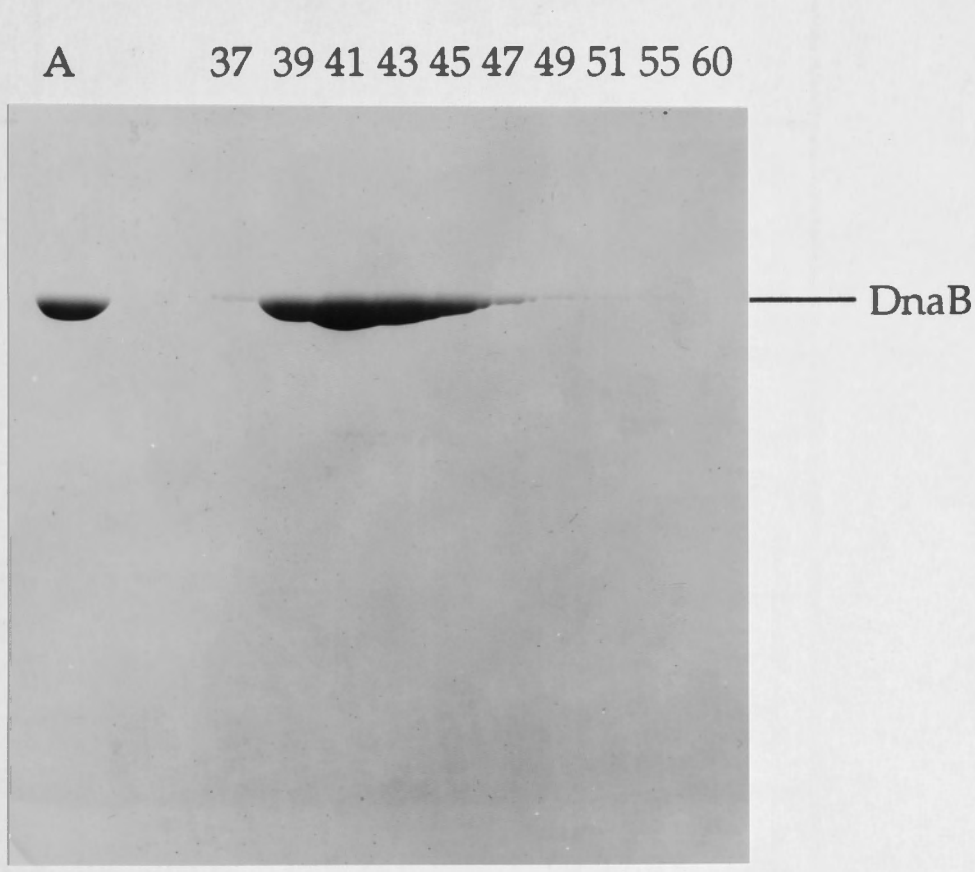
A
37 39 41 43 45 47 49 51 55 60
DnaB

Fraction	Volume [ml]	Protein concentration [mg/ml]	Total protein [mg]	Total activity [U] x 10^{-6}	Specific activity [U/mg] x 10^{-3}	Yield [%]	Purification [-fold]
FI *cell lysate*	268	6.5	1742	19.1	10.95	(100)	(0)
FII *ammonium sulfate precipitation*	27.5	9.3	255.75	13.0	50.89	68	4.65
FIIIB *DEAE-Fractogel chromatography*	88.9	1.14	101.35	5.54	54.67	29	5.00
FIVB *hydroxyapatite chromatography*	38.2	2.36	90.15	5.36	59.5	28	5.43

Table 3.3

Purification of the DnaB protein from strain RSC989 (Purification B1). The purification method is described in detail in Section 3.2.1.2. Concentrations of proteins were determined by Bradford assay (Section 2.14), enzymatic activities by ABC-primosome assay (Section 3.2.2).

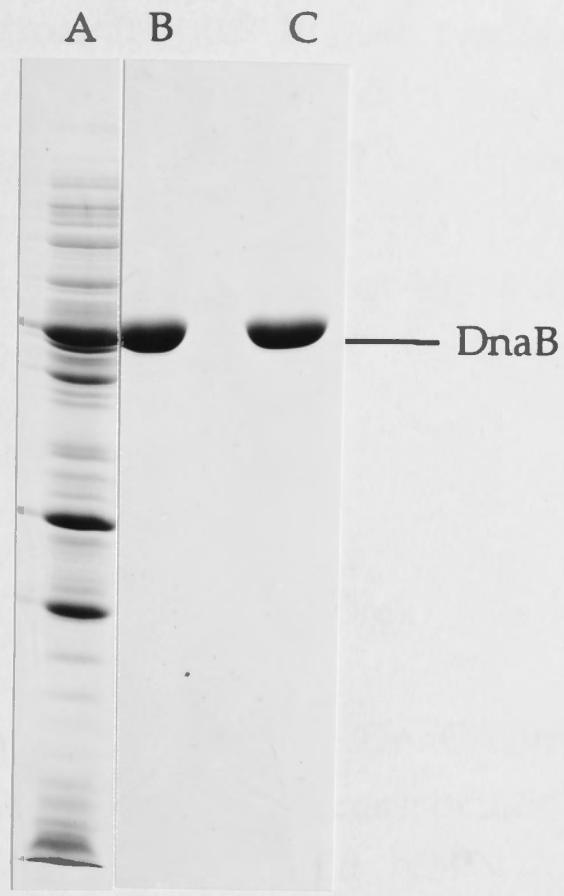

Figure 3.5

SDS-PAGE of the cell lysate of temperature induced strain RSC989 (lane A) and fractions FIVB/Purification B1 (lane B) and FIVB/Purification B2 (lane C; Section 3.2.1.2). In lanes B and C, 20 μg of the DnaB protein were electrophoresed through a 12.5% SDS-polyacrylamide gel (Section 2.15).

Fractions after DEAE-Fractogel chromatography containing the DnaB.DnaC complex were pooled in Purifications B1 and B2 and separately loaded on the column of hydroxyapatite. In both cases, only a portion of the DnaB and DnaC proteins remained associated in the DnaB.DnaC complex. The portion was larger in Purification B1 (~70 %; Figure 3.6), only ~40 % of DnaB and DnaC still formed the complex after the hydroxyapatite chromatography in Purification B2 (data not shown). The DnaB.DnaC complex from Purifications B1 and B2 was not used for crystallization experiments.

3.3.1.3 Reassociation of the DnaB.DnaC Complex

In addition to purification of the DnaB.DnaC complex directly from a cell lysate, the complex can be prepared by reassociation of pure DnaB and DnaC proteins in the presence of Mg^{2+} and ATP (Kobori and Kornberg, 1982b). In our experiment, DnaB and DnaC proteins used for reassociation of the complex were only partially purified. ~90% pure DnaB protein (~0.11 pmol) was mixed with approximatelly 6.5-fold molar excess of DnaC (~0.72 pmol) as described in Section 3.2.1.3. DnaB was reassociated with DnaC almost quantitatively, only traces of the DnaB protein were detected in fractions 61 and 62 (Figure 3.7). The yield of purified DnaB.DnaC complex was 4.5 mg.

The stoichiometry of DnaB and DnaC in the DnaB.DnaC complex purified using Method A and in the purified DnaB.DnaC complex reassociated from separate DnaB and DnaC proteins was verified by high-performance electrophoretic chromatography.

3.3.2 *High-performance Electrophoretic Chromatography*

Protein samples for HPEC were prepared as described in Section 3.2.3. Before the samples of the DnaB.DnaC complex were applied on the HPEC gel column, a control run of the DnaB and DnaC proteins mixed in equimolar ratio was carried out to test the method. A sample for this experiment was prepared as follows. The DnaB and DnaC proteins purified using Method A were dialysed separately against Tris.PO_4 pH 7.5 to remove

Figure 3.6

(a) Hydroxyapatite chromatography of the DnaB.DnaC complex (Purification B1). Elution profile of proteins in a linear gradient of K_2HPO_4-KH_2PO_4 pH 7.17 (0 to 160 mM). No DnaB or DnaC protein was detected in the flowthrough. The particular peaks correspond to the DnaB protein, DnaC protein and the DnaB.DnaC complex as indicated.

(b) SDS-PAGE of proteins separated during chromatography on ceramic hydroxyapatite. Portions (13 µl) of the column fractions (total volume 3.475 ml; numbers of fractions are as indicated) were electrophoresed through a 12.5 % SDS - polyacrylamide gel as described in Section 2.15.

(a)

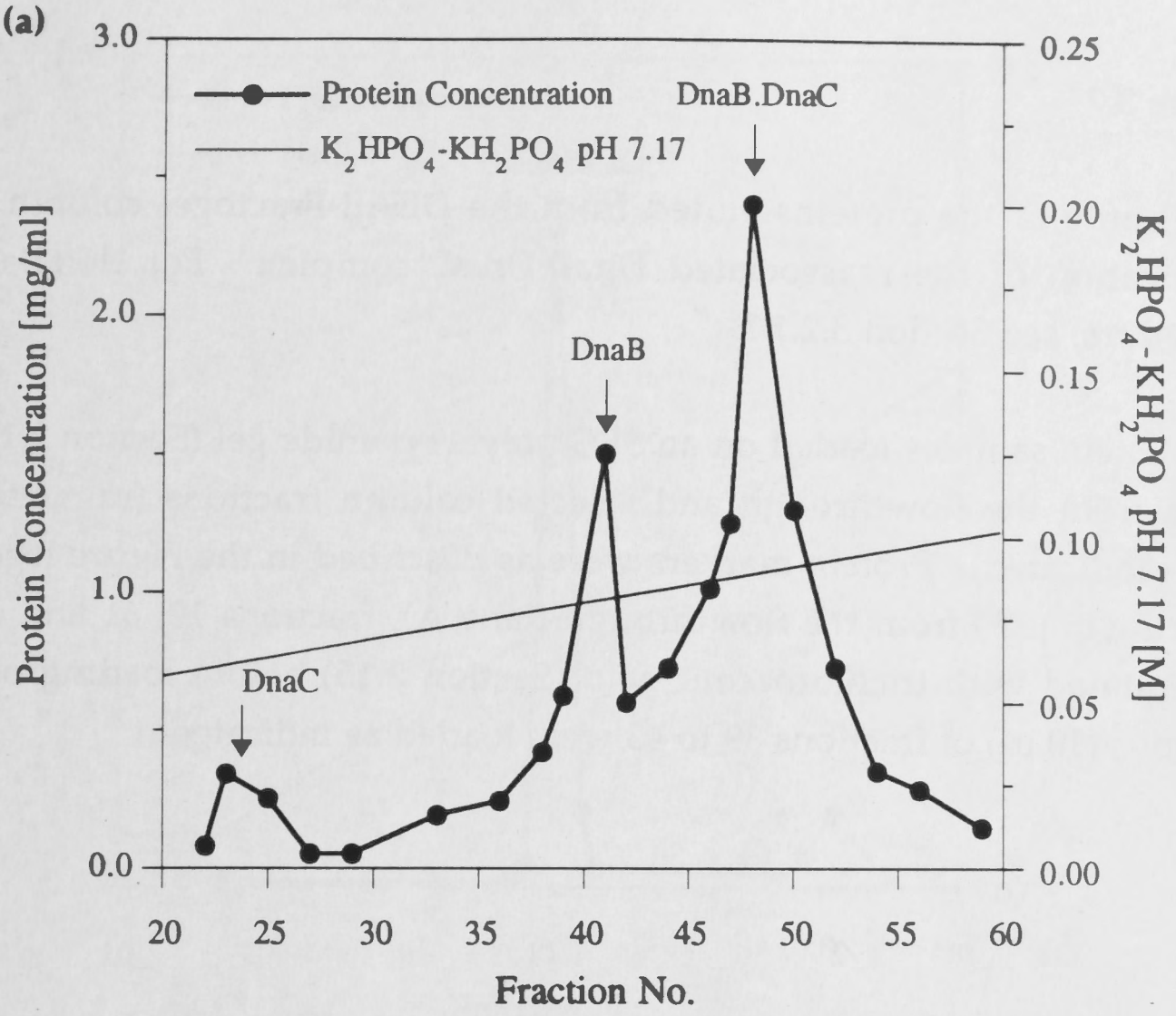
Protein Concentration
DnaB.DnaC
K2HPO4-KH2PO4 pH 7.17
DnaB
DnaC
Protein Concentration [mg/ml]
K2HPO4-KH2PO4 pH 7.17 [M]
Fraction No.
3.0
2.0
1.0
0.0
0.25
0.20
0.15
0.10
0.05
0.00
20
25
30
35
40
45
50
55
60

(b)

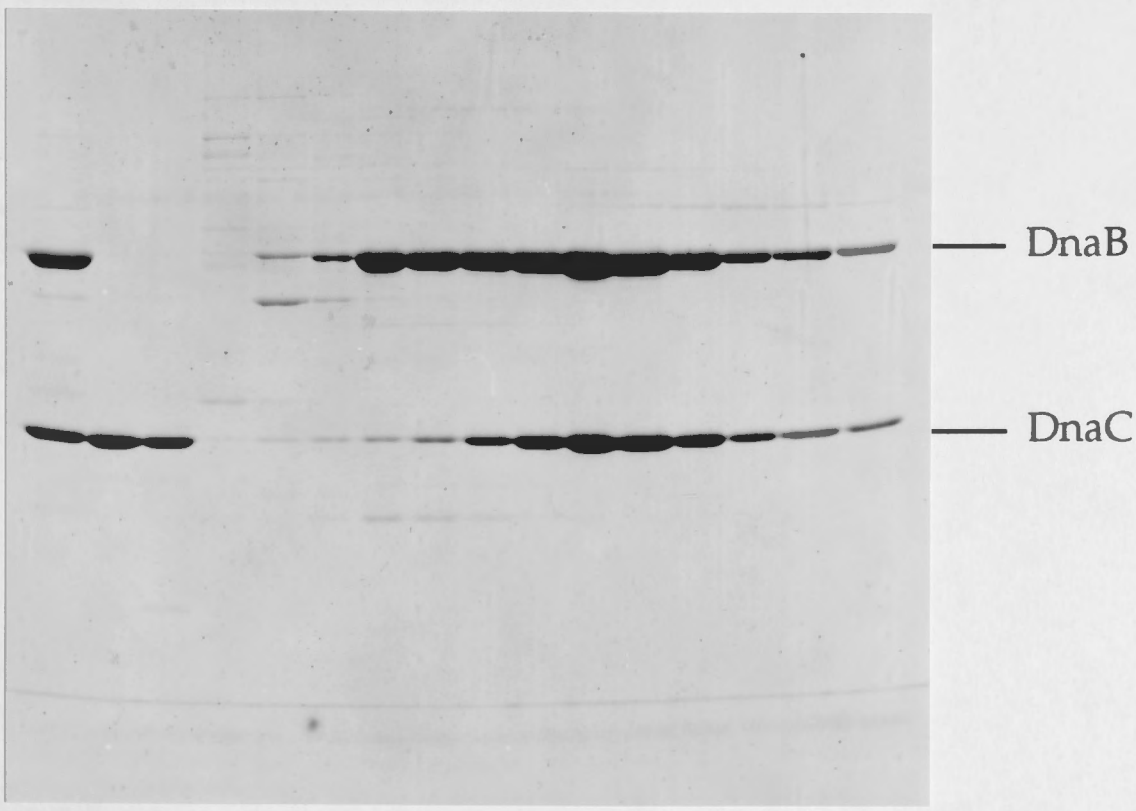
A 23 25 32 35 38 40 42 44 46 48 50 52 54 56 58
DnaB
DnaC

Figure 3.7

(a) Profile of the proteins eluted from the DEAE-Fractogel column during purification of the reassociated DnaB.DnaC complex. For details of the procedure, see Section 3.2.1.3.

(b) Protein samples loaded on an SDS-polyacrylamide gel (Section 2.15) were taken from the flowthrough and selected column fractions (numbers 10 to 65, as indicated). Protein markers were as described in the Figure legend 3.1. Protein (15 µg) from the flowthrough (lane A), fractions 10, 61 and 62 were precipitated with trichloroacetic acid (Section 2.15) before loading on a gel. Portions (10 µl) of fractions 39 to 43 were loaded as indicated.

(a)

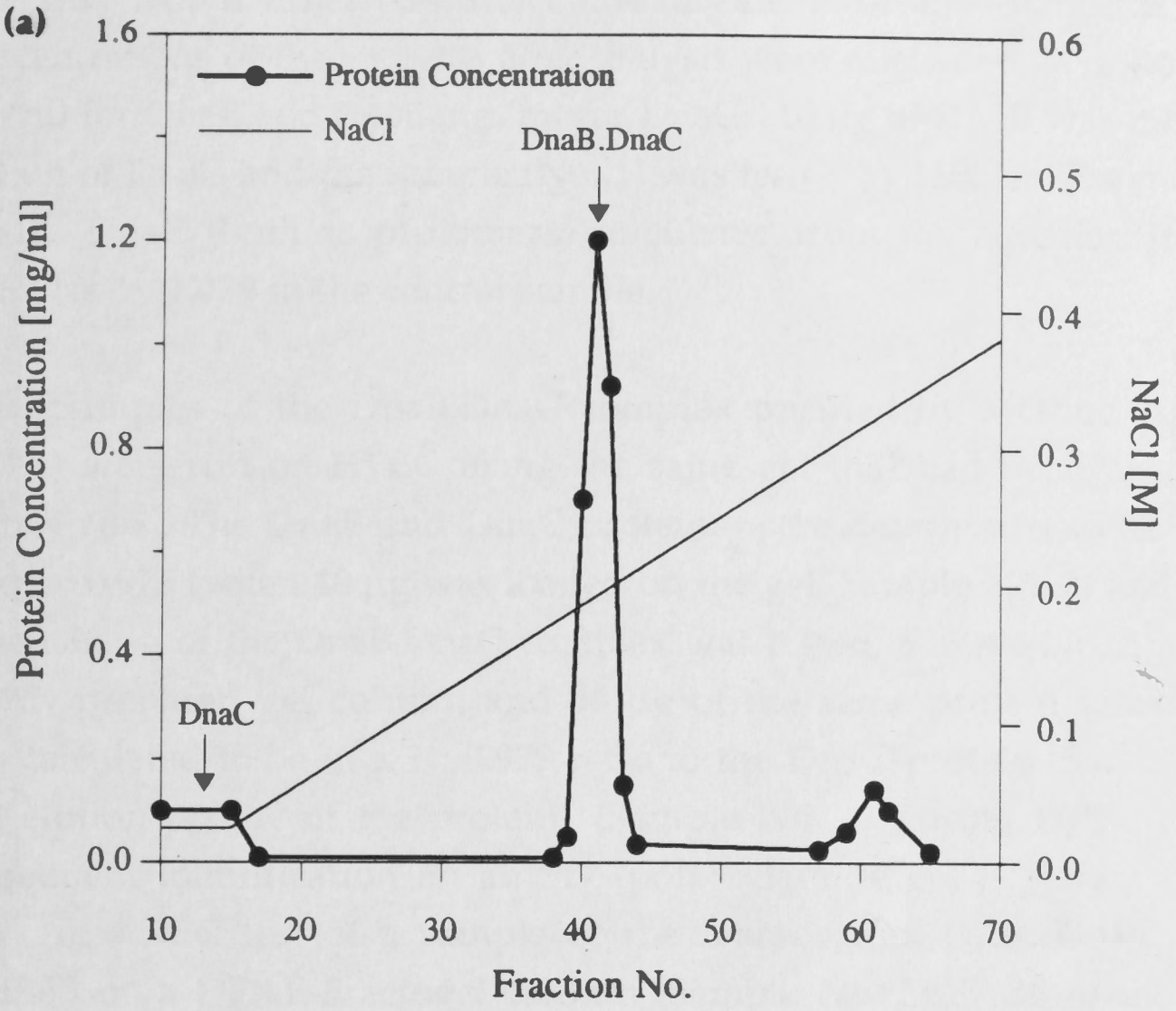
Protein Concentration
NaCl
DnaB.DnaC
DnaC
Protein Concentration [mg/ml]
NaCl [M]
Fraction No.
1.6
1.2
0.8
0.4
0.0
0.6
0.5
0.4
0.3
0.2
0.1
0.0
10
20
30
40
50
60
70

(b)

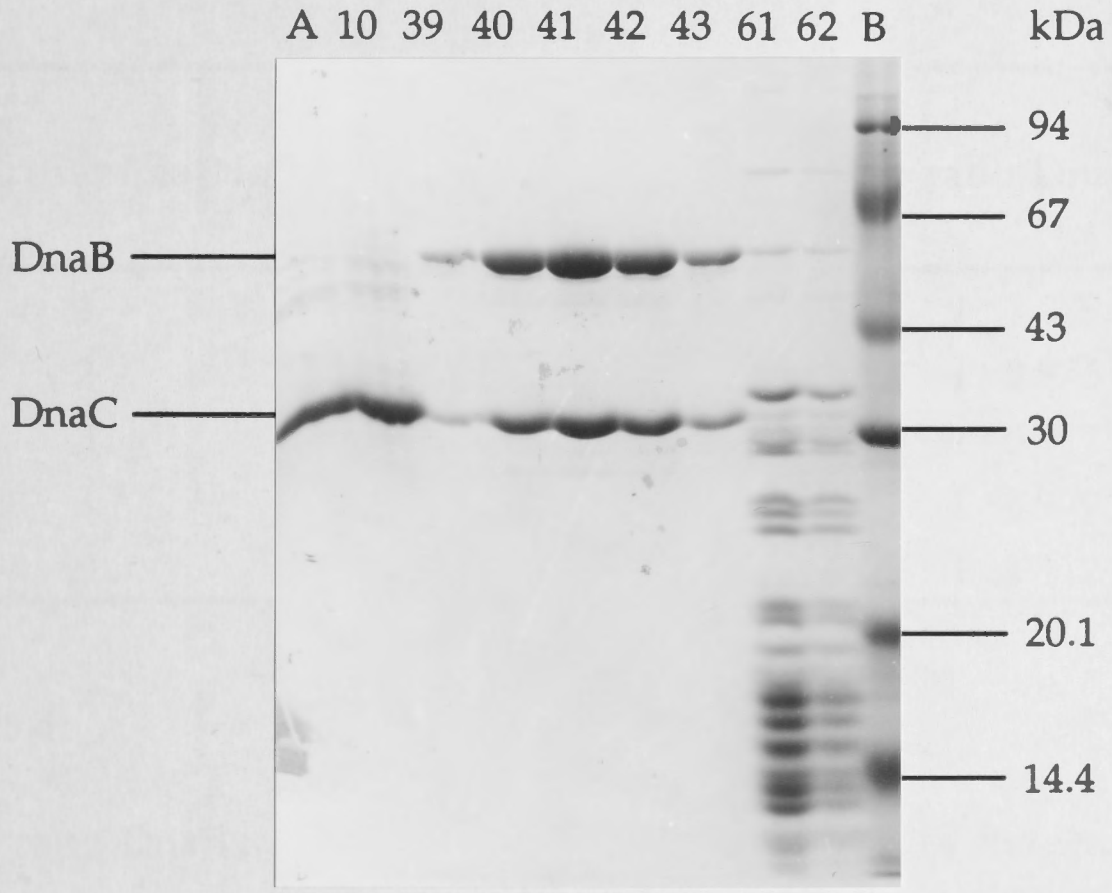
A 10 39 40 41 42 43 61 62 B
kDa
DnaB
DnaC
94
67
43
30
20.1
14.4

ATP that would otherwise affect measurements of absorbance at 280 nm. Concentrations of the proteins after dialysis were calculated (A_{280})to be 0.797 mg/ml for DnaB and 0.406 mg/ml for DnaC. 16 µg of DnaB was mixed with 8.54 µg of DnaC and the sample (No. 1) was tested by HPEC. The molar ratio DnaB : DnaC (both as protomers) calculated from the equation in Section 3.2.3 was 1 : 1.079 in the control sample.

Samples of the DnaB.DnaC complex purified by Method A (Section 3.2.1.1) were run on HPEC using the same gel that had been used for the control run. The DnaB and DnaC proteins were determined to be in molar ratio 1 : 0.975 (when 40 µg was loaded on the gel; Sample No. 2) and 1 : 0.977 (when 30 µg of the DnaB.DnaC complex was tested; Sample No. 3). Using a freshly-prepared gel column and 40 µg of the same protein sample, DnaB was calculated to be in a 1 : 0.979 ratio to the DnaC protein (Sample No. 4). The elution profile of the proteins (Sample No. 4) during HPEC and their subsequent identification on an SDS-polacrylamide gel is shown in Figure 3.8. An HPEC test of a sample of the reassociated DnaB.DnaC complex purified on a DEAE-Fractogel column (Sample No. 5; 25 µg of the protein) revealed the molar ratio DnaB : DnaC = 1 : 1.112. The results are summarized in Table 3.4.

Protein sample No.	Total protein [µg]	Molar ratio DnaB:DnaC
1	25	1 : 1.079
2	40	1 : 0.975
3	30	1 : 0.977
4	40	1 : 0.979
5	25	1 : 1.112

Table 3.4

Molar ratio DnaB : DnaC (as protomers) in samples of the DnaB.DnaC complexes prepared as indicated in the text (Section 3.3.2). The method is described in detail in Section 3.2.3. Molar extinction coeficients at 280 nm were calculated by the method of Gill and von Hippel (1989) to be ε_M(DnaB) = 29, 870 $M^{-1}cm^{-1}$ and ε_M(DnaC) = 22, 190 $M^{-1}cm^{-1}$.

Figure 3.8

(a) Elution profile of the DnaB.DnaC complex (Sample No. 4, Section 3.3.2) during the high-performance electrophoretic chromatography as was recorded by the printer connected to the HPEC system. The molar ratio DnaB : DnaC in the DnaB.DnaC complex purified by Method A (Section 3.2.1.1) was determined from this graph to be 1 : 0.979. The procedure is described in Section 3.2.3.

(b) Electrophoresis on a 12.5% SDS-polyacrylamide gel (Section 2.15) was used to identify proteins separated on HPEC. Protein markers in lane A are as in Figure 3.1. Proteins from the control experiment (Sample No. 1, Section 3.3.2) were loaded in lanes B and C. Fractions containing the DnaB protein (16 μg) were pooled, precipitated with trichloroacetic acid, mixed with the sample buffer (Section 2.15) and loaded in lane B. Fractions containing DnaC (8.54 μg) were treated in the same way and loaded in lane C. Protein from pooled HPEC fractions numbers 12 and 13 (Sample No. 4, Figure 3.8a) was precipitated with trichloroacetic acid and loaded in lane D, from 14 and 15 in lane E, 23 and 24 in lane G and the protein from fractions 27 and 28 was loaded in lane H.

(a)

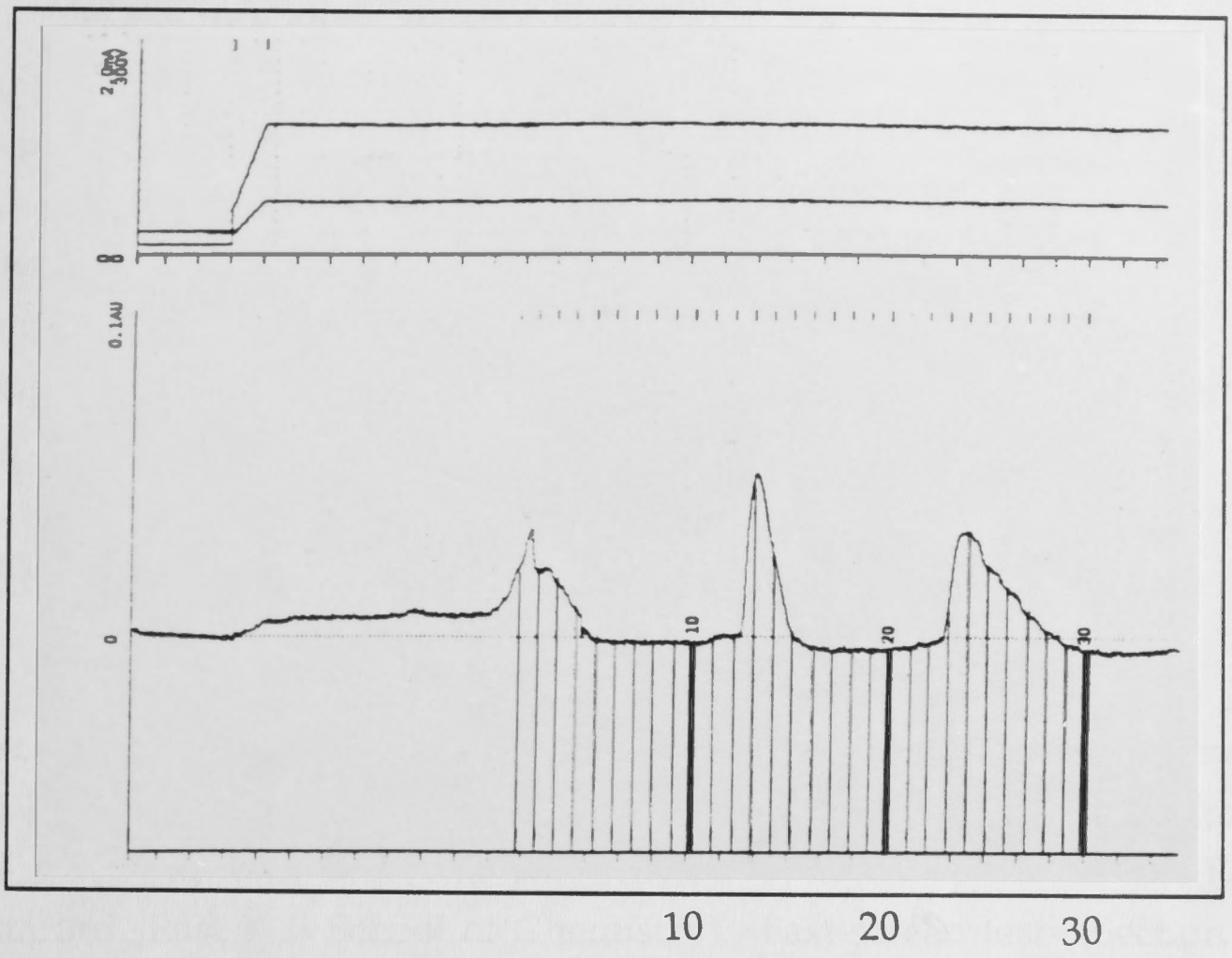

Fraction No.

(b)

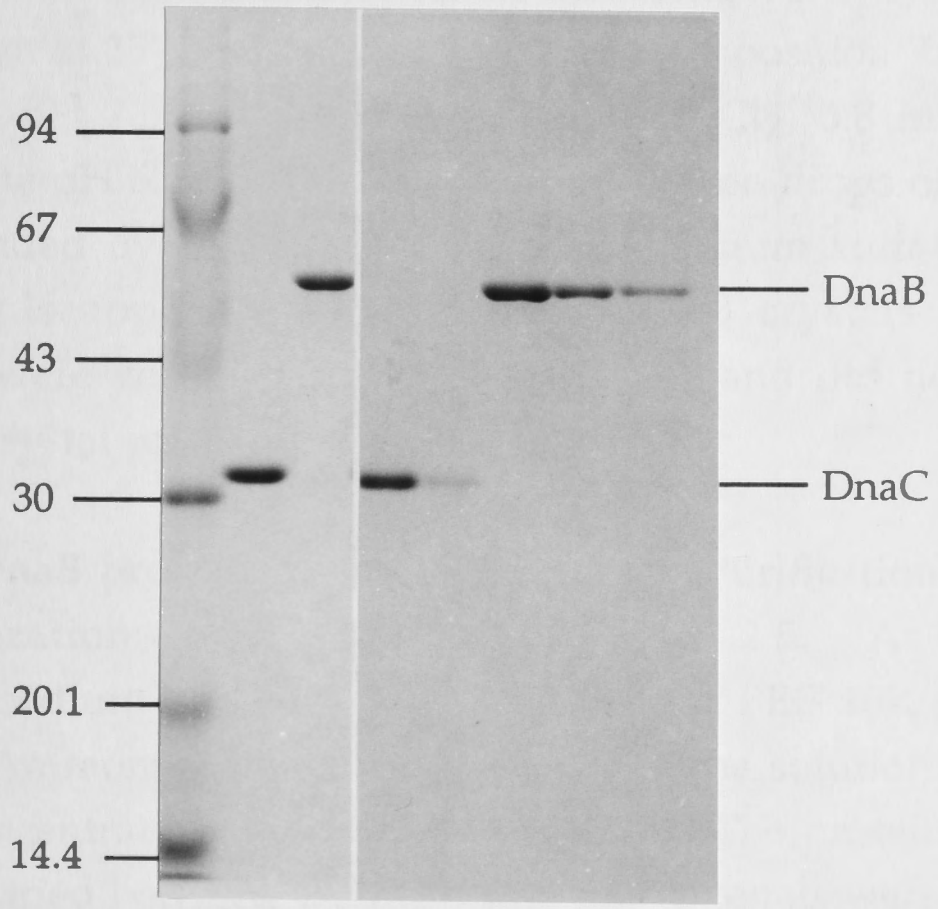

Taken together, stoichiometry of the DnaB and DnaC proteins in complexes tested by HPEC confirmed that an intact DnaB.DnaC complex can be purified using Method A or prepared by reassociation from separate proteins and purified afterwards. The DnaB.DnaC complex obtained in either way satisfied the strict requirements for crystallization of protein complexes, when a correct and accurate molar ratio of the proteins composing the complex is the primary prerequisite for growing crystals.

3.3.3 *Crystallization of the Proteins*

The hanging-drop method of protein crystallization was used as described in Section 3.2.5. Initial crystallization experiments were carried out in collaboration with Dr J. Thorn (Research School of Chemistry) using the DnaB protein and the DnaB.DnaC complex purified by Dr N.P.J. Stamford (Research School of Chemistry). Fast-screen tests (Section 3.2.5) of conditions for crystallization of the DnaB.DnaC complex were set up at 4°C and 25°C. The results identified PEG as a potentially useful precipitant. A wide range of conditions for crystallization of DnaB and the DnaB.DnaC complex was tested. The best result achieved were crystals of the DnaB protein grown at 25°C from a drop of initial composition 7.2 mg/ml DnaB, 8 mM HEPES pH 7.5, 1.6 mM DTT, 4 mM $MgCl_2$, 0.8 mM ATP, 100 mM sodium citrate pH 6.5 and 2% PEG 8K-20K. When drops of this composition were suspended over wells containing ammonium sulfate (0.4 - 0.6 M at 25°C), crystals appeared in two days. DnaB crystals prepared in this experiment were very thin in two dimensions and did not diffract X-rays. No protein crystal was obtained at 4°C.

The DnaB protein (fraction FIVB) from Purification A was prepared for crystallization as described in Section 3.2.5. As in the previous experiment, sodium citrate (100 mM) pH 6.5 and PEG 10K (2%) were used in the drops. Ammonium sulphate (0.4 M) was the solution in the reservoirs. Different concentrations of DnaB were tested. The protein concentration in drops was varied between 4.4 and 9 mg/ml. Crystals were prepared at 25°C as well as at 4°C. Those grown at 4°C were better formed and larger. Further experiments were therefore carried out only at this temperature. On mixing the protein with sodium citrate and PEG, a precipitate formed. Depending on the concentration of the protein, this appeared either immediately, the

next day or took as long as a few weeks (when the initial protein concentration was <5 mg/ml). The concentration of DnaB optimal for formation of large protein crystals was ~7 mg/ml. The first DnaB (Purification A) crystals (Figure 3.9) that were analyzed on the RAXIS-II X-ray diffractometer had been grown from 150 mM sodium citrate pH 6.5 and diffracted X-rays to 24 Å. Similar crystallization of the DnaB protein dialysed against Dial B containing 0.1 mM ADP instead of ATP provided crystals that did not diffract X-rays at all. Further crystallization experiments of DnaB (ATP-form) were set up over a range of pH and concentrations of sodium citrate. PEG 400, 3.4K, 8K, 10K and 20K of different concentrations were used. Although PEG was not essential for crystallization of DnaB, it affected the size of the crystals significantly. The kinetics of crystallization were regulated by the concentration of ammonium sulfate or sodium citrate (0.2 - 0.6 M) in wells. The best results were achieved using 100 - 150 mM sodium citrate buffer pH 6.25 - 6.5, 0.25 - 0.5 % PEG 10K in the drops and 0.4 M ammonium sulfate in the wells. Crystals were formed in 6 days. However, these bigger crystals did not diffract X-rays any better.

The same conditions for crystallization were used for the DnaB protein purified in the presence of ADP (Purification B2). The concentrations of ADP in crystallization buffers were varied between 0.1 and 0.25 mM. A crystal (0.08 x 0.08 x 0.7 mm) taken for X-ray diffraction analysis was exposed to 1.5418 Å radiation (50 kV, 100 mA) three times for 20 minutes. The crystal was kept stationary. An ordered diffraction pattern of discrete spots was obtained to about 14 Å resolution and a defined pattern of thermal diffuse scattering to 7 Å resolution was observed (Figure 3.10b). The dimensions of another DnaB (ADP-form) crystal prepared under the same conditions were 0.4 x 0.4 x 2 mm (Figure 3.10a) and it diffracted X-rays to 8 Å. The morphologies of all DnaB (Purification B2) crystals were trigonal prisms.

Crystallization experiments were focused on crystallization of the uncomplexed DnaB protein. Nevertheless, a few sets of crystallization experiments were also set up for the DnaB.DnaC complex (fraction FIVBC; Purification A) and the DnaC protein (fraction FIVC; Purification A). Proteins were prepared for crystallization as described in Section 3.5. The DnaB.DnaC complex formed hexagonal crystals from 100 mM sodium citrate pH 6 - 7 (Figure 3.9; ~0.625 mm in each dimension) at 4°C, but they were fragile, difficult to handle and did not diffract X-rays. Initial crystallization

Figure 3.9

(a) Crystals of the DnaB protein purified by Method A (Section 3.2.1.1). The DnaB protein (Fraction FIVB) was dialysed against buffer Dial B and concentrated in Amicon ultrafiltration cells and Centricon concentrators (Section 3.2.4) to ~7 mg/ml. 150 mM sodium citrate pH 6.5 was used as a crystallization reagent (Section 3.3.3). Crystals were prepared by the hanging-drop method (Section 3.2.5) at 4°C in six days and diffracted X-rays to 24 Å (Section 3.2.6).

(b) Crystals of the DnaB.DnaC complex (Purification A) were prepared (Section 3.3.3) from Fraction FIVBC dialysed against buffer Dial BC (Section 3.2.5), concentrated (Section 3.2.4) and mixed with sodium citrate pH 6.0 (100 mM). Crystals of size ~0.625 mm in each dimension did not diffract X-rays.

(a)

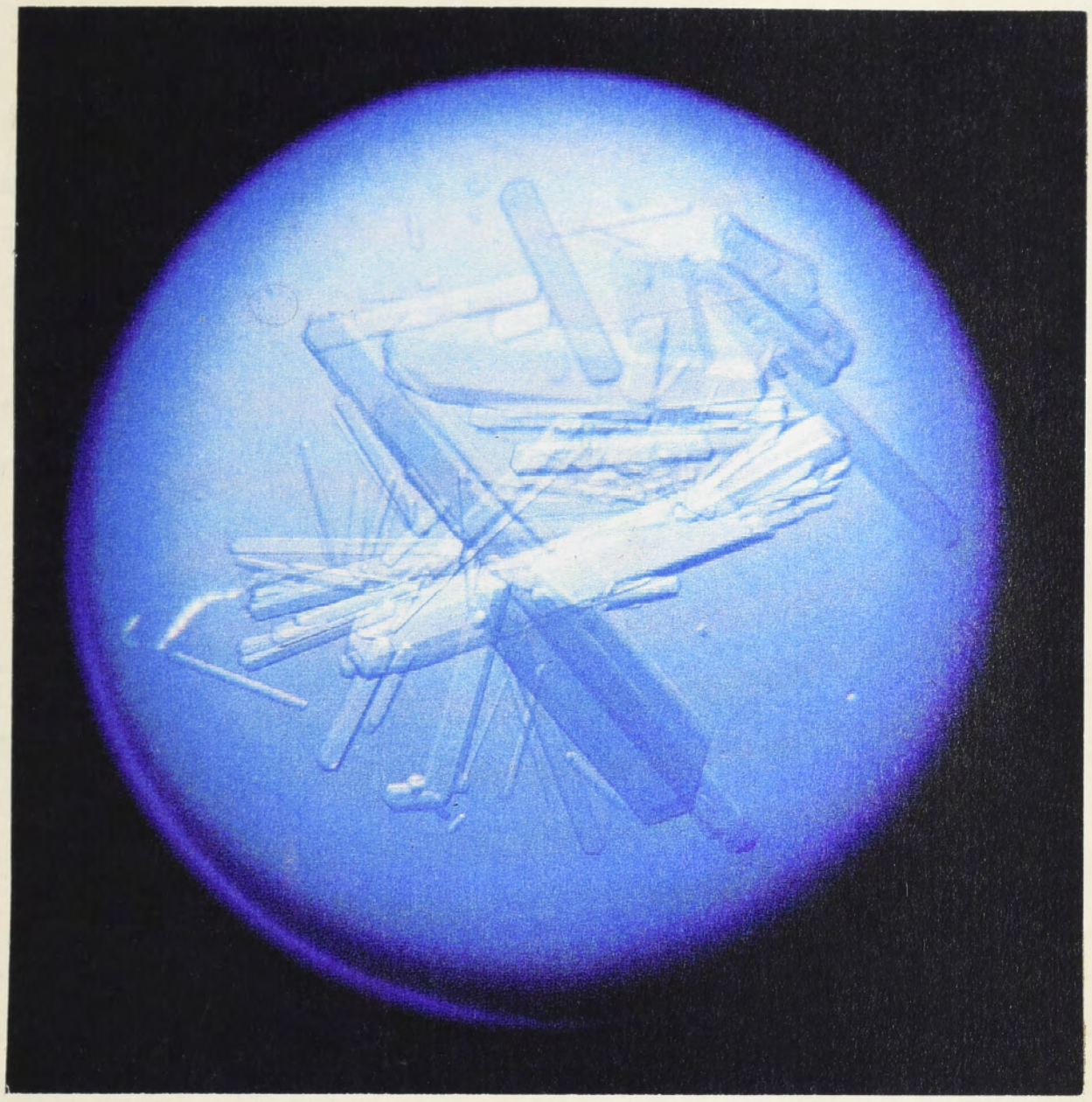

(b)

Figure 3.10

(a) Crystal of the DnaB protein complexed with ADP. The actual size of the crystal was measured to be 0.4 x 0.4 x 2 mm. The DnaB protein (Fraction FIVB; Purification B2) was dialysed against Dial B buffer (Section 3.2.5) containing 0.25 mM ADP instead of ATP and concentrated in a vacuum ultrafiltration apparatus (Section 3.2.4) to 7.7 mg/ml. The crystal was prepared by the hanging-drop method at 4°C using 100 mM sodium citrate pH 6.5 and 0.5% PEG 10K as crystallization reagents. The crystal was formed in 6 days and diffracted X-rays to ~8 Å.

(b) Photograph of the diffraction pattern of a DnaB-ADP crystal (0.08 x 0.08 x 0.7 mm) similar to the one presented in Figure 3.10a (Section 3.3.3). The diffraction pattern was obtained using 1.5418 Å radiation (50 kV, 100 mA). The crystal was kept stationary and exposed to the radiation three times for 20 minutes. X-rays were diffracted strongly at ~14 Å. A pattern of thermal diffuse scattering detected at ~7 Å may indicate discrete but so far undefined conformational transitions of parts of the molecules ordered within the lattice.

(a)

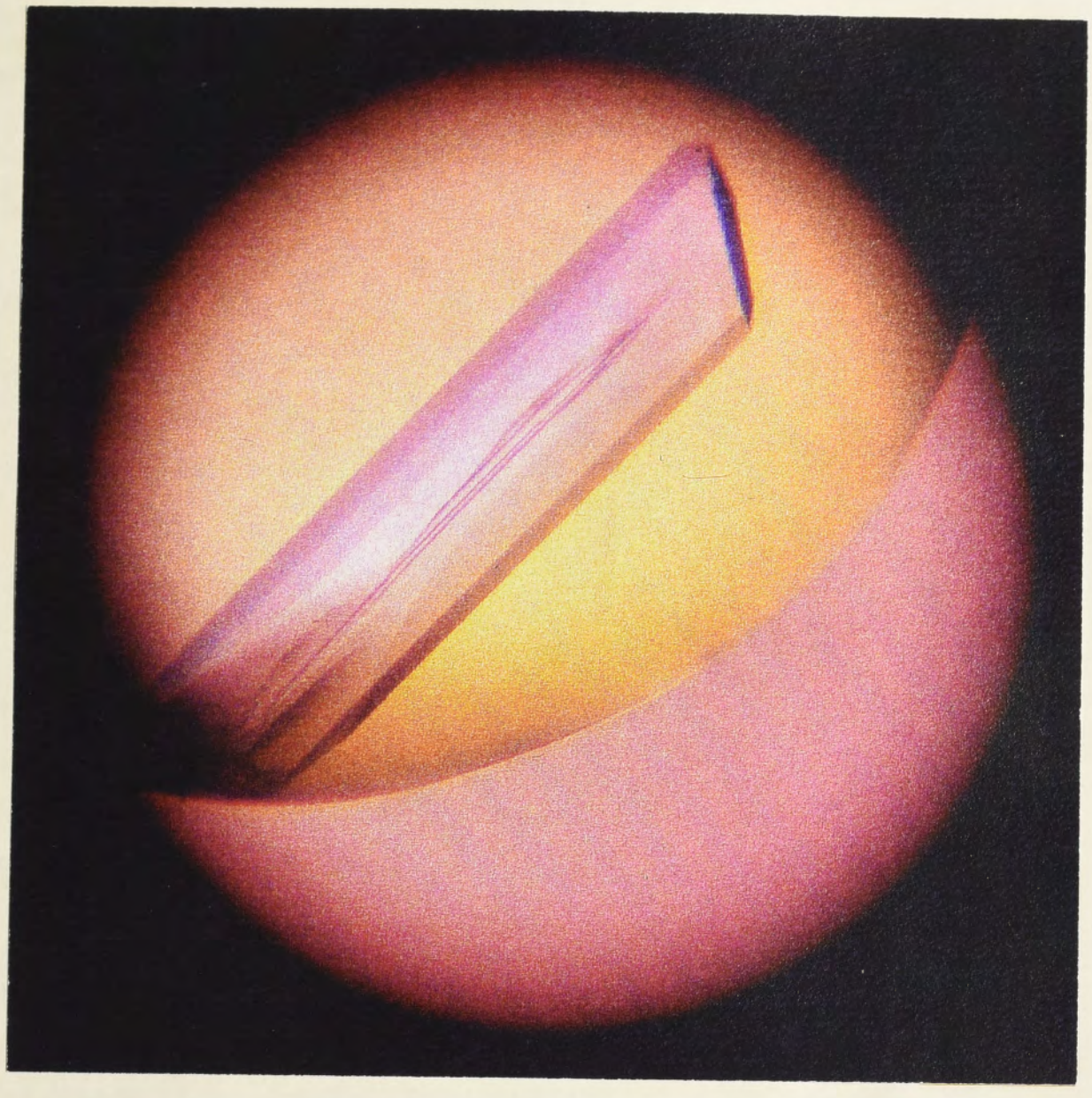

(b)

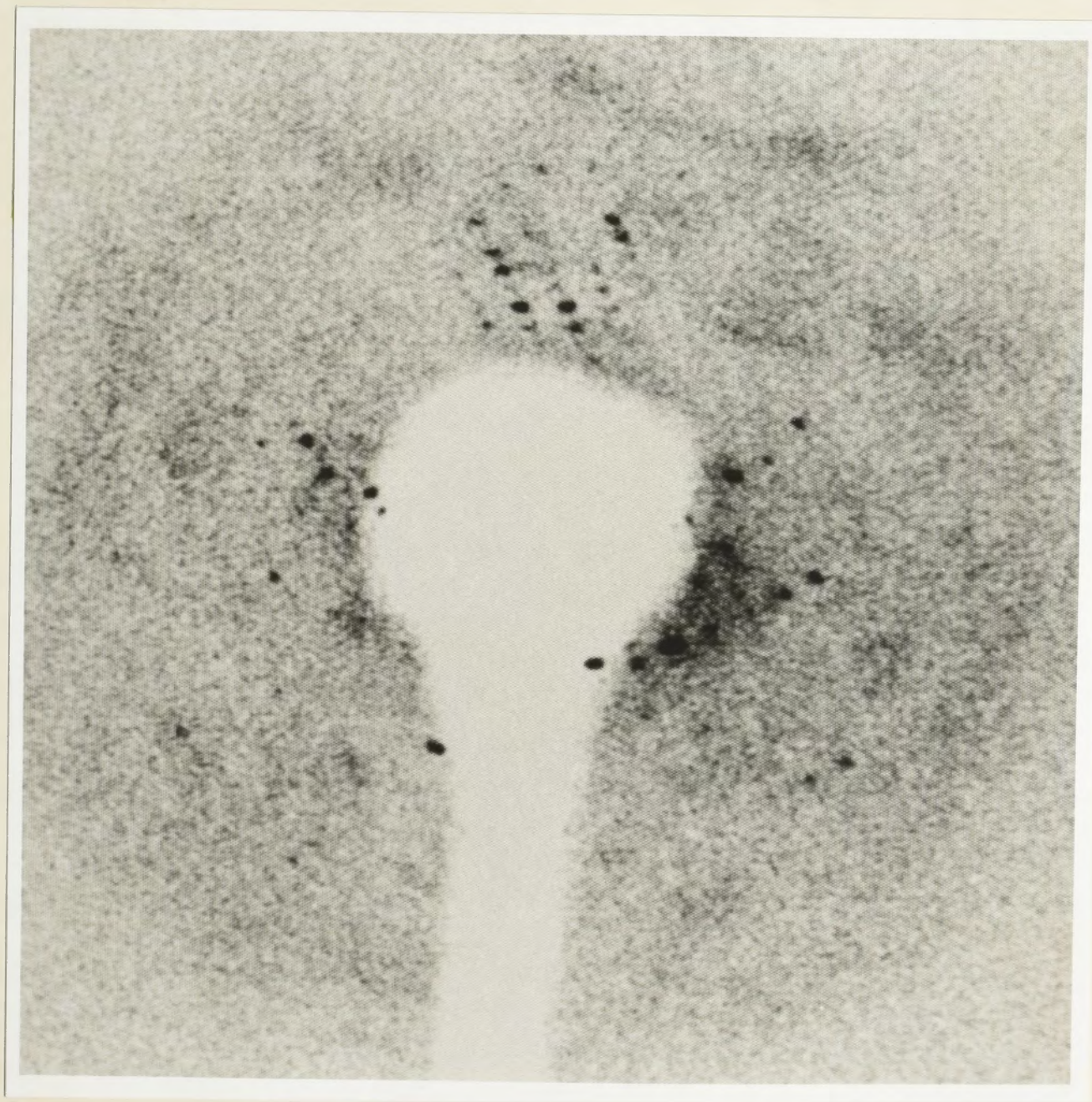

experiments only (a fast screen at 4°C) were performed with the purified DnaC protein, without production of any crystals.

3.4 Discussion

The first prerequisite for solving the three-dimensional structure of a protein by X-ray crystallography is a well-ordered crystal that diffracts X-rays to high resolution. One of the crucial parameters that affect formation of such crystals is purity of the protein. A protein to be crystallized should ideally be more than 97% pure, but the protein purity required for crystallization varies for different proteins. Some can accommodate a certain level of contamination, while for others, absolute purity is necessary.

The purification method of DnaB, DnaC and the DnaB.DnaC complex used by Stamford (1991) provided us with proteins of ~98% purity. Nevertheless, traces of the DnaC protein in DnaB after purification on the column of DEAE-cellulose and Sephacryl S400 were extremely undesirable because of the known interaction of DnaC with the DnaB protein. The DnaC contamination was probably due to the slight overlap between peaks of the DnaB protein and the DnaB.DnaC complex in the purification carried out by Stamford (1991). To improve protein resolution during anion-exchange chromatography, a shallower gradient of NaCl and DEAE-Fractogel resin were used. As documented in Figure 3.1, separation of DnaB and the DnaB.DnaC complex was complete.

The elution profile of the DnaB.DnaC complex showed a double-peak. Since dissociation of the complex was unlikely in the presence of 0.1 mM ATP and 5 mM $MgCl_2$, a possible explanation is that DNA (or oligonucleotides) still bound to the DnaB protein in fraction FII (Section 3.1.4.1) induces ATPase activity of the protein and as a consequence of this, not all subunits of the DnaB hexamer are in an ATP-bound form. It is probable that only some of them bind ATP, while others bind ADP, the product of ATP hydrolysis. To present this hypothesis schematically, some subunits of the $(adenosinephosphate)_6 . (DnaB)_6 . (DnaC)_6 . (adenosinephosphate)_6$ complex would be ATP.DnaB.DnaC.ATP and others ADP.DnaB.DnaC.ATP. In thermodynamic studies of the interactions of nucleotides with the DnaB helicase, Bujalowski and Klonowska (1993)

determined the intrinsic binding constants of fluorescent ATP- and ADP-analogues to be $K_{TNP\text{-}ATP} = (5.9 \pm 1) \times 10^5$ M^{-1} and $K_{TNP\text{-}ADP} = (2.1 \pm 0.4) \times 10^6$ M^{-1} respectively, confirming thus that ADP is bound to the DnaB hexamer even more strongly than ATP. The DnaC protein cannot bind ADP. A molecule of ATP is more tightly bound to DnaC ($K_D = 6 \times 10^{-6}$ M; Nakayama *et al.*, 1989a) than to DnaB ($K_D = 1.9 \times 10^{-5}$ M; Arai and Kornberg, 1989b). Therefore in solution containing ADP and ATP of concentrations just high enough to allow formation of the ATP complex with DnaC protein, DnaB can bind either ATP or ADP or might even be nucleotide-free.

Another possible explanation of the DnaB.DnaC double-peak is the presence of protein inpurities in fractions 24 - 29 (Figure 3.1), some of which might interact with the DnaB.DnaC complex and affect its affinity for the DEAE fractogel. In Purification A, fractions 26 - 36 (Figure 3.1) were pooled (fraction FIIIBC) and purified on Sephacryl S400. The final Fraction FIVBC was ~99% free of protein contaminants. However, crystals of the DnaB.DnaC complex, although of reasonable size (Section 3.2.3), did not diffract X-rays. Crystals of the DnaB protein from the same purification showed a diffraction pattern only at ~24 Å resolution.

In Purification B2 (Section 3.2.1.2), ADP was used instead of ATP to maintain the DnaB protein in a single conformation. However, this method could not give the DnaB.DnaC complex in a single and stable conformation either. According to Wahle *et al.* (1989a), 6 DnaC monomers interact with the DnaB hexamer to form the DnaB.DnaC complex, which is then stabilised by binding of one molecule of ATP to each DnaC monomer (Section 1.3.1). ADP cannot be bound to DnaC to stabilize the complex (Wahle *et al.*, 1989a). The results of hydroxyapatite chromatography (Section 3.2.1.2) were therefore not surprising.

Results of the reassociation of the DnaB.DnaC complex from partially purified DnaB and DnaC proteins (Section 3.2.1.3) confirmed this method as an acceptable alternative for a large-scale preparation of an intact DnaB.DnaC complex. The DnaB.DnaC complex obtained in the experiment was used for studying conditions of stability of the complex (data not shown). Results of its crystallization are therefore not available. However, they would probably be similar to those obtained with the DnaB.DnaC complex purified in Purification A.

The DnaB (Purification B2) crystals prepared under the same conditions as the DnaB (Purification B1) crystals (Section 3.2.3) diffracted X-rays to a resolution of ~8 Å. Nevertheless, patterns of thermal diffuse scattering still indicated the likely existence of discrete conformational transitions of parts of the molecules within the lattice. At this stage it is not possible to define these changes, but we can speculate about several alternatives, where they take place, what they are caused by, and how to eliminate (minimize) them.

There are several approaches that could help to solve the three-dimensional structure of the DnaB protein at atomic level, namely:

(a) stabilization of the conformation of wild-type (*wt*) DnaB by using ribonucleoside phosphate ligands of the correct type and relative ratio, and/or growing crystals of the *wt*DnaB protein complexed with DNA;
(b) stabilization of the DnaB conformation by introducing specific modifications into its amino-acid sequence (see Section 4);
(c) solving the structure of the separate domains of the DnaB monomer (see Section 5);
(d) solving the structure of analogues of the *E. coli* DnaB protein described in Section 1.4 or a functional analog from a thermophilic organism that is expected to be conformationally more stable at accessible temperatures than analogues from mesophilic bacteria,
(e) solving the structure of protein complexes of *E. coli* DnaB with *E. coli* DnaC analogues (*e.g.*, λP protein, Section 1.3.1);
(f) stabilization of protein crystals by cross-linking agents (*e.g.*, glutaraldehyde);
(g) low-temperature diffraction studies. This would require stabilization of crystals by cryoprotectants (*e.g.*, methylpentendiol, methanol, ethyleneglycol, glycerol, ethanol).

Growing protein crystals in the presence of different ribonucleotide ligands was shown as a necessity in the case of the bovine mitochondrial F_1-ATPase (Abrahams *et al.*, 1994). The F_1-ATPase which is involved in synthesis of ATP from ADP and inorganic phosphate is a complex of five different proteins with the stoichiometry $3\alpha : 3\beta : 1\gamma : 1\delta : 1\varepsilon$. The α- and β-subunits are homologous and both contain the same nucleotide-binding motif (G.X.X.X.X.G.K.T/S; Walker *et al.*, 1982). Whereas the nucleotides in the α-subunits do not change and their function is unknown, the structures of three catalytic sites, which are in the β-subunits, are always different.

Each of them passes through 'open', 'loose' and 'tight' states. The structure found in the crystal is compatible with one of the states to be expected in the cyclical binding change mechanism. In the crystal, each of the α-subunits and one β-subunit binds nucleoside triphosphate analogue, one β-subunit binds nucleotide diphosphate and one β-subunit is nucleotide-free. Interconversion of the states under native conditions may be achieved by rotation of the $\alpha_3\beta_3$ subassembly relative to the γ-subunit.

The DnaB helicase catalyses hydrolysis of ATP. The energy released in the reaction is, presumably, utilised in the unwinding of the DNA duplex. The DnaB protein contains the same nucleotide-binding motif as F_1-ATPase (Biswas and Biswas, 1987; Walker *et al.*, 1982) and was shown to be able to bind both ribonucleoside triphosphates and ribonucleoside diphosphate ligands (Arai and Kornberg, 1981b). The conformations of the ATP- and ADP-bound forms are different (Nakayama *et al.*, 1984b). One can speculate that each of the DnaB monomers might pass through similar cycles as do β-units of the F_1-ATPase. If this is the case, binding of the correct type of ribonucleotide ligand in the particular DnaB monomer might be the crucial factor to get well-ordered crystal of *wt*DnaB helicase.

For more details about options (b) and (c) see Sections 4 and 5 respectively. Work on *S. typhimurium* DnaB, P1 Ban protein and λP protein is now in progress (Dr N.E. Dixon, Ms P.E. Lilley). Stabilization of crystals by cross-linking agents or collecting diffraction data at subzero temperatures has not yet been examined extensively. This might potentially improve the resolution to which X-rays can be diffracted for any crystal of the DnaB protein.

4 DOMINANT-LETHAL MUTANTS OF THE *E. coli* DnaB PROTEIN

4.1 Introduction

X-ray diffraction analysis of DnaB crystals prepared under conditions identical except for the presence of ATP in one sample and ADP in the other gave ordered diffraction patterns of discrete spots to 24 Å and 8 Å, respectively (Section 3.3.3). These results suggested that stabilization of the DnaB molecule in a single conformation might be one of the decisive factors in growing crystals of quality suitable for high-resolution X-ray diffraction analysis.

A minimization of nucleotide-induced conformational changes in the molecule of DnaB should be also possible to achieve by specific modifications of the amino-acid sequence of the protein.

Several *S. typhimurium dnaB* mutants with dominant-lethal phenotypes were isolated and identified by Maurer and Wong (1988). The dominance of their lethal phenotypes indicated that the encoded proteins, although not fully functional, are structurally intact since they interfere with host DNA replication. Such mutations were identified in both domains of DnaB defined by proteolysis as well as in the protease-sensitive "hinge-region" of the DnaB molecule.

Considering the conformational changes that are induced in the DnaB molecule in connection with ATP hydrolysis, two types of the isolated *dnaB* mutants commended themselves as useful candidates for crystallization and high-resolution structural studies: (a) mutants with deficiency in hydrolysis of ATP, and (b) the "hinge-region" mutants (Maurer and Wong, 1988).

In an *S. typhimurium* ATPase$^-$ mutant, the nucleotide-binding motif (residues 230-237; Section 1.5) was affected by replacing arginine at residue 231 by cysteine (R231C mutant, Maurer and Wong, 1988). An *E. coli* DnaB-R231C analog (Shrimankar *et al.*, 1992, Marszalek and Kaguni, 1992) has been shown to be able to form hexamers, interact with ATP, ATPγS, ADP, and poly(dT), form complexes with DnaC, and stimulate activity of primase

in general priming. A dominant-negative effect of the mutant on replication of the *E. coli* chromosomal DNA has been demonstrated to be due to a profound deficiency in ATP hydrolysis and helicase activity. The dominant-lethal effect of DnaB-R231C *in vivo* was observed at 30°C as well as 42°C, suggesting that a properly-folded structure of the protein is expected to be stable also upon overexpression induced at 42°C.

The non-mutated "hinge-region" is presumed to be the part of the DnaB molecule that undergoes changes in conformation during hydrolysis of ATP, as reflected by its different sensitivity to trypsin in the ATPγS-bound form compared with the ADP-bound form (Nakayama *et al.*, 1984b). Mutations in this region could therefore potentially stabilize the DnaB molecule in a single conformation too.

Oligonucleotide-directed mutagenesis of the *E. coli dnaB* gene, performed with a view to prepare DnaB molecules that would be conformationally stable, is reported in this chapter. The mutant proteins were purified on a large scale and DnaB-R231C was crystallized.

4.2 Materials and Methods

4.2.1 *Construction of Phagemid pND604*

Phagemid vector pTZ18U (Mead *et al.*, 1986) was used for subcloning of the *dnaC*$^+$*dnaB*$^+$ operon from pPS562 (performed by Dr N.E. Dixon). Plasmid pPS562 was digested with *Bam*HI and *Eco*RI enzymes and a 2897-bp fragment containing the intact *dnaC* and *dnaB* genes was isolated and inserted between the corresponding sites of pTZ18U. Competent cells of AN2666 were transformed with the product of ligation and double-stranded phagemid DNAs from separate transformants were analyzed by *Bam*HI/*Eco*RI and *Eco*RI/*Nco*I double digests. A phagemid of predicted construction was designated pND604 (Figure 4.1). Strain RSC937 (AN2666/pND604) was used for preparation of ssDNA templates for oligonucleotide-directed mutagenesis (Section 2.16).

Figure 4.1

A scheme for construction of phagemid pND604, ssDNA of which was used in oligonucleotide RSC89-directed mutagenesis of the *dnaB* gene. The mutagenesis provided pND711 (*dnaB-R231C*$^+$, *dnaC*$^+$). Details of the genetic manipulations are in Sections 4.2.1 and 4.2.2.

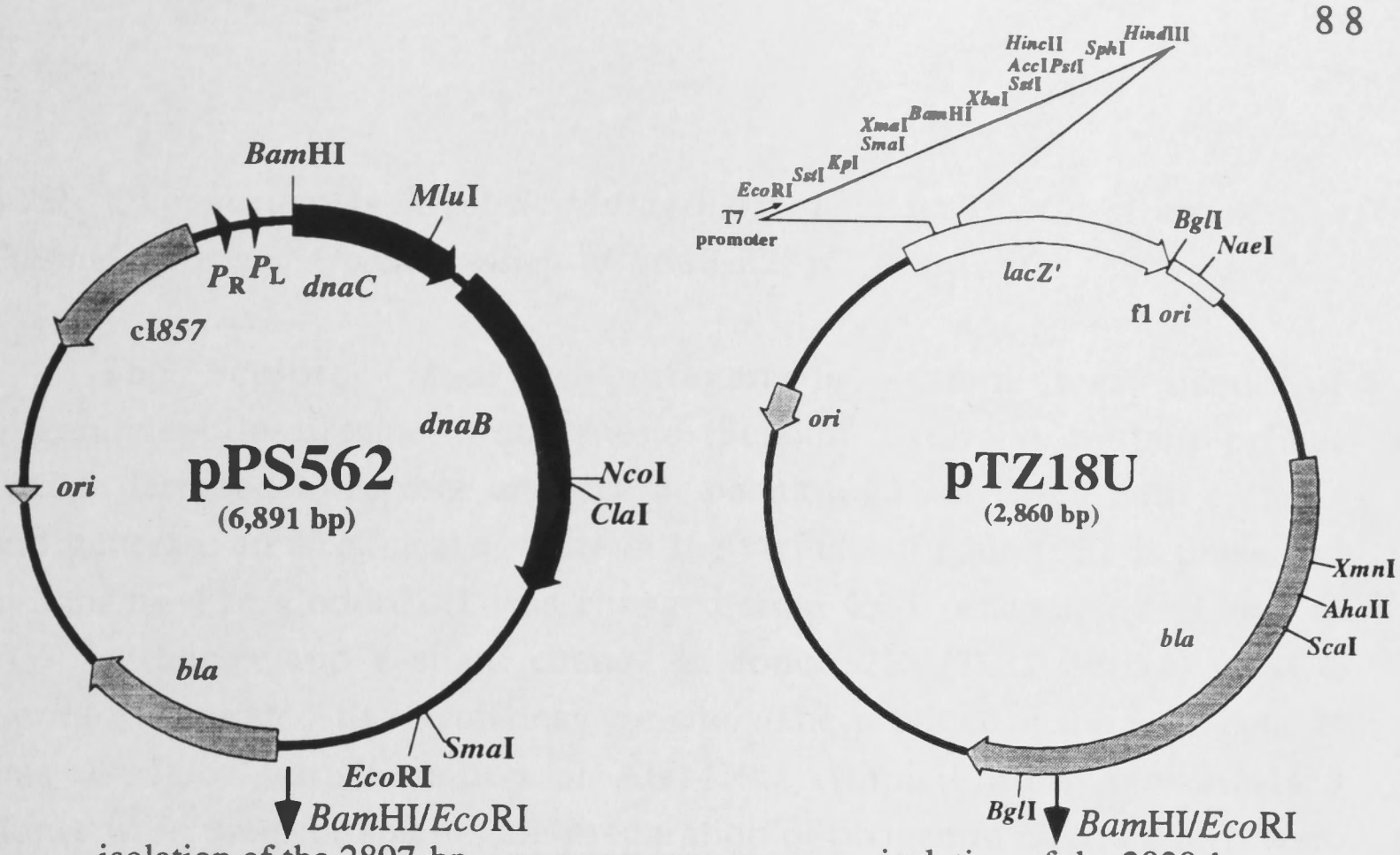
BamHI
MluI
PR PL
dnaC
cI857
dnaB
pPS562
(6,891 bp)
ori
NcoI
ClaI
bla
SmaI
EcoRI
BamHI/EcoRI
isolation of the 2897-bp
dnaC+dnaB+ fragment
HincII SphI HindIII
AccI PstI
SstI
XbaI
XmaI BamHI
SmaI
KpI
SstI
EcoRI
T7
promoter
BglI
NaeI
lacZ'
f1 ori
ori
pTZ18U
(2,860 bp)
XmnI
AhaII
ScaI
bla
BglI
BamHI/EcoRI
isolation of the 2839-bp
fragment
ligation
BamHI
BglI
NaeI
f1 ori
XmnI
AhaII
ScaI
dnaC
bla
pND604
(5,736 bp)
dnaB
BglI
NcoI
ori
T7 promoter
EcoRI
mutagenesis (mutant primer RSC89)
BamHI
BglI
NaeI
f1 ori
XmnI
AhaII
ScaI
dnaC
bla
pND711
(5,736 bp)
dnaB
R231C
BglI
NcoI*
NcoI
ori
T7 promoter

4.2.2 *Oligonucleotide-directed Mutagenesis of* dnaB - *Construction of a Plasmid Directing Overexpression of* dnaB-R231C *and* dnaC

The Sculptor *in-vitro* mutagenesis system was used for oligonucleotide-directed mutagenesis (Section 2.16). A mutant primer RSC89 designed to replace arginine at position 231 of DnaB with cysteine and generate an *Nco*I cleavage site in the vicinity of codon 231 is presented in Scheme 4.1. Codon 231 was changed from CGT (encoding arginine) to TGT (cysteine), and a silent change in codon 233 [TCG (serine) to TCC (serine)] generated the *Nco*I cleavage site. The product of the mutagenesis was used for transformation of AN1459. Ampicillin-resistant AN1459 clones were used for small-scale preparation of phagemid DNAs which were then analysed by a *Bam*HI/*Nco*I double digest. Identification of a 1500-bp fragment indicated the presence of a new *Nco*I site downstream of the mutated codon 231. A 1698-bp *Bam*HI-*Nco*I fragment was the result of the cleavage of phagemids containing the non-mutated *dnaB* gene. The sequence of the mutated region was confirmed by dideoxy sequencing and the mutant DNA was designated pND711 (5736 bp, Figure 4.1). The mutant *E. coli dnaB* gene will be designated *dnaB-R231C* and its encoded protein will be referred to as DnaB-R231C.

A 2897-bp *Bam*HI-*Eco*RI fragment of pND711 containing *dnaC* and *dnaB-R231C* was isolated after a *Bam*HI/*Eco*RI/*Bgl*I-triple digest of the phagemid and ligated between the *Bam*HI and *Eco*RI sites of pMA200U (Elvin *et al.*, 1990). The product of ligation was used for transformation of AN1459. Ampicillin-resistant transformants were selected at 30°C and plasmid DNAs from separate clones were analysed by *Bam*HI/*Eco*RI and *Bam*HI/*Nco*I double digests. The results of digestions identified strains harbouring the recombinant plasmid containing the $dnaC^{+}dnaB\text{-}R231C^{+}$ operon under the control of P_R and P_L promoters (pND712, 7039 bp; Figure 4.2). Overproduction of DnaB-R231C and DnaC was tested at 42°C (Figure 4.4). The experiment described in this section was performed by Dr N. E. Dixon.

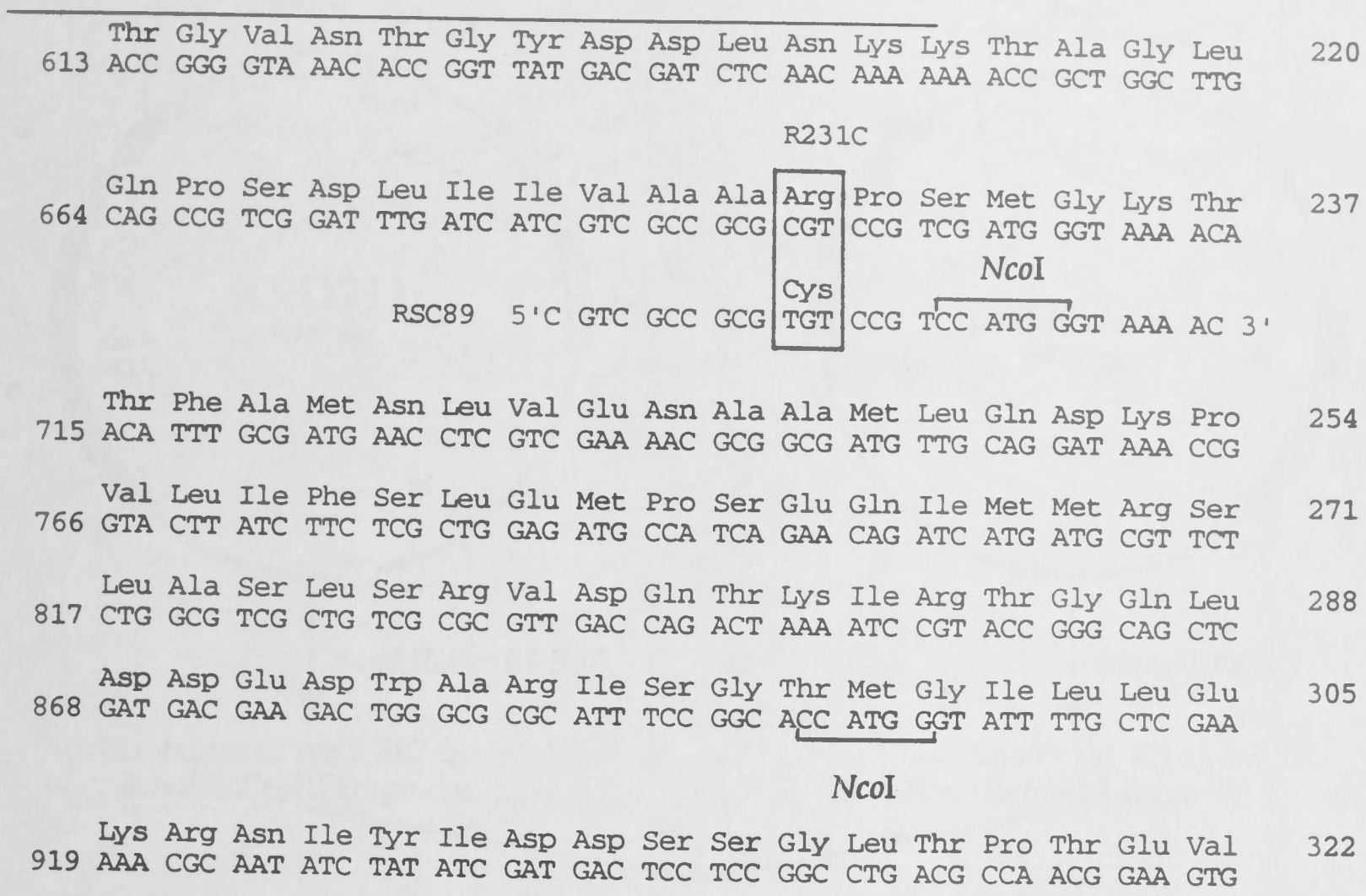

Scheme 4.1

A strategy for site-directed mutagenesis of codon 231 of the *dnaB* gene. Presented is the *dnaB* sequence between nucleotides 613 and 969. In the case of successful mutagenesis directed by mutant primer RSC89, the codon 231 (CGT) encoding arginine was replaced by codon TGT for cysteine. A mutation in codon 233 generated an *Nco*I site, which was used for screening of phagemid DNAs after transformation of strain AN1459 with the product of the mutagenesis and selection of ampicillin-resistant transformants at 30°C. The product of successful mutagenesis of *dnaB* codons 231 and 233 in pND604 was designated pND711 (Figure 4.1)

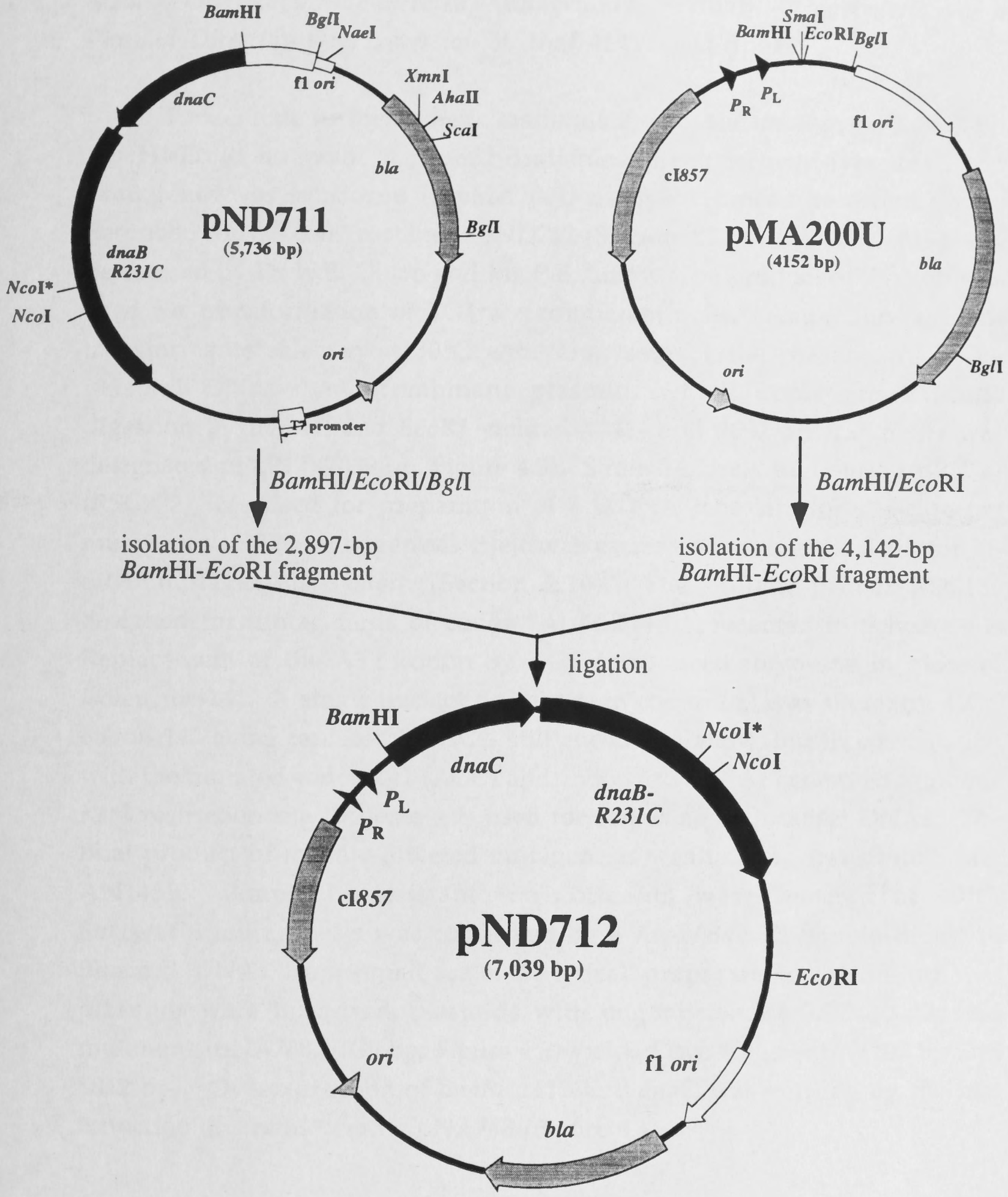

Figure 4.2

Subcloning of the *Bam*HI-*Eco*RI *dnaC*$^+$-*dnaB-R231C*$^+$ fragment of pND711 in pMA200U provided pND712, which directed high-level overexpression of both genes (Figure 4.4).

4.2.3 *Oligonucleotide-directed Mutagenesis of* dnaB - *Construction of a Plasmid Directing Overexpression of* dnaB-I141T *and* dnaC

To facilitate further genetic manipulations of the *dnaB* gene, a 2897-bp *Bam*HI-*Eco*RI fragment of pPS562 containing the intact wild-type *dnaC* and *dnaB* genes was subcloned in pMA200U using the procedure essentially as described for the construction of pND712 (Section 4.2.2). The subcloning was performed by Dr N.E. Dixon and Ms P.E. Lilley. The product of ligation was used for transformation of TG1*recA* competent cells. Ampicillin-resistant transformants selected at 30°C were analysed for the presence of ~7-kb plasmid DNA. A recombinant plasmid, which upon simultaneous digestion by *Bam*HI and *Eco*RI yielded 4142- and 2897-bp fragments was designated pPL717 (7039 bp; Figure 4.3). Strain TG1*recA* harbouring pPL717 (RSC972) was used for preparation of a ssDNA template for site-directed mutagenesis. The mutagenesis itself was carried out using the Sculptor *in-vitro* mutagenesis system (Section 2.16). The mutant primer RSC130 designed for mutagenesis of codon 141 (ATT) is presented in Scheme 4.2. Replacement of the ATT codon by ACC introduced threonine in place of isoleucine-141. A single nucleotide change in codon 142 was silent: the GCC codon 142 being replaced by GCG still encoded alanine, but in combination with the mutated codon 141 (ACC) and codon 143 (GAA) generated a unique *Ksp*I restriction site (Scheme 4.2) used for screening of plasmid DNAs. The final product of the site-directed mutagenesis was used to transform strain AN1459. Ampicillin-resistant transformants were selected at 30°C. Successful mutagenesis was confirmed by a *Ksp*I/*Bam*HI-double digest of plasmid DNAs from small-scale analytical preparations. Non-mutated plasmids were linearised, plasmids with oligonucleotide RSC130-directed mutations (pNA788, 7039 bp; Figure 4.3) yielded two fragments (1227 bp and 5812 bp). Overexpression of *dnaB-I141T* and *dnaC* was verified by thermal induction of strains bearing pNA788 (Figure 4.4).

4.2.4 *Purification and Crystallization of DnaB-R231C and DnaB-I141T*

Dominant-lethal mutants DnaB-R231C and DnaB-I141T were purified from strains RSC990 (AN1459/pND712, pLysS) and RSC2047 (AN1459/pNA788, pLysS), respectively.

Figure 4.3

Construction of pPL717, a derivative of phagemid pMA200U. Using pPL717, ssDNA containing the coding strands of the *dnaC* and *dnaB* genes was produced for use as a template for site-directed mutagenesis. Plasmid pNA788 was then immediately available for high-level expression of *dnaC* and *dnaB-I141T*. Details of genetic manipulation are described in Section 4.2.3.

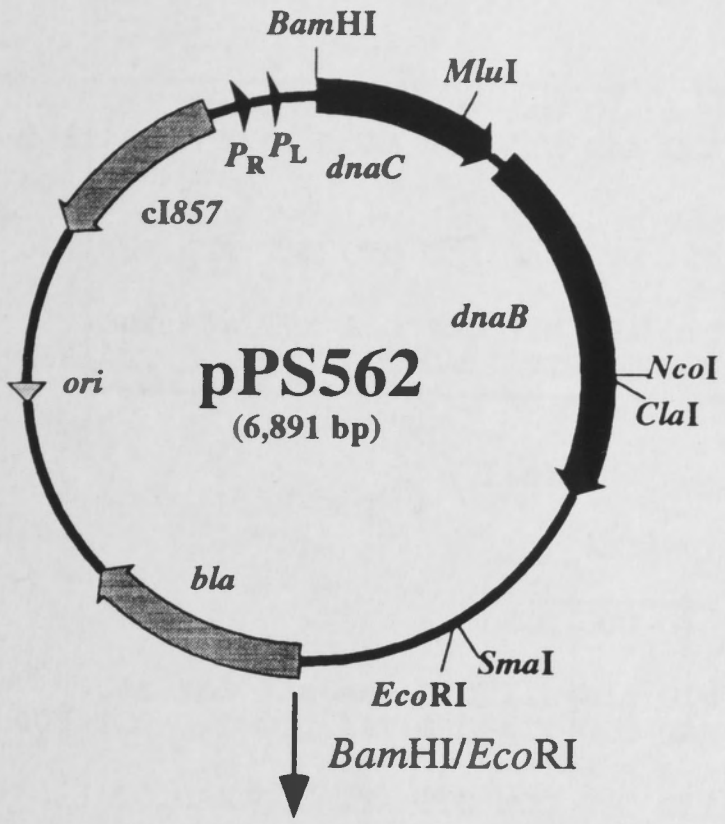

BamHI/EcoRI

isolation of the 2897-bp
dnaC$^+$*dnaB*$^+$ fragment

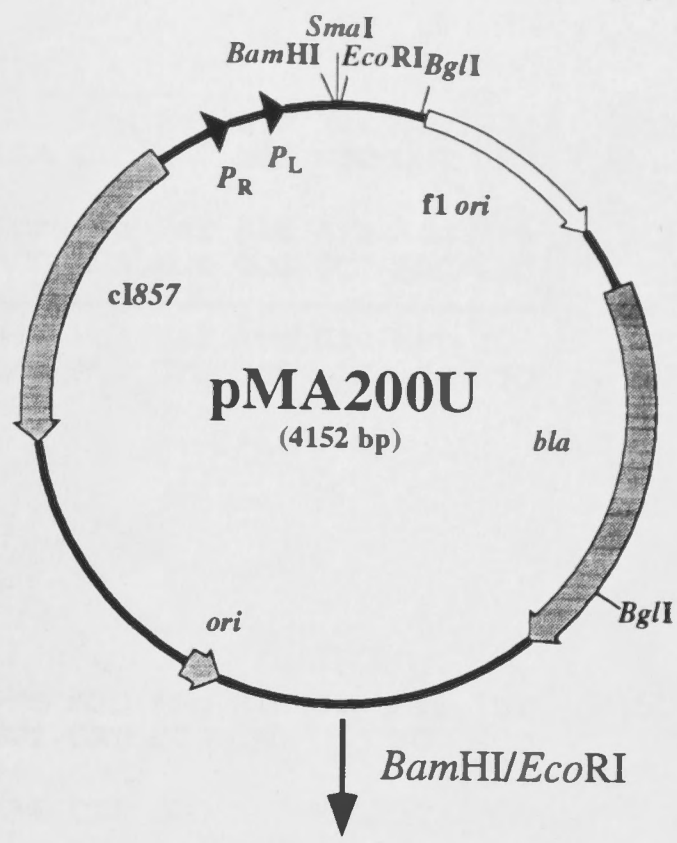

BamHI/EcoRI

isolation of the 4142-bp
fragment

ligation

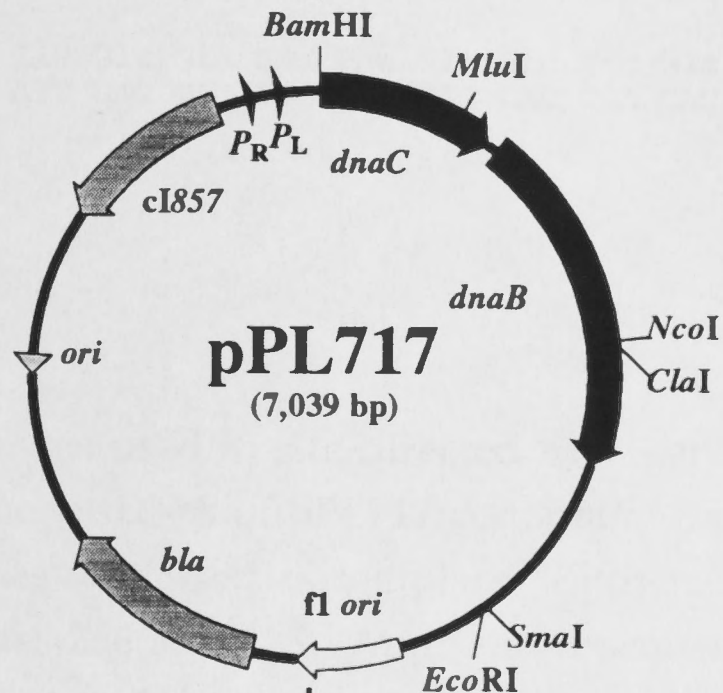

mutagenesis
(mutant primer RSC130)

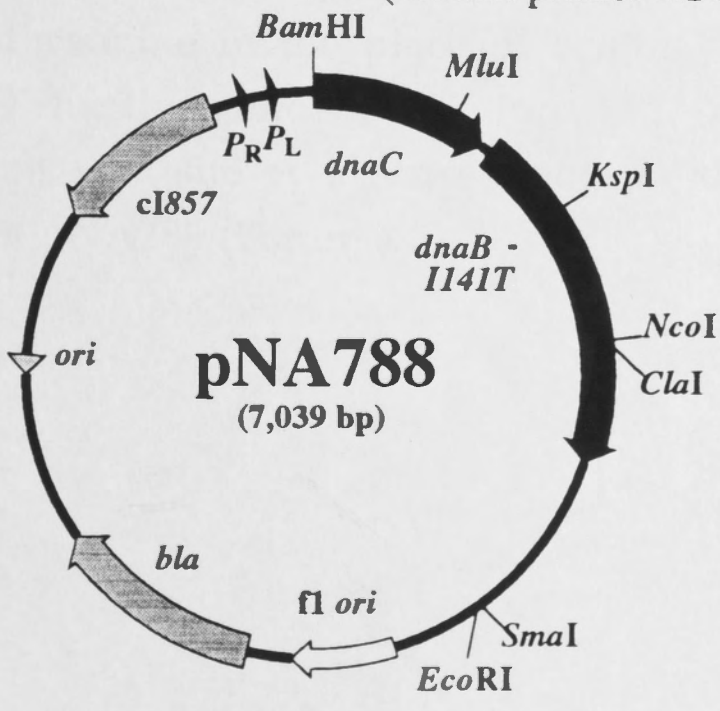

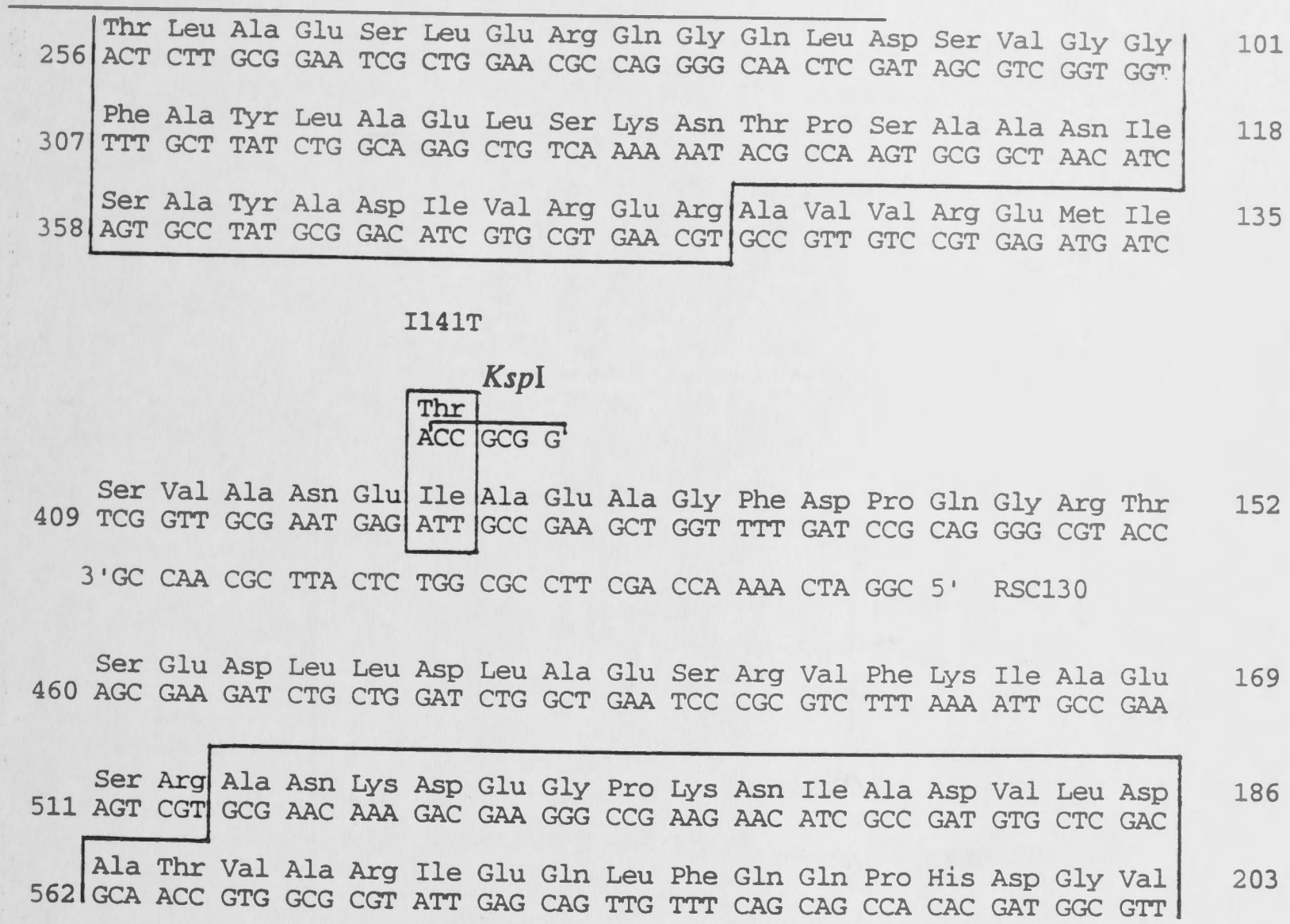

Scheme 4.2

Mutant primer RSC130 was used in site-directed mutagenesis of codons 141 and 142 of the *dnaB* gene. ssDNA of pPL717 containing the coding strand of the *dnaC* and *dnaB* genes was used as template. Shown is the sequence of *dnaB* between nucleotides 256 and 613. Amino acid sequences of the part of NH_2-terminal domain (residues 85 - 126) and part of COOH-terminal domain (residues 173 - 203) are indicated. Successful mutagenesis generated codon ACC encoding threonine in the place of original codon 141 (ATT; isoleucine), and GCG in the place of codon 142 (originally GCC). Introduction of a unique *Ksp*I site as a consequence of the mutations was used for identification of pNA788 (Figure 4.3).

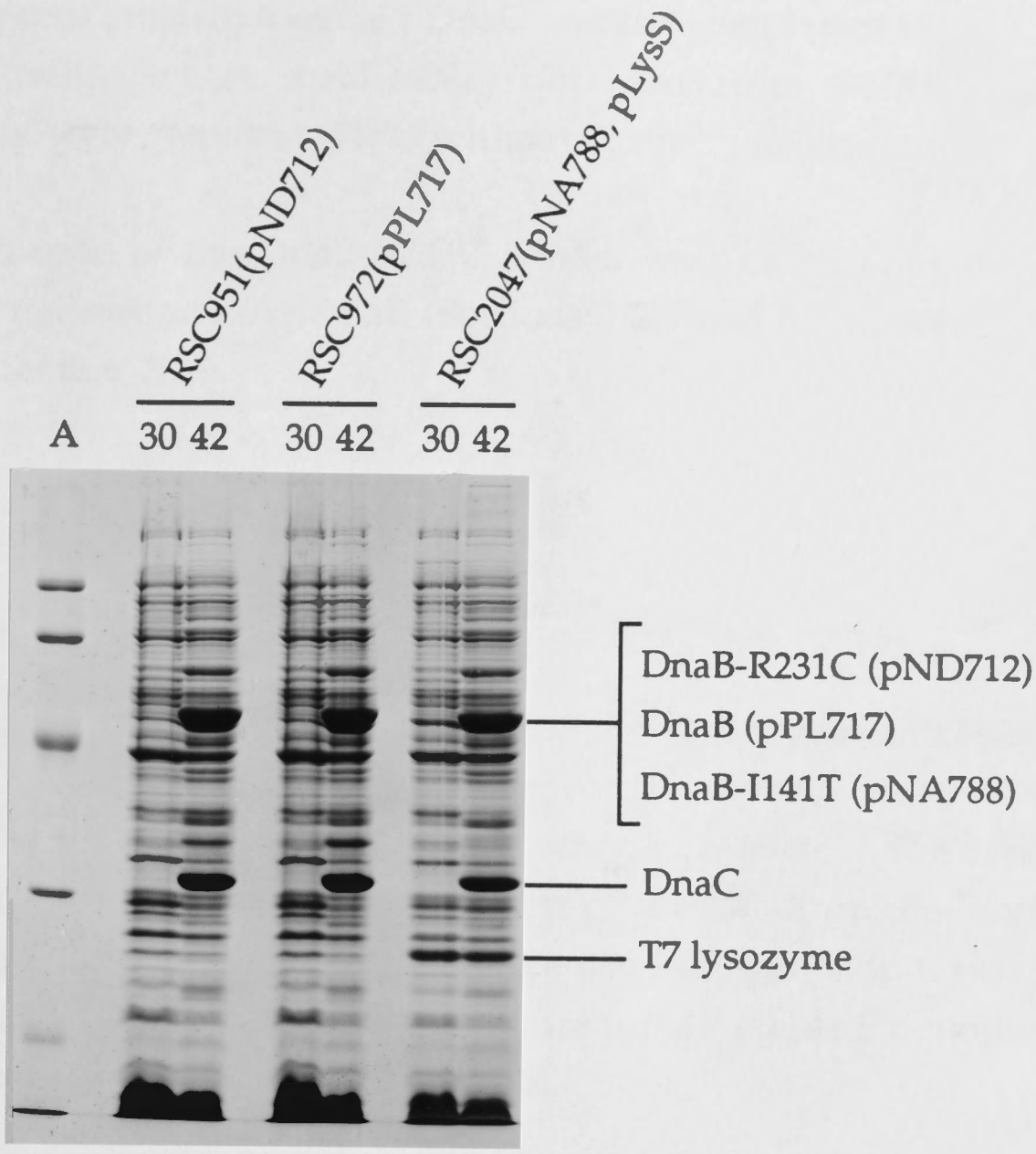

Figure 4.4

SDS-PAGE of cell lysates. Cultures (20 ml) of RSC951 (AN1459/pND712), RSC972 (AN1459/pPL717), and RSC2047 (AN1459/pNA788, pLysS) were grown at 30°C to A_{595}~0.5 in the presence of ampicillin (50 μg/ml) as described in Section 2.2. Cells were harvested from a portion (1 ml) and the remainder of the culture was incubated at 42°C with vigorous shaking. After 4 hours, further 1-ml samples were taken. The sedimented cells were resuspended to A_{595}=10 in SDS-gel loading buffer (Section 2.15) and treated for 2 min at 95-100°C. Portions (20 μl) were loaded on a 12.5% SDS-polyacrylamide gel and electrophoresed as described in Section 2.15. Protein markers in lane A were as in Figure 3.1. Overproduction of the particular proteins is indicated.

The purification procedure was essentially as described in Section 3.2.1.2. Fractions of partially-purified DnaC and the complex of DnaC with the mutant DnaBs (where applicable) obtained from DEAE-Fractogel chromatography were stored at -70°C without further purification.

Crystallization of the DnaB-R231C protein was carried out using the method for crystallization of *wt*DnaB (Sections 3.2.5 and 3.3.3); crystals were analysed as in Section 3.2.6.

4.3 Results

In attempts to obtain a preparation of the DnaB protein containing molecules of DnaB in a single and stable conformation, two dominant-lethal mutants were prepared: *dnaB-R231C* and *dnaB-I141T*. The missense mutation of codon 231 resulted in expression of the DnaB protein deficient in ATPase and helicase activities. Replacement of the codon 141 (ATT encoding isoleucine) by ACC (encoding threonine) yielded a dominant-lethal "hinge-region" mutant of DnaB.

4.3.1 *ATPase⁻ Mutant of the DnaB Protein*

The *E. coli dnaB-R231C* mutant - an analog of *S. typhimurium dnaB-R231C* (Maurer and Wong, 1988) - was prepared by Shrimanakar *et al.* (1992). The gene was subcloned and overexpressed in the Studier T7-promoter expression system (1990). Shrimankar *et al.* (1992) observed that cell growth was very sensitive to background expression of DnaB; the lethal effect of DnaB-R231C was even more profound. In our case, having the intact *dnaC⁺dnaB⁺* operon subcloned in a tightly-regulated derivatives of vector pCE30 (Elvin *et al.*, 1990) under the control of tandem $\lambda P_R P_L$ promoters, we chose to prepare our own system for overexpression of this ATPase⁻ mutant.

ssDNA utilized in oligonucleotide-directed mutagenesis was prepared from pND604 - a derivative of pTZ18U containing the *Bam*HI-*Eco*RI *dnaC⁺dnaB⁺* fragment of pPS562 (Section 4.2.1; Figure 4.1). Because of the orientation of the fragment (Figure 4.1), expression of *dnaC* and *dnaB* from

the *lac* promoter of the vector was not possible. The site-directed mutagenesis was carried out as described in Section 4.2.1. Phagemid pND604 having the original *dnaB* codon 231 encoding arginine replaced with a TGT codon for cysteine was designated pND711 (Figure 4.1). pND711 was used as a source of the mutant *dnaC*$^+$*dnaB-R231C*$^+$ operon, which was subcloned downstream of the tandem P_RP_L promoters of pMA200U yielding phagemid pND712 (Section 4.2.1; Figure 4.2). Simultaneous overproduction of the DnaB-R231C protein and DnaC directed by pND712 (strain RSC951) is documented in Figure 4.4. There was no apparent effect of the mutant plasmid on cell growth at 30°C.

In order to make the lysis of the cells (strain RSC951) easier in purification of the ATPase$^-$ DnaB-R231C mutant protein, plasmid pLysS (*cat*$^+$) was introduced into the strain. Overproduction of DnaB-R231C, DnaC and T7 lysozyme in strain RSC990 (RSC951/pLysS) is illustrated in Figure 4.4. The purification of DnaB-R231C was performed as described in Section 4.2.4. The elution profile of the proteins from DEAE-Fractogel showed good resolution of DnaB-R231C and the DnaB-R231C.DnaC complex (Figure 4.5). The DnaB-R231C.DnaC complex was apparently eluted in a single peak. This fact supports the hypothesis that the elution profile of the *wt*DnaB.DnaC complex from chromatography on DEAE-Fractogel in the presence of ATP (Purification A; Section 3.3.1.1) formed a double peak due to some of the DnaB molecules forming a complex with ATP and some forming a complex with ADP - the product of a DnaB-promoted hydrolysis of ATP (Section 3.4). Protein contaminants from Fraction FIIIB-R231C were removed by chromatography on hydroxyapatite. 37.6 mg of ~98% pure DnaB-R231C protein was isolated from 6 litres of the heat-induced culture of RSC990 (Table 4.1; Figure 4.5). An ABC-primosome assay (Section 3.2.2) confirmed deficiency of DnaB-R231C in promoting DNA replication (Figure 4.6)

Crystallization of the DnaB-R231C protein was carried out essentially as described for *wt*DnaB (Sections 3.2.5 and 3.3.3) with one exception. The *wt*DnaB doesn't contain cysteines. The only modification was therefore the addition of DTT (2 mM) to all buffers in order to protect the thiol group of the cysteine which had been introduced into DnaB at position 231.

Figure 4.5

(a) Elution profile of DnaB-R231C and the DnaB-R231C.DnaC complex from chromatography on a column of DEAE-Fractogel (Section 4.2.4). Protein concentrations were determined by Bradford assay (Section 2.14). Volumes of fractions were 7.4 ml.

(b) SDS-PAGE of the proteins eluted from DEAE-Fractogel in the gradient of NaCl. A sample (5 µl) of the protein fraction obtained after ammonium-sulfate precipitation and the following dialysis (lane A) was electrophoresed through a 12.5% SDS-polyacrylamide gel, together with a 12-µl portion of the flowthrough and portions (12 µl) of fractions indicated above the photograph. A sample (30 µg) of the DnaB-R231C obtained after the last purification step - chromatography on hydroxyapatite - was electrophoresed in lane C.

(a)

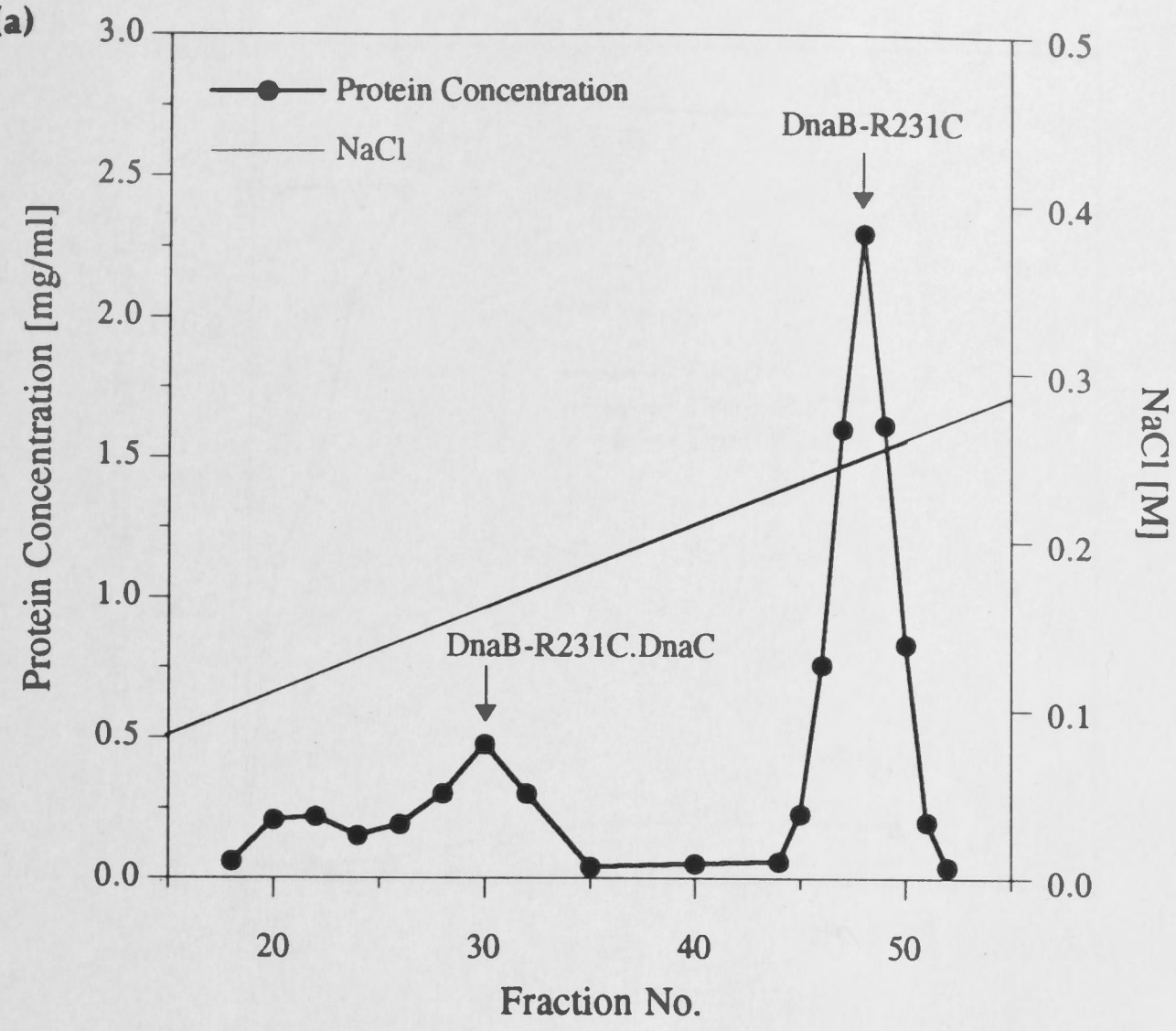
Protein Concentration
NaCl
DnaB-R231C
DnaB-R231C.DnaC
Protein Concentration [mg/ml]
NaCl [M]
Fraction No.
3.0
2.5
2.0
1.5
1.0
0.5
0.0
0.5
0.4
0.3
0.2
0.1
0.0
20
30
40
50

(b)

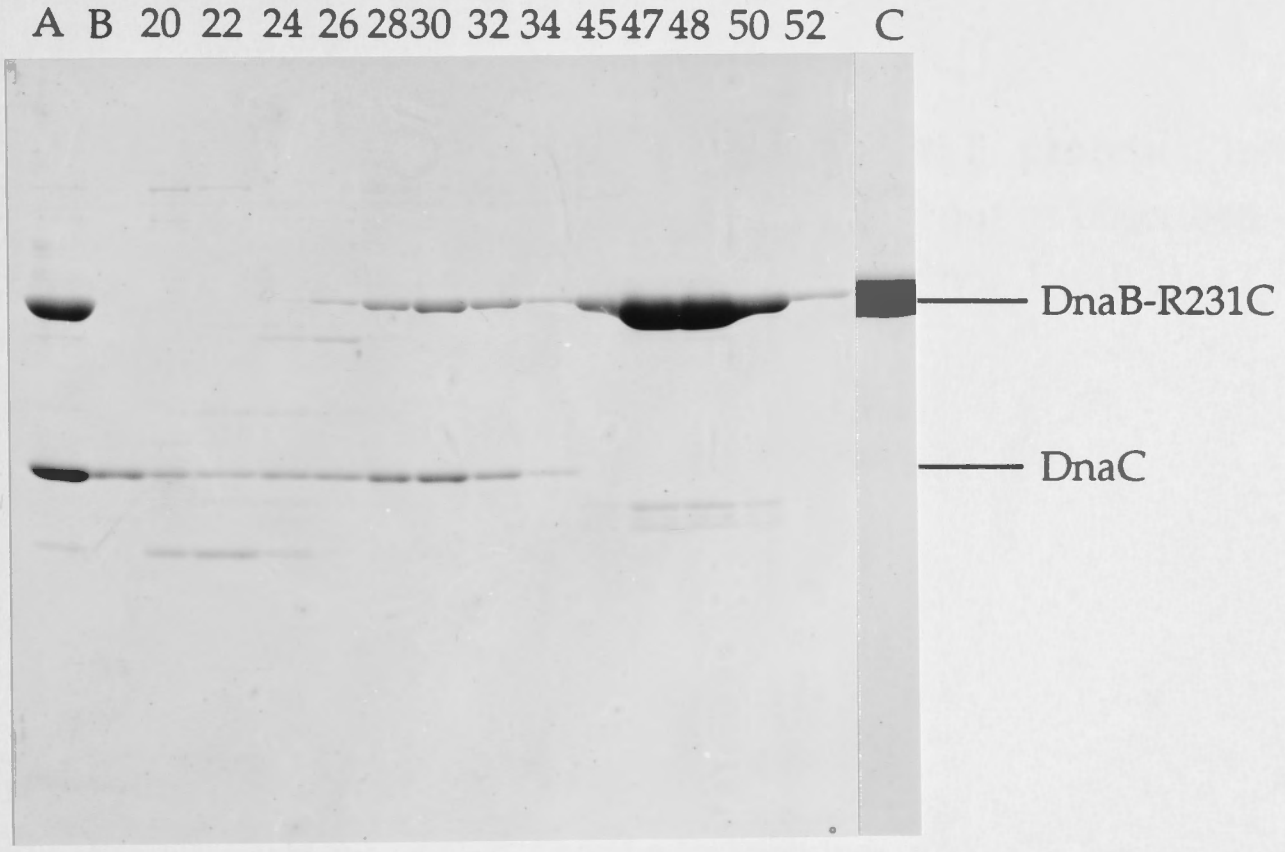
A B 20 22 24 26 28 30 32 34 45 47 48 50 52 C
DnaB-R231C
DnaC

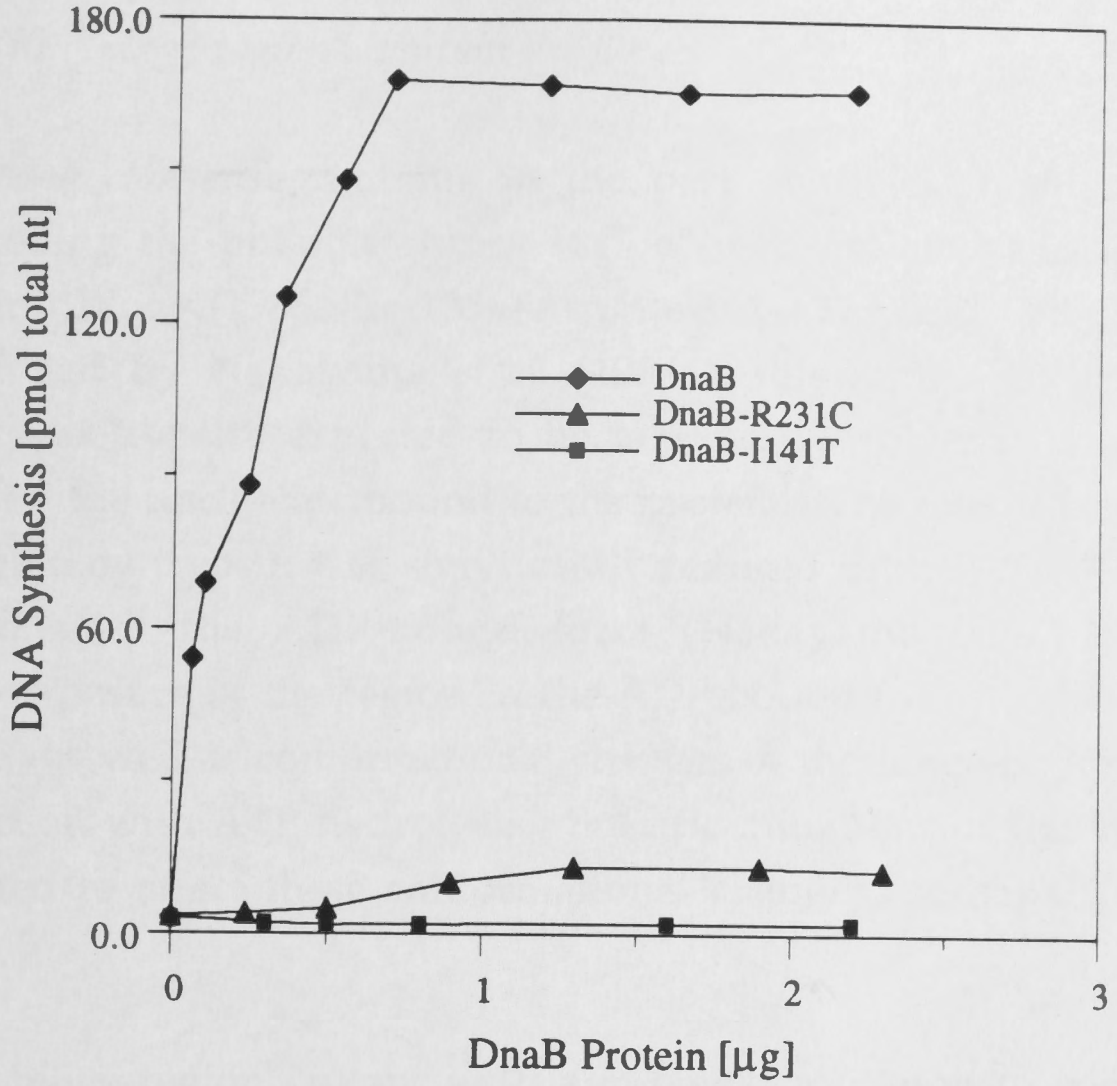

Figure 4.6

Activities of the *wt*DnaB, DnaB-R231C, and DnaB-I141T proteins in replication of DNA. The ABC-primosome assay was carried out as described in Section 3.2.2, and confirmed that neither DnaB-R231C, nor DnaB-I141T could substitute for *wt*DnaB in DNA replication.

4.3.2 *The "hinge-region" mutant of DnaB*

Three missense mutants in the part of the *S. typhimurium dnaB* gene encoding the putative "hinge region" were isolated and identified by Maurer and Wong (1988): Ile-135→Asn, Ile-141→Thr, and Leu-156→Pro. As was deduced by Nakayama *et al.* (1984a), this region is, because of its sensitivity to trypsin, expected to be exposed to solvent. The sensitivity depends on the nucleotide bound to the protein. The rate of cleavage of the hinge-region by trypsin was significantly reduced in the ATPγS-bound form compared with the ADP-bound form (Nakayama *et al.*, 1984b). This indicates exposure of the region in the ADP-bound form to the solvent (*i.e.*, to trypsin) as well as conformational changes of the hinge-region in *wt*DnaB in connection with ATP hydrolysis. Specific mutations of this region might be expected to affect these conformational changes, perhaps "freezing" the structure.

A hinge-region mutant with a missense mutation in codon 141 was prepared. Phagemid pPL717, a pMA200U derivative containing an intact *dnaC*$^{+}$*dnaB*$^{+}$ operon downstream the λ $P_R P_L$-promoter system, was constructed in the first place to facilitate this and any further manipulations of the *dnaB* gene (Figure 4.3, Section 4.2.3). High-level overproduction of DnaB and DnaC in strain RSC972 (TG1*recA*/pPL717) was confirmed by visualization of the total cell protein after the heat induction at 42°C (Figure 4.4). The alternative of using pPL717 for site-directed mutagenesis eliminates the necessity of subcloning of the mutated *dnaC*$^{+}$*dnaB*$^{*+}$ operon from pND604, a derivative of pTZ18U.

ssDNA of pPL717 (Figure 4.3) was used as a template for mutagenesis of codon 141 of the *dnaB* gene. Phagemid pNA788 was prepared encoding DnaB with threonine instead of isoleucine in position 141 (Section 4.2.3, Figure 4.3, Scheme 4.2). A silent mutation in codon 142 generated a unique *Ksp*I restriction site which was used for identification of mutant genes (Scheme 4.2). Strain RSC2036 (AN1459/pNA788) was tested for overproduction of DnaB-I141T and DnaC at 42°C. The high-level overproduction of both proteins is documented in Figure 4.4.

Cell paste of RSC2047 (14 g) was used for purification of the mutant DnaB protein (Section 4.2.4). The most noticeable result was the apparent

inability of the DnaB-I141T to form a stable complex with *wt*DnaC protein (Figure 4.7). The purification yielded 22.3 mg of ~98% pure DnaB-I141T (Table 4.1). The mutant DnaB-I141T protein was inactive in the DNA-replication assay, as expected (Figure 4.6).

4.4 Discussion

Subcloning of the *E. coli dnaC*$^+$*dnaB*$^+$ operon in pTZ18U and pMA200U phagemid vectors, the following oligonucleotide-directed mutageneses and further subcloning of the *dnaC*$^+$*dnaB-R231C*$^+$ operon in pMA200U provided bacterial strains simultaneously overproducing dominant-lethal DnaB mutants and the DnaC protein.

Shrimankar *et al.* (1992) placed *dnaB* and the gene encoding DnaB-R231C under T7 transcriptional and translational signals in vectors of the pET series (Studier *et al.*, 1990) using BL21(DE3) as host strain. No overexpression of DnaB or DnaB-R231C was seen in the absence of plasmid pLysS, which bears the gene encoding T7 lysozyme. Introduction of pLysS into the expression systems enabled overproduction of both proteins. The T7 lysozyme presumably inhibited the background of T7 RNA polymerase activity and the associated lethal expression of DnaB and DnaB-R231C - the proteins with a lethal effect on the cells.

In our case, both mutant genes were subcloned downstream from the strong and very tightly-regulated P_RP_L-promoter system. Because of the elimination of background expression of the *dnaB* mutants, no inhibitory effect on cell growth at 30°C was detected (data not shown) and high-level overproduction of the mutant proteins was achieved after thermal induction.

The inhibitory effect of DnaB-R231C on the action of DnaB in DNA replication (Marszalek and Kaguni, 1992) has not been tested, although the inability of the mutant to replace *wt*DnaB protein has been confirmed in an ABC-primosome assay (Figure 4.6). As is evident from the elution profile of proteins from DEAE-Fractogel chromatography, the DnaB-R231C protein

Figure 4.7

(a) Elution profile from DEAE-Fractogel chromatography of the proteins produced by strain RSC2047 (AN1459/pNA788, pLysS). Purification of DnaB-I141T was carried out as described in Section 4.2.4. Protein concentrations were determined by Bradford assay (Section 2.14); volumes of fractions were 7.4 ml.

(b) SDS-PAGE of a portion (8.5 µl) of the fraction obtained after selective ammonium-sulfate precipitation of proteins from the cell lysate (lane A); flowthrough (12 µl; lane B); and 12-µl portions of separate fractions (7.4 ml; numbered as indicated). No DnaB-I141T.DnaC complex was obtained. A sample (30 µg) of DnaB-I141T which was further purified by hydroxyapatite chromatography (lane C) demonstrates the purity of the protein.

(a)

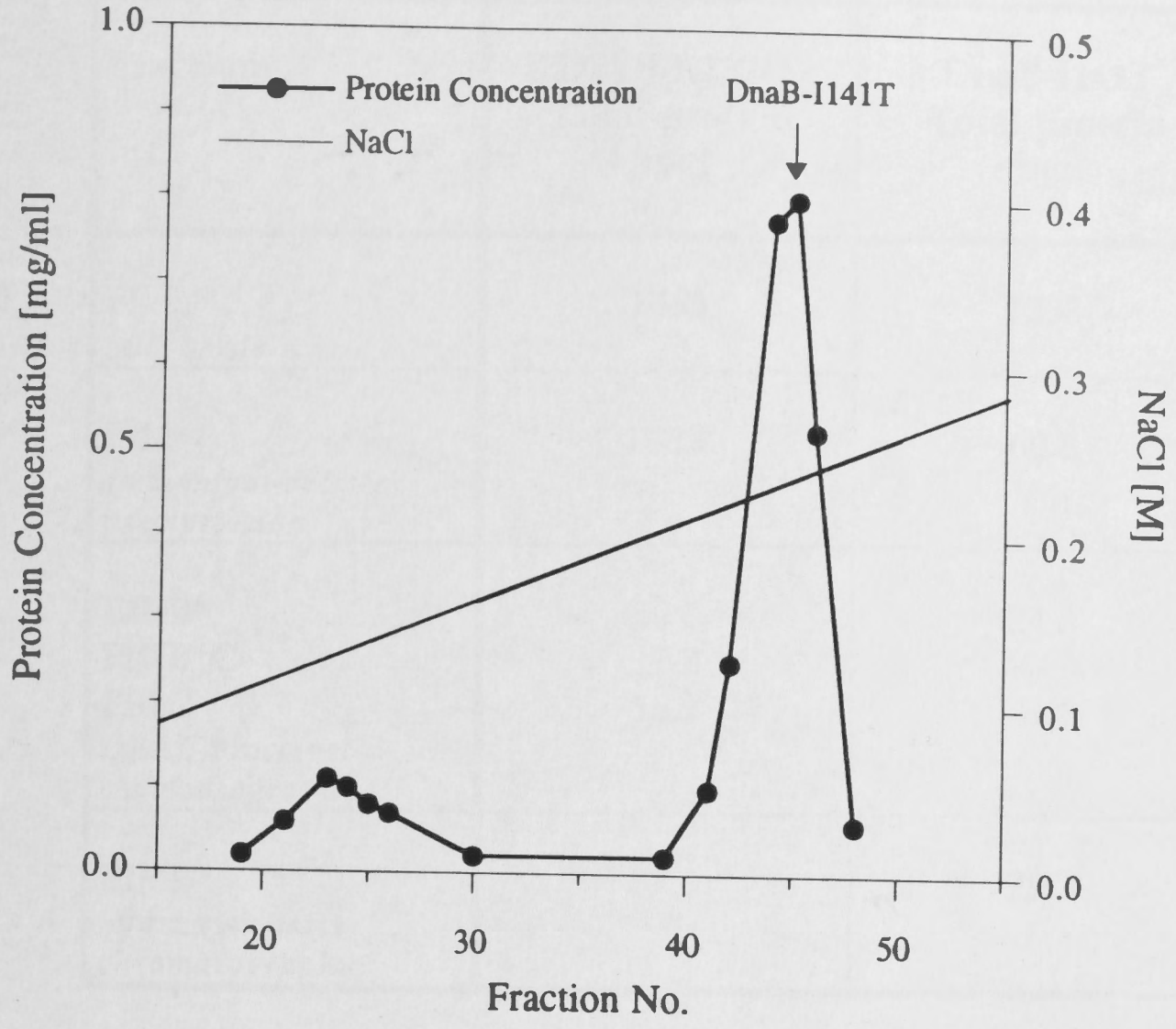
1.0
0.5
0.0
Protein Concentration
NaCl
DnaB-I141T
Protein Concentration [mg/ml]
0.5
0.4
0.3
0.2
0.1
0.0
NaCl [M]
20
30
40
50
Fraction No.

(b)

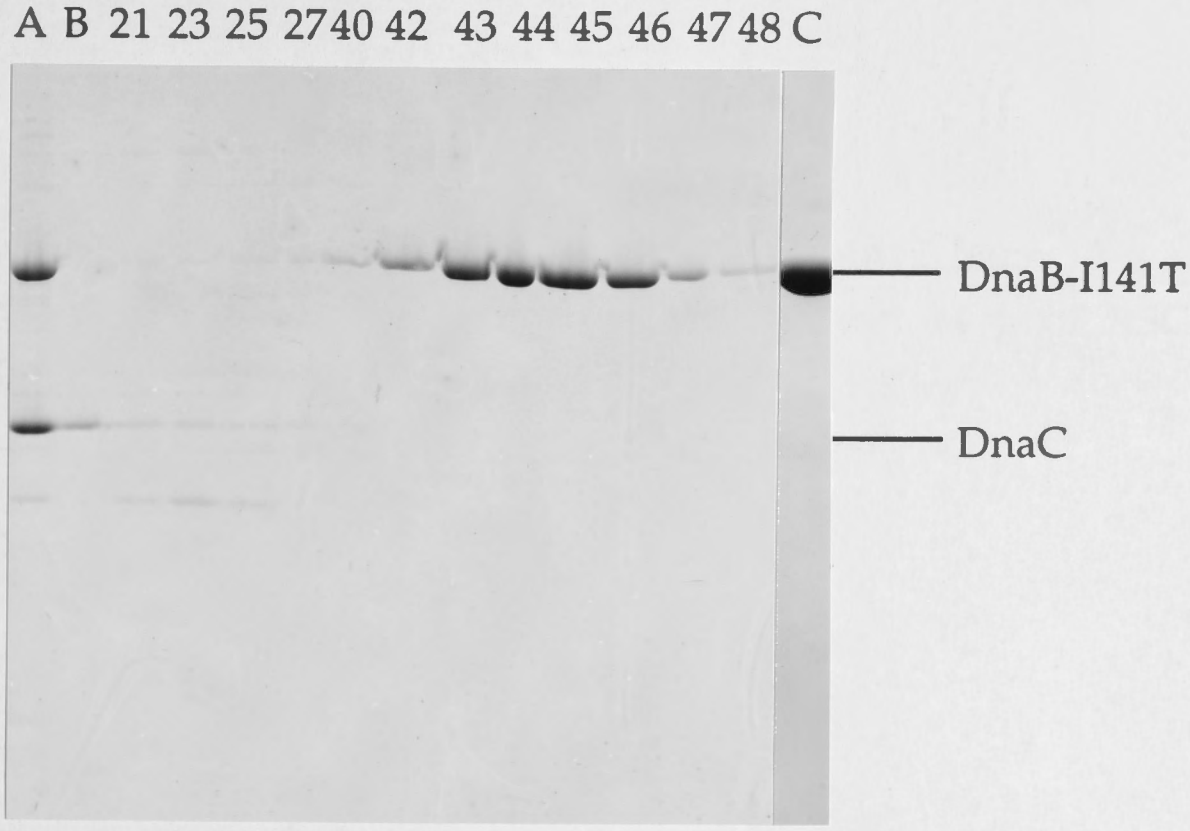
A B 21 23 25 27 40 42 43 44 45 46 47 48 C
DnaB-I141T
DnaC

Fraction	DnaB-R231C Total protein [mg]	DnaB-I141T Total protein [mg]
FI *cell lysate*	1463	1233
FII *ammonium-sulfate precipitation*	106.7	60.8
FIIIB*	50.6	24.3
FIIIB*C	17.8	N/A
FIIIC *DEAE-Fractogel chromatography*	18.9	7.7
FIVB* *hydroxyapatite chromatography*	37.6	22.3

Table 4.1

Purification of lethal mutants DnaB-R231C and DnaB-I141T from 15 g of cell paste of strain RSC990 (AN1459/pND712, pLysS) and 14 g of RSC2047 (AN1459/pNA788, pLysS), respectively.

forms a complex with *wt*DnaC. This characteristic was also reported by Marszalek and Kaguni (1992). Considering the fact that the complex was eluted in a single peak in the presence of ATP, this mutant might be the right candidate for crystallization and structural studies of the DnaB.DnaC complex. ATP is bound not only to DnaB-R231C (Shrimankar *et al.*, 1992) but also to DnaC and stabilizes the complex. At the same time, no DnaB-induced hydrolysis of ATP can take place and most of the subunits of the complex are expected to be in the ATP.DnaB-R231C.DnaC.ATP form (see also Section 3.4). Although crystals of DnaB-R231C did not diffract X-rays to high resolution, conditions for crystallization have not yet been examined extensively.

The DnaB-I141T protein together with DnaC were overproduced to a high level in strain RSC2036 (AN1459/pNA788) and the DnaB mutant was purified on a large scale. No evidence that comments on whether this mutation prevents conformational changes of the hinge region has yet been obtained. Involvement of isoleucine-141 in binding of another protein (Maurer and Wong, 1988) has been confirmed. Replacement of the isoleucine by threonine had a profound effect on an interaction of DnaB with the DnaC protein. As is evident from the elution profile on DEAE-Fractogel chromatography, no stable DnaB-I141T.DnaC complex was formed. Nevertheless, the solubility of the mutant DnaB protein suggests at least transient interaction with DnaC, since neither *wt*DnaB nor any DnaB mutant was obtained in a soluble form in the absence of simultaneous overexpression of the DnaC protein (Stamford, 1991).

DnaB-I141T could not substitute for *wt*DnaB in the ABC-replication assay. Inability of the mutant to form a stable complex with DnaC may affect loading of the DnaB protein onto the DNA template. However, even if this could be completed, the I141T mutation might prevent nucleotide-induced conformational changes in the molecule and probably thus affect mobility of the primosome along the template DNA.

5 DELETION MUTANTS OF THE DnaB PROTEIN

5.1 Introduction

Partial proteolytic cleavage of native DnaB protein (Nakayama *et al.*, 1984) indicated that each protomer is composed of at least two relatively stable domains. The smaller NH_2-terminal domain (estimated M_r=12,000) comprises amino-acid residues 15-126 and has a high degree of secondary structure (particularly α-helix). The 14 amino-acid "tail" (residues 1-14) can be easily cleaved off by trypsin without any significant effect on the DnaB activities. The COOH-terminal domain (M_r~33,000, residues 173-470) forms oligomers and is necessary for all catalytic activities of DnaB which have been detected to date. The domain is predicted to contain a relatively high content of β-sheet structure, is flexible, and highly susceptible to tryptic attack unless stabilized by binding of nucleotide. The COOH- and NH_2-terminal domains are joined through an ~45-amino-acid hinge region (residues 127-172). For a more detailed description of characteristics of the domains and regions of DnaB, see Section 1.5.

By solving the three-dimensional structure of the COOH- and NH_2-terminal domains of the DnaB protein, a signifficant contribution to the elucidation of the structure of the whole DnaB molecule could be made.

The *dnaB* gene was genetically manipulated and a series of DnaB deletion mutants were cloned by Stamford (1991) in derivatives of vector pCE30 (Elvin *et al.*, 1990) in order to generate overproducers of DnaB domains. The products of these experiments included two plasmids containing genes encoding NH_2-terminal deletion mutants of the DnaB protein (DnaBΔN), and two others designed for overexpression of COOH-terminal deletion mutants (DnaBΔC; Figure 5.1). However, the DnaBΔC162-470 deletion mutant (pPS503; strain RSC571) was the only one overproduced to high levels in a partially soluble form. The COOH-terminal polypeptides DnaBΔN1-156 (pPS431; RSC353) and DnaBΔN1-177 (pPS433; RSC537), as well as the DnaBΔC404-470 mutant (pPS501; RSC569), were completely insoluble.

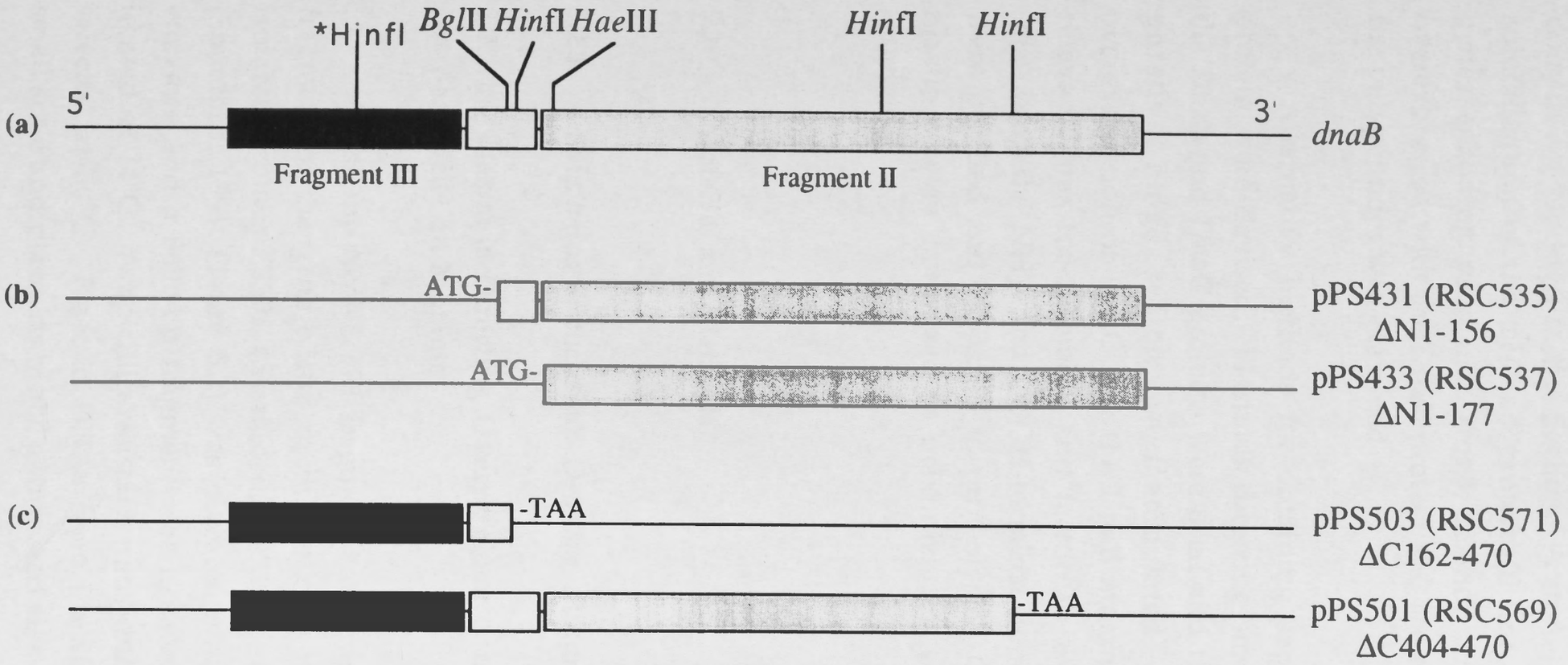

Figure 5.1

Schematic representation of the region encoding the *wt*DnaB protein (a), the NH_2-terminal deletion mutants of DnaB (encoded by plasmids pPS431 and pPS433; b), and the COOH-terminal deletion mutants of the protein (encoded by plasmids pPS503 and pPS501; c). Adapted from Stamford (1991).

Further genetic manipulations that were used in attempts to prepare strains overproducing both DnaB domains in soluble form are described, and purification and crystallization experiments with the NH_2-terminal domain are reported in this Section. A strategy similar to the one used for solubilization of the *wt*DnaB protein (Stamford, 1991) was applied. The genes encoding particular DnaB deletion mutants were simultaneously overexpressed with the DnaC protein and the effect of DnaC on solubility of the polypeptides was examined.

Alternative methods for obtaining separate domains of the DnaB protein were devised. Plasmids directing simultaneous overproduction of the DnaB and DnaC proteins were used and the part of *dnaB* encoding the putative hinge region was manipulated. Several new vectors for overexpression of DnaC and the DnaB mutants were prepared. Protease-cleavage sites for thrombin and factor Xa were inserted into the region separating the NH_2- and COOH-terminal domains. The insertion mutants were purified and subjected to proteolysis. Conditions of the proteolytic reactions were optimized to maximize the yields of the desired protein fragments.

5.2 Material and Methods

5.2.1 *Subcloning of the* dnaB *Deletion Mutants*

5.2.1.1 Plasmids Directing Overproduction of the DnaC Protein and the DnaBΔC Deletion Mutants

A 1201-bp *Nco*I-*Eco*RI fragment containing a 316-bp COOH-terminal fragment of the gene encoding the deletion mutant DnaBΔC404-470 was isolated from pPS501 (Stamford, 1991; Figure 5.2). Plasmid pPS562 (Stamford, 1991; Figure 5.2) was digested with *Nco*I and *Eco*RI restriction enzymes and a 5690-bp fragment was isolated. The two fragments were ligated at 14°C. Ampicillin-resistant transformants of strain AN1459 were selected at 30°C. Plasmid DNAs from transformants were isolated on a small scale and plasmids of the anticipated size (6891 bp) were digested with

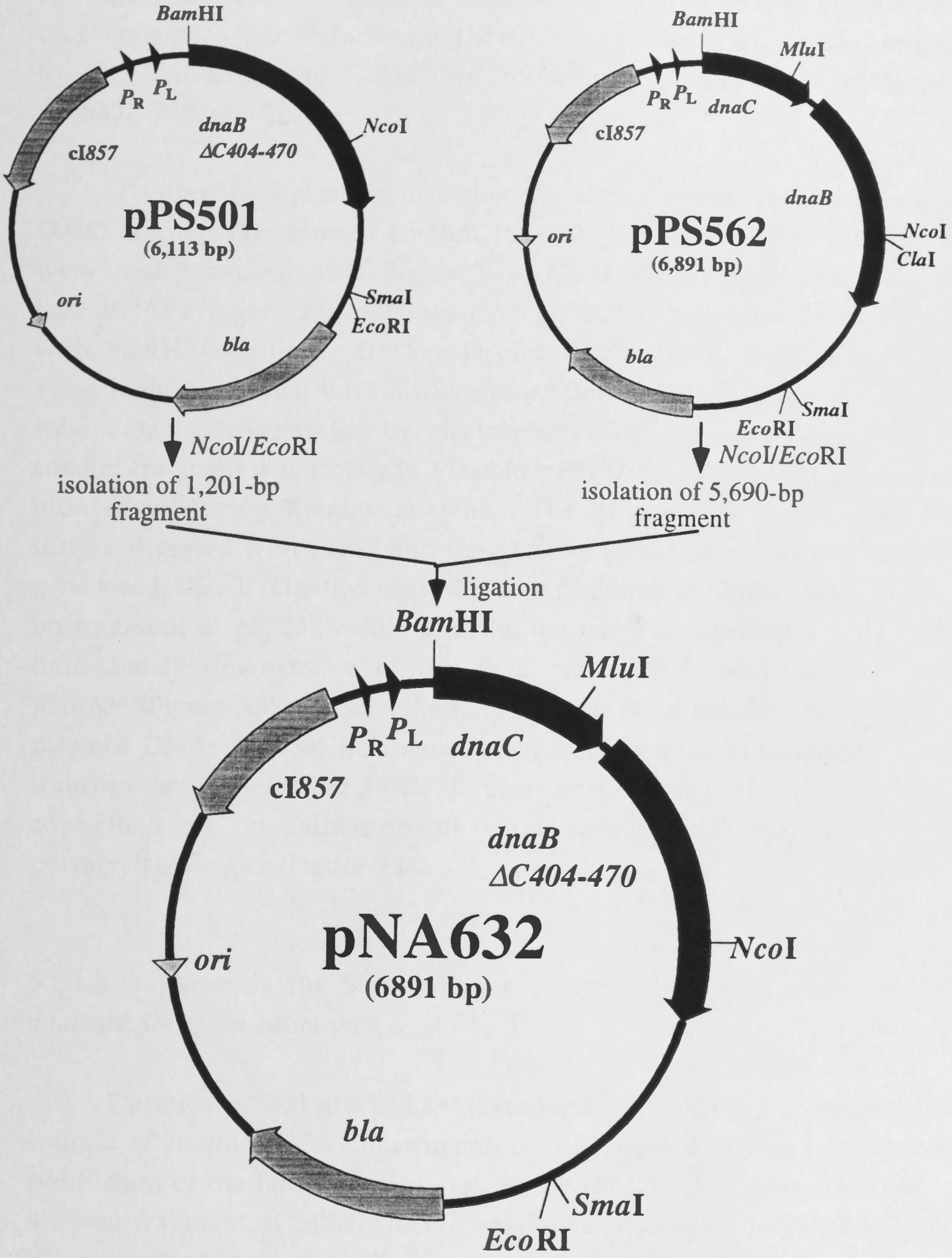

Figure 5.2

Construction of pNA632, a plasmid directing simultaneous overexpression of *dnaBΔC404-470* and *dnaC* (Section 5.2.1.1).

*Nco*I and *Eco*RI endonucleases to confirm the presence of 5690-bp and 1201-bp fragments. Overproduction of the desired proteins at 42°C was confirmed by SDS-PAGE (Figure 5.14). The constructed plasmid was designated pNA632 (Figure 5.2).

To prepare a plasmid directing the simultaneous overproduction of DnaC and deletion mutant DnaBΔC162-470, plasmids pPS503 and pPS237 were used (Stamford, 1991; Figure 5.3). A 2121-bp fragment containing the *dnaBΔC162-470* gene was obtained from pPS503. This plasmid was digested with *Bam*HI, the linear DNA was end-filled with Klenow enzyme and subsequently digested with *Eco*RI endonuclease. The 2121-bp and 3992-bp fragments were separated by electrophoresis in an agarose gel and the smaller fragment was isolated. Plasmid pPS237 was linearized by *Acc*I and blunt-ended using Klenow enzyme. The linear blunt-ended DNA was further digested with *Eco*RI and the 4770-bp fragment containing the *dnaC* gene was isolated. Ligation of the 2121-bp fragment of pPS503 with the 4770-bp fragment of pPS237 resulted in the fusion of the *dnaBΔC162-470* gene immediately downstream of the *dnaC* terminus. The product plasmid pNA636 (Figure 5.3) was identified on the basis of an *Eco*RI/*Bam*HI digest of plasmid DNAs isolated in a small scale from ampicillin-resistant AN1459 transformants selected at 30°C. Expression of both proteins at 42°C was confirmed by visualization of total cell protein on 12.5% SDS-polyacrylamide gels (Figure 5.14).

5.2.1.2 Plasmids for Simultaneous Overexpression of *dnaC* and the *dnaBΔN* Deletion Mutants

Plasmids pPS431 and pPS237 (Stamford, 1991; Figure 5.4) were used as sources of fragments for construction of a plasmid directing simultaneous production of the DnaC protein and the DnaBΔN1-156 deletion mutant. A 4770-bp fragment of pPS431 was prepared as described in Section 5.2.1.1. Plasmid pPS431 was partially digested with *Bam*HI and linearized plasmid DNA was isolated. After end-filling with Klenow enzyme, the DNA was digested with *Eco*RI. A 1318-bp *dnaBΔN1-156*$^+$ fragment was isolated and ligated with the 4770-bp fragment of pPS237. The ligation product was used for transformation of strain AN1459 and ampicillin-resistant transformants were selected at 30°C. Plasmid DNAs from the separate clones were isolated

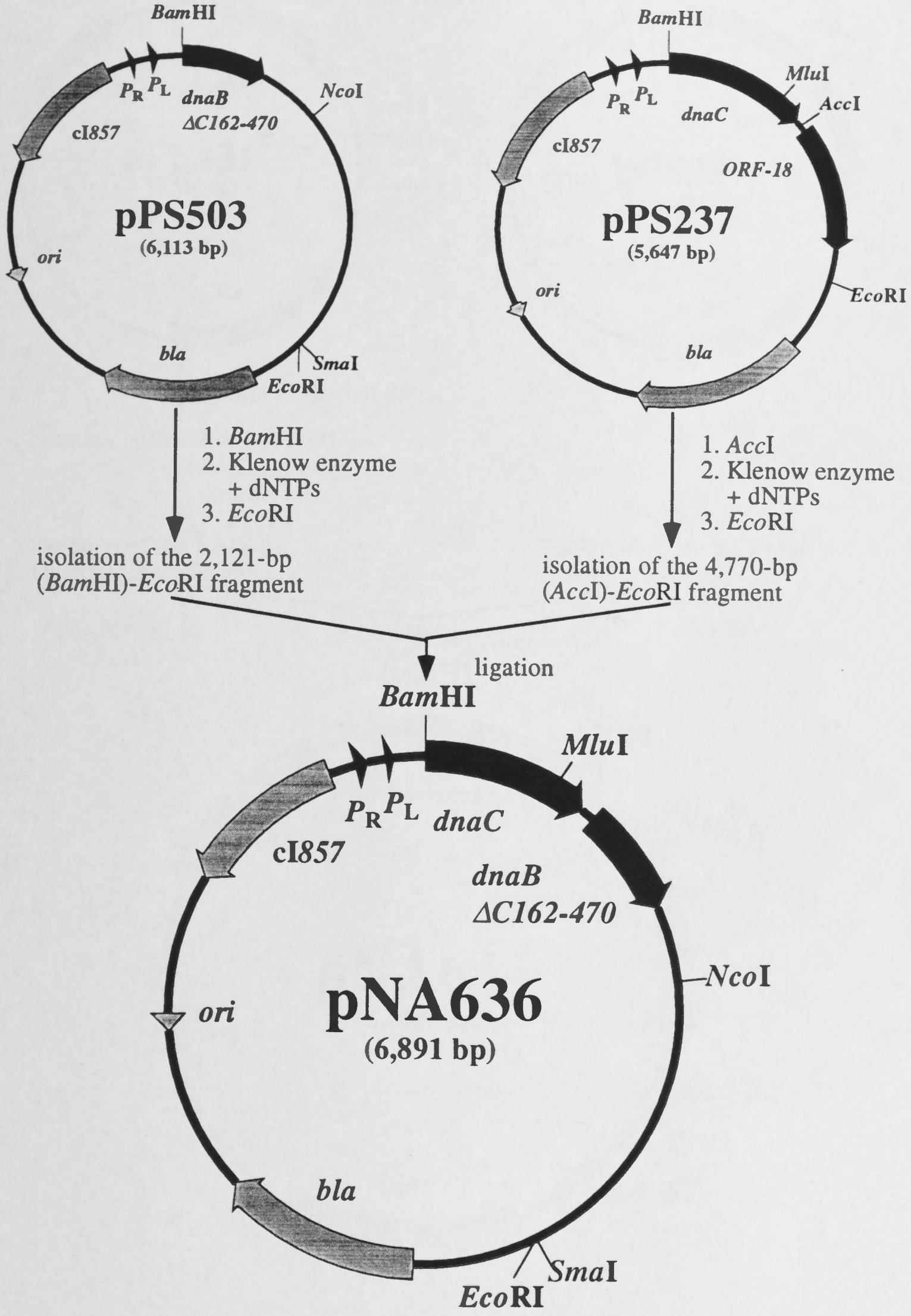

Figure 5.3

Plasmid pNA636 containing *dnaC* and *dnaBΔC162-470* under the control of P_R and $P_L$promoters was prepared as described in Section 5.2.1.1.

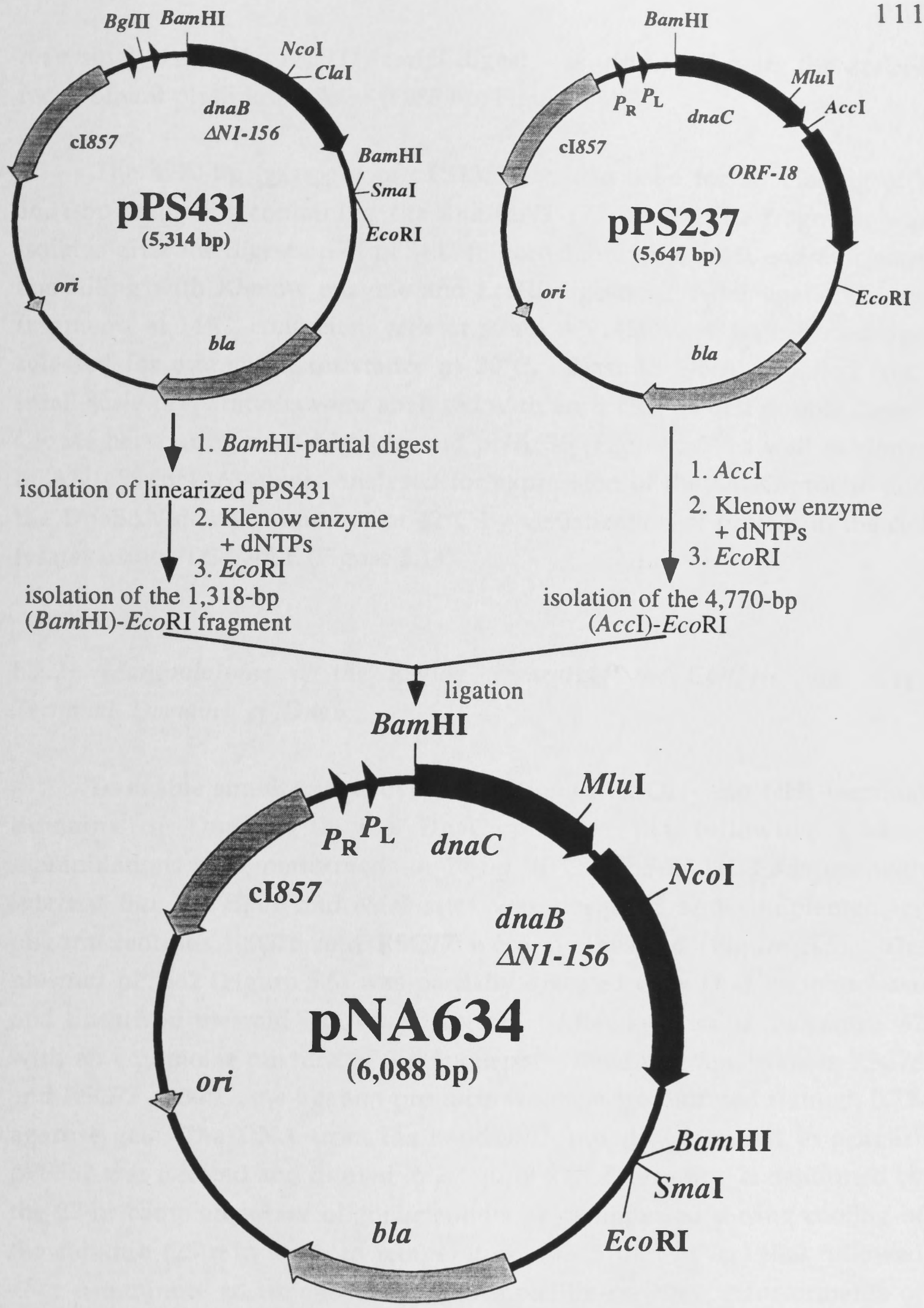

Figure 5.4

Plasmid pNA634 was constructed to direct a simultaneous overexpression of *dnaC* and *dnaBΔN1-156*. Details of the genetic manipulations are described in Section 5.2.1.2.

on a small scale. An *Eco*RI/*Bam*HI digest was used to identify the desired recombinant plasmid pNA634 (6088 bp; Figure 5.4).

The 4770-bp fragment of pPS237 was also used for subcloning of a 1634-bp fragment containing the *dnaBΔN1-177* gene. The fragment was isolated after the digestion of pPS433 (Figure 5.5) with *Bam*HI endonuclease, end-filling with Klenow enzyme and *Eco*RI digestion. After ligation of the fragments at 14°C, competent cells of strain AN1459 were transformed and selected for ampicillin resistance at 30°C. Plasmid DNAs isolated from small-scale preparations were analysed with an *Eco*RI/*Bam*HI double digest. Clones harbouring a 6404-bp plasmid pNA635 (Figure 5.5) as well as clones of AN1459/pNA634 were analysed for expression of the DnaC protein and the DnaBΔN-deletion mutants at 42°C by visualization of protein in the cell lysates using SDS-PAGE (Figure 5.14).

5.2.2 *Manipulations of the Region Separating the COOH- and NH_2-Terminal Domains of DnaB*

To enable simultaneous overproduction of COOH- and NH_2-terminal domains of DnaB with the DnaC protein, the following genetic manipulations were performed. A 27-bp "STOP-RBS-START" adaptor with internal *Bam*HI, *Hpa*I, and *Nde*I sites was designed and complementary oligonucleotides RSC76 and RSC77 were synthesized (Figure 5.6). The plasmid pPS562 (Figure 5.6) was partially digested with *Dra*I endonuclease and linearized plasmid DNA was isolated. After ligation of linear pPS562 with an equimolar mixture of 5'-unphosphorylated oligonucleotides RSC76 and RSC77 at 30°C, the ligation products were electrophoresed through 0.7% agarose gel. The DNA from the band with mobility identical to a linear pPS562 was isolated and diluted in 200 µl of TE. Protruding ends formed by the 27-nt complementary oligonucleotides were annealed during cooling of the mixture (25 min at room temperature and 5 min in ice) that followed after a 6-minute treatment at 70°C. Ampicillin-resistant transformants of strain AN1459 were selected at 30°C. Plasmid DNAs of the anticipated size (6918 bp) isolated on a small scale from 108 transformants were screened for insertion of the adaptor in the required *Dra*I site (between codons 165 and 166 of the *dnaB* gene) following digestion with *Bam*HI restriction endonuclease. No such recombinant plasmid was identified, so a different strategy was therefore used. All ampicillin-resistant AN1459 transformants

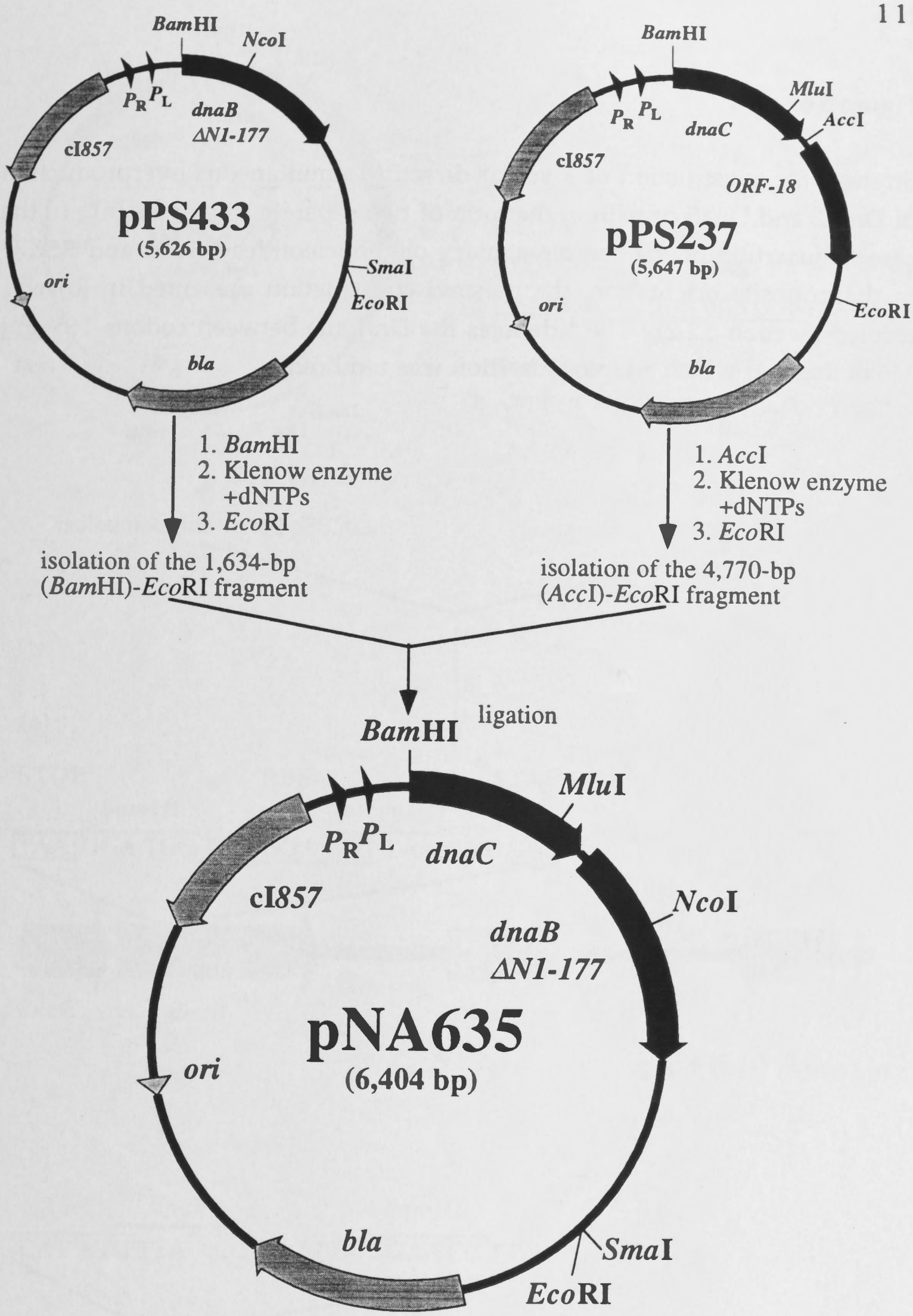

Figure 5.5

Construction of pNA635 directing overproduction of DnaC together with DnaBΔN1-177 (Section 5.2.1.2).

Figure 5.6

Strategy for construction of a vector directing simultaneous overproduction of DnaC, and DnaB protein in the form of two separate fragments (a). In the case of insertion of the complementary oligonucleotides RSC76 and RSC77 in the opposite orientation, the plasmid construction presented in (b) was formed (Section 5.2.2). The * denotes the *Dra*I site between codons 165 and 166 of *dnaB*, at which adaptor insertion was required.

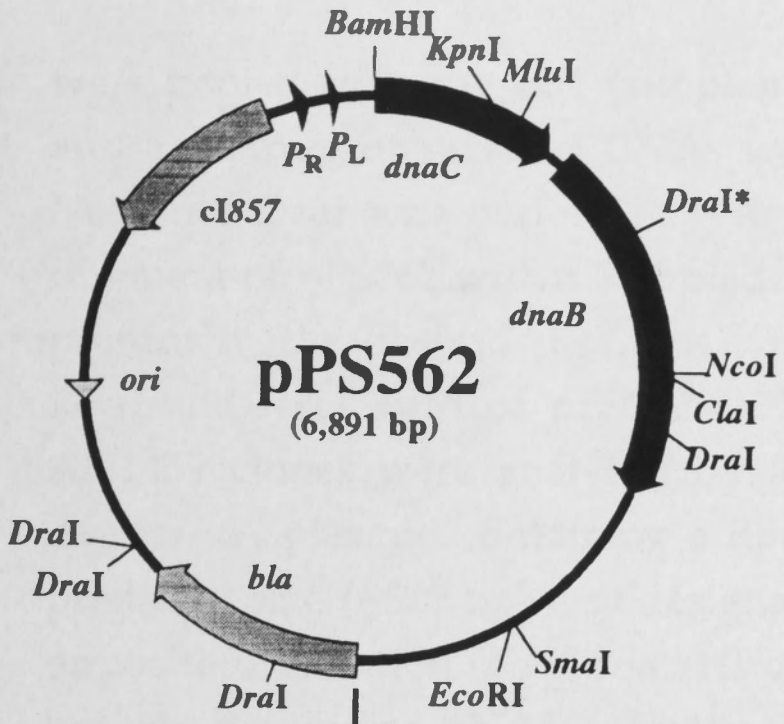

RSC76

STOP **RBS** **START**

5' TAA GGA TCC TAA GGA GGT TAA CAT ATG 3'

RSC77

3' ATT CCT AGG ATT CCT CCA ATT GTA TAC 5'

*Dra*I partial digest

isolation of linearized pPS562

ligation

(a)

STOP **RBS** **START**

*Bam*HI *Hpa*I *Nde*I

TAA GGA TCC TAA GGA GGT TAA CAT ATG

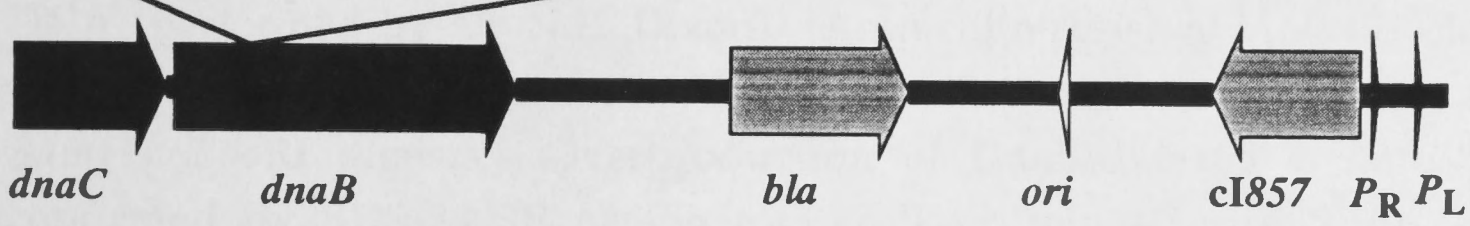

pNA640 (6,918 bp)

(b)

*Nde*I *Hpa*I *Bam*HI

CAT ATG TTA ACC TCC TTA GGA TCC TTA

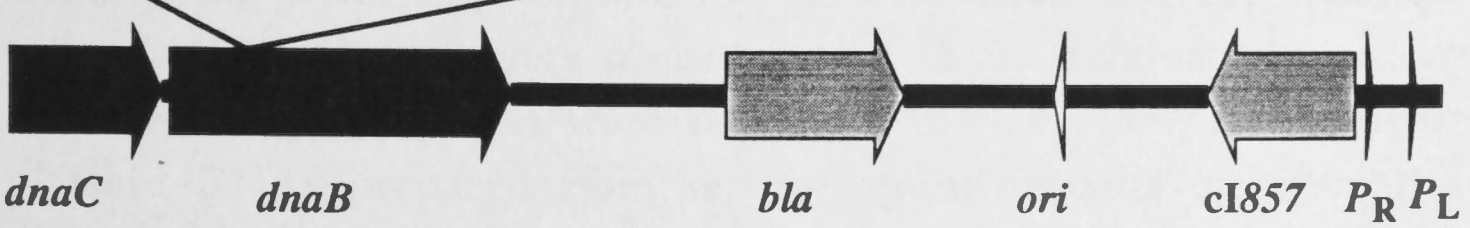

pNA641 (6,918 bp)

were pooled from the LBT (supplemented with 50 μg/ml ampicillin) plate, and a mixture of plasmid DNAs was isolated. A triple digest with *Kpn*I, *Nco*I and *Dra*I was performed. A 1255-bp *Nco*I-*Kpn*I fragment (1228-bp fragment of pPS562 with a 27-bp adaptor in the *Dra*I site, which is no longer present in the desired plasmid) was isolated and reinserted between the *Kpn*I and *Nco*I sites of pPS562. Plasmid DNAs from ampicllin-resistant AN1459 clones were analysed by *Bam*HI, *Bam*HI/*Kpn*I and *Bam*HI/*Nco*I digests. A plasmid containing a *Kpn*I-*Bam*HI fragment judged to be of the predicted size (~829 bp) was designated pNA640, and one with the insert in opposite orientation (*Kpn*I/*Bam*HI digest produced a fragment of size ~844 bp) was designated pNA641 (Figure 5.6). Overproduction of the proteins was tested at 42°C (Figure 5.16). Plasmids of the predicted size corresponding to pNA640 from several clones were further screened for *Hpa*I sites in the adaptors and sequenced (performed by Dr N.E. Dixon). The experiments provided three types of recombinant plasmids that were designated: pNA640*, pNA641, and pNA645 (Section 5.3.1, Figure 5.7).

5.2.3 *Plasmids Directing Overproduction of DnaBΔN1-165*

Plasmid pNA645 (Figure 5.7, Scheme 5.2) was digested with *Bam*HI; a 5615-bp fragment was isolated and a ligation was carried out to reclose the DNA (performed by Dr N.E. Dixon). Ampicillin-resistant AN1459 clones were selected at 30°C, plasmids of a correct size (5615 bp) were analysed by *Bam*HI/*Eco*RI digests. Overproduction of DnaBΔN1-165 at 42°C was confirmed by SDS-PAGE of the total cell protein (Figure 5.16). The recombinant plasmid was designated pND713 (Figure 5.8).

Because of a deletion in the RBS in pNA645 (Figure 5.7, Scheme 5.2), the *dnaBΔN165*$^{+}$ *Nde*I-*Eco*RI fragment was subcloned in an RBS-(*Nde*I)start vector pND706 (Dr N. E. Dixon and Mr C. Neylon; Figure 5.9). A 4282-bp *Nde*I-*Eco*RI fragment of pND706 was ligated with a 1585-bp *Nde*I-*Eco*RI fragment of pNA645 containing the gene for DnaBΔN1-165. Competent cells of strain AN1459 were transformed with the product of ligation and ampicillin-resistant clones were selected at 30°C. *Nde*I/*Eco*RI digests of plasmid DNAs prepared from separate transformants on a small scale enabled identification of the correct recombinant plasmid (pCN718, 5867 bp; Figure 5.9). Selected transformants were analysed for the expression of the DnaBΔN1-165 mutant at 42°C (Figure 5.15).

Figure 5.7

Plasmids prepared by genetic manipulation described in Section 5.2.2 and schematically presented in Figure 5.6. Plasmid pNA641 corresponded to the expected construction (Figure 5.6b), pNA640* and pNA645 were deletion mutants (Section 5.3.1, Scheme 5.2) of the plasmid originally designated pNA640 (Figure 5.6a).

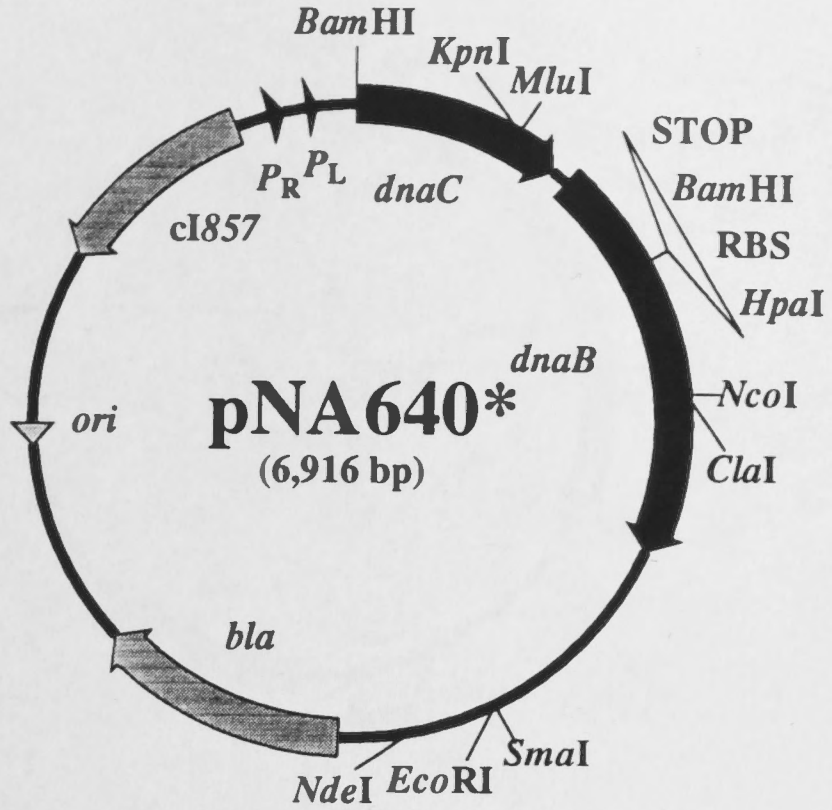
BamHI
KpnI
MluI
STOP
BamHI
RBS
HpaI
PR PL
dnaC
cI857
dnaB
pNA640*
(6,916 bp)
ori
NcoI
ClaI
bla
SmaI
NdeI
EcoRI

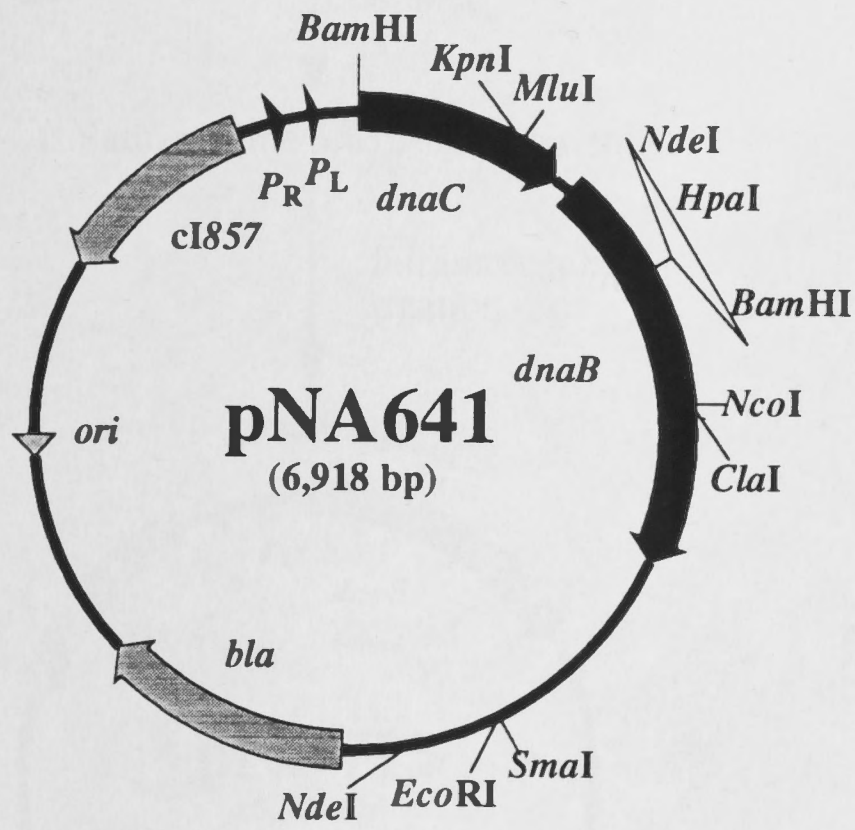
BamHI
KpnI
MluI
NdeI
HpaI
PR PL
dnaC
cI857
BamHI
dnaB
pNA641
(6,918 bp)
ori
NcoI
ClaI
bla
SmaI
NdeI
EcoRI

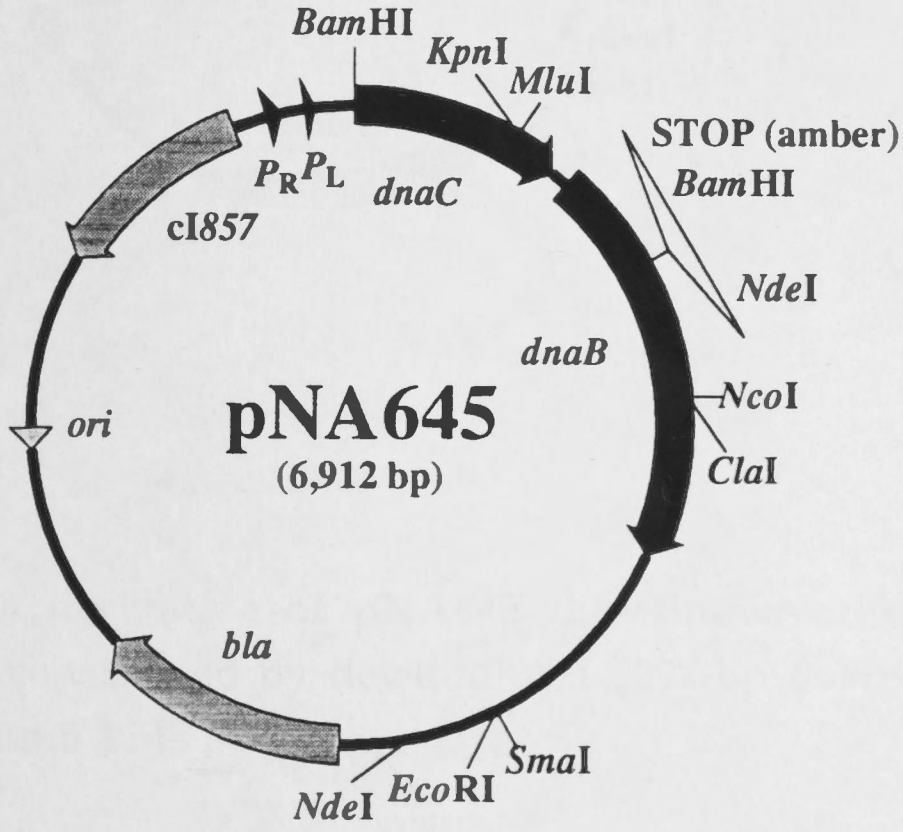
BamHI
KpnI
MluI
STOP (amber)
BamHI
PR PL
dnaC
cI857
NdeI
dnaB
pNA645
(6,912 bp)
ori
NcoI
ClaI
bla
SmaI
NdeI
EcoRI

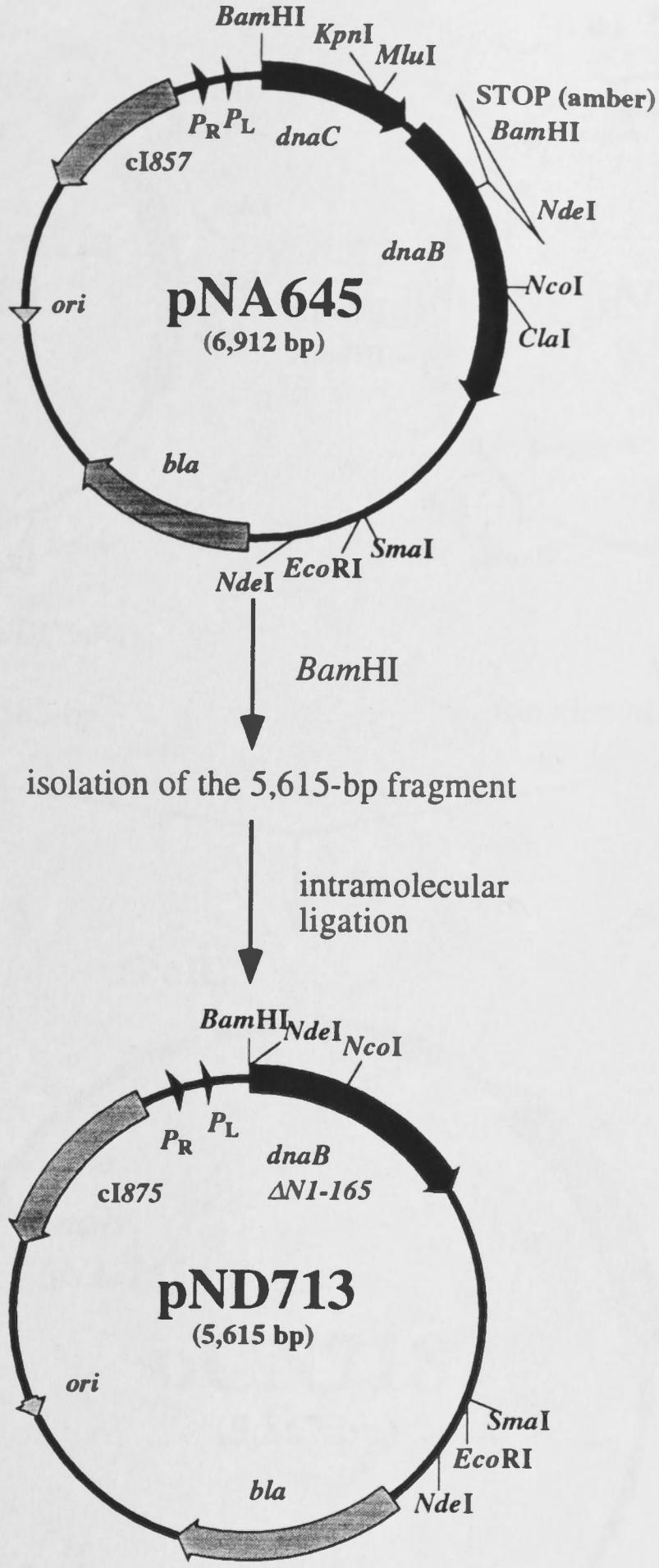

Figure 5.8

Plasmid pND713, a derivative of pNA645 directing overexpression of *dnaBΔN1-165*, was constructed by deletion of a 1297-bp *Bam*HI fragment from pNA645 (Section 5.2.3).

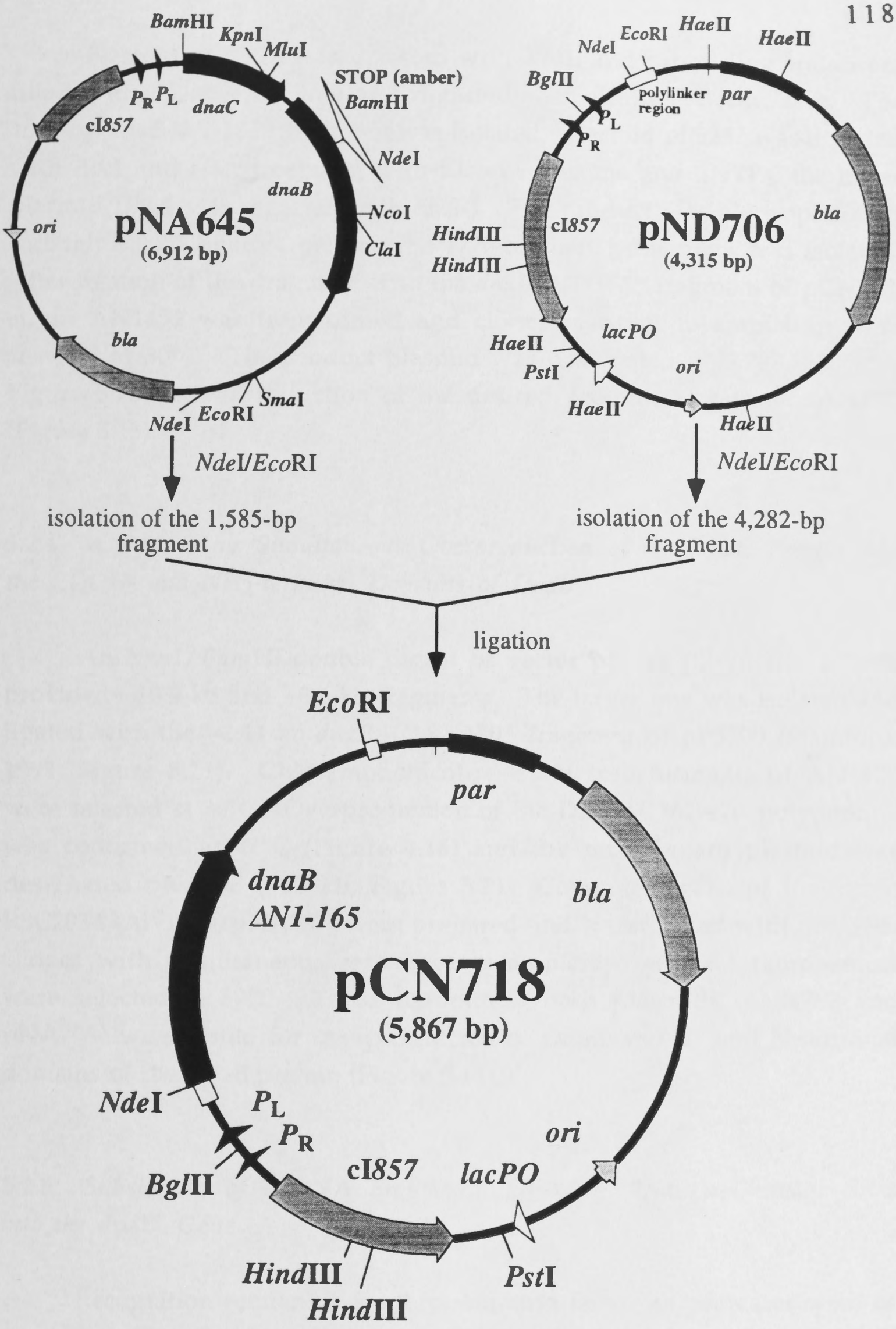

Figure 5.9

Subcloning of the *dnaBΔN1-165*$^{+}$ *Nde*I-*Eco*RI fragment of pNA645 in a RBS-(*Nde*I)START vector pND706 (Section 5.2.3). pCN718 directed high-level overproduction of DnaBΔN1-165 (Figure 5.15)

Plasmid pCN718 was digested with *Xba*I, and protruding ends were filled with Klenow enzyme and digested with *Eco*RI endonuclease. The 1625-bp *dnaBΔN1-165*$^+$ fragment was isolated. Plasmid pPS237 was digested with *Acc*I and after treatment with Klenow enzyme and dNTPs, the linear plasmid DNA was digested with *Eco*RI. The product was electrophoresed through a 0.7% agarose gel and the 4770-bp *dnaC*$^+$ fragment was isolated. After ligation of this fragment with the *dnaBΔN1-165*$^+$ fragment of pCN718, strain AN1459 was transformed and clones resistant to ampicillin were selected at 30°C. The product plasmid was designated pNA787 (6395 bp; Figure 5.10). Overproduction of the desired proteins was tested at 42°C (Figure 5.15).

5.2.4 *A System for Simultaneous Overproduction of the DnaC Protein and the COOH- and NH_2-terminal Domains of DnaB*

An *Nru*I/*Bam*HI-double digest of vector pCE33 (Elvin *et al.*, 1990) provided ~10.9-kb and ~0.6-kb fragments. The larger one was isolated and ligated with the ~2.11-kb *dnaBΔC162-470*$^+$ fragment of pPS503 (Stamford, 1991; Figure 5.11). Chloramphenicol-resistant transformants of AN1459 were selected at 30°C. Overproduction of the DnaBΔC162-470 polypeptide was confirmed at 42°C (Figure 4.16) and the recombinant plasmid was designated pNA798 (~13 kb; Figure 5.11). Competent cells of the strain RSC2034 (AN1459/pNA787) were prepared and transformed with pNA798. Clones with simultaneous resistance to ampicillin and chloramphenicol were selected at 30°C. Those harbouring both plasmids (pNA787 and pNA798) were tested for overproduction of DnaC and C- and N-terminal domains of the DnaB protein (Figure 5.15).

5.2.5 *Subcloning of a DNA Fragments Encoding Protease-Cleavage Sites into the* dnaB *Gene*

Recognition sequences for thrombin and factor Xa proteases were as used in vectors of the pGEX series (Pharmacia Biotech; Scheme 5.1). Oligonucleotide adaptors designed for insertion of thrombin and factor Xa cassettes into the plasmid pNA641 (Section 5.3.1, Figure 5.7) in the form of *Nde*I-*Bam*HI fragments are in Scheme 5.1. The plasmid pNA641 was digested with *Pst*I and *Bam*HI (Figure 5.12). The products were separated by

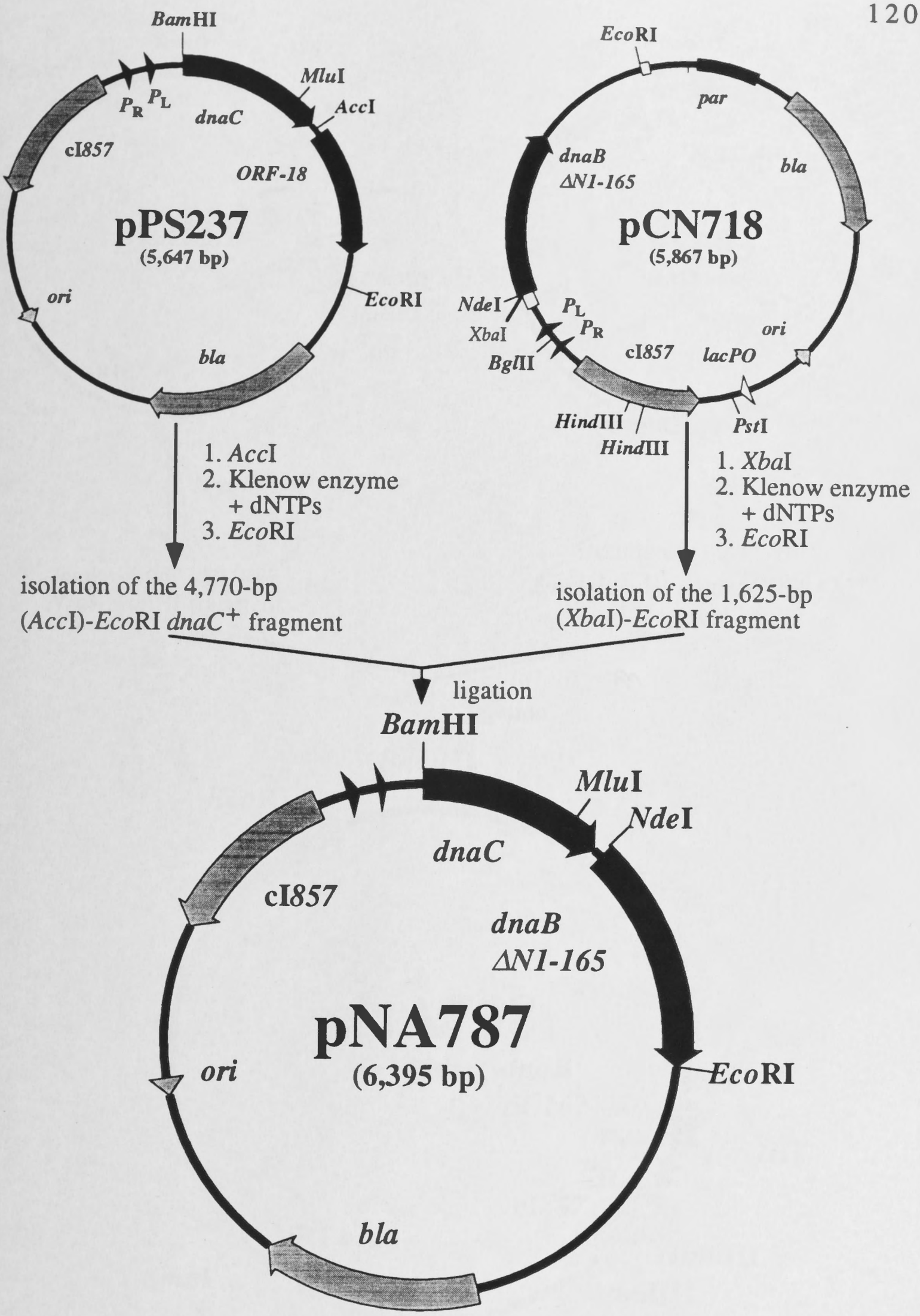

Figure 5.10

Construction of pNA787, directing co-transcription of *dnaC* and *dnaBΔN1-165* from a synthetic operon. Details of construction are described in Section 5.2.3.

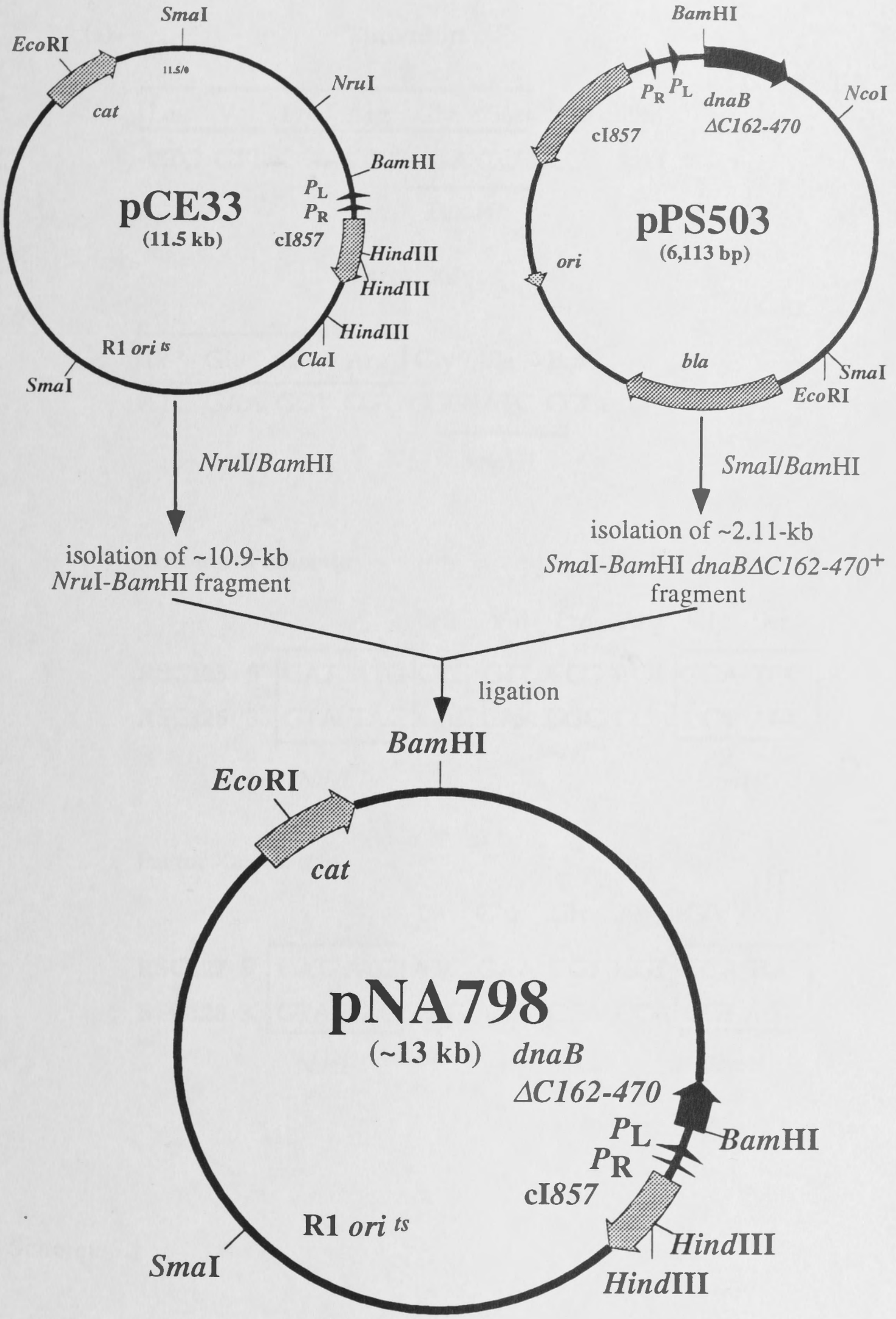

Figure 5.11

Plasmid pNA798 was constructed by subcloning of ~2.11-kb *Sma*I-*Bam*HI *dnaBΔC162-470*+ fragment of pPS503 into vector pCE33 (Section 5.2.4).

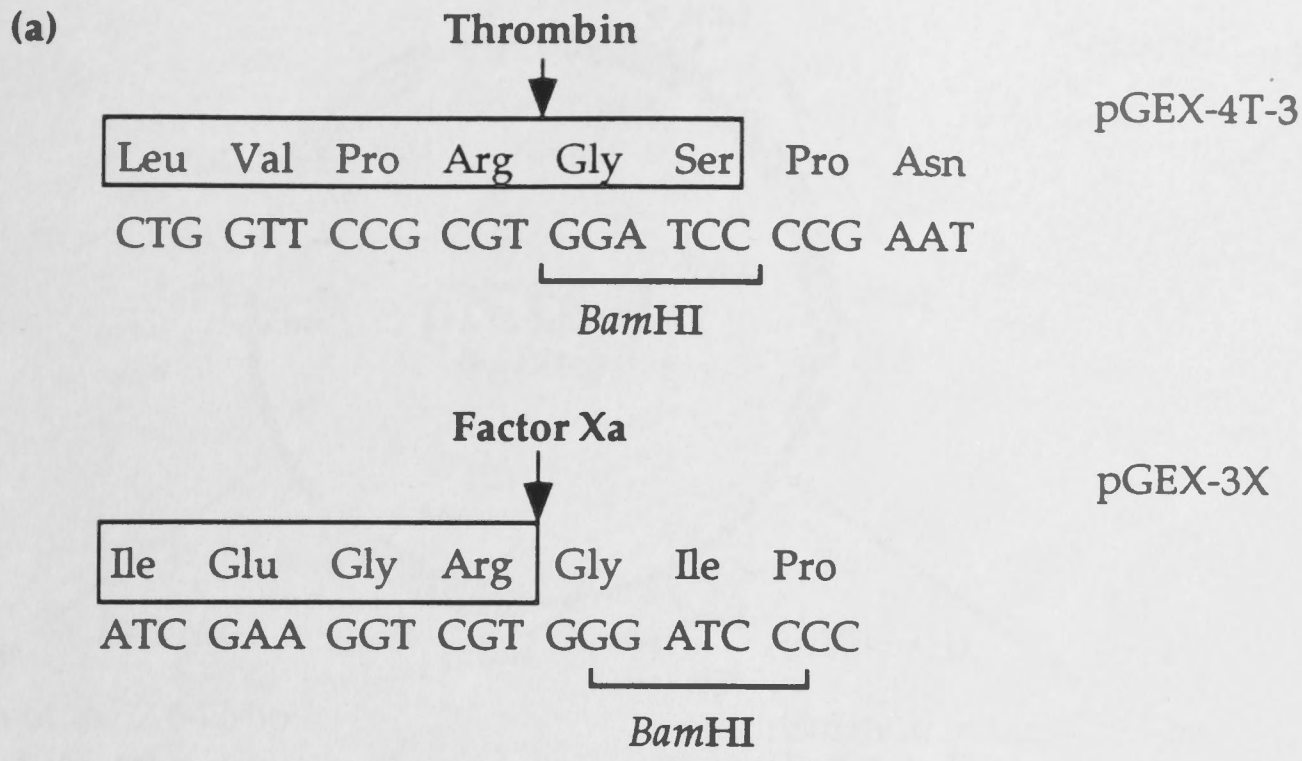

(b) Thrombin cassette

			Leu	Val	Pro	Arg	Gly	Ser	
RSC125	5'	CAT ATG	CTG	GTT	CCG	CGT	GGA TCC		3'
RSC126	3'	GTA TAC	GAC	CAA	GGC	GCA	CCT AGG		5'
		*Nde*I						*Bam*HI	

Factor Xa cassette

			Ile	Glu	Gly	Arg	Gly		
RSC127	5'	CAT ATG	ATC	GAA	GGT	CGT	GGA TCC		3'
RSC128	3'	GTA TAC	TAG	CTT	CCA	GCA	CCT AGG		5'
		*Nde*I						*Bam*HI	

Scheme 5.1

(a) Recognition sequences for thrombin and factor Xa proteases (Pharmacia Biotech Molecular and Cell Biology Catalogue 1994/1995; Section 5.2.5)

(b) Oligonucleotides designed for insertion of thrombin and factor Xa cassettes into pNA641 between dnaB codon 165 and 166 (Section 5.2.5)

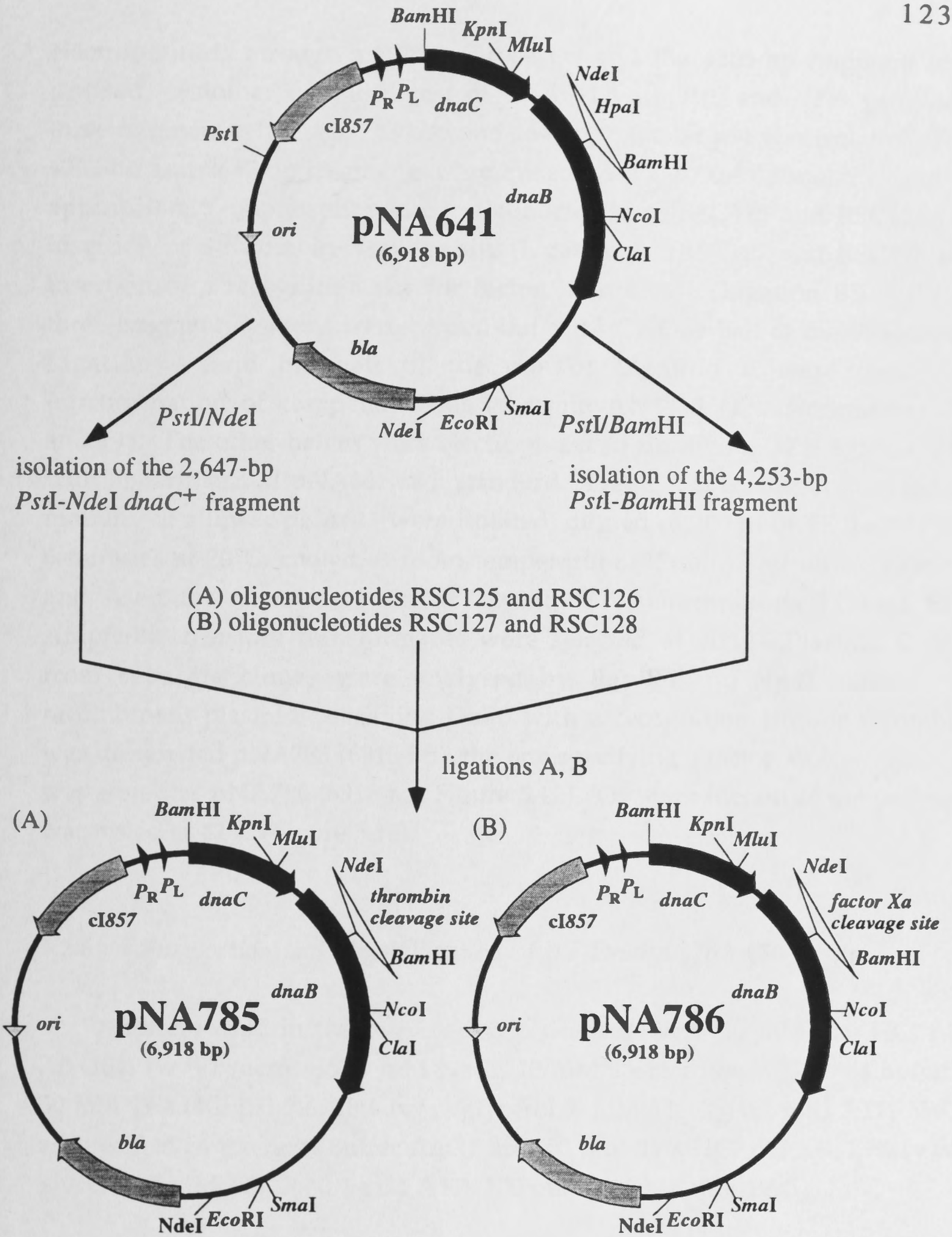

Figure 5.12

A scheme for subcloning of fragments encoding the thrombin and factor Xa recognition sites into the *dnaB* gene (Section 5.2.5). Thrombin- and factor Xa- *Nde*I-*Bam*HI cassettes are presented in Scheme 5.1.

electrophoresis through a 0.7% agarose gel and the 4253-bp fragment was isolated. Another double digest of pNA641 with *Pst*I and *Nde*I provided three fragments (1841 bp, 2430 bp and 2647 bp); the largest was isolated. The 4253-bp and 2647-bp fragments were mixed with a 1000-fold molar excess of appropriate 5'-unphosphorylated oligonucleotides [RSC125 and RSC126 for insertion of a thrombin-cleavage site (Ligation A); RSC127 and RSC128 for insertion of a recognition site for factor Xa protease (Ligation B)] and the three-fragment ligations were carried out at 14°C. One-half of the product of Ligation A and one-half of the one of Ligation B were used for transformation of competent cells of strain AN1459 (Transformations T1 and F1). The other halves were electrophoresed through a 0.7% agarose gel, with linear plasmid pNA641 as a standard. Fragments corresponding to the mobility of a linear pNA641 were isolated, diluted in 200 µl of TE, heated for 6 minutes at 70°C, cooled at room temperature (25 min) and on ice (5 min) and used for transformation of AN1459 (Transformations T2 and F2). Ampicillin-resistant transformants were selected at 30°C. Plasmid DNAs from separate clones were analysed by *Bam*HI and *Hpa*I digests. A recombinant plasmid specifying DnaB with a recognition site for thrombin was designated pNA785 (6918 bp), the one specifying a factor Xa cleavage site was stored as pNA786 (6918 bp; Figure 5.12). Overproduction of the proteins was tested at 42°C (Figure 5.16).

5.2.6 *Purification and Crystallization of the DnaBΔC162-470 Mutant*

Buffers used in the purification procedure were 50 mM Tris.HCl pH 7.6, 10% (w/v) sucrose, 200 mM NaCl, 10 mM spermidine.HCl (lysis buffer); 50 mM Tris.HCl pH 7.6, 20% (v/v) glycerol, 5 mM $MgCl_2$, 0.1 mM ATP, NaCl as specified in the text (Buffer AΔC); and 50 mM Tris.HCl pH 7.6, 15% (v/v) glycerol, 5 mM $MgCl_2$, 0.1 mM ATP, 100 mM NaCl (Buffer BΔC).

Columns of DEAE-Fractogel [TSK DEAE-650 (M); Merck] and Sephadex G-50 (Pharmacia) were prepared according to manufacturers' instructions. A column of DEAE-Fractogel (12.5 x 2.5 cm) was then washed with 120 ml of Buffer AΔC containing 1 M NaCl and equilibrated with ten volumes of Buffer AΔC without NaCl. A column of Sephadex G-50 (45 x 2.5 cm) was washed with 800 ml of BufferBΔC at a flow rate of 27 ml/hour.

Strain RSC571 (AN1459/pPS503; Stamford, 1991; see Figure 5.3) was grown in 6 x 1 l of LBT broth supplemented with ampicillin (50 μg/ml) to A_{595} = 0.5. Induction at 42°C, and preparation of a cell suspension were carried out as described in Section 3.2.1.1. The yield was ~15 g of cell paste.

The cell suspension was thawed in 230 ml of lysis buffer and lysozyme (0.25 mg/ml) was added. The cell lysate (fraction FIΔC) was obtained as described in Section 3.2.1.1. Finely-ground ammonium sulfate was added to 0.27 g/ml and after being stirred for 2 hours, the protein precipitate was sedimented (40,000 x g, 45 min, 0°C). The pellet was dissolved in 25 ml of Buffer AΔC (not containing NaCl), dialysed against the same buffer (2 l overnight and 1 l for 3 hours) and centrifuged (12,000 x g, 15 min, 4°C). The supernatant (fraction FIIΔC) was collected, diluted with Buffer AΔC to a volume of 50 ml and loaded on a column of DEAE-Fractogel. The column was washed with 120 ml of Buffer AΔC and a linear gradient (600 ml) of NaCl (0 to 300 mM) in Buffer AΔC was used for elution of proteins at a fow rate of 60 ml/hour. Fractions Nos. 36 - 42 were pooled (fraction FIIIΔC; Figure 5.19), dialysed overnight against 1.5 l of Buffer BΔC, concentrated in an Amicon stirred ultrafiltration cell (Section 3.2.4) to 29.3 mg/ml and loaded onto a column of Sephadex G-50. The protein was eluted at a flow rate of 36 ml/hour. Fractions of DnaBΔC162-470 were frozen in liquid nitrogen (fraction FIVΔC) and stored at -70°C. Fraction No. 47 (Figure 5.20) was dialysed against buffer DialB containing 0.1 mM ATP and fast screens for protein crystallization were set up at 4°C and 25°C (Section 3.2.5).

5.2.7 *Purification of the DnaB-9αα165/166, DnaB-T165/166, and DnaB-F165/166 Mutants*

The DnaB protein with a 9-amino-acid insertion in the putative hinge region (DnaB-9αα165/166) was purified from strain RSC934 (AN1459/pNA641). The mutant DnaB proteins containing recognition sites for thrombin (DnaB-T165/166) and factor Xa (DnaB-F165/166) proteases were purified from strains RSC2045 (AN1459/pNA785, pLysS) and RSC2046 (AN1459/pNA786, pLysS), respectively.

Purifications were carried out in the presence of 0.1 mM ATP as described in Section 3.2.1.2. DNA replication activity of the proteins was determined with the ABC-primosome assay (Section 3.2.2).

5.2.8 *Proteolysis of the DnaB-T165/166 and DnaB-F165/166 Mutants*

The purified DnaB-T165/166 and DnaB-F165/166 proteins (Section 5.3.2) were dialysed against reaction buffers for thrombin and factor Xa proteases: 40 mM Tris.HCl pH 8.0, 100 mM NaCl, 0.25 mM $CaCl_2$, 5 mM $MgCl_2$, 0.1 mM ATP was the buffer for thrombin cleavage (Buffer T); 20 mM Tris.HCl pH 8.0, 100 mM NaCl, 2 mM $CaCl_2$, 5 mM $MgCl_2$, 0.1 mM ATP was the composition of Buffer F for factor Xa proteolysis of DnaB. Thrombin (2.5 U) and factor Xa (1.5 U) were used for the cleavage of each 50 µg of the particular protein. In each case, the cleavage was carried out in a volume of 150 µl containing 1.15 mg/ml DnaB-T165/166 and 0.89 mg/ml DnaB-F165/166, respectively. Products of the cleavage reactions were electrophoresed through 12.5% SDS-polyacrylamide gels (Figures 5.17 and 5.18).

5.3 Results

5.3.1 *Subcloning of the* dnaB *Deletion Mutants*

Strains RSC569 (AN1459/pPS501), RSC571 (AN1459/pPS503), RSC535 (AN1459/pPS431) and RSC537 (AN1459/pPS433) overproducing the deletion mutants of the DnaB protein (Stamford 1991; Figure 5.1) were not suitable sources for the purification of NH_2- and COOH-terminal domains of DnaB. All of them (except RSC571) accumulated the synthesized polypeptides in an insoluble form. DnaBΔC162-470 was partially soluble (Stamford, 1991). In attempts to overproduce the deletion mutants in soluble form, strategies involving simultaneous expression with DnaC were used.

The genes *dnaBΔN1-156*, *dnaBΔN1-177*, and *dnaBΔC162-470* were subcloned into the *dnaC*$^+$ vector pPS237 (Section 5.2.1, Figures 5.3, 5.4, and 5.5). A 316-bp COOH-terminal part of *dnaBΔC404-470* was inserted in a 1201-bp *Nco*I-*Eco*RI fragment into the vector containing the complete *dnaB-dnaC* operon (pPS562; Figure 5.2). Strain AN1459 was used as the host strain. These manipulations provided strains RSC832 (AN1459/pNA632), simultaneously overproducing DnaBΔC404-470 and the DnaC protein, RSC861 (AN1459/pNA636) for overproduction of DnaBΔC162-470 and

DnaC, RSC859 (AN1459/pNA634) for production of DnaBΔN1-156 and DnaC, and RSC860 (AN1459/pNA635) for simultaneous production of DnaBΔN1-177 and the DnaC protein (Figure 5.13). Both DnaBΔC-deletion mutants were co-overproduced with DnaC at 42°C to high levels, while significantly lower levels of the DnaBΔN-deletion mutants were detected. The solubilities of all DnaB mutants synthesized simultaneously with DnaC were examined extensively (lysozyme-heat lysis, freeze-thaw lysis, solubilization with sodium deoxycholate). However, their solubility was not improved (data not shown).

A new genetic manipulation was undertaken with a view to simultaneously overproduce NH_2- and COOH-terminal domains of DnaB with the DnaC protein. An experiment was carried out as described in Section 5.2.2 and schematically presented in Figure 5.6. Restriction analyses of plasmid DNAs from the separate ampicillin-resistant clones and the following dideoxy sequencing revealed that the experiment yielded three different recombinant plasmids pNA641, pNA640*, and pNA645 (Figure 5.7). The sequence of the adaptor inserted in the "wrong" orientation was confirmed to be as predicted (pNA641; Figure 5.6). This resulted in a mutant *dnaB* encoding the DnaB protein with a 9-amino-acid insertion in the putative hinge region between phenylalanine (codon 165) and lysine (codon 166) as presented in Scheme 5.3. The mutant protein will be referred to as DnaB-9αα165/166. On the other hand, the plasmid originally designated as pNA640 (Figure 5.6) was found only in a form of deletion mutants pNA640* or pNA645 (Figure 5.7). The sequences of the adaptors in pNA640* and pNA645 are presented in Scheme 5.2. A clone of strain AN1459 containing pNA640* was designated RSC933, the one bearing pNA641 was retained as RSC934. The strain designated RSC945 contains plasmid pNA645. Production of proteins in these strains after being treated at 42°C is illustrated in Figure 5.14.

Good overproduction of DnaC and the DnaB-9αα165/166 insertion mutant was achieved in strain RSC934. The mutant protein was purified from 16 g of cell paste (Section 5.2.7), and 13.6 mg of ~99% pure DnaB-9αα165/166 protein was obtained. The specific activity of the protein in DNA replication (Section 3.2.2) was determined to be 55.5 U/μg [53.4 U/μg was the specific activity of *wt*DnaB (Purification A), 59.5 U/μg was the value in Purification B1 (Sections 3.3.1.1 and 3.3.1.2)].

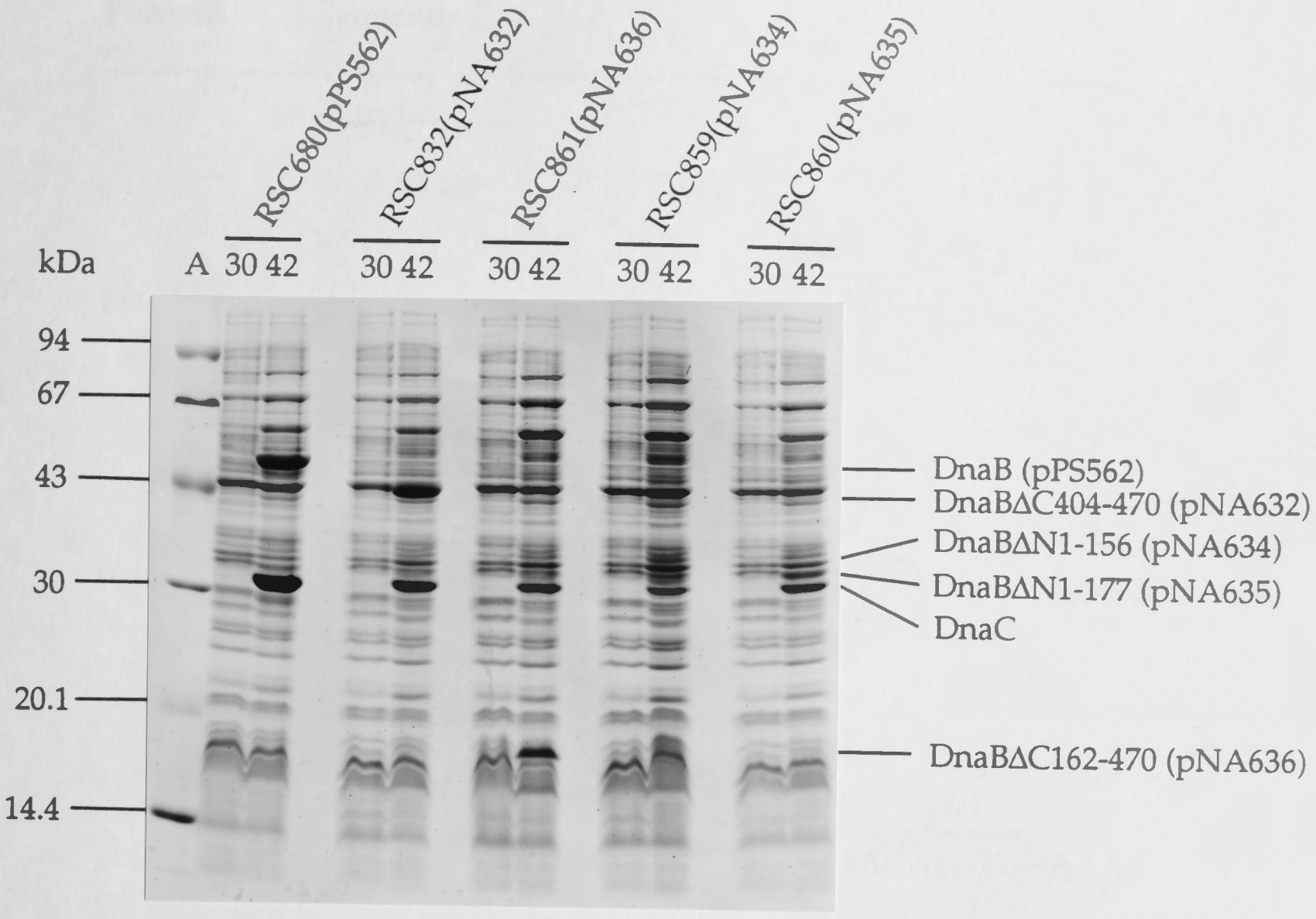

Figure 5.13

SDS-PAGE of lysed cells. Cultures (20 ml) of RSC680, RSC832, RSC861, RSC859, and RSC860 were grown at 30°C to A_{595}~0.5 in the presence of ampicillin (50 μg/ml) as described in Section 2.2. Cells were harvested from a portion (1 ml) and the remainder of the culture was incubated at 42°C, with vigorous shaking. After 4 hours at 42°C, further 1-ml samples were taken. The sedimented cells were resuspended to A_{595}=10 in a loading buffer (Section 2.7) and treated for 2 min at 95-100°C. 20-μl portions were loaded on a 12.5% SDS-polyacrylamide gel and electrophoresed as described in Section 2.7. Protein markers in lane A were as in Figure 3.1. Overproduction of the particular proteins is indicated.

Plasmid	Sequence
pNA640	STOP RBS START 165 *Bam*HI *Hpa*I *Nde*I 166 TTT - TAA GGATCC TAAGGAG GTTAACATATG - AAA
pNA640*	STOP RBS 165 *Bam*HI *Hpa*I 166 TTT - TAA GGATCC TAAGGA•GTTAACATA•G - AAA
pNA645	STOP START 165 *Bam*HI *Nde*I 166 TTT - TA •GGATCC TA •GG• • ••TAACATATG - AAA

Scheme 5.2

The results of dideoxy sequencing of plasmids pNA640* and pNA645 helped to determine deletions (•) in the STOP-RBS-START which was designed for plasmid pNA640. A 1-bp deletion in the RBS together with a 1-bp deletion in the start codon, caused a shift in the reading frame. As a consequence of this, pNA640* directed overproduction of DnaC and DnaBΔC166-470 only (Figure 5.14). Because of a deletion in the originally designed stop codon (TAA) in plasmid pNA645, an amber stop codon was generated. The start codon remained intact. Strain RSC945 (AN1459/pNA645) overproduced DnaC together with DnaBΔC166-470 and DnaBΔN1-165, but due to extensive deletion in the RBS, the *dnaBΔN1-165* was overexpressed to a low level (Figure 5.14).

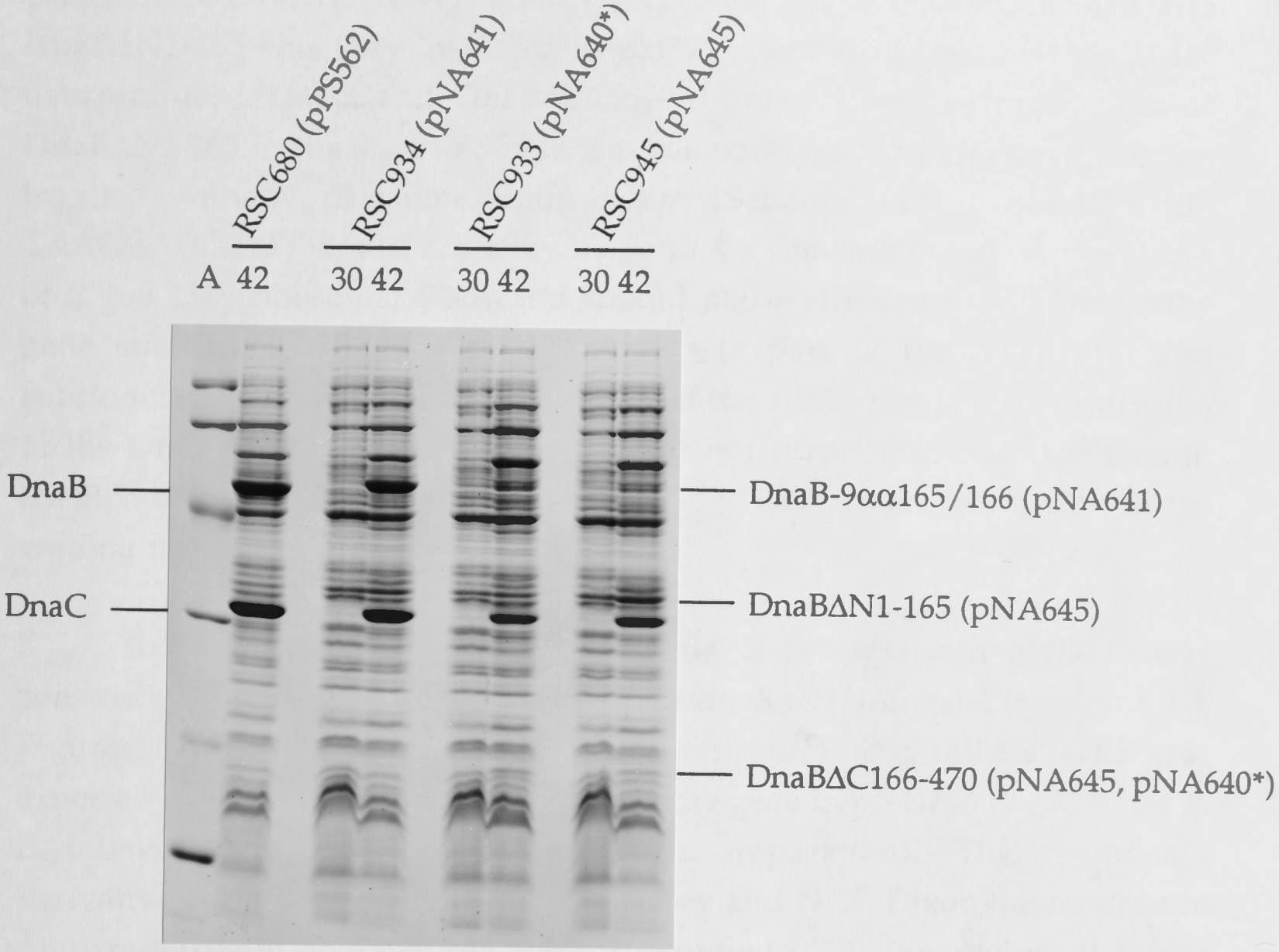

Figure 5.14

Overproduction of the proteins directed by plasmids pPS562 (*wt*DnaB and DnaC), pNA641 (DnaB-9αα165/166 and DnaC), pNA640* (DnaBΔC166-470, DnaC) and pNA645 (DnaBΔN1-165, DnaBΔC166-470, DnaC; Figure 5.7) in strains RSC680, RSC934, RSC933, and RSC945, respectively. SDS-PAGE of the cell lysates. Cells were grown and treated as described in the legend to Figure 5.13. Protein markers (lane A) are as described in Figure 3.1.

Plasmid pNA645 (strain RSC945) directed expression of the DnaC protein to a moderate level, while overproduction of DnaBΔC166-470 and DnaBΔN1-165 was very low. Strain RSC933 harbouring plasmid pNA640* overproduced DnaC and DnaBΔC166-470 only. Low overproduction of DnaBΔN1-165 in the strain RSC945 is presumabely due to extensive deletion in the synthetic ribosome-binding site (Scheme 5.2). This RBS (5'-TAAGGAGGT-3') would normally be perfectly complementary to the 3'-end of *E. coli* 16-S ribosomal RNA and should allow efficient translation of the gene starting with the ATG start codon (a part of the *Nde*I site) and subcloned with an acceptable spacing from the RBS. The lack of expression of the DnaBΔN1-165 domain in RSC933 is not surprising - the deletions in the RBS and *Nde*I site upstream the DnaBΔN1-165 resulted in a shift in the reading frame (Scheme 5.2, Figure 5.14).

To achieve overproduction of DnaBΔN1-165, plasmid pND713 was constructed using pNA645 as source of the *dnaBΔN1-165* gene (Section 5.2.3, Figures 5.8 and 5.15). The translation efficiency of *dnaBΔN1-165* was expected to be increased by subcloning of the gene in pND706 (C. A. Love, P. E. Lilley and N. E. Dixon, manuscript in preparation). This vector is a derivative of pPL452 (C. A. Love, P. E. Lilley and N. E. Dixon, manuscript in preparation) and contains the ϕ10-translational initiation region of phage T7, essentially as it appears in the Studier T7 expression system (pET vectors, 1990), linked to tandem λ promoters. Insertion of a 1585-bp *Nde*I-*Eco*RI fragment of pNA645 yielded plasmid pCN718 (Section 5.2.3, Figures 5.9 and 5.15), that overproduces the COOH-terminal domain of DnaB (DnaBΔN1-165) to an acceptable level. Plasmid pNA787, constructed by subcloning of the *dnaBΔN165*$^{+}$ fragment in pPS237 (strain RSC2034; Section 5.2.3, Figure 5.10) directed simultaneous overexpression of the DnaBΔN1-165 domain with DnaC as illustrated in Figure 5.15. About 25% of the DnaBΔN1-165, when overproduced alone, was soluble and co-overproduction of DnaC did not seem to affect this yield (data not shown).

In order to create a system that would simultaneously overproduce the NH_2- and COOH-terminal domains of DnaB with the DnaC protein, a new strategy was devised and the experiment described in Section 5.2.3 was carried out. Since the strain simultaneously overproducing DnaBΔN1-165 and DnaC was available [RSC2034 (AN1459/pNA787)], a compatible plasmid encoding the NH_2-terminal domain of the DnaB protein together with a gene encoding resistance to an antibiotic other than ampicillin was required

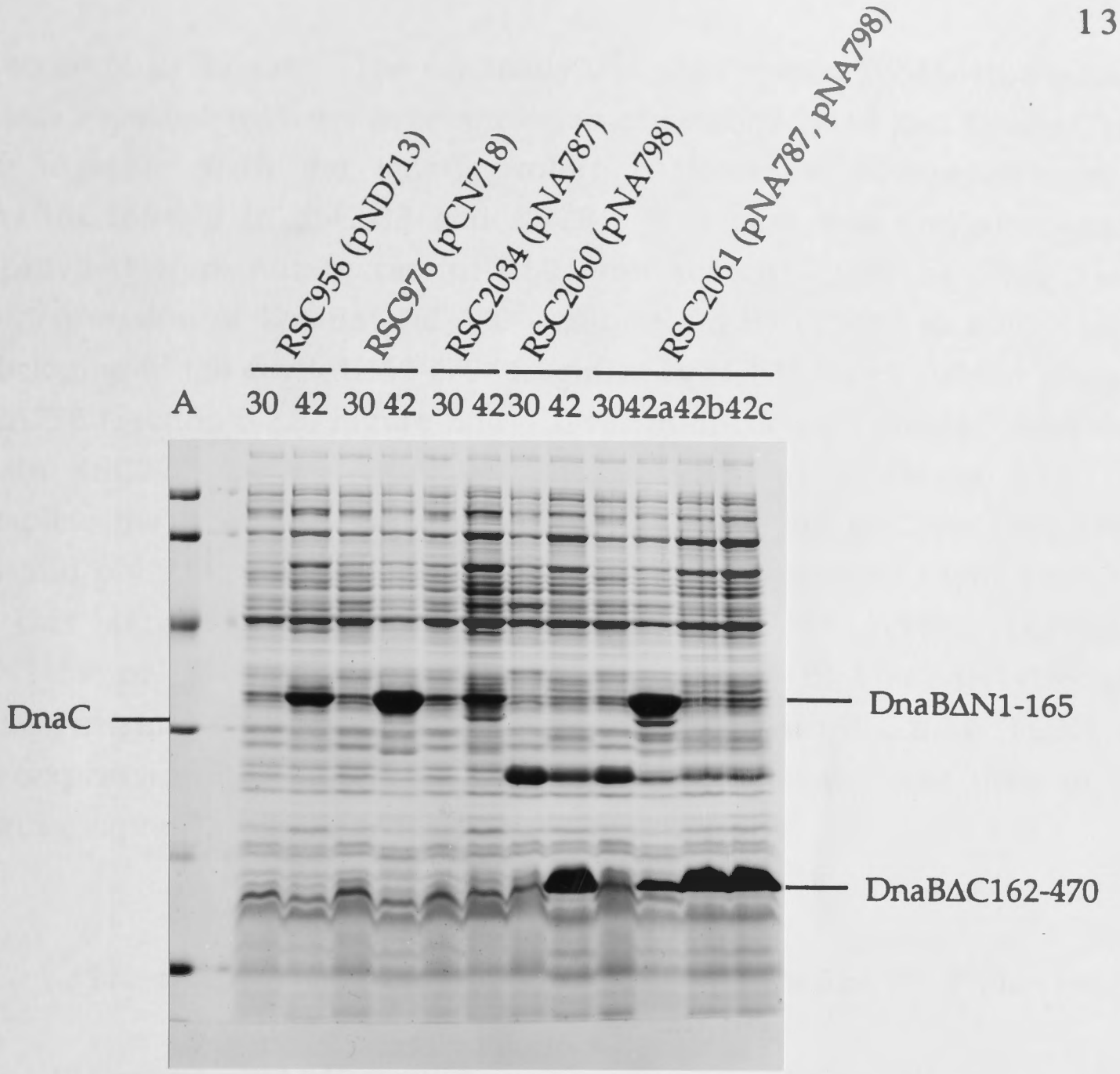

Figure 5.15

Several systems for overexpression of the *dnaBΔN1-165* deletion mutant were prepared. Strains RSC956 harbouring plasmid pND713 (*dnaBΔN1-165*$^+$), RSC976 [pCN718 (*dnaBΔN1-165*$^+$)], RSC2034 [pNA787 (*dnaBΔN1-165*$^+$, *dnaC*$^+$)], RSC2060 [pNA798 (*dnaBΔC162-470*$^+$)], and RSC2061 [pNA798 (*dnaBΔC162-470*$^+$), pNA787 (*dnaBΔN1-165*$^+$, *dnaC*$^+$)] were grown and induced as described in the legend to Figure 5.13. The LBT medium was supplemented with ampicillin (50 μg/ml) for RSC956, RSC976, and RSC2034. Chloramphenicol (7 μg/ml) was used to maintain pNA798 in strain RSC2060. The two-plasmid system RSC2061 was grown at 30°C and thermally induced at 42°C in the presence of ampicillin (50 μg/ml) and chloramphenicol, the concentration of which was varied. When 7 μg/ml was used, the overproduction of DnaBΔC162-470 (lane 42a) was only ~10% of the level in RSC2060 but at the same time, the overproduction of DnaBΔN1-165 was maintained very high and overproduction of DnaC remained at the original level (RSC2034). In the presence of higher concentrations of chloramphenicol (30 μg/ml and 50 μg/ml, respectively; lanes 42b and 42c), no overproduction of DnaBΔN1-165 or DnaC was detected.

to accomplish the task. The originally designed system (pNA640, Figure 5. 6) was expected to direct overexpression of DnaBΔN1-165 and DnaBΔC166-470 together with the DnaC protein. However, overproduction of DnaBΔC166-470 in RSC933 and RSC945 was very low and attempts to improve it were not successful (data not shown). On the other hand, overexpression of DnaBΔC162-470 was directed by pPS503 to a high level. Subcloning of the *dnaBΔC162-470*$^+$ fragment in pCE33 (*cat*$^+$) yielded plasmid pNA798 (Section 5.2.3, Figure 5.11). Overproduction of DnaBΔC162-470 in strain RSC2060 (AN1459/pNA798) is documented in Figure 5.15. To complete the experiment, an ampicillin-resistant strain RSC2034 containing plasmid pNA787 (*dnaBΔN165*$^+$, *dnaC*$^+$, *bla*$^+$) was transformed with pNA798. In this ampicillin- and chloramphenicol-resistant system [RSC2061 (AN1459/pNA787, pNA798)], the overproduction of DnaBΔN1-165 and DnaC remained at the same level as observed in strain RSC2034. However, overexpression of DnaBΔC162-470 was significantly lower than in the original expression system (RSC2060; Figure 5.15).

5.3.2 *Mutants of the DnaB Protein Generated for the Specific Proteolyses*

Plasmids pNA785 encoding the DnaB protein with an inserted thrombin-cleavage site (DnaB-T165/166), and pNA786 encoding a factor Xa-recognition site within the putative hinge region of the DnaB protein (DnaB-F165/166) were prepared as described in Section 5.2.4 (Figure 5.12). Different treatments of the three-fragment ligation products before transformations of strain AN1459 affected the results of the experiments. Tranformations T1 and F1 that were carried out with one half of the ligation mixtures provided only a few tens of ampicillin-resistant clones. On the other hand, several thousands of transformants were the results of Transformations T2 and F2. The proportions of plasmids pNA785 and pNA786 among the ampicillin-resistant clones also commended electrophoretic separation of the linear plasmid DNA with oligonucleotides attached to its *Nde*I- and *Bam*HI-protruding ends, followed by their annealing before the transformation of competent cells. The resulting modification of the primary structure of DnaB after insertion of the thrombin- and factor Xa-recognition sites is presented in Scheme 5.3. High-level overproduction of the mutant DnaB proteins and DnaC at 42°C was detected in strains RSC2032 (AN1459/pNA785) and RSC2033 (AN1459/pNA786; Figure 5.16).

(a) pNA641

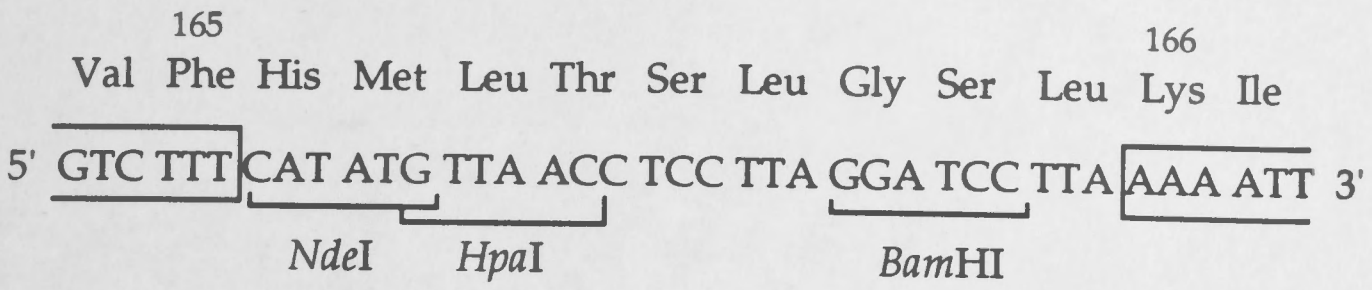

(b) pNA785

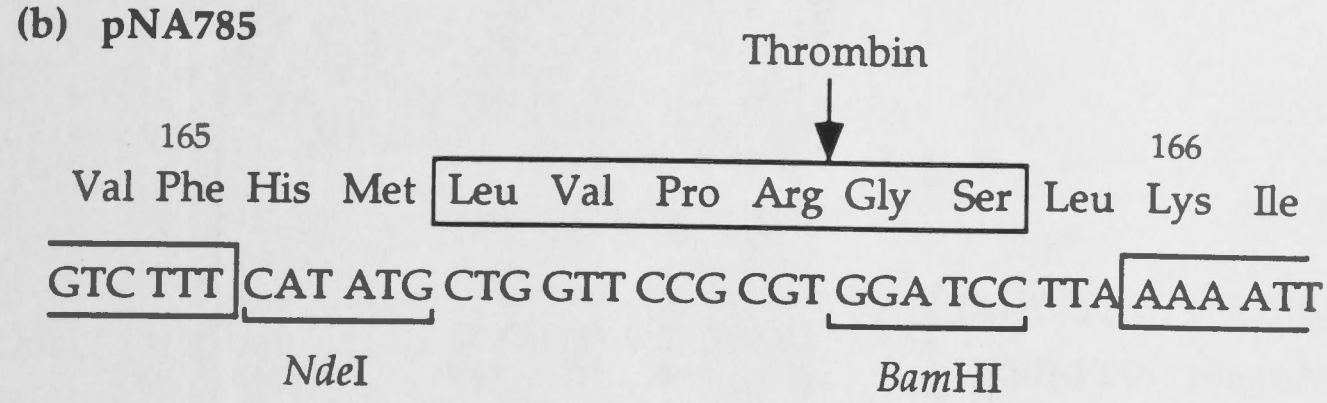

(c) pNA786

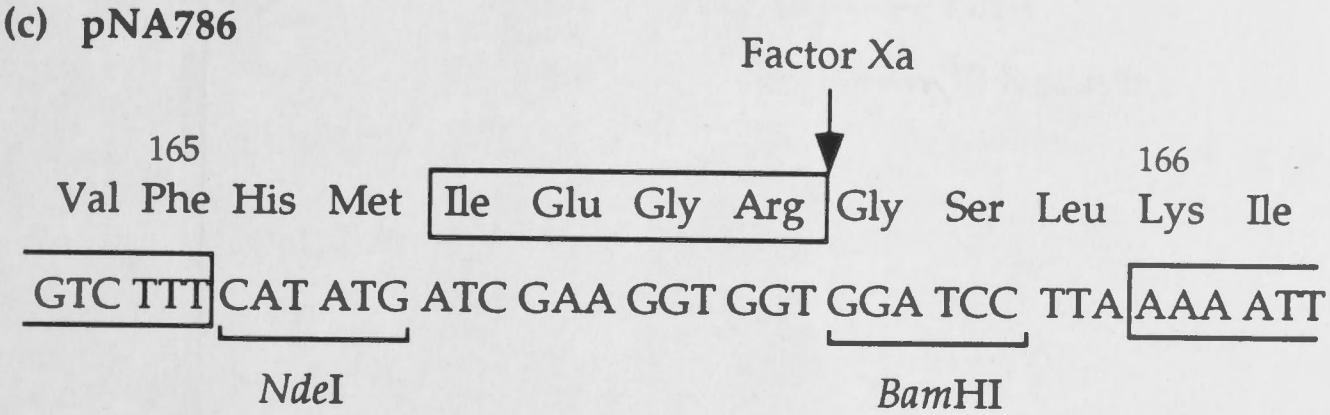

Scheme 5.3

Insertion of a STOP-RBS-START adaptor (Figure 5.6) in the opposite orientation between codons 165 and 166 of *dnaB* generated plasmid pNA641 encoding DnaB with a 9-amino-acid insertion between phenylalanine (codon 165) and lysine (codon 166). Replacement of the 17-bp *Nde*I-*Bam*HI fragment of pNA641 by the *Nde*I-*Bam*HI thrombin cassette (Scheme 5.1b) resulted in plasmid pNA785. Replacement of the same fragment by the *Nde*I-*Bam*HI factor Xa cassette (Scheme 5.1b) yielded pNA786. Amino-acid residues inserted into the DnaB protein as a consequence of these genetic manipulations are indicated above the particular nucleotide sequences.

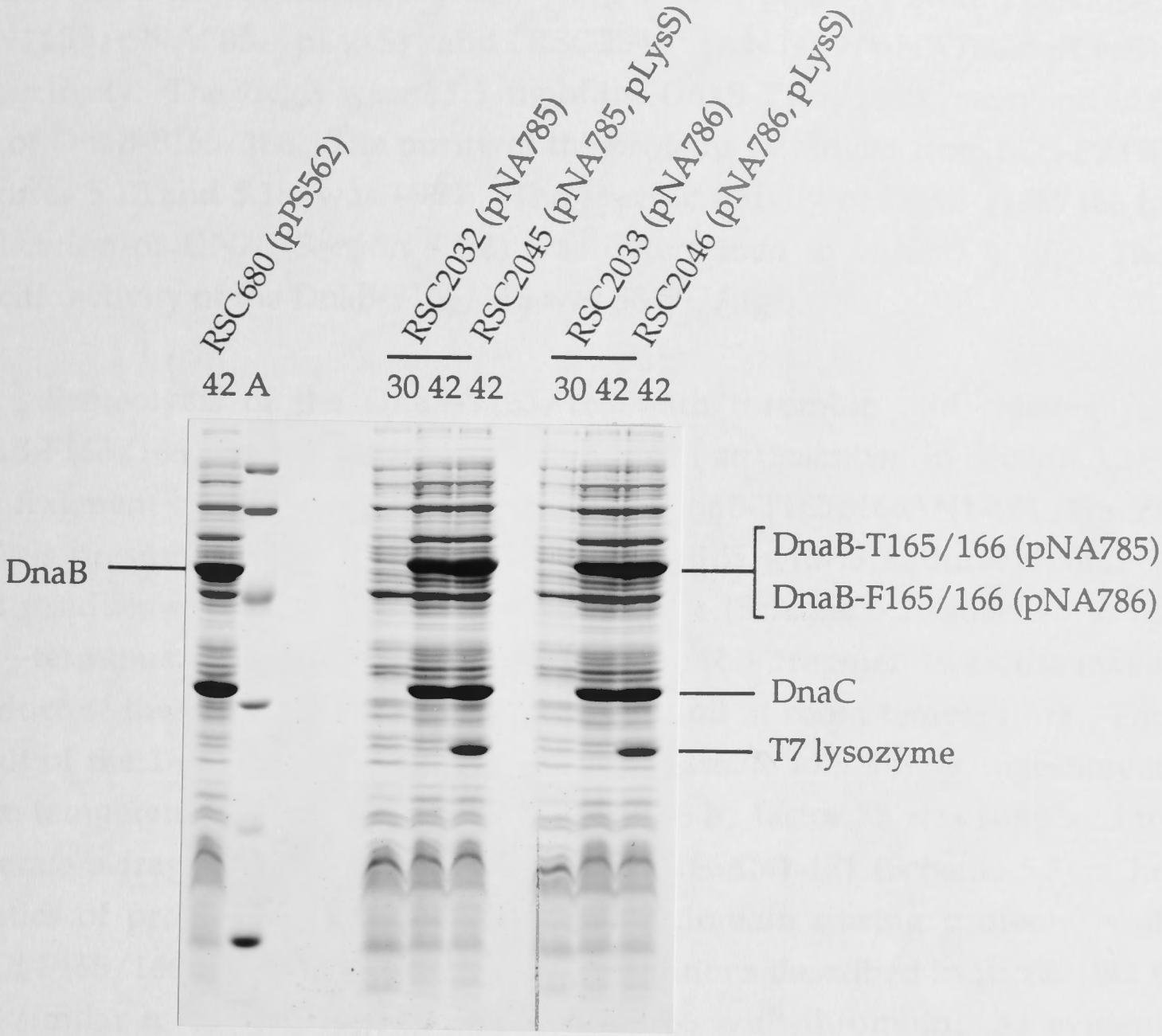

Figure 5.16

SDS-PAGE of cell lysates of strains RSC2032, RSC2045, RSC2033 and RSC2046. Cells were grown, induced and samples for the electrophoresis were taken as in the legend to Figure 5.13. pNA785 directed high-level co-overproduction of DnaC and a DnaB mutant having the thrombin-recognition site inserted between phenylalanine (codon 165) and lysine (codon 166) of the protein. pNA786 directed simultaneous overexpression of *dnaB-F165/166* and *dnaC*. Plasmid pLysS (*cat*$^+$) directing production of T7 lysozyme was introduced into the strains to facilitate lysis of the cells. A sample of a cell lysate of thermally-induced strain RSC680 and protein markers (lane A) were used as standards.

Purifications of DnaB-T165/166 and DnaB-F165/166 were performed as described in Section 5.2.7 from ~15 g of cell paste of strains RSC2045 (AN1459/pNA785, pLysS) and RSC2046 (AN1459/pNA786, pLysS), respectively. The yields were 13.3 mg of the DnaB-T165/166 protein and 12.5 mg of DnaB-F165/166. The purity of the proteins as judged from SDS-PAGE (Figures 5.17 and 5.18) was ~98%. The specific activity of DnaB-T165/166 in replication of DNA (Section 3.2.2) was determined to be 58.5 U/μg. The specific activity of the DnaB-F165/166 was 58.8 U/μg.

Proteolysis of the DnaB-T165/166 with thrombin and cleavage of DnaB-F165/166 with factor Xa were carried out as described in Section 5.2.8. The fragment of DnaB-T165/166 designated DnaB-T165/166ΔN1-171 (Figure 5.17) is presumed to correspond to DnaBΔN1-165 with 3 additional amino-acid residues encoded by the thrombin cassette (Scheme 5.2) attached to its NH_2-terminus. As evident from Figure 5.17, this fragment was the major product of the digestion by thrombin at 4°C and at room temperature. The result of the 1-day digestion at 4°C was comparable to a 5-hour digestion at room temperature. Cleavage of DnaB-F165/166 by factor Xa was supposed to generate a fragment identical to DnaB-T165/166ΔN1-171 (Scheme 5.3). The kinetics of production of the DnaBΔN1-165 domain during proteolysis of DnaB-F165/166 with factor Xa under the conditions described in Section 5.2.8 was similar to the cleavage of DnaB-T165/166 with thrombin. As evident from Figures 5.17 and 5.18, the COOH-terminal domain was prone to further unspecific degradation.

The mobility of the fragments supposedly corresponding to the NH_2-terminal domains was higher than the mobility of DnaBΔC166-470 or DnaBΔC162-470, in the case of cleavage by thrombin as well as in proteolysis with factor Xa (Figures 5.17 and 5.18). Determination of the NH_2- and COOH-terminal amino-acid sequences of the fragments and alignment of the sequences with the primary structure of DnaB would enable specification of the fragments.

Figure 5.17

SDS-PAGE of the products of proteolysis of DnaB-T165/166 by thrombin. The protein was dialysed against Buffer T and the reaction was carried out at 4°C, room temperature, or 37°C, as described in Section 5.2.8. 2.5 U of thrombin was used for the cleavage for each 50 μg of the protein. Bands labelled DnaBΔN1-165, DnaC, DnaBΔC166-470, and DnaBΔC162-470 correspond to the particular proteins overproduced in strains RSC2061 (AN1459/pNA798, pNA787), RSC33/640 [AN1459/pNA33-640 (*cat*$^+$)], and RSC2034 (AN1459/pNA787). Plasmid pNA33-640 was prepared as a part of an alternative strategy for the preparation of a system simultaneously overproducing DnaC, DnaBΔC166-470, and DnaBΔN1-165. Because of a low overproduction of DnaC and the NH_2-terminal domain of DnaB the strain was not used in further experiments. The band labelled DnaB-T165/166ΔN1-171 is presumed to correspond to the DnaBΔN1-165 polypeptide with 3 amino-acid residues encoded by the thrombin cassette and attached to the NH_2-terminus of DnaBΔN1-165 (Scheme 5.3). Mobility of the fragment supposedly corresponding to the NH_2-terminal fragment and designated DnaBΔCX was higher than the mobility of DnaBΔC162-470 probably due to unspecific degradation of the COOH- and NH_2-termini of the NH_2-terminal fragment.

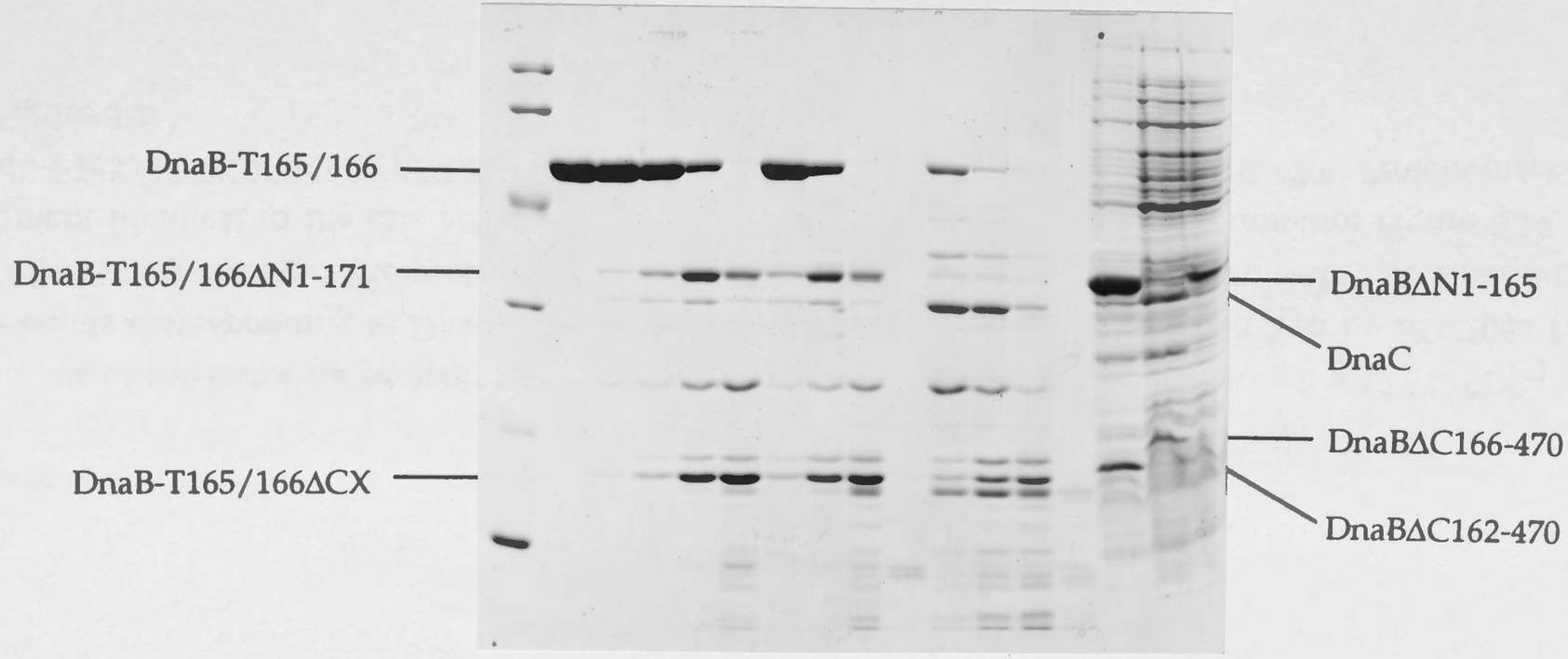
RSC2061(pNA798, pNA787)
RSC33/640 (pNA33/640)
4°C
ROOM TEMPERATURE
37°C
42 42 42
A 0 1 5 24 72 1 5 24 72 1 5 24 72
DnaB-T165/166
DnaB-T165/166ΔN1-171
DnaB-T165/166ΔCX
DnaBΔN1-165
DnaC
DnaBΔC166-470
DnaBΔC162-470

Figure 5.18

Products of the factor Xa-proteolysis of DnaB-F165/166 were electrophoresed through a 12.5% SDS-polyacrylamide gel. The bands corresponding to DnaC and the deletion mutants of *wt*DnaB overproduced by RSC2061 (AN1459/pNA798, pNA787) are indicated. The proteolysis yielded two major products that are presumed to be DnaB-F165/166ΔN1-171 (a fragment identical to the one generated in proteolysis of DnaB-T165/166 by thrombin; Figure 5.17, Scheme 5.3), and DnaB-F165/166ΔCX which probably represents a truncated version of DnaBΔC162-470. Protein markers (lane A) are as in Figure 3.1.

RSC2061 (pNA798, pNA787)

4°C ROOM TEMPERATURE 37°C 42°C

A 0 1 5 24 72 1 5 24 72 1 5 24 72

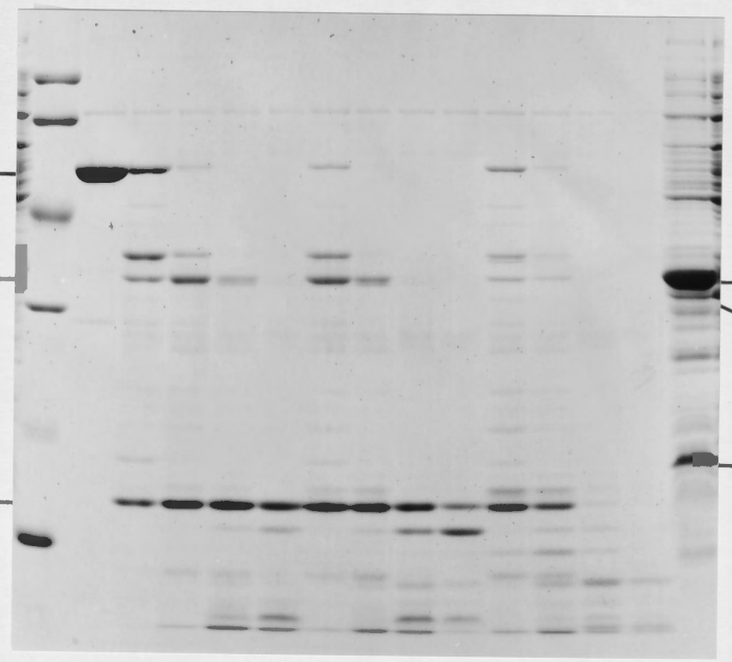

DnaB-F165/166

DnaB-F165/166ΔN1-171

DnaB-F165/166ΔCX

DnaBΔN1-165

DnaC

DnaBΔC162-470

5.3.3 *Purification and Crystallization of the NH_2-terminal Domain of the DnaB Protein*

The NH_2-terminal domain of the DnaB protein was overproduced to a high level in strain RSC571 (AN1459/pPS503). Simultaneous overproduction of the domain with DnaC did not seem to improve its solubility (Section 5.3.1). Strain RSC571 was therefore used as a source of the partially-soluble DnaBΔC162-470 deletion mutant which represents the entire NH_2-terminal domain with a 14-amino-acid "tail" on its NH_2-terminus together with ~35 amino-acid residues of the putative hinge region (estimated M_r=17,880).

A concentration of ammonium sulfate optimal for precipitation of DnaBΔC162-470 from the cell lysate was determined experimentally. On addition of 0.27 mg to each ml of lysate, most of the DnaBΔC162-470 precipitated and about 30% of protein inpurities remained in the solution. Fractions Nos. 36-42 obtained from DEAE-Fractogel chromatography (Figure 5.19) contained 150 mg of total protein (fraction FIIIΔC). Non-denaturing SDS-PAGE indicated that the deletion mutant exists as a monomer (data not shown), and gel filtration through a column of Sephadex G-50 was therefore used as a final purification step. As illustrated in Figure 5.20, DnaBΔC162-470 from fraction FIIIΔC was eluted in a single peak. The final yield of ~97% pure DnaBΔC162-470 was 136 mg (Table 5.1).

An experiment carried out with a view to form a DnaBΔC162-470.DnaC complex was not successful. The trial was essentially performed in the same way as reassociation of *wt*DnaB with the DnaC protein (Section 3.2.1.3). The following anion-exchange chromatography on a column of DEAE-Fractogel completely separated DnaBΔC162-470 from DnaC (data not shown).

Initial crystallization experiments did not suggest any potentially useful crystallization reagents.

5.4 **Discussion**

Several systems for overexpression of NH_2- and COOH-terminal DnaB deletion mutants were prepared in attempts to purify and crystallize

Figure 5.19

(a) Elution profile of the DnaBΔC162-470 from chromatography on a column of DEAE-Fractogel. Chromatography was performed as described in Section 5.2.7. Protein concentrations were determined by Bradford assay (Section 2.14).

(b) SDS-PAGE of the proteins eluted from DEAE-Fractogel in a gradient of NaCl. Protein markers (lane A) were as usual (Figure 3.1). A sample of Fraction FIΔC (lane B) together with a sample of Fraction FIIΔC (lane C) and 4.5-μl portions of selected fractions (as indicated above the photograph) were electrophoresed through a 12.5% SDS-polyacrylamide gel (Section 2.15).

(a)

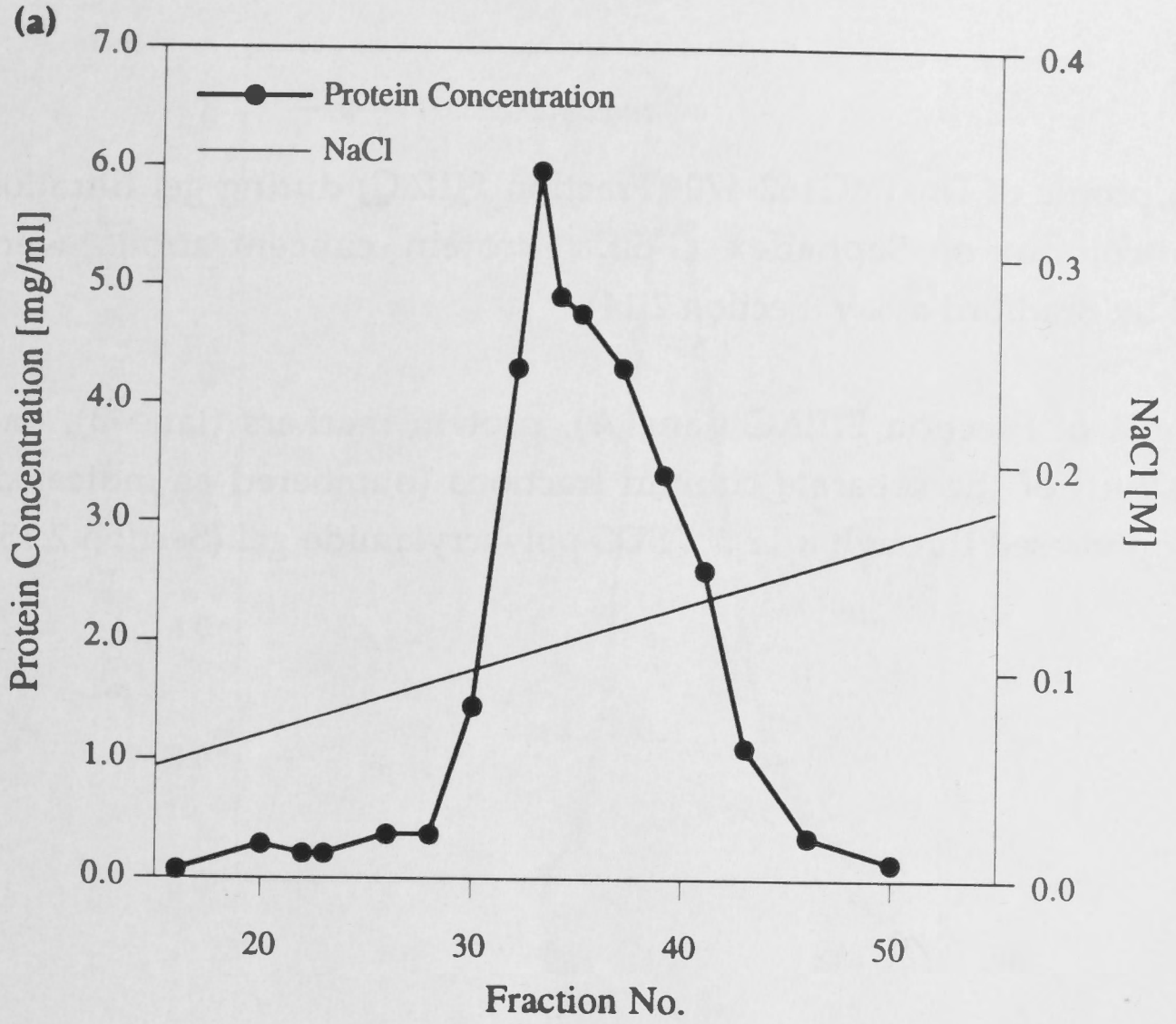

(b)

A B C 22 26 28 30 32 33 34 35 36 37 38 39 41 43

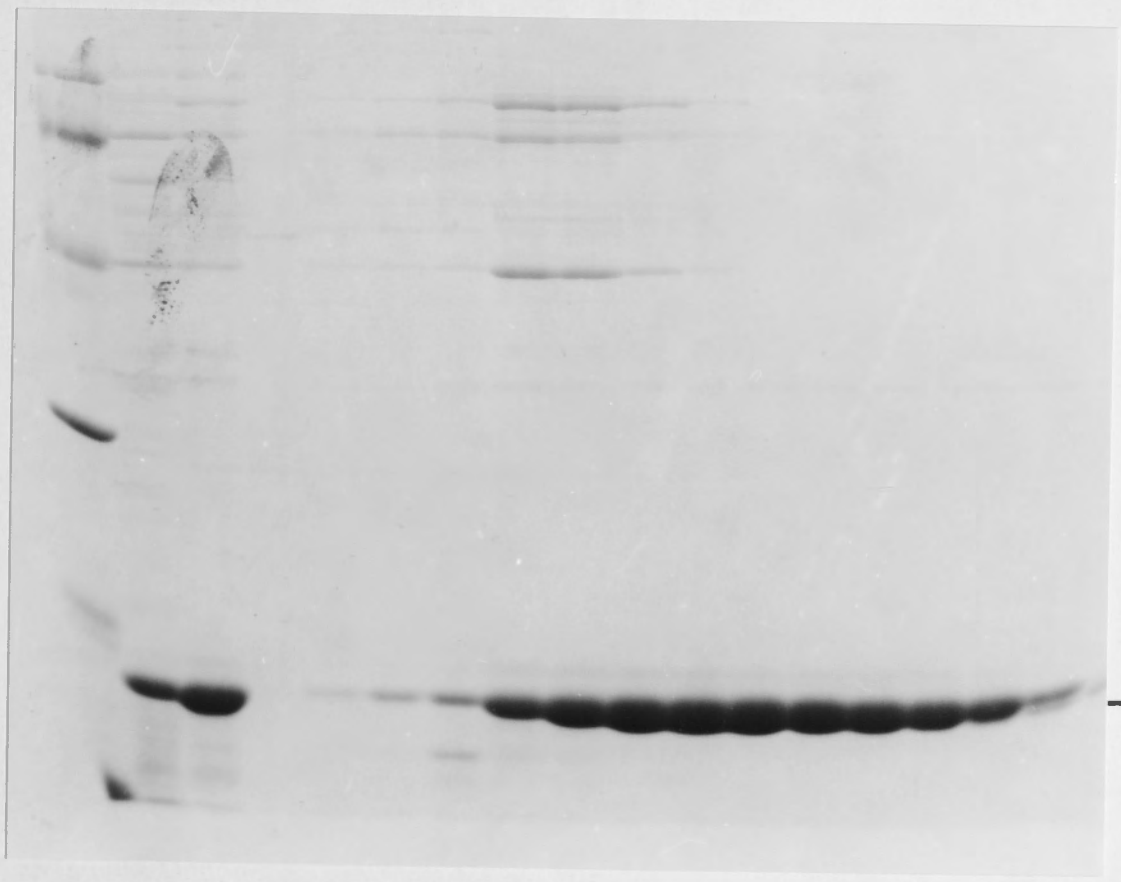

DnaBΔC162-470

Figure 5.20

(a) Elution profile of DnaBΔC162-470 (Fraction FIIIΔC) during gel filtration through a column of Sephadex G-50. Protein concentrations were determined by Bradford assay (Section 2.14).

(b) A sample of Fraction FIIIΔC (lane A), protein markers (lane B), and portions (2.5 µl) of the separate column fractions (numbered as indicated) were electrophoresed through a 12.5% SDS-polyacrylamide gel (Section 2.15)

(a)

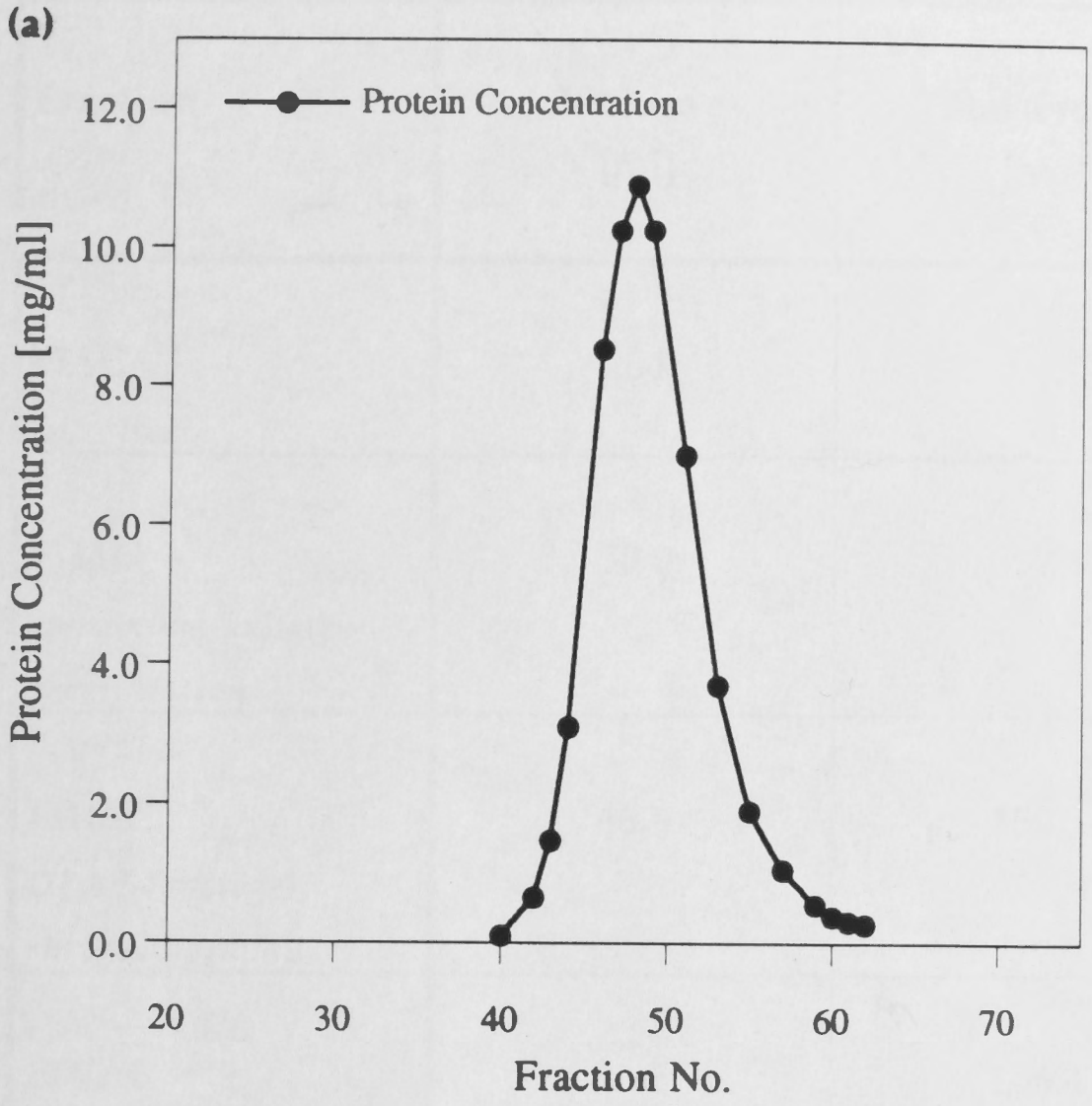
Protein Concentration
12.0
10.0
8.0
6.0
4.0
2.0
0.0
Protein Concentration [mg/ml]
20
30
40
50
60
70
Fraction No.

(b)

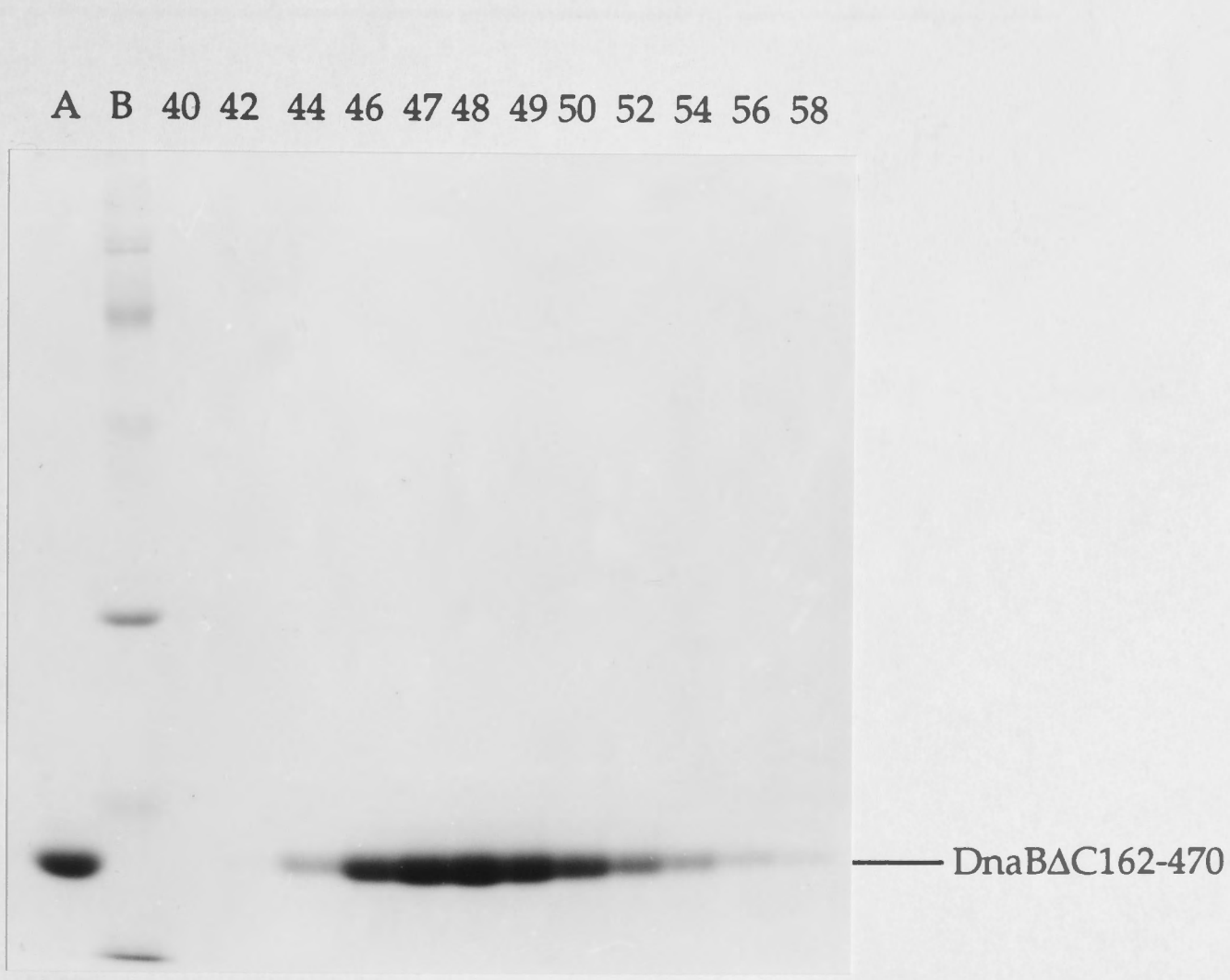
A B 40 42 44 46 47 48 49 50 52 54 56 58
DnaBΔC162-470

Fraction	Volume [ml]	Total Protein [mg]
FIΔC *cell lysate*	264	943
FIIΔC *ammonium-sulfate precipitation*	50.0	397.3
FIIIΔC *DEAE-Fractogel chromatography*	46.4	150.3
FIVΔC *Sephadex G-50 gel filtration*	24.6	136.4

Table 5.1

Purification of the DnaBΔC162-470 deletion mutant from ~15 g of cell paste of strain RSC571 (Section 5.2.6). Activity of the mutant could not be measured, because no independently assayable catalytic activity of the NH_2-terminal domain of DnaB has been detected so far.

the separate domains of DnaB. These experiments were conducted simultaneously with the preparation of dominant lethal mutants of DnaB (Section 4) as another alternative that, if succesful, could significantly contribute to elucidation of the three-dimensional structure of the DnaB protein.

A strain overproducing the NH_2-terminal domain in a soluble form was available, so the major interest was therefore focused on subcloning of the genes encoding the COOH-terminal domain, which retains most of the DnaB catalytic activities. The DnaBΔN1-156 and DnaBΔN1-177 mutants (Stamford, 1991) remained insoluble even after their co-overproduction with DnaC. Possible explanations are that they cannot fold properly, or that they don't interact with DnaC. As to the interaction of DnaB with DnaC, it has not yet been confirmed if it involves only the NH_2-terminal domain (Nakayama, 1984b), the COOH-terminal domain (Chang *et al.*, 1991) or both. In fact, inability of the DnaB-I141T mutant to form a stable complex with DnaC (Section 4.3.2) indicates an important role of the hinge region in this interaction too.

Further attempts were therefore focused on the preparation of a system for simultaneous overexpression of DnaC, DnaBΔC166-470 and DnaBΔN1-165 with a view to reconstitute the native protein from discrete fragments (even transiently) and thus to obtain a soluble COOH-terminal domain of DnaB. Because of very low overproduction of DnaBΔC166-470 directed by different recombinant plasmids (data not shown), a system for overproduction of DnaC, DnaBΔN1-165, and DnaBΔC162-470 was prepared. The DnaBΔN1-165 polypeptide was partially soluble. Other systems were prepared, one overproducing this polypeptide only, and one directing overexpression of DnaBΔN1-165 together with the DnaC protein. All these expression systems will have to be examined and compared with each other in order to choose the best one for large-scale overproduction and purification of the COOH-terminal domain.

The COOH-terminal part of the molecule representing the DnaBΔN1-165 deletion mutant together with three amino-acid residues of the thrombin/factor Xa cassette attached to its NH_2-terminus was generated by specific proteolysis. Purification of this fragment is another possibility for obtaining the COOH-terminal domain. However, considering the further degradation of the domain under the conditions of proteolyses, obtaining a

homogeneous preparation of the desired polypeptide suitable for extensive crystallization experiments might be a problem. This approach could, however, be extended to use of other more specific proteases when and if they become available.

No crystals of the DnaBΔC162-470 mutant representing the NH_2-terminal domain together with a 35-amino-acid part of the hinge region have been prepared yet. We suppose that the polypeptide is folded properly. It has then a high degree of secondary structure (Section 1.5) between residues 15-126, but also contains a 14-amino-acid "tail" on the NH_2-terminus and ~35-amino-acid part of the "hinge region", which could make its crystallization difficult. Alternatively, the structure of this polypeptide or a somewhat smaller soluble version yet to be prepared might be elucidated by multidimensional NMR spectrometry.

6 ELECTRON-MICROSCOPIC STUDIES OF THE DnaB HELICASE

6.1 Introduction

Electron microscopy is another powerful technique that gives us information about protein structure. It can reveal the quaternary structure of large proteins or aggregates, the shape of individual subunits, or, in rare cases, even determine the pathway of the polypeptide chain within a protein molecule. Although one always must be wary of potential artifacts inherent in the use of the electron microscope, this technique in many cases provides an unparalleled glimpse of a protein structure. The value of such information is appreciated especially where other techniques have not been successful.

In the case of the DnaB helicase, further extensive experimental studies are required to obtain high-resolution X-ray diffraction data and to solve the structure of the protein at atomic level. However, in the meantime, electron-microscopic studies of negatively stained DnaB oligomers carried out by Dr José M. Carazo and Ms M. Carmen San Martin (Centro Nacional de Biotechnología (C.S.I.C.), Campus Universidad Autonóma de Madrid) have provided information about the general structure of the aggregate at medium resolution (San Martin *et al.*, 1995). Their results of the two-dimensional analysis and three-dimensional reconstruction of the DnaB helicase are reported in this section.

6.2 Material and Methods

6.2.1 *Electron Microscopy*

The DnaB protein was purified in the presence of ATP (Section 3). Immediately before the electron-microscopy assays, glycerol was removed from the samples by chromatography on a Sephadex G100 column (Pharmacia) in Buffer B (Section 3.2.1) without glycerol, and diluted in the

same buffer to 5 µg/ml. Carbon-coated holey grids were treated by glow discharge. A sample of DnaB (5 µg/ml) was loaded onto the grids and negatively stained with 2% uranyl acetate. Grids were examined in a Jeol 1200 EX-II transmission electron microscope at 100 kV accelerating voltage and x60,000 magnification. Micrographs were taken on Kodak SO - 163 plates under minimum-dose conditions. Tilting pairs were taken first at 55° and then at 0°, using an eucentric goniometer and minimum dose conditions.

6.2.2 *Image Processing*

Micrographs were digitized in an Eikonix IEEE 488 camera with a pixel size of approximately 4 Å and processed using the Xmipp package (software developed in the group of Dr J. M. Carazo). The particle projections were selected from the digitized micrographs to form an homogeneous population of views. Then, 64 x 64 pixel single-particle images were extracted and translationally aligned by cross-correlation with a circular mask. Assessment of the population's homogeneity was carried out by means of a neural network self-organizing map (S.O.M.) based classificator (Marabini and Carazo, 1994). Images of particles were then processed by a reference-free alignment method (Penczek *et al.*, 1992) and again examined by the S.O.M. classificator. A rotational power spectrum (Crowther and Amos, 1971) was obtained for a significant area of the specimen containing the perifery of the particle. Resolution was estimated by the spectral signal to noise ratio method (Unser *et al.*, 1987) with the threshold set at 4.

6.2.3 *Three-Dimensional Reconstruction*

Three-dimensional reconstruction was performed following the random conical tilting method (Rademacher *et al.*, 1987) by means of a filtered backprojection algorithm. Three-dimensional resolution was estimated by the differential phase residual method with the cut-off set at 45° (Frank *et al.*, 1988). After backprojection, the reconstructed volume was low-pass filtered to the estimated reproducible resolution and visualized with AVS (Advanced Visual Systems, Inc.). The percentage of reconstructed protein mass was calculated considering a mean protein density of 1.33 g/cm^3.

6.3 Results

6.3.1 *Two-Dimesional Analysis of the DnaB Oligomer*

The preparations of DnaB (in the presence of ATP) when observed in the electron microscope showed triangle-shaped views with a central region of lower density (Figure 6.1a). A total of 1373 single-particle images were visually selected and extracted. A subset of this population is shown in Figure 6.1b. Single-particle images were processed as described in Section 6.2.2. The average image (Figure 6.2a) contains reproducible signal information to 1.8 nm. The general morphology of this image shows a triangle shaped particle with an external diameter of 14 nm penetrated by a channel of 4 nm diameter. The edges of the triangle have length of about 11 nm. The specimen presents 3 peripheral stain-excluding regions surrounding another 6 more massive lobules. The three small regions appear to be connected preferentially to one of its two large neighbours, providing the oligomer with a certain handedness. A rotational analysis (Figure 6.2.b) carried out at the peripheral region of the average image (between radii 35 and 70 Å) confirmed the significance of the triangular features upon the general hexagonal structure with two strong peaks of energy at the three-fold and six-fold rotational harmonics (39% and 43% of the total energy, respectively).

6.3.2 *Three-dimensional Reconstruction of the DnaB Oligomer.*

A three-dimensional reconstruction of the DnaB oligomer at a resolution of 2.7 nm was obtained from an initial set of 1351 images of particle pairs viewed at tilt angles of 0 and 55° (Section 6.2.3).

A representative surface rendering of the volume of the oligomer is presented in Figure 6.3a. The planes corresponding to the reconstructed DnaB oligomer are in Figure 6.3b.

The three-dimensional reconstruction of DnaB further extended the results of the two-dimensional analysis. The reconstructed volume is about 3.8 nm high and shows that the low contrast region at the centre of the particle is a channel running through the whole structure that appears to be fully open on both sides. As evident from Figure 6.3b, the reconstructed

(a)

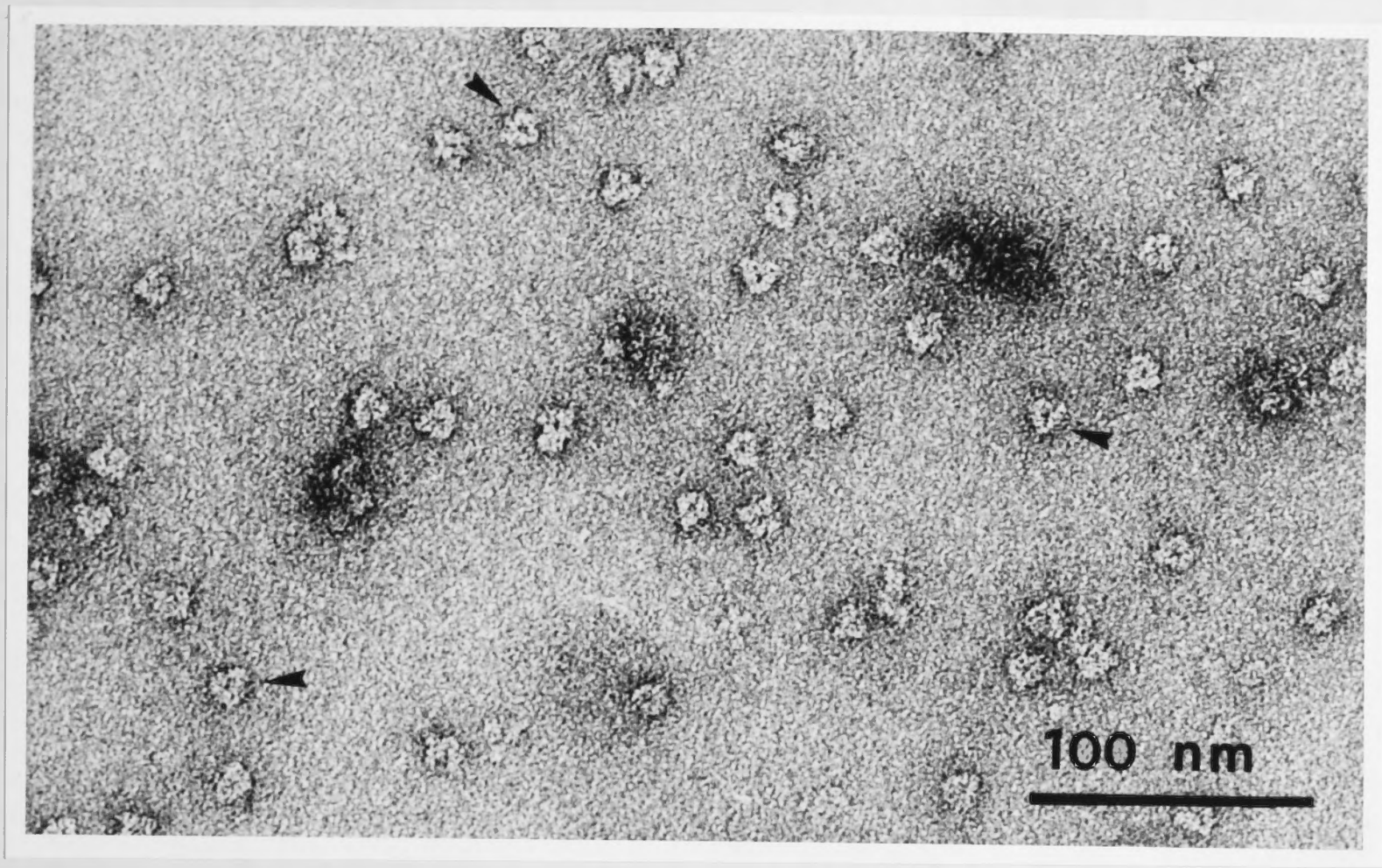

(b)

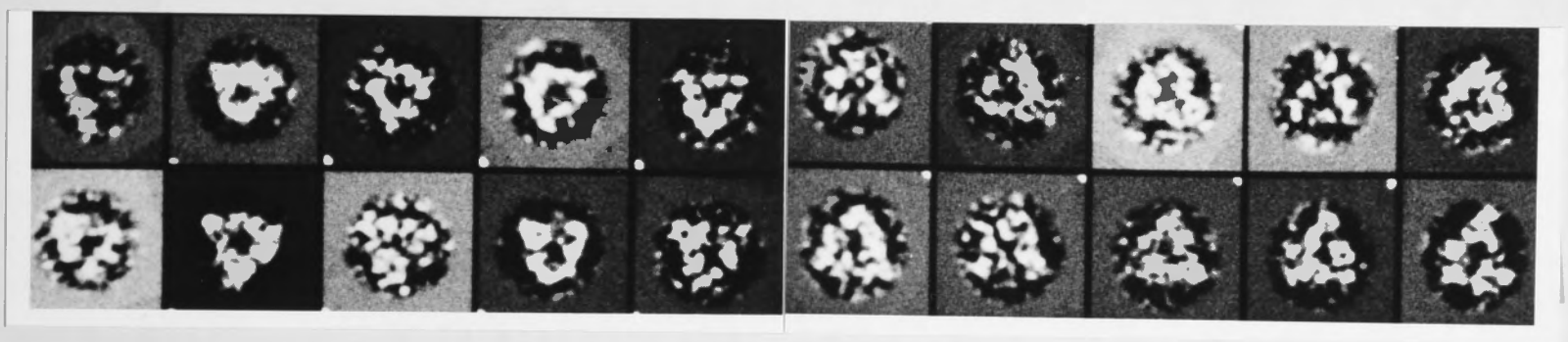

Figure 6.1

Typical electron micrograph (a) and gallery of views (b) of negatively stained DnaB oligomers.

(a)

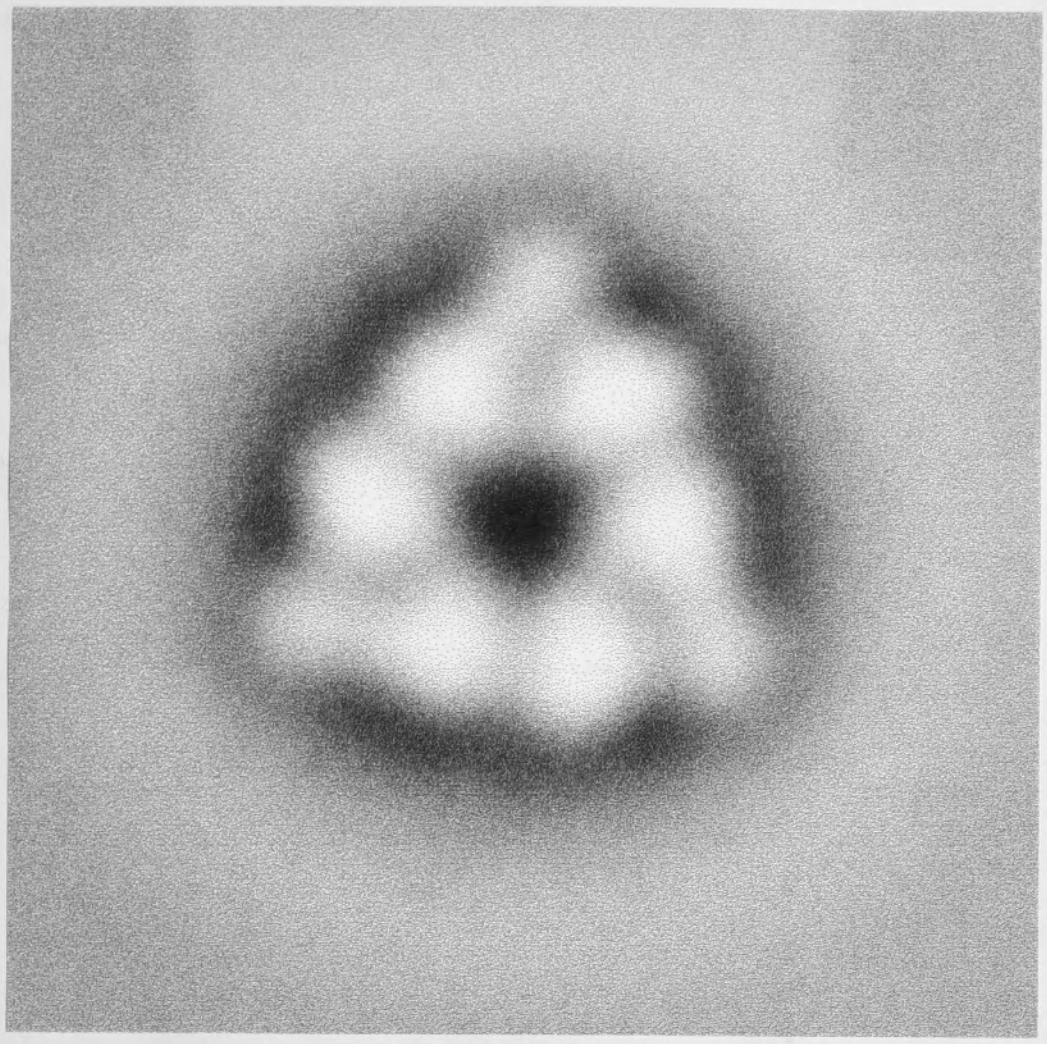

(b)

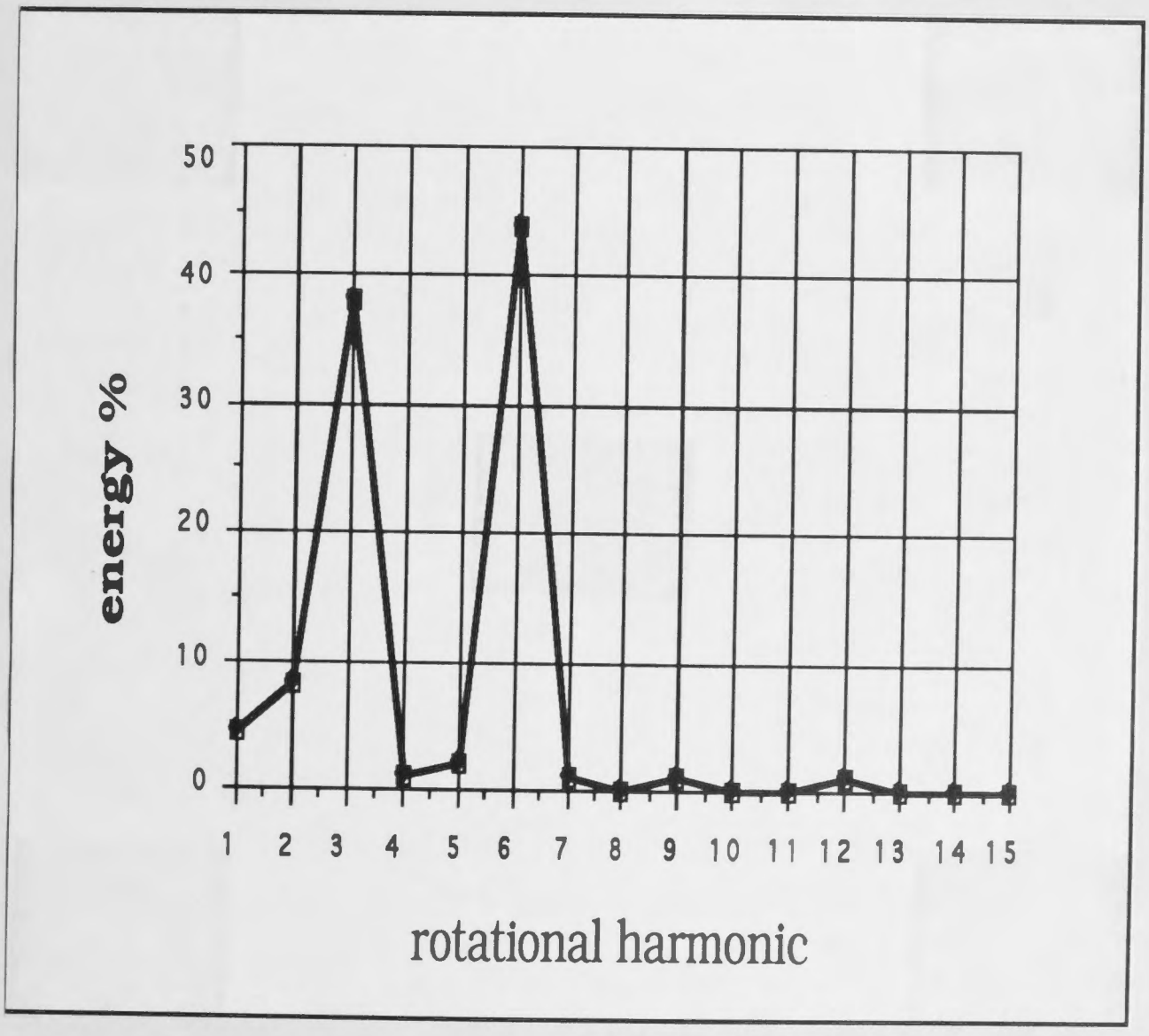

Figure 6.2

Two-dimensional analysis of views of the DnaB oligomer. (a) Average projection image filtered to 18 Å resolution. (b) Rotational analysis of the average image between radii 35 and 70 Å.

(a)

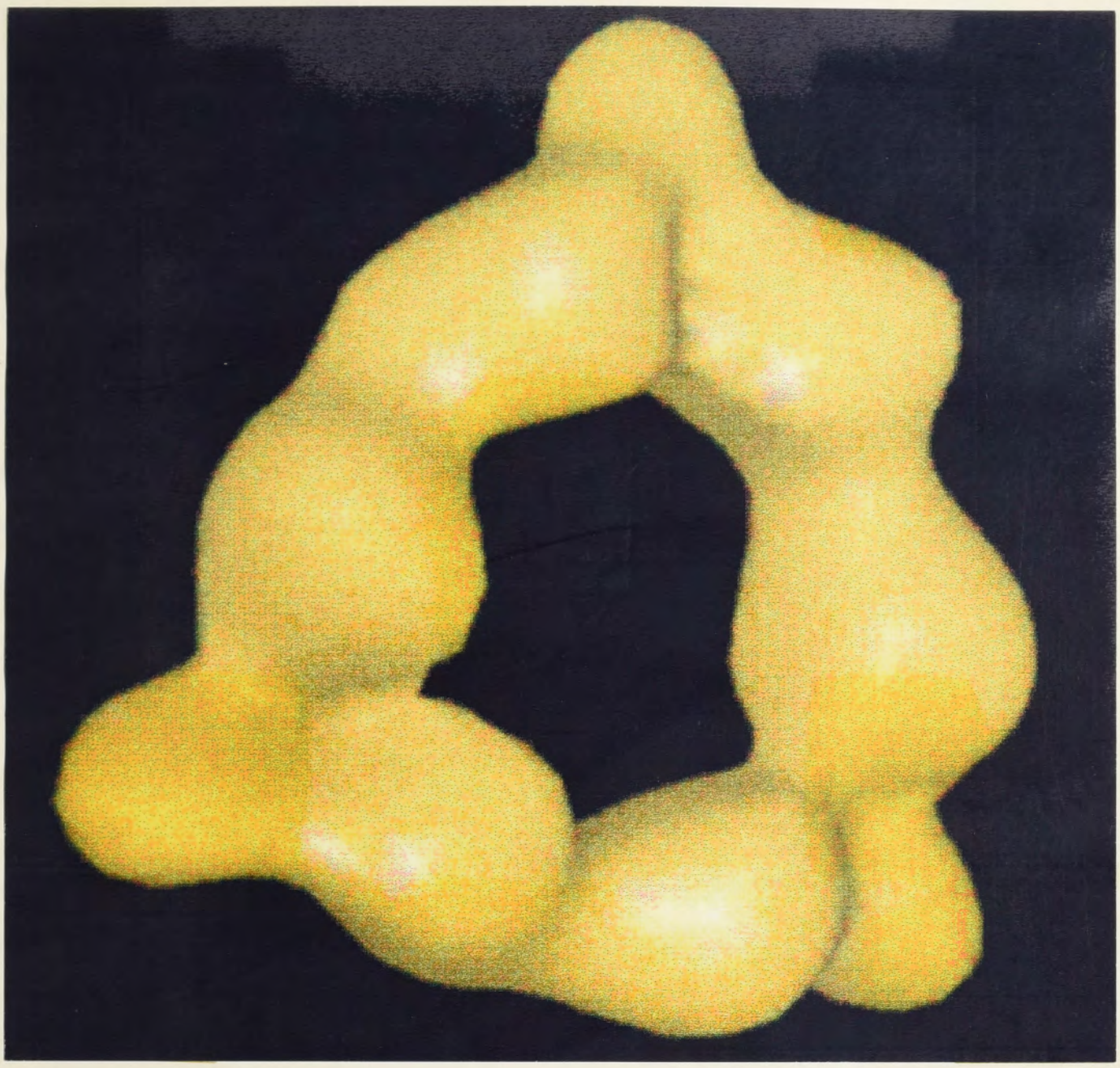

(b)

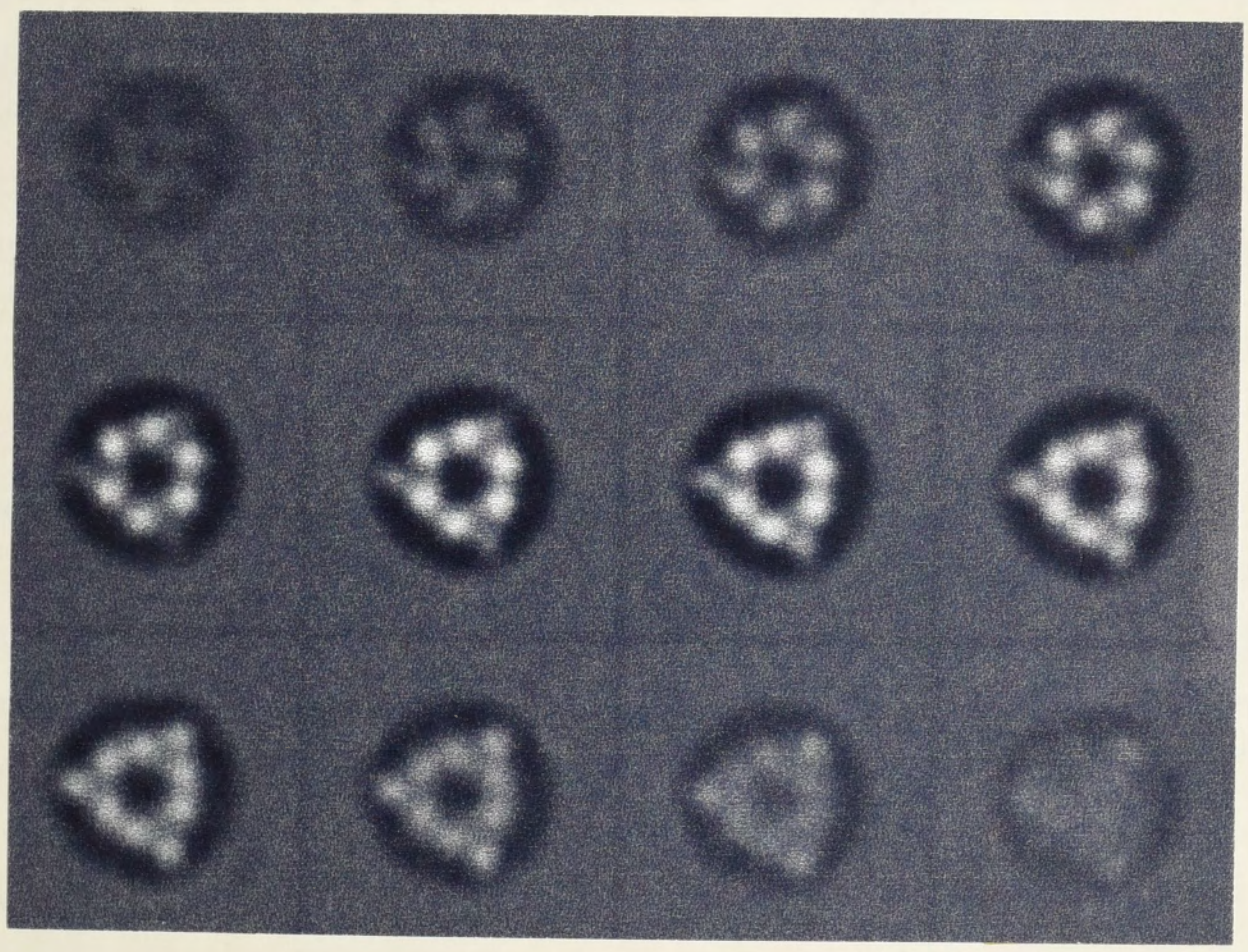

Figure 6.3

Three-dimensional reconstruction of the DnaB oligomer. (a) Surface rendering the reconstructed volume. (b) Sections through the reconstructed volume.

particle shows a degree of polarity between its two faces, with six inner lobules running from side to side and another three, less massive, appearing only in one of the sides.

Assuming a mean protein density of 1.33 g/cm^3, the reconstructed volume represents 55% of the volume expected for a protein of about 300,000 molecular weight. This is a not a surprising result for negatively-stained proteins, where both flattening of the molecules and stain penetration during sample preparation usually lead to volumes smaller than those predicted for globular proteins (Celia *et al.*, 1994).

6.4 Discussion

As determined by analytical sedimentation equilibrium studies (Bujalowski *et al.*, 1994), the *E.coli* DnaB helicase exists in solution as a stable hexamer over a wide range of protein concentrations. In thermodynamic studies carried out by Bujalowski and Klonowska (1993), a hexagonal arrangement of the subunits was suggested as the most probable physiological form of the DnaB hexamer. The six monomers building up the aggregate were established to be identical (Reha-Krantz and Hurwitz, 1978a; Arai *et al.*, 1981c). Based on these facts, a regular structure of hexagonal symmetry would be automatically expected for the DnaB helicase. However, the structural results of electron-microscopic studies indicated a somewhat different situation.

When DnaB is negatively stained and observed in the electron microscope, the oligomer shows a triangle-shaped characteristic view with a diameter of about 14 nm and a central stain-penetrating region. The two-dimensional study at 1.8 nm resolution (Figure 6.2a) showed that the six identical monomers are arranged in the particle such that it presents a most typical electron microscopy view with three-fold rather than six-fold symmetry. There are six large stain-excluding regions and, in between these regions, there are three additional smaller masses.

The three-dimensional reconstruction at 2.7 nm resolution, presented in Figure 6.3, further extends the results of the two-dimensional analysis. In particular, the relative spatial distribution of the large and small

regions becomes apparent. The three small regions are asymmetrically placed in the reconstructed volume, lying closer to that surface of the aggregate that is in contact with the carbon film. The central area of the oligomer appears as a channel fully opened at both ends, and it is clear that the six large masses are connected to the three smaller ones by narrower bridges.

To summarize these results, a structural model of the DnaB helicase has the following characteristics:

(a) The DnaB oligomer is a trimer of dimers with a very pronounced triangular shape;

(b) there is a channel that wholly traverses the centre of the helicase structure;

(c) the two faces of the DnaB helicase at the ends of the channel are different, producing a structural polarity.

The DnaB protein has always been purified as a hexamer and although there have been reports of its dissociation (Reha-Krantz and Hurwitz, 1978b; Lanka and Schuster, 1983; Gunther *et al.*, 1981a,b), the presence of DnaB dimers has not been reported. Bujalowski *et al.* (1994) only detected hexamers over a wide protein concentration range. However, the "leucine zipper" in the C-terminal domain of DnaB (Nakayama *et al.*, 1988a,b; Biswas *et al.*, 1994) might be involved in interactions that stabilize subunit dimers. Biswas *et al.* (1994) carried out glutaraldehyde-crosslinking studies of DnaB helicase and tryptic fragments of the protein. A kinetic crosslinking experiment with DnaB showed that a dimer was the predominant product in initial stages of the reaction and that higher oligomers were formed only subsequently. The COOH-terminal tryptic fragment formed stable dimers, but not stable hexamers. Our structural model of the DnaB hexamer as a trimer of dimers requires that at least two different regions of each subunit participate in interactions with different neighbouring subunits. Biswas *et al.* (1994) have proposed the existence of a site for protein-protein interactions other than the leucine zipper, further towards the NH_2-terminal end of the COOH-terminal domain. If such a site really exists, the leucine zipper might be responsible for dimerization of the two monomers, and the two monomers in the neighbourhood of this dimer would interact with it each through two sites: one in the NH_2-terminal domain (Nakayama *et al.*, 1984b), the other one in the COOH-terminal domain (the existence of which was suggested by Biswas *et al.*,

1994). Disruption of the interaction mediated through the leucine zipper or the one mediated through the other two sites could produce either of two different dimeric species. This would be also compatible with the findings of Bujalowski *et al.* (1994). In this context (Stamford, 1992), mutant DnaB proteins with (conservative) substitutions of valine residues for leucines in the heptad repeat were examined. One of these, a triple mutant at positions 367, 374 and 381, was still partially active in promoting replication but appeared to be predominantly dimeric as assessed by gel filtration in the presence of ATP. However, the mutant protein as overproduced was largely insoluble, and has not yet been further characterized. Nevertheless, the observation of a dimeric species is consistent with the proposed symmetry of the hexamer.

Bujalowski and Klonowska (1993) carried out thermodynamic studies of interactions of the DnaB helicase with nucleotides. Their results confirmed that there are six nucleotide-binding sites per DnaB hexamer as observed previously (Arai and Kornberg, 1981c), but revealed that the binding process is biphasic. Three nucleotide molecules are bound with high affinity; three others are bound in a subsequent low-affinity binding phase. The biphasic character of nucleotide binding to the DnaB hexamer is interpreted in terms of negative cooperativity among nucleotide-binding sites on the hexamer. The present structural model involving a trimer of dimers provides a reasonable structural basis for interpretation of these data.

There are some other facts that support the three-fold symmetry of the DnaB hexamer. As described in Section 1.3.3.1, the DnaT protein is one of the components involved in primosome assembly on the ϕX174 template (Lehman and Kornberg, 1992; Allen amd Kornberg, 1993) and in the interstrand transfer of DnaB that initiates rolling-circle replication following complementary-strand synthesis on ϕX174 and M13-A site DNA (Allen *et al.*, 1993). DnaT exists as a trimer of 19.5-kDa subunits. Although the role of DnaT in these processes remains uncertain, available evidence is consistent with it interacting at least transiently with DnaB and/or the DnaB.DnaC complex. Furthermore, as reported in Section 1.3.1, the λP protein (λ-specific analog of *E. coli* DnaC) forms a complex with DnaB during phage λ replication, and delivers it to the λO.*oriλ* complex. Again, in the isolable DnaB.λP complex, there appear to be only three λP protomers bound to the DnaB hexamer (Klein *et al.*, 1980; Mallory *et al.*, 1990), which is consistent with the observation of three-fold symmetry in the helicase molecule.

The existence of a channel of diameter ~4 nm running through the DnaB oligomer provokes a notion of one or both strands of DNA at a replication fork passing through the enzyme. Previous studies (Arai and Kornberg, 1981c) assumed that DNA wraps around the DnaB protein. Arai and Kornberg (1981c) observed that DnaB protects ~70-80 nucleotides of ssDNA from nuclease degradation. The inner channel of the reconstructed DnaB oligomer is only 3 nm high, which would probably be insufficient to protect that length of DNA and a model of DNA wrapping around the DnaB hexamer might be correct. However, the nuclease-protection experiments were carried out under conditions where the interaction of DnaB with DNA occurs distributively as it is in the general priming reaction (Section 1.3.2). On the other hand, the processive interactions of DnaB with DNA in specific priming require a specific mechanism for loading DnaB onto an SSB-coated DNA template (Section 1.3.3), perhaps such that the ssDNA passes through the channel. As was demonstrated by LeBowitz and McMacken (1986), the DnaB helicase requires a preformed forked structure in helicase assays on synthetic substrates with at least 40-nt (optimum 90-nt) 3'-terminal extension of ssDNA in the strand to which DnaB was not bound (Section 1.3.1). One might speculate, that the template strand on which DnaB is tracking as it moves in the 5' to 3' direction passes through the channel of the hexamer. The strand displaced during strand separation would then pass with the opposite polarity around the outside of the DnaB helicase.

As to the polarity of the presented structural model of DnaB, further electron-microscopic studies are required, since this feature could also be induced by a differential attachment with the carbon film and does not neccesarily have to be a characteristic of the particle under physiological conditions. Only the examinations of the particles by cryo-electron-microscopic studies in frozen buffer without contact with the carbon support film could probably confirm or disprove the structural polarity of the DnaB helicase. However, the possible polarity of DnaB is particularly relevant to consideration of the unidirectional (5' to 3') nature of translocation of DnaB on ssDNA and of its helicase activity. The indications of structural polarity could provide a simple mechanism for a defined directional interaction of the helicase with its ss DNA substrates. In this way it could be properly loaded onto ss DNA in the correct orientation for directional translocation. The handedness appearing in the symmetrized two-dimensional average could also point in this same direction.

The first model for secondary and tertiary structure of the DnaB monomer that was proposed by Nakayama *et al.* (1984a) is described in Section 1.5 and presented in Figure 1.8. Bujalowski and co-workers (1994) have recently provided new information on the shape of both the monomer and the hexamer of DnaB. Analytical ultracentrifuge experiments indicated that the monomer has an elongated structure with a ratio between its two main axes of $a/b = 5.2 \pm 0.8$ and that the oligomer has a nonspherical shape with an axial ratio $a/b = 2.6 \pm 0.6$, when modelled as prolate ellipsoids of revolution. In our results, with a particle 14 nm in diameter and 3.8 nm high, this ratio would be of about 3.6 for the oligomer, a figure compatible with that from Bujalowski *et al.* (1994), especially if we consider the possible flattening induced in the molecule by sample processing for electron microscopy.

A hypothetical model that accomodates both the results presented in this section as well as the previously established monomer model (Nakayama *et al.*, 1984b; Figure 6.4a) is shown in Figure 6.4b. The schematic representation of the arrangement of the six monomers in the oligomer fully agrees with the structural results of electron microscopy. The equivalence between the monomers in this model and the model proposed by Nakayama *et al.* (1984b) is obvious.

The six massive lobules in the particle would correspond to the COOH-terminal domains of the six monomers. The ATP- and DNA-binding regions would be located in this inner region of the particle. On the other hand, the three small masses at the vertices of the triangle would account for the NH_2-termini of a pair of monomers. The predicted dimerization (leucine heptad repeat) sites in the COOH-terminal domains would be responsible for the dimerization of the tryptic fragment corresponding to this domain, but the presence of the second area of contact between monomers in the NH_2-terminal domain would be essential for the arrangement of three dimers into a stable hexamer, and hence for the helicase action of DnaB.

The proposed detailed structural model is, of course, subject to the known limitations of the techniques that have been used, *i.e.*, specimen preservation in heavy metal stain and limited resolution, and further detailed analyses are also needed to assess the validity of the hypotheses. Nevertheless, the new data do present a three-dimensional framework

(a)

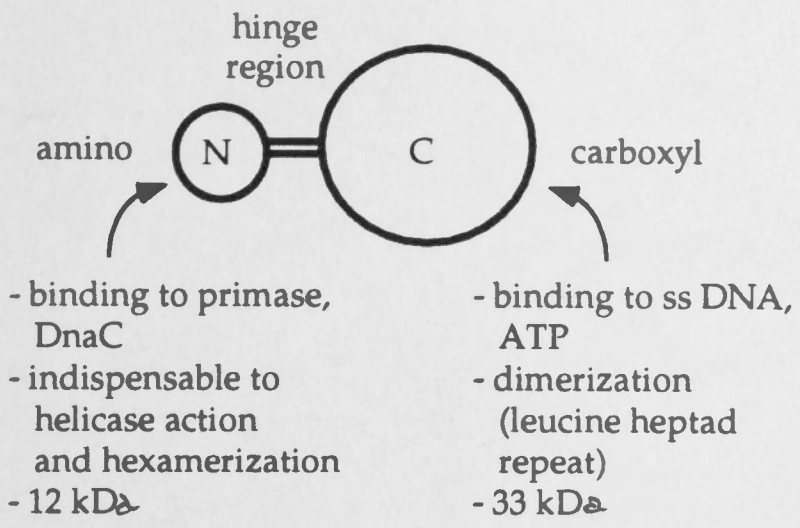

(b)

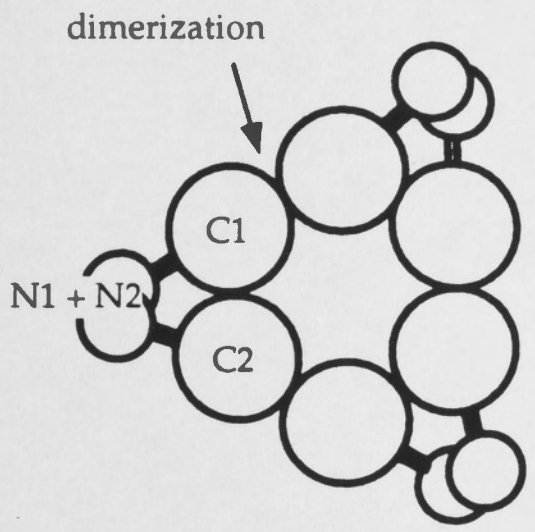

Figure 6.4

(a) Model of the DnaB monomer (adapted from Nakayama *et al.*, 1984b).

(b) Structural model of the DnaB oligomer. Schematic representation of the arrangement of the six monomers in the oligomer.

from which to approach structure-function relationships, not only for DnaB, but also in the growing family of related helicases (San Martin *et al.*, 1995).

CONCLUDING STATEMENT

In spite of a large number of enzymes that belongs to the helicase protein family and their importance in replication, recombination, and repair of DNA, there is a lack of high-resolution structural information about any DNA helicase. The DnaB helicase is a multifunctional enzyme with a unique role in the replication system of *E. coli*. Because of a good knowledge of the DnaB functions in this well-characterised bacterium, together with at least a certain notion of the domain and quaternary structure of the protein, the *E. coli* DnaB helicase seemed to be an ideal protein for further structural studies.

The aim of the work presented in this thesis was to investigate possibilities of obtaining high-resolution structural data about DnaB primarily using X-ray diffraction analysis of protein crystals. The extensive crystallization experiments were made feasible by improving the large-scale purification procedure of the DnaB protein and isolation of large quantities of ~99% pure DnaB and the DnaB.DnaC complex. Different nucleoside-phosphate ligands were used in purification and crystallization buffers in attempts to stabilise the DnaB in a single conformation. Preparation of the DnaB (ADP-bound form) crystals that diffracted X-rays to ~8Å is an important result, since to our knowledge, there has not been published any information about DnaB crystals suitable for X-ray diffraction analysis so far. Nevertheless, the conformation of DnaB in the prepared crystals was probably not completely stable as was deduced from the patterns of thermal diffuse scattering.

Several alternative strategies to generate variant DnaB proteins for structural studies either by X-ray crystallography or multidimensional NMR spectrometry were therefore explored.

An ATPase$^-$ mutant of DnaB (DnaB-R231C) was prepared, purified in large quantities and crystallized. The DnaB-I141T mutant, with modification of the region that is believed to undergo conformational changes on hydrolysis of ATP, was generated and purified. Conditions for crystallization of both mutants will have to be examined more extensively. The DnaB-R231C.DnaC complex, which seemed to be more stable than

*wt*DnaB.DnaC, might be the right candidate for crystallization and structural studies of the complex. DnaB-I141T did not form a stable complex with the DnaC protein.

In recognition of the fact that solving the three-dimensional structure of DnaB deletion mutants could contribute to elucidation of the structure of the whole DnaB protein, a significant effort was invested in the generation of systems overproducing the separate COOH- and NH_2-terminal fragments of DnaB in soluble form. Simultaneous overproduction of the DnaC protein with insoluble DnaB deletion mutants did not seem to improve their solubility.

Several systems for overproduction of the partially-soluble DnaBΔN1-165 mutant (the COOH-terminal domain) were prepared by subcloning of the *dnaBΔN1-165* gene in various expression vectors. In addition to this strategy, two DnaB insertion mutants with thrombin and factor Xa cleavage sites in the hinge region of the protein (DnaB-T165/166 and DnaB-F165/166, respectively) were prepared. The fragment of DnaB that approximately mimics the COOH-terminal domain can thus also be generated by proteolysis of DnaB-T165/166 or DnaB-F165/166 and subsequently purified by protein chromatography. All these systems will have to be further examined to choose the best one for large-scale overproduction and purification of the COOH-terminal domain.

The method for purification of the soluble NH_2-terminal domain of the DnaB protein (DnaBΔC162-470) was devised and large quantities of homogeneous DnaBΔC162-470 were purified. Crystallization experiments were not successful, however. The structure of this monomeric polypeptide might be resolved in the future by NMR spectrometry.

Electron microscopic images of negatively-stained DnaB protein have been studied and processed (Dr José M. Carazo and Ms M. Carmen San Martin, Centro Nacional de Biotecnología (C.S.I.C.), Madrid) to produce a three-dimensional reconstruction of the DnaB oligomer at 2.7 nm resolution. The model depicts the hexameric molecule as a trimer of dimers with a pronounced triangular shape with a channel that traverses the centre of the oligomer.

REFERENCES

Abdel-Monem, M., Durwald, H. and Hoffmann-Berling, H. (1976) Enzymic unwinding of DNA. 2. Chain separation by an ATP-dependent DNA unwinding enzyme. *Eur. J. Biochem.* 65:441-449.

Abrahams, J.P., Leslie, A.G.W., Lutter, R. and Walker, J.E. (1994) Structure at 2.8Å resolution of F1-ATPase from bovine heart mitochondria. *Nature* 370:621-628.

Alfano, C. and McMacken, R. (1989a) Ordered assembly of nucleoprotein structures at the bacteriophage λ replication origin during the initiation of DNA replication. *J.Biol.Chem.* 264:10699-10708.

Alfano, C. and McMacken, R. (1989b) Heat shock protein-mediated disassembly of nucleoprotein structures is required for the initiation of bacteriophage λ DNA replication. *J.Biol.Chem.* 264:10709-10718.

Allen, G.C., Jr., Dixon, N.E. and Kornberg, A. (1993) Strand switching of a replicative DNA helicase promoted by the *E. coli* primosome. *Cell* 74:713-722.

Allen, G.C., Jr. and Kornberg, A. (1991) Fine balance in the regulation of DnaB helicase by DnaC protein in replication in *Escherichia coli*. *J.Biol.Chem.* 266:22096-22101.

Allen, G.C., Jr. and Kornberg, A. (1993) Assembly of the primosome of DNA replication in *Escherichia coli*. *J.Biol.Chem.* 268:19204-19209.

Arai, K. and Kornberg, A. (1979) A general priming system employing only *dnaB* protein and primase for DNA replication. *Proc.Natl.Acad.Sci.USA* 76:4308-4312.

Arai, K. and Kornberg, A. (1981a) Mechanism of DnaB protein action. II. ATP hydrolysis by DnaB protein dependent on single- or double-stranded DNA. *J.Biol.Chem.* 256:5253-5259.

Arai, K. and Kornberg, A. (1981b) Mechanism of DnaB protein action. III. Allosteric roles of ATP in the alteration of DNA structure by DnaB protein in priming replication. *J.Biol.Chem.* 256:5260-5266.

Arai, K. and Kornberg, A. (1981c) Mechanism of DnaB protein action. IV. General priming of DNA replication by DnaB protein and primase compared with RNA polymerase. *J. Biol. Chem.* 256:5267-5272.

Arai, K. and Kornberg, A. (1981d) Unique primed start of phage ϕX174 DNA replication and mobility of the primosome in a direction opposite chain synthesis. *Proc.Natl.Acad.Sci.USA* 78:69-73.

Arai, K., Low, R., Kobori, J., Shlomai, J. and Kornberg, A. (1981a) Mechanism of *dnaB* protein action. V. Association of *dnaB* protein, protein n′, and other prepriming proteins in the primosome of DNA replication. *J.Biol.Chem.* 256:5273-5280.

Arai, K., Low, R.L. and Kornberg, A. (1981b) Movement and site selection for priming by the primosome in phage ϕX174 DNA replication. *Proc.Natl.Acad.Sci.USA* 78:707-711.

Arai, K., Yasuda, S. and Kornberg, A. (1981c) Mechanism of DnaB protein action. I. Crystallization and properties of DnaB protein, an essential replication protein in *Escherichia coli*. *J.Biol.Chem.* 256:5247-5252.

Bachmann, B.J. (1990) Linkage map of *Escherichia coli* K-12, edition 8. *Microbiol.Rev.* 54:130-197.

Baker, T.A., Funnell, B.E. and Kornberg, A. (1987) Helicase action of DnaB protein during replication from the *Escherichia coli* chromosomal origin *in vitro*. *J.Biol.Chem.* 262:6877-6885.

Baker, T.A., Sekimizu, K., Funnell, B.E. and Kornberg, A. (1986) Extensive unwinding of the plasmid template during staged enzymatic initiation of DNA replication from the origin of the *Escherichia coli* chromosome. *Cell* 45:53-64.

Baker, T.A. and Wickner, S.H. (1992) Genetics and enzymology of DNA replication in *Escherichia coli*. *Annu.Rev.Genet.* 26:447-477.

Biswas, S.B. and Biswas, E.E. (1987) Regulation of DnaB function in DNA replication in *Escherichia coli* by *dnaC* and λ*P* gene products. *J.Biol.Chem.* 262:7831-7838.

Biswas, S.B., Chen, P.-H. and Biswas, E.E. (1994) Structure and function of *Escherichia coli* DnaB protein: Role of the N-terminal domain in helicase activity. *Biochemistry* 33:11307-11314.

Bittner, M. and Vapnek, D. (1981) Versatile cloning vectors derived from the runaway replication plasmid pKN402. *Gene* 15:319-329.

Bouché, J.P., Rowen, L. and Kornberg, A. (1978) The RNA primer synthetized by primase to initiate phage G4 DNA replication. *J.Biol.Chem.* 253:765-769.

Bradford, M.M. (1976) A rapid and sensitive method for the quantitation of microgram quantities of protein utilizing the principle of protein-dye binding. Anal. Biochem. 72:248-254.

Bramhill, D. and Kornberg, A. (1988a) Duplex opening by DnaA protein at novel sequences in initiation of replication at the origin of the *E. coli* chromosome. *Cell* 52:743-755.

Bramhill, D. and Kornberg, A. (1988b) A model for initiation at origins of DNA replication. *Cell* 54:915-918.

Bujalowski, W. and Klonowska, M.M. (1993) Negative cooperativity in the binding of nucleotides to *Escherichia coli* replicative helicase DnaB protein. Interactions with fluorescent nucleotide analogues. *Biochemistry* 32:5888-5900.

Bujalowski, W. and Klonowska, M.M. (1994) Structural characteristics of the nucleotide-binding site of *Escherichia coli* primary replicative helicase DnaB protein. Studies with ribose and base-modified fluorescent nucleotide analogues. *Biochemistry* 33:4682-4694.

Bujalowski, W., Klonowska, M.M. and Jezewska, M.J. (1994) Oligomeric structure of *Escherichia coli* primary replicative helicase DnaB protein. *J. Biol. Chem.* 50:31350-31358.

Celia, H., Hoermann, L., Schultz, P., Lebeau, L., Mallough, V., Wigley, D.B., Wang, J.C., Mioskowski, C. and Oudet, P. (1994) Three-dimensional model of *Escherichia coli* gyrase B subunit crystallized in two-dimensions on novobiocin-linked phospholipid films. *J. Mol. Biol.* 236:618-628.

Chang, S.-F., Ng, D., Baird, L. and Georgopoulos, C. (1991) Analysis of an *Escherichia coli dnaB* temperature-sensitive insertion mutation and its cold sensitive extragenic suppressor. *J. Biol. Chem.* 266:3654-3660

Chase, J.W. and Williams, K.R. (1986) Single-stranded DNA binding proteins required for DNA replication. *Annu.Rev.Biochem.* 55:103-136.

Chou, P.Y. and Fasman, G.D. (1978) Empirical predictions of protein conformation. *Annu.Rev.Biochem.* 47:251-276.

Crowther. R.A. and Amos, L.A. (1971) Harmonic analysis of electron microscope images with rotational symmetry. *J. Mol. Biol.* 60:123-130.

Davis, R.W., Botstein, D. and Roth, J.R. (1980) *Advanced Bacterial Genetics.* Cold Spring Harbor Laboratory, Cold Spring Harbor, New York.

D'Ari, R., Jaffe-Brachet, A., Touati-Schwartz, D. and Yarmolinsky, M. (1975) A *dnaB* analog specified by bacteriophage P1. *J.Mol.Biol.* 94:341-366.

De Massy, B., Bejar, S., Louarn, J., Louarn, J.M. and Bouché, J.P. (1987) Inhibition of replication forks exiting the terminus region of the *Escherichia coli* chromosome occurs at two loci separated by 5 min. *Proc.Natl.Acad.Sci.USA* 84:1759-1763.

Dixon, N.E. and Kornberg, A. (1984) Protein HU in the enzymatic replication of the chromosomal origin of *Escherichia coli.* *Proc.Natl.Acad.Sci.USA* 81:424-428.

Dodson, M., Echols, H., Wickner, S. Alfano, C., Mensa-Wilmot, K., Gomez, B., LeBowitz, J., Roberts, J.D. and McMacken, R. (1986) Specialized

nucleoprotein structures at the origin of replication of bacteriophage lambda: localized unwinding of duplex DNA by a six-protein reaction. *Proc.Natl.Acad.Sci.USA* 83:7638-7642.

Dodson, M., McMacken, R. and Echols, H. (1989) Specialized nucleoprotein structures at the origin of replication of bacteriophage λ. Protein association and disassociation reactions responsible for localized initiation of replication. *J.Biol.Chem.* 264:10719-10725.

Elvin, C.M., Dixon, N.E. and Rosenberg, H. (1986) Molecular cloning of the phosphate (inorganic) transport (*pit*) gene of *Escherichia coli* K12. Identification of the *pit*$^+$ gene product and physical mapping of the *pit-gor* region of the chromosome. *Mol. Gen. Genet.* 204:477-484.

Elvin, C.M., Thompson, P.R., Argall, M.E., Hendry, P., Stamford, N.P.J., Lilley, P.E. and Dixon, N.E. (1990) Modified bacteriophage lambda promoter vectors for overproduction of proteins in *Escherichia coli*. *Gene* 87:123-126.

Fayet, O. and Prère, M.-F. (1987) Method for localization of cloned DNA fragments on the *Escherichia coli* chromosome. *J.Bacteriol.* 169:5641-5647.

Frank, J., Radermacher, M., Wagenknecht, T. and Verschoor, A. (1988) Studying ribosome structure by electron microscopy and computer image processing. *Methods Enzymol.* 164:3-35.

Fuller, R.S., Funnel, B.E. and Kornberg, A. (1984) The DnaA protein complex with the *E. coli* chromosomal replication origin (*oriC*) and other DNA sites. *Cell* 38:889-900.

Funnell, B.E., Baker, T.A. and Kornberg, A. (1986) Complete enzymatic replication of plasmids containing the origin of the *Escherichia coli* chromosome. *J.Biol.Chem.* 261:5616-5624.

Funnell, B.E., Baker, T.A. and Kornberg, A. (1987) *In vitro* assembly of a prepriming complex at the origin of the *Escherichia coli* chromosome. *J.Biol.Chem.* 262:10327-10334.

Gibson, F., Cox, G.B., Downie, J.A. and Radik, J. (1977) A mutation affecting a second component of the F_o portion of the magnesium ion-stimulated

adenosine triphosphatase of *Escherichia coli* K12. The *uncC424* allele. *Biochem. J.* 164:193-198.

Gill, S.C. and von Hippel, P.H. (1989) Calculation of protein extinction coefficients from amino-acid sequence data. *Anal. Biochem* . 182: 319-326.

Günther, E., Lanka, E., Mikolajczyk, M. and Schuster, H. (1981) The DnaB protein of *Escherichia coli groP*B mutants. *J.Biol.Chem.* 256:10712-10716.

Heisig, A., Severin, I., Seefluth, A.-K. and Schuster, H. (1987) Regulation of the *ban* gene containing operon of prophage P1. *Mol.Gen.Genet.* 206:368-376.

Hermes, J.D., Parekh, S.M., Blackow, S.C., Köster, H. and Knowles, J.R. (1989) A reliable method for random mutagenesis: The generation of mutant libraries using spiked oligodeoxyribonucleotide primers. *Gene* 88:143-151.

Hiasa, H. and Marians, K.J. (1992) Differential inhibition of the DNA translocation and DNA unwinding activities of DNA helicases by the *Escherichia coli* Tus protein. *J.Biol.Chem.* 267:11379-11385.

Hiasa, H., Sakai, H. and Komano, T. (1989) Identification of single-strand initiation signals in the *terC* region of the *Escherichia coli* chromosome. *FEBS Lett.* 246:21-24.

Hidaka, M., Kobayashi, T. and Horiuchi, T. (1991) A newly identified DNA replication terminus site, *TerE*, on the *Escherichia coli* chromosome. *J.Bacteriol.* 173:391-393.

Hill, T.M., Henson, J.M. and Kuempel, P.L. (1987) The terminus region of the *Escherichia coli* chromosome contains two separate loci that exhibit polar inhibition of replication. *Proc.Natl.Acad.Sci.USA* 84:1754-1758.

Hill, T.M., Kopp, B.J. and Kuempel, P.L. (1988) Termination of DNA replication in *Escherichia coli* requires a transacting factor. *J.Bacteriol.* 170:662-668.

Hines, J.C. and Ray, D.S. (1980) Construction and characterization of new coliphage M13 cloning vectors. *Gene* 11:207-218.

Hwang, D.S. and Kornberg, A. (1992) Opposed actions of regulatory proteins, DnaA and IciA, in opening the replication origin of *Escherichia coli*. *J.Biol.Chem.* 267:23087-23091.

Katz, L., Kingsbury, D.T. and Helinski, D.R. (1973) Stimulation by cyclic adenosine monophosphate of plasmid deoxyribonucleic acid replication and catabolite repression of the plasmid deoxyribonucleic acid-protein relaxation complex. *J. Bacteriol.* 114:577-591.

Khatri, G.S., MacAllister, T., Sista, P.R. and Bastia, D. (1989) The replication terminator protein of *E. coli* is a DNA sequence-specific contra-helicase. *Cell* 59:667-674.

Klein, A., Lanka, E. and Schuster, H. (1980) Isolation of a complex between the P protein of phage λ and the *dnaB* protein of *Escherichia coli*. *Eur.J.Biochem.* 105:1-6.

Kobayashi, T., Hidaka, M. and Horiuchi, T. (1989) Evidence of a *ter* specific binding protein essential for the termination reaction of DNA replication in *Escherichia coli*. *EMBO J.* 8:2435-2441.

Kobori, J.A. and Kornberg, A. (1982a) The *Escherichia coli dnaC* gene product. II. Purification, physical properties, and role in replication. *J.Biol.Chem.* 257:13763-13769.

Kobori, J.A. and Kornberg, A. (1982b) The *Escherichia coli dnaC* gene product. III. Properties of the dnaB-dnaC protein complex. *J.Biol.Chem.* 257:13770-13775.

Kolodner, R. and Richardson, C.C. (1977) Replication of duplex DNA by bacteriophage T7 DNA polymerase and gene 4 protein is accompanied by hydrolysis of nucleotide 5'-triphosphates. *Proc.Natl.Acad.Sci.USA* 74:1525-1529.

Kornberg, A. and Baker, T.A. (1991) *DNA Replication*, 2nd Edn, W.H. Freeman & Co., New York, N.Y.

Kuempel, P.L., Pelletier, A.J. and Hill, T.M. (1989) Tus and the terminators: The arrest of replication in prokaryotes. *Cell* 59:581-583.

Laemmli, U.K. (1970) Cleavage of structural proteins during the assembly of the head of bacteriophage T4. *Nature* 227:680-685.

Lanka, E., Geschke, B. and Schuster, H. (1978) *Escherichia coli dnaB* mutant defective in DNA initiation: Isolation and properties of the DnaB protein. *Proc.Natl.Acad.Sci.USA* 75:799-803.

Lanka, E., Mikolajczyk, M., Schlicht, M. and Schuster, H. (1978) Association of the prophage P1 *ban* protein with the DnaB protein of *Escherichia coli*. *J.Biol.Chem.* 253:4746-4753.

Lanka, E. and Schuster, H. (1983) The DnaC protein of *Escherichia coli*. Purification, physical properties and interaction with DnaB protein. *Nucleic Acids Res.* 11:987-997.

LeBowitz, J.H. and McMacken, R. (1984) The bacteriophage lambda O and P protein initiators promote the replication of single-stranded DNA. *Nucleic Acids Res.* 12:3069-3088.

LeBowitz, J.H. and McMacken, R. (1986) The *Escherichia coli* DnaB replication protein is a DNA helicase. *J.Biol.Chem.* 261:4738-4748.

LeBowitz, J.H., Zylicz, M., Georgopoulos, C. and McMacken, R. (1985) Initiation of DNA replication on single-stranded DNA templates catalyzed by purified replication proteins of bacteriophage λ and *Escherichia coli*. *Proc.Natl.Acad.Sci.USA* 82:3988-3992.

Lee, E.H. and Kornberg, A. (1991) Replication deficiencies in *priA* mutants of *Escherichia coli* lacking the primosomal replication n' protein. *Proc.Natl.Acad.Sci.USA* 88:3029-3032.

Lee, E.H., Kornberg, A., Hidaka, M., Kobayashi, T. and Horiuchi, T. (1989) *Escherichia coli* replication termination protein impedes the action of helicases. *Proc.Natl.Acad.Sci.USA* 86:9104-9108.

Lee, M.S. and Marians, K.J. (1989) The *Escherichia coli* primosome can translocate actively in either direction along a DNA strand. *J.Biol.Chem.* 264:14531-14542.

Legerski, R.J. and Robberson, D.L. (1985) Analysis and optimization of recombinant DNA joining reactions. *J. Mol. Biol.* 181:297-312.

Lehman, I.R. and Kornberg, A. (1992) DNA replication in prokaryotes and eukaryotes. *Chemtracts-Biochem.Mol.Biol.* 3:1-18.

Liberek, K., Osipiuk, J., Zylicz, M., Ang, D., Skorko, J. and Georgopoulos, C. (1990) Physical interactions between bacteriophage and *Escherichia coli* proteins required for initiation of lambda DNA replication. *J.Biol.Chem.* 265:3022-3029.

Lilley, P.E., Stamford, N.P.J., Vasudevan, S.G. and Dixon, N.E. (1993) The 92-min region of the *Escherichia coli* chromosome: Location and cloning of the *ubiA* and *alr* genes. *Gene* 129:9-16.

Lohman, T.M. (1992) *Escherichia coli* DNA helicases: Mechanisms of DNA unwinding. *Mol.Microbiol.* 6:5-14.

Low, R.L., Arai, K. and Kornberg, A. (1981) Conservation of the primosome in successive stages of ϕX174 DNA replication. *Proc.Natl.Acad.Sci.USA* 78:1436-1440.

Luria, S.E. and Burrous, J.W. (1957) Hybridization between *Escherichia coli* and *Shigella*. *J. Bacteriol.* 74:461-476.

Mallory, J.B., Alfano, C. and McMacken, R. (1990) Host virus interactions in the initiation of bacteriophage lambda DNA replication. Recruitment of *Escherichia coli* DnaB helicase by lambda P replication protein. *J.Biol.Chem.* 265:13297-13307.

Marabini, R. and Carazo, J. M. (1994) Pattern recognition and classification of images of biological macromolecules using artificial neural networks. *Biophys. J.* 66:1804-1814.

Marians, K.J. (1992) Prokaryotic DNA replication. *Annu.Rev.Biochem.* 61:673-719.

Marszalek, J. and Kaguni, J.M. (1994) DnaA protein directs the binding of DnaB protein in initiation of DNA replication in *Escherichia coli*. *J.Biol.Chem.* 269:4883-4890.

Masai, H. and Arai, K. (1988) Operon structure of *dnaT* and *dnaC* genes essential for normal and stable DNA replication of *Escherichia coli* chromosome. *J.Biol.Chem.* 263:15083-15093.

Masai, H. and Arai, K. (1989) Leading strand synthesis of R1 plasmid replication *in vitro* is primed by primase alone at a specific site downstream of *oriR*. *J.Biol.Chem.* 264:8082-8090.

Masai, H., Bond, M.W. and Arai, K. (1986) Cloning of the *Escherichia coli* gene for primosomal protein i: The relationship to DnaT, essential for chromosomal DNA replication. *Proc.Natl.Acad.Sci.USA* 83:1256-1260.

Masai, H., Nomura, N. and Arai, K. (1990a) The ABC-primosome. A novel priming system employing DnaA, DnaB, DnaC, and primase on a hairpin containing a DnaA box sequence. *J.Biol.Chem.* 265:15134-15144.

Masai, H., Nomura, N., Kubota, Y. and Arai, K. (1990b) Roles of ϕX174 type primosome- and G4 type primase-dependent primings in initiation of lagging and leading strand syntheses of DNA replication. *J.Biol.Chem.* 265:15124-15133.

Matson, S.W. (1991) DNA helicases of *Escherichia coli*. *Prog.Nucleic Acid Res.Mol.Biol.* 40:289-326.

Matson, S.W., Bean, D.W. and George, J.W. (1994) DNA helicases: Enzymes with essential roles in all aspects of DNA metabolism. *BioEssays* 16:13-22.

Matson, S.W. and Kaiser-Rogers, K.A. (1990) DNA helicases. *Annu.Rev.Biochem.* 59:289-329.

Maurer, R., Osmond, B.C. and Botstein, D. (1984a) Genetic analysis of DNA replication in bacteria: *dnaB* mutations that suppress *dnaC* mutations and *dnaQ* mutations that suppress *dnaE* mutations in *Salmonella typhimurium*. *Genetics* 108:25-38.

Maurer, R., Osmond, B.C., Shekhtman, E., Wong, A. and Botstein, D. (1984b) Functional interchangeability of DNA replication genes in *Salmonella typhimurium* and *Escherichia coli* demonstrated by a general complementation procedure. *Genetics* 108:1-23.

Maurer, R. and Wong, A. (1988) Dominant lethal mutations in the *dnaB* helicase gene of *Salmonella typhimurium*. *J.Bacteriol.* 170:3682-3688.

McHenry, C.S. (1988) DNA polymerase III holoenzyme of *Escherichia coli*. *Annu.Rev.Biochem.* 57:519-550.

McMacken, R., Ueda, K. and Kornberg, A. (1977) Migration of *Escherichia coli* DnaB protein on the template DNA strand as a mechanism in initiating DNA replication. *Proc.Natl.Acad.Sci.USA* 74:4190-4194.

Mead, D.A., Szczesna-Skorupa, E. and Kemper, B. (1986) Single-stranded DNA 'blue' T7 promoter plasmids: a versatile tandem promoter system for cloning and protein engineering. *Protein Eng.* 1:67-74.

Minden, J.S. and Marians, K.J. (1985) Replication of pBR322 DNA *in vitro* with purified proteins. Requirement for topoisomerase I in the maintenance of template specificity. *J.Biol.Chem.* 260:9316-9325.

Mok, M. and Marians, K.J. (1987) The *Escherichia coli* preprimosome and DnaB helicase can form replication forks that move at the same rate. *J.Biol.Chem.* 262:16644-16654.

Monod, J., Cohen-Bazire, G. and Cohn, M. (1951) Sur la biosynthèse de la β-galactosidase (lactase) chez *Escherichia coli*. La specificité de l'induction. *Biochim. Biophys. Acta.* 7:585-599.

Morrison, D.A. (1979) Transformation and preservation of competent bacterial cells by freezing. *Methods Enzymol.* 68:326-331.

Nakayama, N., Arai, N., Bond, M.W., Kaziro, Y. and Arai, K. (1984a) Nucleotide sequence of *dnaB* and the primary structure of the DnaB protein from *Escherichia coli*. *J.Biol.Chem.* 259:97-101.

Nakayama, N., Arai, N., Kaziro, Y. and Arai, K. (1984b) Structural and functional studies of the DnaB protein using limited proteolysis. Characterization of domains for DNA-dependent ATP hydrolysis and for protein association in the primosome. *J.Biol.Chem.* 259:88-96.

Nurse, P., Zavitz, K.H. and Marians, K.J. (1991) Inactivation of the *Escherichia coli* PriA DNA replication protein induces the SOS response. *J.Bacteriol.* 173:6686-6693.

Ollis, D. and White, S. (1990) Proteein crystallization. *Methods Enzymol.* 182:646-662.

O'Shea, E.K., Rutkowski, R. and Kim, P.S. (1989a) Evidnece that the leucine zipper is a coiled coil. *Science* 243:538-542

O'Shea, E.K., Rutkowski, R., Stafford III, W.F. and Kim, P.S. (1989b) Preferential heterodimer formation by isolated leucine zippers from Fos and Jun. *Science* 245:646-648

Oka, A., Sugimoto, K., Takanami, M. and Hirota, Y. (1980) Replication origin of *Escherichia coli* K12: the size and structure of the minimum DNA segment carrying information for autonomous replication. *Mol.Gen.Genet.* 178:9-20.

Pedré, X., Weise, F., Chai, S., Lüder, G. and Alonso, J.C. (1994) Analysis of *cis* and *trans* acting elements required for the initiation of DNA replication in the *Bacillus subtilis* bacteriophage SPP1. *J. Mol. Biol.* 236:1324-1340.

Pelletier, A.J., Hill, T.M. and Kuempel, P.L. (1988) Location of sites that inhibit progression of replication forks in the terminus region of *Escherichia coli. J.Bacteriol.* 170:4293-4298.

Penczek, P., Radermacher, M. and Frank, J. (1992) Three-dimensional reconstruction of single particles embedded in ice. *Ultramicroscopy* 40:33-53.

Radermacher, M., Wagenknecht, T., Verschoor, A. and Frank, J. (1987) Three-dimensional reconstruction from a single-exposure, random conical tilt series applied to the 50S ribosomal subunit of *Escherichia coli. J. Microsc.* 146:113-136.

Reha-Krantz, L.J. and Hurwitz, J. (1978a) The *dnaB* gene product of *Escherichia coli*. I. Purification, homogeneity, and physical properties. *J.Biol.Chem.* 253:4043-4050.

Reha-Krantz, L.J. and Hurwitz, J. (1978b) The *dnaB* gene product of *Escherichia coli*. II. Single-stranded chromatography DNA-dependent ribonucleoside triphosphatase activity. *J.Biol.Chem.* 253:4051-4057.

Sambrook, J., Fritsch, E.F. and Maniatis, T. (1989) *Molecular Cloning. A Laboratory Manual.* 2nd Edn. Cold Spring Harbor Laboratory, Cold Spring Harbor, New York, N.Y.

San Martin, M.C., Stamford, N.P.J., Dammerova, N., Dixon, N.E. and Carazo, J.M. (1995) A structural model for the *Escherichia coli* DnaB helicase based on electron-microscopy data. *J.Struct.Biol.* (in the press).

Schekman, R., Weiner, J.H., Weiner, A. and Kornberg, A. (1975) Ten proteins required for conversion of ϕX174 single-stranded DNA to duplex form *in vitro*. *J.Biol.Chem.* 250:5859:5865.

Sclafani, R.A. and Wechsler, J.A. (1981) Suppression of *dnaC* alleles by the *dnaB* analog (*ban* protein) of bacteriophage P1. *J.Bacteriol.* 146:321-324.

Sekimizu, K., Bramhill, D. and Kornberg, A. (1988) Sequential early stages in the in vitro initiation of replication at the origin of the *Escherichia coli* chromosome. *J.Biol.Chem.* 263:7124-7130.

Seufert, W. and Messer, W. (1987) DnaA protein binding to the plasmid origin region can substitute for primosome assembly during replication of pBR322 in vitro. *Cell* 48:73-78.

Shlomai, J. and Kornberg, A. (1980) An *Escherichia coli* replication protein that recognizes a unique sequence within a hairpin region in ϕX174 DNA. *Proc.Natl.Acad.Sci.USA* 77:799-803.

Shlomai, J., Polder, L., Arai, K. and Kornberg, A. (1981) Replication of ϕX174 DNA with purified enzymes. I. Conversion of viral DNA to a supercoiled biologically active duplex. *J.Biol.Chem.* 256:5233-5238.

Shrimankar, P., Stordal, L., Maurer, R. (1992) Purification and characterization of a mutant DnaB protein specifically defective in ATP hydrolysis. *J. Bacteriol.* 174:7689-7696.

Silhavy, T.J., Berman, M.L. and Enquist, L.W. (1984) *Experiments with Gene Fusions.* Cold Spring Harbor Laboratory, Cold Spring Harbor, New York, N.Y.

Sriprakash, K.S. and MacAvoy, E.S. (1988) A gene for DnaB like protein in chlamydial plasmid. *Nucleic Acids Res.* 15:10596.

Stamford, N.P.J. (1992) *PhD thesis: Proteins of the E. coli primosome,* Canberra: Aust National University.

Studier, W., Rosenberg, A.H., Dunn, J.J. and Dubendorff, J.W. (1990) Use of T7 polymerase to direct expression of cloned genes. *Methods Enzymol.* 185:61-89.

Stuitje, A.R., Weisbeek, P.J. and Meijer, M. (1984) Initiation signals for complementary strand synthesis in the region of the replication origin of the *Escherichia coli* chromosome. *Nucleic Acids Res.* 12:3321-3332.

Thommes, P. and Hübscher, U. (1992) Eucaryotic DNA helicases: Essential enzymes for DNA transactions. *Chromosoma* 101:467-473.

Touati-Schwartz, D. (1979) A *dnaB* analog *ban*, specified by bacteriophage P1: Genetic and physiological evidence for functional analogy and interactions between the two products. *Mol.Gen.Genet.* 174:173-188.

Tougu, K., Peng, H. and Marians, K.J. (1994) Identification of a domain of *Escherichia coli* primase required for functional interaction with the DnaB helicase at the replication fork. *J.Biol.Chem.* 269:4675-4682.

Turner, R. and Tjian, R. (1989) Leucine repeats and an adjacent DNA binding domain mediate the formation of functional cFos-cJun heterodimers. *Science* 243:1689-1694.

Ueda, K., McMacken, R. and Kornberg, A. (1978) DnaB protein of *Escherichia coli*. Purification and role in the replication of ΦX174 DNA. *J.Biol.Chem.* 253:261-269.

Unser, M., Trus, B. L. and Steven, A. C. (1987) A new resolution criterion based on spectral signal-to-noise ratios. *Ultramicroscopy* 23:39-52.

Vieira, J. and Messing, J. (1987) Production of single-stranded plasmid DNA. *Methods Enzymol.* 153:3-11.

Wahle, E., Lasken, R.S. and Kornberg, A. (1989a) The dnaB-dnaC replication protein complex of *Escherichia coli*. I. Formation and properties. *J.Biol.Chem.* 264:2463-2468.

Wahle, E., Lasken, R.S. and Kornberg, A. (1989b) The dnaB-dnaC replication protein complex of *Escherichia coli*. II. Role of the complex in mobilizing dnaB functions. *J.Biol.Chem.* 264:2469-2475.

Walker, J.E., Saraste, M., Runswick, M.J. and Gay, N.J. (1982) Distantly related sequences in the a and b subunits of ATP synthase, myosin, kinases and other ATP-requiring enzymes and a common nucleotide binding fold. *EMBO J.* 1:945-951.

Wang, P.Y. and Iyer, V.N. (1978) Analogues of the *dnaB* gene of *Escherichia coli* K12 associated with conjugative R plasmids. *J.Bacteriol.* 134:765-770.

Wechsler, J.A. and Gross, J.D. (1971) *Escherichia coli* mutants temperature-sensitive for DNA synthesis. *Mol.Gen.Genet.* 113:273-284.

Weiner, J.H., McMacken, R. and Kornberg, A. (1976) Isolation of an intermediate which precedes DnaG RNA polymerase participation in enzymatic replication of bacteriophage ϕX174 DNA. *Proc.Natl.Acad.Sci.USA* 73:752-756.

Wickner, S. (1984) DNA-dependent ATPase activity associated with phage P22 gene 12 protein. *J.Biol.Chem.* 259:14038-14043.

Wickner, S. and Hurwitz, J. (1974) Conversion of ϕX174 viral DNA to double-stranded chromatography form by purified *Escherichia coli* proteins. *Proc.Natl.Acad.Sci.USA* 71:4120-4124.

Wickner, S. and Hurwitz, J. (1975) Interaction of *Escherichia coli dnaB* and *dnaC(D)* gene products *in vitro*. *Proc.Natl.Acad.Sci.USA* 72:921-925.

Woelker, B. and Messer, W. (1993) The structure of the initiation complex at the replication origin, *oriC*, of *Escherichia coli*. *Nucleic Acids Res.* 21:5025-5033.

Wong, A., Kean, L. and Maurer, R. (1988) Sequence of the *dnaB* gene of *Salmonella typhimurium*. *J.Bacteriol.* 170:2668-2675.

Wu, C.A., Zechner, E.L. and Marians, K.J. (1992a) Coordinated leading- and lagging-strand synthesis at the *Escherichia coli* DNA replication fork. I. Multiple effectors act to modulate Okazaki fragment size. *J.Biol.Chem.* 267:4030-4044.

Wu, C.A., Zechner, E.L., Reems, J.A., McHenry, C.S. and Marians, K.J. (1992b) Coordinated leading- and lagging-strand synthesis at the *Escherichia coli* DNA replication fork. V. Primase action regulates the cycle of Okazaki fragment synthesis by polymerase III holoenzyme. *J.Biol.Chem.* 267:4074-4083.

Yanisch-Perron, C., Vieira, J. and Messing, J. (1985) Improved M13 phage cloning vectors and host strains: nucleotide sequences of the M13mp18 and pUC19 vectors. *Gene.* 33:103-119.

Zechner, E.L., Wu, C.A. and Marians, K.J. (1992a) Coordinated leading- and lagging-strand synthesis at the *Escherichia coli* DNA replication fork. II. Frequency of primer synthesis and efficiency of primer utilization control Okazaki fragment size. *J.Biol.Chem.* 267:4045-4053.

Zechner, E.L., Wu, C.A. and Marians, K.J. (1992b) Coordinated leading- and lagging-strand synthesis at the *Escherichia coli* DNA replication fork. III. A polymerase-primase interaction governs primer size. *J.Biol.Chem.* 267:4054-4063.

Zipursky, S.L. and Marians, K.J. (1981) *Escherichia coli* factor Y sites of plasmid pBR322 can function as origins of DNA replication. *Proc. Natl. Acad. Sci. U.S.A.* 78:6111-6115.

Zyskind, J.W., Cleary, J.M., Brusilow, W.S., Harding, N.E. and Smith, D.W. (1983) Chromosomal replication origin from the marine bacterium *Vibrio harveyi* functions in *Escherichia coli: oriC* consensus sequence. *Proc.Natl.Acad.Sci.USA* 80:1164-1168.

Zyskind, J.W. and Smith, D.W. (1977) Novel *Escherichia coli dnaB* mutant: Direct involvement of *dnaB*252 gene product in the synthesis of an origin-ribonucleic acid species during initiation of a round of deoxyribonucleic acid replication. *J.Bacteriol.* 129:1476-1486.

APPENDIX

The nucleotide sequence of the coding region of the *E.coli dnaB* gene and the primary structure of the DnaB protein (Nakayama *et al.*, 1984a). In the mature protein, the initiator methionine residue is removed *in vivo* leaving alanine as the NH_2-terminal residue (Nakayama *et al.*, 1984a). The region encoding the DnaB protein is composed of 1413 bp, the DnaB protein contains 470 amino acid residues and has a calculated molecular weight of 52,265.

```
    Met Ala Gly Asn Lys Pro Phe Asn Lys Gln Gln Ala Glu Pro Arg Glu Arg     16
  1 ATG GCA GGA AAT AAA CCC TTC AAC AAA CAG CAG GCT GAA CCC CGC GAA CGC

    Asp Pro Gln Val Ala Gly Leu Lys Val Pro Pro His Ser Ile Glu Ala Glu     33
 52 GAT CCA CAA GTT GCC GGG CTG AAA GTG CCT CCG CAC TCG ATC GAA GCG GAG

    Gln Ser Val Leu Gly Gly Leu Met Leu Asp Asn Glu Arg Trp Asp Asp Val     50
103 CAG TCG GTG TTG GGC GGT TTA ATG CTA GAT AAC GAA CGC TGG GAT GAT GTA

    Ala Glu Arg Val Val Ala Asp Asp Phe Tyr Thr Arg Pro His Arg His Ile     67
154 GCC GAG CGT GTG GTA GCA GAC GAT TTT TAC ACC CGC CCA CAC CGT CAT ATC

    Phe Thr Glu Met Ala Arg Leu Gln Glu Ser Gly Ser Pro Ile Asp Leu Ile     84
205 TTT ACT GAA ATG GCG CGT TTG CAG GAA AGC GGT AGC CCT ATC GAT CTG ATT

    Thr Leu Ala Glu Ser Leu Glu Arg Gln Gly Gln Leu Asp Ser Val Gly Gly    101
256 ACT CTT GCG GAA TCG CTG GAA CGC CAG GGG CAA CTC GAT AGC GTC GGT GGT

    Phe Ala Tyr Leu Ala Glu Leu Ser Lys Asn Thr Pro Ser Ala Ala Asn Ile    118
307 TTT GCT TAT CTG GCA GAG CTG TCA AAA AAT ACG CCA AGT GCG GCT AAC ATC

    Ser Ala Tyr Ala Asp Ile Val Arg Glu Arg Ala Val Val Arg Glu Met Ile    135
358 AGT GCC TAT GCG GAC ATC GTG CGT GAA CGT GCC GTT GTC CGT GAG ATG ATC

    Ser Val Ala Asn Glu Ile Ala Glu Ala Gly Phe Asp Pro Gln Gly Arg Thr    152
409 TCG GTT GCG AAT GAG ATT GCC GAA GCT GGT TTT GAT CCG CAG GGG CGT ACC

    Ser Glu Asp Leu Leu Asp Leu Ala Glu Ser Arg Val Phe Lys Ile Ala Glu    169
460 AGC GAA GAT CTG CTG GAT CTG GCT GAA TCC CGC GTC TTT AAA ATT GCC GAA

    Ser Arg Ala Asn Lys Asp Glu Gly Pro Lys Asn Ile Ala Asp Val Leu Asp    186
511 AGT CGT GCG AAC AAA GAC GAA GGG CCG AAG AAC ATC GCC GAT GTG CTC GAC

    Ala Thr Val Ala Arg Ile Glu Gln Leu Phe Gln Gln Pro His Asp Gly Val    203
562 GCA ACC GTG GCG CGT ATT GAG CAG TTG TTT CAG CAG CCA CAC GAT GGC GTT

    Thr Gly Val Asn Thr Gly Tyr Asp Asp Leu Asn Lys Lys Thr Ala Gly Leu    220
613 ACC GGG GTA AAC ACC GGT TAT GAC GAT CTC AAC AAA AAA ACC GCT GGC TTG

    Gln Pro Ser Asp Leu Ile Ile Val Ala Ala Arg Pro Ser Met Gly Lys Thr    237
664 CAG CCG TCG GAT TTG ATC ATC GTC GCC GCG CGT CCG TCG ATG GGT AAA ACA

    Thr Phe Ala Met Asn Leu Val Glu Asn Ala Ala Met Leu Gln Asp Lys Pro    254
715 ACA TTT GCG ATG AAC CTC GTC GAA AAC GCG GCG ATG TTG CAG GAT AAA CCG

    Val Leu Ile Phe Ser Leu Glu Met Pro Ser Glu Gln Ile Met Met Arg Ser    271
766 GTA CTT ATC TTC TCG CTG GAG ATG CCA TCA GAA CAG ATC ATG ATG CGT TCT

    Leu Ala Ser Leu Ser Arg Val Asp Gln Thr Lys Ile Arg Thr Gly Gln Leu    288
817 CTG GCG TCG CTG TCG CGC GTT GAC CAG ACT AAA ATC CGT ACC GGG CAG CTC

    Asp Asp Glu Asp Trp Ala Arg Ile Ser Gly Thr Met Gly Ile Leu Leu Glu    305
868 GAT GAC GAA GAC TGG GCG CGC ATT TCC GGC ACC ATG GGT ATT TTG CTC GAA

    Lys Arg Asn Ile Tyr Ile Asp Asp Ser Ser Gly Leu Thr Pro Thr Glu Val    322
919 AAA CGC AAT ATC TAT ATC GAT GAC TCC TCC GGC CTG ACG CCA ACG GAA GTG

    Arg Ser Arg Ala Arg Arg Ile Ala Arg Glu His Gly Gly Ile Gly Leu Ile    339
970 CGT TCC CGC GCA CGC CGT ATT GCC CGT GAA CAC GGC GGC ATC GGG CTT ATC
```

```
     Met Ile Asp Tyr Leu Gln Leu Met Arg Val Pro Ala Leu Ser Asp Asn Arg    356
1021 ATG ATC GAC TAC CTG CAA CTG ATG CGC GTA CCG GCG CTT TCC GAT AAC CGT

     Thr Leu Glu Ile Ala Glu Ile Ser Arg Ser Leu Lys Ala Leu Ala Lys Glu    373
1072 ACG CTG GAA ATT GCA GAA ATC TCT CGC TCG CTG AAA GCA CTG GCG AAA GAA

     Leu Asn Val Pro Val Val Ala Leu Ser Gln Leu Asn Arg Ser Leu Glu Gln    390
1123 CTG AAC GTG CCG GTG GTG GCG CTG TCC CAG TTG AAC CGT TCT CTG GAA CAA

     Arg Ala Asp Lys Arg Pro Val Asn Ser Asp Leu Arg Glu Ser Gly Ser Ile    407
1174 CGT GCC GAC AAA CGC CCG GTC AAC TCC GAC CTG CGT GAA TCT GGC TCT ATC

     Glu Gln Asp Ala Asp Leu Ile Met Phe Ile Tyr Arg Asp Glu Val Tyr His    424
1225 GAG CAG GAT GCG GAC TTG ATC ATG TTT ATC TAT CGT GAT GAG GTG TAT CAC

     Glu Asn Ser Asp Leu Lys Gly Ile Ala Glu Ile Ile Ile Gly Lys Gln Arg    441
1276 GAA AAC AGT GAT TTA AAA GGC ATC GCG GAA ATT ATT ATC GGT AAA CAA CGT

     Asn Gly Pro Ile Gly Thr Val Arg Leu Thr Phe Asn Gly Gln Trp Ser Arg    458
1327 AAC GGC CCA ATC GGG ACG GTA CGC CTG ACC TTT AAC GGT CAA TGG TCG CGC

     Phe Asp Asn Tyr Ala Gly Pro Gln Tyr Asp Asp Glu Stop                   470
1378 TTC GAC AAC TAT GCG GGG CCG CAG TAC GAC GAC GAA TAA
```